Mariam Abdulkareem

ENVIRONMENTAL SUSTAINABILITY OF GEOPOLYMER COMPOSITES

ACTA UNIVERSITATIS LAPPEENRANTAENSIS 992

Mariam Abdulkareem

ENVIRONMENTAL SUSTAINABILITY OF GEOPOLYMER COMPOSITES

Dissertation for the degree of Doctor of Science (Technology) to be presented with due permission for public examination and criticism in the Auditorium 1316 at Lappeenranta-Lahti University of Technology LUT, Lappeenranta, Finland on the 3rd of December, 2021, at noon.

Acta Universitatis
Lappeenrantaensis 992

Supervisors Professor Mika Horttanainen
LUT School of Energy Systems
Lappeenranta-Lahti University of Technology LUT
Finland

Associate Professor Jouni Havukainen
LUT School of Energy Systems
Lappeenranta-Lahti University of Technology LUT
Finland

Reviewers Professor Dr. Matthias Finkbeiner
Department of Environmental Technology
Technische Universität Berlin
Germany

Associate Professor Lidia Lombardi
Department of Energy Systems and Environment
University Niccolò Cusano - Rome
Italy

Opponent Associate Professor Sara González-Garcìa
Department of Chemical Engineering
University of Santiago de Compostela
Spain

ISBN 978-952-335-738-9
ISBN 978-952-335-739-6 (PDF)
ISSN-L 1456-4491
ISSN 1456-4491

Lappeenranta-Lahti University of Technology LUT
LUT University Press 2021

Abstract

Mariam Abdulkareem
Environmental Sustainability of Geopolymer Composites
Lappeenranta 2021
101 pages
Acta Universitatis Lappeenrantaensis 992
Diss. Lappeenranta-Lahti University of Technology LUT
ISBN 978-952-335-738-9, ISBN 978-952-335-739-6 (PDF), ISSN-L 1456-4491, ISSN 1456-4491

Portland cement (PC) production is resource-intensive and contributes 4–8% of global CO_2 emissions. The quest for reduced CO_2 emissions from PC production has led to the development of geopolymer binders. Geopolymers are produced from aluminosilicate precursors such as coal fly ash and granulated blast furnace slag and are developed from the polycondensation of polymeric aluminosilicates and alkali-silicates, yielding three-dimensional polymeric frameworks. This study was conducted to determine the environmental sustainability of geopolymers with respect to PC and PC concrete.

The primary aim of this dissertation is to compare the environmental performance of geopolymer materials to conventional materials and to support decision-making in the development of environmentally sustainable construction materials. To this end, the objectives of this dissertation are as follows: (1) to identify the most important factors contributing to the environmental impact of geopolymers that could be considered in future development, by quantifying the environmental performance of different geopolymer binders and composite mix designs in comparison to PC and PC concrete; (2) to quantify the potential to improve the environmental performance of geopolymers by utilising chemically modified waste-derived alkali-silicates instead of conventional sodium silicate, and (3) to quantify and compare the environmental performance of a product (low-height noise barrier) made from either PC concrete or geopolymer, identify hotspots, and evaluate the impact of product system changes on the performance.

The aim and objectives of this dissertation were met using the life cycle assessment (LCA) methodology which addresses the environmental performance and potential environmental impacts throughout a product's life cycle. Four LCA studies were conducted in this regard. The LCA studies were progressive, with results from the first two LCA studies providing the basis for the last two LCA studies.

The results obtained from the first two LCA studies reveal that alkali activator (sodium silicate) is the major contributor to the environmental performance of geopolymer mix designs. The best mix design from these analyses has 4% sodium silicate and 50% reduced global warming potential (GWP) when compared to PC concrete, and 61% reduced GWP when compared to steel fibre reinforced PC concrete. Based on the above results, the third LCA study was carried out by substituting chemically modified glass waste and rice husk ash derived alkali-silicate, respectively, with conventional sodium silicate powder and sodium silicate solution which led to 72% and 90% GWP reduction.

These results supported decision-making and guided the development of geopolymer composite mix designs in a project involving LUT university and partners. The environmental performance of these locally developed geopolymer composite mix designs shows the possibility of developing a geopolymer composite from 83% weight-% of industrial waste and by-products and 0.3% weight-% of alkali activator with a 73% GWP reduction when compared to conventional concrete.

This dissertation shows the differences in the environmental performance of geopolymers with different precursors, alkali activators, and system boundaries (cradle-to-gate and cradle-to-grave) and provides insight into how the environmental performance of geopolymers is influenced by these factors. It also enables a better understanding of the development of geopolymer composites as sustainable construction materials and facilitates environmentally sustainable decision-making in this area of study. This supports the often-emphasised view that geopolymer binders can be considered a low-carbon substitute for PC.

Keywords: Portland cement, geopolymer composites, industrial waste, life cycle assessment, environmental sustainability, environmental performance, waste recycling, industrial by-products, industrial side streams, waste management.

Acknowledgements

This dissertation was carried out at Sustainability Science and Solutions Unit in the School of Energy Systems at Lappeenranta-Lahti University of Technology LUT, Finland, between 2018 and 2021.

My sincerest gratitude goes to my supervisors, Professor Mika Horttanainen and Associate Professor Jouni Havukainen for their guidance, support, and supervision. I also wish to extend my gratitude to Associate Professor Mika Luoranen and Professor Risto Soukka.

I wish to acknowledge and thank my dissertation reviewers Professor Dr. Matthias Finkbeiner and Associate Professor Lidia Lombardi for their valuable comments and feedback which has helped improve my dissertation.

My research journey has been a roller coaster ride. There were the beautiful days and struggle days. As I am happy to see it through, I wouldn't have achieved all these without support of my family, friends, and colleagues. I appreciate your impacts such as catching up in the hallway for a quick chat, the jokes and banters, the social invites, putting a smile on my face, playing games, supporting me, and motivating me not to give up especially in challenging times.

So, many thanks to the SuSci unit members for an uplifting, inclusive and supportive working atmosphere. I also wish to express my utmost and sincerest gratitude to my family and friends. Thank you all for the smiles, laughter, and treasured moments. Also, a special shoutout to my Kongila. *I am citing you now ooo*...but really, May you always be happy. To my Muhammad Bashir… I am grateful for you.

I wish to acknowledge NASRDA for their support.

To everyone that has contributed to this journey of mine, I express my deepest gratitude and appreciation. Thank you all for making me better in my career and personal life.

Mariam Abdulkareem
November 2021
Lappeenranta, Finland

Our deepest fear is not that we are inadequate.
Our deepest fear is that we are powerful beyond measure.
It is our light, not our darkness that most frightens us.
We ask ourselves, who am I to be brilliant, gorgeous,
talented, fabulous?
Actually, who are you not to be?
Your playing small does not serve the world.
There is nothing enlightened about shrinking so that other
people won't feel insecure around you.
We are all meant to shine, as children do.
We are born to make manifest God's glory that is within us.
It is not just in some of us; it is in everyone.
And as we let our own light shine, we unconsciously give
other people permission to do the same.
As we are liberated from our own fear, our presence
automatically liberates others.

Marianne Williamson

In loving memory of my dad, Ibrahim Ayinla Kareem.

Contents

List of publications

This dissertation is based on the following papers: The publications are depicted using Roman numerals, for example, Publication I or PI.

This dissertation contains materials from the following papers: The rights were granted by publishers to include the material in the dissertation.

I. Niu, H., Abdulkareem M., Sreenivasan H., Kantola A. M., Havukainen J., Horttanainen M., Telkki V., Kinnunen P., Illikainen M. (2020). Recycling mica and carbonate-rich mine tailings in alkali-activated composites: synergy with metakaolin. *Minerals Engineering*, 157, doi: 10.1016/J.MINENG.2020.106535.

II. Abdulkareem, M., Havukainen, J., Horttanainen, M. (2019). How environmentally sustainable are fibre reinforced alkali-activated concrete? *Journal of Cleaner Production*: 236. doi: 10.1016/j.jclepro.2019.07.076.

III. Abdulkareem, M., Havukainen, J., Nuortila-Jokinen, J., Horttanainen, M. (2021). Environmental and economic perspectives of waste-derived activators in alkali-activated mortars *Journal of Cleaner Production*, 280, 124651. doi: 10.1016/j.jclepro.2020.124651.

IV. Abdulkareem, M., Havukainen, J., Nuortila-Jokinen, J., Horttanainen, M. (n.d.). Life-cycle assessment of a low-height noise barrier for railway traffic noise. *Journal of Cleaner Production* Submitted 2021.

Author's contribution

Mariam Abdulkareem was the principal investigator and author of Publications II–V. In paper I, He Niu was the principal investigator and author, and Mariam Abdulkareem conducted LCA modelling and assessment and contributed to article writing regarding the LCA aspect of the study.

Nomenclature

Symbol

eq	equivalent
℃	degree celcius
%	percent

Abbreviations

3D	Three-dimensional
ADP	Abiotic Depletion Potential
AM	Additive Manufacturing
AP	Acidification Potential
CFA	Coal fly ash
EC	European Commission
EC-JRC	European Commnision Joint Research Centre
EP	Euthrophication Potential
EU	European Union
FAETP	Freshwater Aquatic Ecotoxicity Potential
FRGC	Fibre reinforced geopolymer composite
GBFS	Granulated blast furnace slag
GGBFS	Ground granulated blast furnace slag
GHG	Greenhouse gas
GWP	Global Warming Potential
HTP	Human Toxicity Potential
ILCD	International Reference Life Cycle Data
kWh	Kilo Watt hour
LCA	Life Cycle Assessment
LCI	Life Cycle Inventory
LCIA	Life Cycle Impact Assessment
LHNB	Low-height noise barrier
LUT	Lappeenranta-Lahti University of Technology
MAETP	Marine Aquatic Ecotoxicity Potential
MJ	Mega Joules
MPa	Mega Paschal
ODP	Ozone Depletion Potential
P	Publication
PC	Portland cement
POCP	Photochemical Ozone Creation Potential
PM	Particulate matter
PP	Polypropylene
RHA	Rice husk ash
S	Scenario
TETP	Terrestrial Ecotoxicity Potential

TWh	Tera Watt hour

Chemical compounds

Al_2O_3	Aluminium oxide
$CaCO_3$	Calcium carbonate
CaO	Calcium oxide
CO_2	Carbon dioxide
Fe_2O_3	Iron oxide
NaOH	Sodium hydroxide
NO_x	Nitrogen oxides
SiO_2	Silicon dioxide
SO_2	Sulphur dioxide
SO_x	Sulphur oxides

1 Introduction

1.1 Background

Cement production from major global producers increased from approximately 2.63 billion tonnes in 2009 to 3.99 billion tonnes in 2018 (CEMBUREAU, 2019), and produces an estimated 4–8% of global CO_2 emissions (Andrew, 2018a; Davidovits, 2015). Cement is a hydraulic binding material that glues aggregates together to form mortar or concrete, constituting 10–15% of the concrete mix by volume (Gagg, 2014). The two main aspects of cement production that produce CO_2 emissions are:

1. The chemical reaction that occurs when heat is applied during clinker production (clinker is the primary constituent of cement). Here, carbonates are decomposed into oxides and CO_2, stoichiometrically indicating the amount of CO_2 emitted for a given amount of produced CaO as shown in Equation 1.1 (Andrew, 2018a; Gagg, 2014).
   $CaCO_3 + HEAT \rightarrow CaO + CO_2$ (1.1)
2. Fuel combustion during heating of raw materials at temperatures over 1000 °C (Andrew, 2018a).

Besides CO_2 emissions, other emissions from cement production include dust, NO_x, and SO_2 (CEMBUREAU, 2019). The most common cement is CEM I Portland cement (PC) (95% to 100% clinker). As clinker is the primary constituent of cement, the higher the clinker share, the higher the CO_2 emissions from the chemical reaction to form clinker. Thus, other cement types "blended cements" were introduced in addition to PC substituting some percentages of clinker with industrial by-products and/or waste such as blast furnace slag and coal fly ash (Davidovits, 2015) to improve the environmental performance of PC (CEMBUREAU, 2015a, 2015b, 2015c). These blended cements are CEM II Portland composite cement (65% to 94% of clinker), CEM III blast furnace cement (5% to 64% of clinker), CEM IV pozzolanic cement (45% to 89% of clinker), and CEM V composite cement (20% to 64% of clinker) (BS-EN197-1, 2011).

Furthermore, the need for binders with even better environmental performance than PC, which could potentially further reduce CO_2 emissions, led to the development of geopolymer binders. Geopolymers result from the "polycondensation of polymeric aluminosilicates and alkali-silicates, yielding three-dimensional polymeric frameworks" They do not necessitate extreme high-temperature kilns with high fuel expenditure as in PC production, thereby reducing energy consumption (Davidovits, 2015, 1994). Geopolymeric raw materials include naturally occurring aluminosilicates such as metakaolin, or industrial by-products or wastes with high silica-to-alumina ratios, such as coal fly ash (CFA) and granulated blast furnace slag (GBFS) (Davidovits, 2015). Geopolymers can be applied for environmental use in the containment of hazardous and toxic wastes, as well as in construction (Davidovits, 1994). The efficient recycling and use of silica and alumina-rich industrial wastes in geopolymers also reduces the potential environmental impacts of final disposal.

Alkali-activation is a common term employed in the reaction of aluminosilicates and alkali-silicates or alkali activators to produce a binder (Provis, 2018). Geopolymers are regarded as a sub-group of alkali-activated materials and are used interchangeably to some degree in the literature. However, the terminology of geopolymer and alkali-activated materials is under debate (Luukkonen et al., 2018). In some of the published articles in which this dissertation is based on, alkali-activated material terminology was used; however, geopolymer terminology is adopted in this dissertation as most of the cited references use this term.

Geopolymer concretes are produced by mixing geopolymer binders with fine and coarse aggregates and water, while geopolymer mortar is produced by mixing geopolymer binders with fine aggregates and water, as in cement concrete and mortar, respectively. On the other hand, geopolymer composites contain hardened binders with a blend of inorganic, metallic, or polymeric materials. Two or three of these mixtures comprise a composite (Wu and Zhang, 2018). Geopolymer binders can be produced in two ways: one- and two-part mixes. Two-part mix is the more conventional method of geopolymer binder production, and it occurs when a solid aluminosilicate powder reacts with an aqueous alkali activator (e.g. sodium silicate and sodium hydroxide). However, managing significant volumes of corrosive and hazardous alkali solutions in the two-part mix is impractical, resulting in one-part mix geopolymer binder which is produced when a solid aluminosilicate powder is reacted with a solid alkali activator and water. A one-part mix can be more scalable in the future as the binder is used in the same way as cement—by simply adding water (Luukkonen et al., 2018; Provis, 2018). The one-part and two-part geopolymer binder mixes are presented in Figure 1.1 and Figure 1.2.

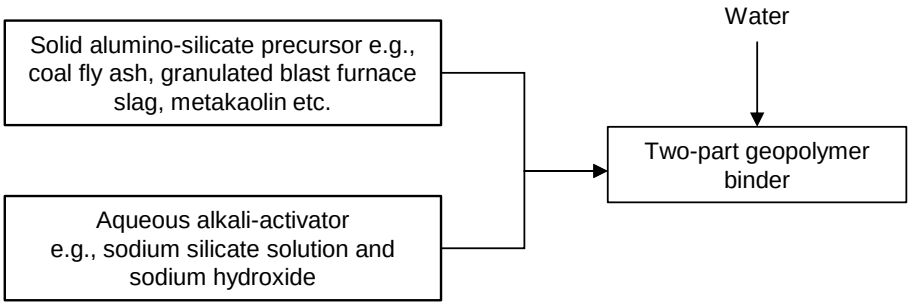

Figure 1.1: Two-part mix geopolymer binder

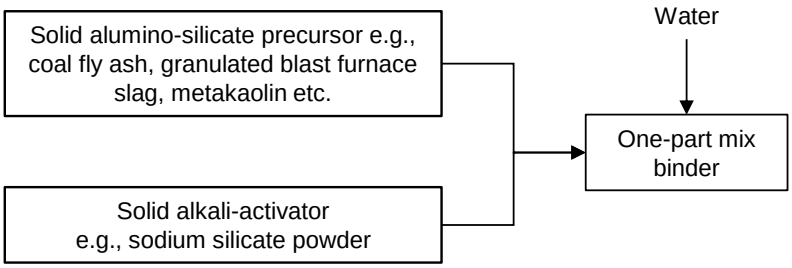

Figure 1.2: One-part mix geopolymer binder

As stated earlier, geopolymers are produced from aluminosilicate precursors, thus providing possibilities for different geopolymeric precursor options. These different options have varying availability, cost, and reactivity globally; hence, they are not standardised materials, in contrast to PC. However, this also makes geopolymers locally adaptable and versatile (Provis, 2018). Furthermore, some precursors such as CFA and GBFS are in demand for blended cements, thereby creating competition for raw materials in the supply chain. In addition, factors such as the long-term availability of precursors, such as in CFA (due to the implementation of renewable energy use), incorporation of sustainability measures in environmental regulations and industries, and varying composition of raw materials (for example, type of coal combustion and source of coal) (Wescott et al., 2010), hinder the future development of geopolymers. Nevertheless, this also leads to the exploration of locally suitable precursors and predisposes the development of geopolymers as a locally adaptable binder than a globally standardised material. In contrast to these concerns, the advantages of geopolymers over PC include acid and temperature resistance, high strength and durability, cold and quick setting, stable bonding of heavy metals and harmful substances, and simple manufacturing techniques (Weil et al., 2005). Compared to PC, geopolymers are considered more environmentally sustainable, as they lead to 70–80% CO_2 reduction (Davidovits, 2015). However, due to differences in precursors, alkali activators, system boundaries, methodologies, transportation, allocation, among others, environmental assessment studies of geopolymers vary and make comparisons challenging.

The most common methodology used in conducting environmental assessments of geopolymers is life cycle assessment (LCA). LCA “addresses the environmental aspects and potential environmental impacts throughout a product’s life cycle from raw material acquisition through production, use, end-of-life treatment, recycling and final disposal” (ISO 14040, 2006). Geopolymer production includes all or some of these life cycle phases which need to be considered when assessing environmental performance.

1.2 Aim and objectives

The aim of this dissertation is to compare the environmental performance of geopolymer materials to conventional materials to support decision-making in the development of environmentally sustainable construction materials. In accordance with the aim, the objectives of this dissertation are as follows.

- To identify the most important factors contributing to the environmental impact of geopolymers that could be considered in future development, by quantifying the environmental performance of different geopolymer binders and composite mix designs in comparison to PC, PC concrete, and steel fibre reinforced PC concrete.
- To quantify the potential to improve the environmental performance of geopolymers by utilising chemically modified waste-derived alkali-silicates instead of conventional sodium silicate.
- To quantify and compare the environmental performance of a product (a low-height noise barrier) made from PC concrete or geopolymer, identify hotspots, and evaluate the impact of product system changes on the performance.

The relationship between the sub-objectives and article publications included in this dissertation is presented in Table 1.1.

Table 1.1: Article publications in relation to sub-objectives.

	Publications	**Sub-objective I**	**Sub-objective II**	**Sub-objective III**
I	Recycling mica and carbonate-rich mine tailings in alkali-activated composites: a synergy with metakaolin	✓		
II	How environmentally sustainable are fibre reinforced alkali-activated concretes from industrial waste materials?	✓		
III	Environmental and economic perspective of waste-derived activators on alkali-activated mortars		✓	
IV	Life cycle assessment of a low-height noise barrier for railway traffic noise	✓		✓

The article publications in the table above and the research gaps identified in these publications formed the basis of this dissertation. The research gaps in the publications are summarised as follows: in Publication I, the environmental performance of alkali activation on mine tailings with metakaolin was investigated in comparison to PC. In Publication II, the environmental performance of various fibre reinforced geopolymer composites (FRGC) designs was compared to PC concrete and steel fibre reinforced PC

concrete. Publications I and II were conducted to identify the materials that predominantly contributed to the environmental performance of the geopolymers. Previously published articles have focused on the environmental performance of geopolymers without fibre reinforcement. However, in Publication II, FRGC was the object of analysis because of the brittle nature of some geopolymers and their sensitivity to cracking when loaded, which sometimes lead to failures and deterioration. Fibres are thus reinforced with geopolymers to enhance their ductility. The results from Publications I and II demonstrated that the key contributing materials to the environmental performance of geopolymers are alkali activators, and this result created the focus for Publication III. Publication III investigated the environmental performance of alkali-silicates developed from chemically modified silica-rich waste materials (rice husk ash and glass wastes) in comparison to conventional sodium silicate. Publication III was carried out to determine whether the chemically modified waste-derived alkali-silicates improved the environmental performance of the geopolymers. Finally, Publication IV assessed the environmental performance of a low-height noise barrier (LHNB) as a case study. Different geopolymer mix designs for this LHNB were developed, and an LCA study was performed.

1.3 Scope and Limitations of current research

This dissertation focuses on the previously mentioned objectives, and the results obtained are limited to the environmental performance studies included within the scope of this dissertation. An overview of the types of precursors, activators, and general scope of each study is presented in Table 1.2.

Table 1.2: Materials and scope of article publications included in this dissertation.

	Precursor	**Alkali activator**	**Aggregate**	**Fibre**	**Product**	**Reference material**	**System boundary**
Publication I	Metakaolin, phosphate mine tailings.	Sodium silicate, NaOH			Binder	PC	Cradle-to gate
Publication II	CFA, GBFS.	Sodium silicate, NaOH	Sand, silica sand, gravel.	Glass fibre, steel fibre, PP fibre.	Concrete	PC concrete	Cradle-to gate
Publication III	CFA, GBFS.	Rice husk ash, glass waste, sodium silicate, NaOH	Sand		Mortar	PC mortar	Cradle-to gate

Publication IV	CFA, GBFS, metakaolin, calcium aluminate cement.	Sodium silicate, NaOH	Sand, gravel, crushed steel slag, bottom ash, tailings.	PP fibre	Low-height noise barrier	PC concrete	Cradle-to grave

CFA, coal fly ash; GBFS, granulated blast furnace slag; NaOH, sodium hydroxide; PC, Portland cement; PP, polypropylene

The industrial by-products contained in this dissertation are mainly considered as waste and are not allocated environmental burdens from previous processes. This is based on the European Union directive that states "a substance is considered a by-product and not waste if the following conditions are met: 1) Further use of the substance is certain; 2) the substance can be used directly without any further processing other than normal industrial practice; 3) the substance is produced as an integral part of a production process; and 4) further use is lawful" (European Parliament and Council, 2008). However, during the sensitivity analysis of some of the studies, mass allocation was applied to waste fractions that may eventually end up as by-products according to the legislation, to determine the effect of allocation on the overall study. Pre-treatment and beneficiation processes needed for different wastes were included during environmental performance assessment.

The environmental performance in this dissertation was quantified using LCA methodology. In Publications I and II, the Centrum voor Milieukunde Leiden (CML) impact assessment method was used, while in Publications III and IV, the ReCiPe 2016 v1.1 (midpoint hierarchist timeframe) method was used. ReCiPe method was adopted in Publications III and IV mainly for its extensive environmental impact categories and endpoint features. Nevertheless, both CML and ReCiPe describe the environmental impacts of the inputs and outputs of the product system. The methodologies are implemented owing to their robustness and ability to reduce uncertainties by restricting quantitative modelling to the early stages in the cause-effect chain (SPhera, 2021). In Publication II, all the CML environmental impact categories were considered. In other publications, the most relevant environmental impact categories in relation to cement and geopolymer production were highlighted, which largely focused on global warming potential (GWP), acidification potential (AP), abiotic depletion potential for fossil fuels (ADP_FF), and photochemical ozone creation (POCP).

This dissertation is based on different geopolymer mix designs, thus making it case- and location-specific because geopolymer production is dependent on the availability of precursors in a given location, unlike PC, which is standardised worldwide. Therefore, this may inhibit the generalisation of the results. However, the information accumulated from these studies fills certain research gaps and contributes to research and knowledge. Due to data limitations and the use of specific regional data (Finland), this dissertation does not provide a global overview of the topic but rather concentrates on the results and conclusions from these specific studies. In addition, this dissertation focuses on the

environmental aspects of sustainability. Consequently, the economic and social sustainability assessments were not conducted.

1.4 Research process and dissertation structure

Publications II, III, and IV were executed as part of the *Urban Infra Revolution project* (project number: UIA02-155). The project lasted three years from 2017 to 2020 and was co-financed by the European Regional Development Fund through the Urban Innovative Actions initiative. The primary objective of the project was to find solutions for reducing CO_2 emissions in urban construction development by incorporating sustainability and circular economy in future construction schemes. This was accomplished by developing novel FRGCs by recycling and reusing local industrial wastes for cement substitutes. Environmental performance calculations were used to guide the design and development of geopolymer composites to ensure better environmental performance compared to conventional PC-based products.

As an article-based dissertation, this dissertation summarises and outlines the main features and results of the four publications presented in Section 1.2. By comparing and linking the findings of these publications, novel findings and conclusions were obtained.

This dissertation comprises five sections:

Section 1. Introduction – This section provides background and an overview of the topic, objectives, scope, and limitations of the current research. The research process and dissertation structure are described.

Section 2. State of the art – This section identifies and reviews the academic literature that is most relevant to the environmental performance of geopolymers and outlines the key differences between the LCA studies performed on geopolymers. This section also provides an overview of the precursors, alkali activator, fibre reinforcement, curing conditions, and carbonation, respectively, within the scope of this dissertation.

Section 3. Materials and Methods – The principle of LCA methodology is discussed in this section, and the LCA studies performed in Publications I, II, III, and IV are described. The goals of the different publications that make up this dissertation, functional units, system boundaries, life cycle inventories, and life cycle impact assessments are provided.

Section 4. Results and discussions – In this section, the key results of the research performed based on the research objectives of this dissertation are highlighted and discussed in a wider context.

Section 5. Conclusions – Recap of the results of this dissertation and conclusions of the research.

2 State of the art

The development of geopolymer binder/concrete has evolved over time. The first geopolymer binder composed of metakaolin-750, slag, and potassium silicate in a ratio of 1:1:2. This mix design was not considered a worthy competitor to PC because it was costly and not environmentally friendly owing to high amount of potassium silicate. Thus, it was promoted for specific niche applications. Subsequently, a second category geopolymer binder, known as a rock-based geopolymer binder, was developed comprising metakaolin-750, slag, volcanic tuff, and alkali-silicate in the ratio 1:1:2:1. The alkali-silicate in the second mix design was reduced to 20% by weight from 50% by weight in the first geopolymer binder. Furthermore, another rock-based geopolymer mix design was developed with slag, weathered granite, and alkali-silicate in the ratio 1.5:3.5:1, reducing alkali-silicate to 17% by weight. This second rock-based cement mix design has high mechanical strength (100–125 MPa on day 28) and becomes a more competitive option with 80% lower CO_2 emissions if slag is considered waste with no allocation, and 70% lower CO_2 emissions if slag is allocated environmental burden from previous processes (Davidovits, 2015). Geopolymer development evolved to a third category, based on low-calcium CFA. This third category is of two types: alkali-activated fly ash material and slag/fly ash-based geopolymer binder. The former requires reacting CFA with NaOH and heat curing at 60–80 °C, while the latter involves obtaining geopolymer binder from CFA, GBFS, and silicate solution at room temperature at a ratio of 5:1:1 with the amount of alkali-silicate reduced to 15–20% by weight from 50% by weight of the first geopolymer binder. This slag/fly ash-based geopolymer binder can produce a compressive strength of 100 MPa at 28 days; however, for a lower strength of approximately 40 MPa, the alkali-silicate can be reduced to 10–15% by weight with a ratio of 8:1:1. Davidovits (2015) contended that alkali-activated fly ash should not be qualified as a geopolymer because of its causticity. However, this is still debated, as many studies have labelled it a geopolymer.

The following subsections present an overview of specific precursors, activators, fibre reinforcement, curing, and carbonation, as included in the scope of this dissertation. In addition, this chapter provides an overview of research on the LCA of geopolymers.

2.1 Aluminosilicate precursors

2.1.1 Coal fly ash (CFA)

CFA is the most common solid aluminosilicate precursor and is usually used with GBFS in a geopolymer mix design (Luukkonen et al., 2018). CFA is a coal combustion residue with an estimated production of 92 million tonnes in 2016 in the EU and an estimated 50% utilisation rate in the construction industry (ECOBA, 2016). CFA is commonly captured from flue gases by electrostatic precipitators or other particle filtration equipment before flue gases enter chimneys (Zhuang et al., 2016). CFA is of two classes: class C, high calcium content, and class F, low-calcium content. Class C CFA is mostly

produced from the combustion of lignite coal and has between 50–70% by weight content of SiO_2, Al_2O_3, and Fe_2O_3, and more than 20% by weight content of CaO; Class F CFA is mainly produced from the combustion of anthracite or bituminous coal and has over 70% by weight content of SiO_2, Al_2O_3, and Fe_2O_3, and less than 10% by weight of CaO (Zhuang et al., 2016). The alumina and silica contents in CFA make it suitable for geopolymer production which typically demonstrates mechanical properties comparable to those of hydrated PC (Zhuang et al., 2016). However, Class C CFA is rarely used in geopolymers because of its low availability and rapid setting (Luukkonen et al., 2018).

2.1.2 Granulated blast furnace slag (GBFS)

GBFS is a by-product of pig iron production in blast furnaces and is generally utilised as a calcium-rich aluminosilicate precursor. Approximately 17 million tonnes of GBFS were produced in Europe in 2018, with approximately 13 million tonnes used in cement and construction, and 3 million tonnes used in road construction (Euroslag, 2019). GBFS has approximately 42% silica and alumina content (Adesanya et al., 2018). Geopolymers made from GBFS have a rapid setting time which is largely unfavourable, but it can be used to enhance the reactivity of low-calcium CFA (Hasnaoui et al., 2019). GBFS is relatively consistent in physical and chemical properties; however, compositions still vary between ores and furnaces (Duxson and Provis, 2008).

2.1.3 Metakaolin

Metakaolin has 97.5% silica and alumina content (Niu et al., 2020) which makes it a great precursor for geopolymers. Metakaolin is produced by heating kaolinite in a regulated manner at temperatures between 500 and 800 °C to expel hydration water. This heating process is referred to as calcination and typically occurs in rotary kilns or fluidised bed processes, which reduce the calcination duration from hours to minutes (NLK, 2002). Kaolinite is a hydrated aluminium disilicate and virgin material formed by the weathering of aluminosilicate minerals (NLK, 2002). Kaolinite production in Europe is estimated to be 35 million tonnes (Euromines, 2019) and has been used to produce ceramics for centuries (NLK, 2002).

2.1.4 Mine tailings

Mine tailings are waste generated from mining and quarrying, accounting for 26% of the total waste generated by economic activities and households in the EU (Eurostat, 2020a), and are currently underutilised. Mine tailings are collected in large sediments, which can lead to several environmental issues including environmental contamination and pollution (Sedira et al., 2017). In addition to the environmental risk involved in storing them, storage and maintenance are also resource intensive. Mine tailings vary in type and composition and are generally not highly reactive precursors; thus, they are largely used in combination with reactive precursors (Niu et al., 2020). Mine tailings often require pre-treatment before use which can include mechanochemical activation, such as grinding,

which can be more energy-efficient and less time consuming than high-temperature pre-treatments (Niu et al., 2020).

2.2 Alkali activators

Alkali activators can provide alkali cations, improve the pH of the reaction mixture, and enable dissolution (Luukkonen et al., 2018). Activators included in this dissertation include conventional sodium silicate and sodium hydroxide (NaOH), a glass waste-derived activator, and a rice husk ash (RHA)-derived activator.

2.2.1 Sodium silicate and sodium hydroxide

Sodium silicate is the most commonly used activator in geopolymer production and is sometimes used together with NaOH (Provis, 2018). NaOH is produced simultaneously with chlorine and hydrogen from the chlor-alkali industry via the decomposition of sodium chloride in water (EU, 2014). The chlor-alkali industry is considered energy-intensive, with 35 TWh of electricity consumed by electrolysis in 2010 in Europe. In addition, the type of cell technique employed also determines whether additional energy (steam or electricity) will be consumed for auxiliary processes (EU, 2014).

Conversely, sodium silicate can be produced in solid or liquid forms (EU, 2007; Fawer et al., 1999). Soluble sodium silicates, also known as waterglass solutions, are liquids containing dissolved glass with some water-like properties which can be used as binders as well as in other applications, including, but not limited to, sealants and emulsifiers (Keawthun et al., 2014). Sodium silicate has two notable basic production routes: furnace and hydrothermal (EU, 2007; Fawer et al., 1999). The furnace route for producing sodium silicate is by direct fusion of pure silica sand and sodium carbonate in gas or oil-fired furnaces at an estimated temperature of 1400 °C to produce sodium silicate lumps. This process also produces CO_2, which is similar to clinker production in cement kilns. After the sodium silicate lumps are produced, they are dissolved in water at elevated pressure and temperature to produce a sodium silicate solution of 37% solids which is subsequently filtered. This furnace-produced sodium silicate liquor has a weight ratio of 3.3 (EU, 2007; Fawer et al., 1999). The hydrothermal route for producing sodium silicate liquor involves dissolving silica sand in NaOH solution hydrothermally in autoclaves. Subsequently, the product is filtered and a sodium silicate solution of 48% solid with a weight ratio of 2.0, is obtained (EU, 2007; Fawer et al., 1999). Other types of sodium silicate products such as sodium metasilicate and sodium silicate powder are produced by drying, crystallisation, sieving, and separation of sodium silicate hydrothermal liquor (Fawer et al., 1999). The molar ratio (SiO_2/Na_2O) of sodium silicate varies between 0.93 and 3.32 (Luukkonen et al., 2018). Sodium silicate activators produce a more durable product with higher compressive strength compared to hydroxide-activated materials. Therefore, a higher amount of sodium silicate is utilised (Mohseni, 2018; Nematollahi et al., 2015). NaOH and sodium silicate have disadvantages, such as energy-intensive production. Thus, using renewable energy for production can help realise a more environmentally

friendly chemical product. Furthermore, NaOH is caustic and produces sodium carbonate when exposed to CO_2 (Luukkonen et al., 2018). Therefore, substituting conventional alkali silicates with other silica-rich sources, such as glass waste and rice husk ash, can be beneficial.

2.2.2 Glass-waste-derived alkali-silicate

Glass and sodium silicate have considerable similarities in their production as they react with silica sand and soda at temperatures above 1100 °C (EU, 2007). In 2019, 37 million tonnes of glass were produced in Europe (Glass Alliance Europe, 2019). Silicon dioxide is the key component of glass; hence, glass waste cullet is a promising source of silicate, with an amorphous silica content of 70–75% (Vinai and Soutsos, 2019). Nevertheless, the composition, colour, and impurities of glass waste can decrease its recycling potential. Alkali-silicate from glass waste is produced using hydrothermal or fusion methods. The hydrothermal method requires heating glass waste in an alkaline solution, whereas the fusion method requires mixing glass waste and NaOH powder and heating at an elevated temperature. The hydrothermal production process produces aqueous alkali silicate, whereas the fusion process produces a powder alkali-silicate (Vinai and Soutsos, 2019).

2.2.3 Rice husk ash derived alkali-silicate

Rice husk is produced during rice paddy milling and has several uses, for example, as a fertiliser and substrate, industrial fuel in power plants, raw material for brick production, etc. (Tong et al., 2018). An efficient way of disposing of rice husks is controlled combustion in kilns or power plants, producing RHA as waste which can also serve as a supplementary cementitious material (Meryman, 2009). RHA has a silica content of approximately 90%, similar to glass (Tong et al., 2018), and is regarded as a possible source of silicates in geopolymer production (Ghosh, 2013; Liu et al., 2016; Ma et al., 2012; Tchakouté et al., 2017). Alkali-silicate from RHA can be produced using the hydrothermal method by dissolving RHA in NaOH solution and heating the constituents (Tong et al., 2018). During the combustion of rice husks, the temperature and combustion time are vital because a shorter duration and higher temperatures likely maximise the amorphous content of RHA and induce the formation of crystalline SiO_2. The share of RHA in rice husks is 18–22% of the dry content by weight. To produce 1 kg of sodium silicate solution, 240 g of RHA is required which results from combusting 1.202 kg of rice husk. (Gursel et al., 2016; Tong et al., 2018).

2.3 Fibre reinforcement

Geopolymer concretes can be sensitive to cracking owing to their brittleness which can result in macro-cracks, failures, and deterioration (Al-mashhadani et al., 2018; Ganesan et al., 2015). To enhance ductility and reduce this shortcoming, geopolymer concrete is reinforced with fibres, which transmit stress between the matrix through the interfacial bond by crossing paths of potential cracks (Alomayri, 2017a). Incorporating fibres into

geopolymers has shown to improve physical and mechanical properties. Polypropylene, polyethylene, polyvinyl alcohol (PVA), and glass fibres have been used as reinforcements for geopolymers in several studies (Al-mashhadani et al., 2018; Alomayri and Low, 2013; Mohseni, 2018; Nematollahi et al., 2017, 2014; Ranjbar et al., 2016). FRGC has received much attention in research because of its improved physical and mechanical properties compared to PC concrete (Alomayri, 2017b). However, the physical and mechanical properties are determined by components such as elastic properties, type, size, dispersion pattern, fibre content and volume fraction, and fibre geometry. (Ganesan et al., 2015). With regard to improvement in FRGC, glass microfibres enhance the post-cracking composite, flexural strength, toughness, modulus properties, and energy absorption (Ganesan et al., 2015). Steel fibres demonstrate high fatigue strength resistance to impact, erosion, and abrasion resistance to splitting, temperature resistance, and shrinkage control of concrete (Rai and Joshi, 2014). Glass and polypropylene fibres enhance the tensile, energy absorption, and impact strength of concrete. However, glass fibres tend to become brittle with time, but this is countered by the introduction of alkali-resistant glass fibres (Rai and Joshi, 2014).

2.4 Curing conditions

Geopolymers are usually cured at ambient temperature (25 °C) but are sometimes cured at elevated temperatures (40–80 °C) subject to mix designs, precursors, etc. Heat curing accelerates early strength development in geopolymers (Luukkonen et al., 2018) and can also be appropriate in cold regions. Relative humidity is an essential factor to control during curing, preferably by sealing geopolymers during curing to avoid dehydration, as it may lead to efflorescence, microcracking, and decreases in compressive strength. In one-part geopolymers, heat is generated owing to solid activator dissolution which can have a positive effect during curing. (Luukkonen et al., 2018).

2.5 Carbonation (CO_2 uptake)

Carbonation "is a chemical reaction by which CO_2 penetrates concrete and reacts with hydration products, forming mainly calcium carbonate" (Andersson et al., 2019). CO_2 emissions from cement production are due to the combustion of fuels required to produce cement and calcination of limestone. The calcination reactions are reversible, and CO_2 can be absorbed back into concrete in a process referred to as carbonation. Carbonation is dependent on several factors, such as the process lasting many years, as it is a slow process. Other factors include CO_2 availability (as concrete must be exposed to CO_2 in the air to carbonate), transport of CO_2 molecules into concrete (which can accelerate the carbonation rate when concrete is crushed), temperature, humidity, and porosity. Consequently, considering carbonation in the emission calculation of concrete is important (Stripple et al., 2018). The carbonation reaction occurs in a number of steps, but the actual uptake reaction between the calcium and carbonate ions takes place in the water phase of the pore solution in the concrete, making water and moisture an important part of carbonation (Andersson et al., 2019). Half of the emissions that come from raw

materials required to produce concrete can be reabsorbed during the carbonation process of concrete during the use phase and partly in the end-of-life phase (Stripple et al., 2018).

2.6 LCA of geopolymer materials

LCA studies provide insight into different aspects of the environmental performance of geopolymers. However, differences in methodologies, system boundaries, functional units, life cycle inventory, allocation method, transportation, etc. make it challenging to compare LCA studies. Teh et al. (2017) applied an input-output hybrid LCA methodology to avoid truncated results due to limiting system boundaries and focused on GWP in geopolymer concrete assessment. The results of the study showed that ground GBFS (GGBFS) had a greater emission reduction compared to CFA. Using the economic allocation method, GGBFS-based and CFA-based geopolymer concrete achieved reductions of 43 and 32%, respectively, when compared to PC concrete. The major contributors to GGBFS-based geopolymer concrete were sodium silicate (20%), GGBFS (16%), and NaOH (11%), while the major contributors to CFA-based geopolymer concrete are CFA (32%) and sodium silicate (17%).

Bajpai et al. (2020) analysed three geopolymer concretes: CFA geopolymer with NaOH and sodium silicate as activators, CFA-silica fume geopolymer with NaOH and sodium silicate as activators, and CFA-silica fume geopolymer with only NaOH as activator. The environmental impact categories assessed were agricultural land use (ALU), GWP, ADP_FF, freshwater ecotoxicity (FAETP), human toxicity (HTP), ozone depletion (ODP), particulate matter formation (PMF), and water depletion (WD). Allocation was not considered in the study, as CFA and silica fume were both considered waste. The endpoint score showed that the different geopolymer concretes had 42–51% better environmental performance compared to PC concrete, with NaOH and sodium silicate been the major contributor to the environmental impacts of the geopolymer concretes. Replacing sodium silicate with silica fume also improved the environmental performance of the geopolymer concrete. The ALU and HTP impact categories showed a marginally higher impact on geopolymer concrete. Transport distances varied by ± 5%; however, the impact of the geopolymer mix was greater than that of PC concrete when the transportation distance was greater.

Furthermore, Salas et al. (2018) modelled a scale-up process from pilot to industrial scale for geopolymer concrete production and considered locally produced NaOH with different energy mixes in comparison to imported NaOH. The environmental impact categories assessed were ADP_FF, GWP, AP, eutrophication potential (EP), photochemical oxidant formation (POF), and ODP. The geopolymer concrete had 64% lower GWP, 26% lower ADP_FF, and 11% lower EP than PC concrete. About AP, POF, and ODP, geopolymer concrete had a higher environmental impact than PC concrete. The comparison between geopolymer concrete and PC concrete entailed limitations due to uncertainty in the characterisation of PC within the life cycle inventory (LCI) of PC concrete. As the LCI of local PC production was not available, an average PC LCI was

considered. Hence, the comparison between geopolymer concrete and PC concrete was only performed under the conditions established in the study. The major contributors to the impact assessment were sodium silicate and NaOH, with the other materials having a lower environmental burden, including zeolite. NaOH production is an important process in geopolymer concrete environmental performance, as it is also a major raw material for sodium silicate production. High electricity consumption caused a high environmental burden in NaOH production; thus, the influence of renewable energy was assessed. The results showed using an average European energy mix was environmentally worse than the local Ecuadorian energy mix because of the higher shares of thermal energy during the NaOH production. In addition, local NaOH produced a better environmental performance than imported European NaOH.

Sandanayake et al. (2018) considered three types of CFA-based geopolymer concretes from different locations in Australia with a focus on GWP impact category. A 5–10% GWP reduction was achieved in comparison to PC concrete in two of the mixes, while a 6% increase in GWP was observed in one of the mixes because of the increased transportation distance. Transportation had a considerable emission in geopolymer concrete due to the lack of local availability of CFA in comparison to PC. Other major contributors include the alkali activation process and heat curing.

Additionally, Heath et al. (2014) focused on clay-based geopolymers as an alternative to PC, using metakaolin as a precursor in a first mix with NaOH and sodium silicate as activators. In a second mix, metakaolin and bentonite meta-clay were used as precursors with NaOH activator. In a third mix, metakaolin precursor and NaOH activator was used. The first mix had a similar GWP to PC but an increased impact in other impact categories. Reductions in GWP of 30% and 40% were achieved in the second and third mixes, respectively, if silica fume was considered as waste. The study concluded that GWP reduction is highly dependent on the mix design and using an alternative form of soluble silica can be influential.

Passuello et al. (2017) assessed the environmental footprint of geopolymer binders using chemically modified RHA as an alternative alkali activator. When the geopolymer binder was produced with conventional sodium silicate as an activator, 7–22% lower GWP emissions were achieved compared to PC. When a geopolymer binder was produced with a chemically modified RHA activator, GWP emissions were reduced by 41–47% compared to PC. However, for other impact categories (AP, EP, FAETP, HTP, POCP, ODP, MAETP and TETP), the chemically modified RHA geopolymer binder and conventional sodium silicate geopolymer binder showed higher impacts than PC. When the chemically modified RHA geopolymer binder was compared to the conventional sodium silicate geopolymer binder, a 16–49% decrease in impacts was observed, especially in the toxicity impact categories (HTP, FAETP, TETP and MAETP) where geopolymer concrete had higher impacts with regards to PC.

Likewise, Mellado et al. (2014) focused on geopolymer mortar from conventional sodium silicate and an alternative activator from chemically modified RHA. The results showed

that conventional sodium silicate was the major contributor to the CO_2 emissions of the geopolymer mortar. Replacing conventional sodium silicate with RHA decreased CO_2 emissions by 50% while maintaining similar mechanical strength. The study showed great advantages in using an RHA alkali activator. Table 2.1 shows a summary of the discussed literature.

Table 2.1: Environmental performance of geopolymer binder and concrete according to literature studies

References	**[1]**	**[2]**	**[3]**	**[4]**	**[5]**	**[6]**	**[7]**
Functional unit	1 m^3 concrete	1 m^3 concrete	1 m^3 hollow blocks	1m^3 concrete	1 kg binder	1 kg paste	ND
System boundary	Cradle-to-shelf	Cradle-to-grave	Cradle-to-gate	Cradle-to-gate	Cradle-to-mixer	Cradle-to-gate	Cradle-to-gate
Reference material	PC concrete	PC concrete	PC concrete	PC concrete	PC	PC	PC
Precursors	90% GGBFS & 10% CFA; 90% CFA & 10% GGBFS	CFA; CFA & silica fume	Natural zeolite	CFA	MK	calcined kaolin sludge	FCC catalyst
Activator	NaOH & sodium silicate	NaOH & sodium silicate; NaOH	NaOH & sodium silicate	NaOH & sodium silicate	NaOH & sodium silicate	NaOH & sodium silicate; NaOH & RHA	NaOH & sodium silicate; NaOH & RHA
Aggregate	Sand & gravel	Sand & gravel	Sand	Sand & gravel	ND	ND	silica sand
Activator to precursor ratio	ND	ND	ND	0.37	ND	0.4	0.5
Curing	ND	Room temperature	60°C for 24h	80°C for 24h	60 - 80°C	50°C for 24h	ND
Data source	Local	Ecoinvent 3.0, testing	Literature, testing Ecoinven	Primary and Secondary data	Ecoinvent	Ecoinvent 3.1	ND

			t 3.3, USLCI				
Region	Australia	India	Ecuador	Australia	ND	Brazil	Italy
Distance for raw materials	National average distance	420–3363 km	4.7–64 km	655–1653 km	ND	ND	45–366 km
Compressive strength	40-50 MPa	35–39 MPa	15 MPa	ND	ND	47–74 MPa	44–60 MPa
Impact categories	GWP	ALU, GWP, ADP_FF, FAETP, HTP, ODP, PMF, WD	ADP_FF, GWP, AP, EP, POF, ODP	GWP	GWP, ADP_FF, AP, EP, ODP, HTP, FAETP, MAETP, TETP; POCP	AP, GWP, EP, FAETP, HTP, MAETP, POCP, ODP, TETP	CO_2 emissions
Impact methodology	Input/Output framework and LCA	ReCiPe	CML 2001	Process based approach	CML 2	CML 01	ND
Software	ND	Umberto NXT	SimaPro	ND	ND	Open LCA	ND
Conclusion	32%-43% reduced GWP in comparison to PC concrete. Sodium silicate and NaOH are key contributors to GWP	42%-51% better environmental performance than PC concrete, sodium silicate and NaOH are key contributors	Better GWP, ADP_FF, EP. Worse AP, POD ODP. NaOH is main contributor	5-10% reduced GWP, transportation and activator had significant contribution	30%-40% GWP reduction, increased impact in all other categories	Reduced GWP emissions	Reduced CO_2 emissions

[1] - Teh et al. (2017); [2] - Bajpai et al. (2020); [3] - Salas et al. (2018); [4] - Sandanayake et al. (2018); [5] - Heath et al. (2014); [6] - Passuello et al. (2017); [7] - Mellado et al. (2014); ADP_FF - abiotic depletion potential_fossil fuel; ALU-Agricultural land use; CFA – coal fly ash; FAETP- freshwater aquatic ecotoxicity potential; FCC - fluid catalytic cracking; GBFS – granulated blast furnace slag; HTP- human toxicity potential; MAETP - marine aquatic ecotoxicity potential; MK – metakaolin; NaOH – sodium hydroxide; ND – not defined; ODP – Ozone depletion potential; PMF-particulate matter formation; POCP-photochemical oxidation creation potential; POF – Photochemical oxidants formation; RHA – rice husk ash; TETP-terrestrial ecotoxicity potential; WD-water depletion.

3 Materials and methods

LCA methodology was employed in this dissertation to determine the environmental performance of geopolymers to support decision-making in the development of environmentally sustainable construction materials. This section details the principles of LCA methodology and the LCA studies included in this dissertation. Four LCA studies on geopolymer binders, mortars, and composites are included. As previously mentioned, geopolymer materials are not standardised like PC, and are developed using different mix designs with different precursors and alkali activators, making each LCA study case- and location-specific, which also aids in decision-making and other developmental measures. The LCA studies contained in this dissertation were performed according to ISO 14040 and 14044 principles and framework (ISO 14040, 2006; ISO 14044, 2007), and follow the main LCA phases which will be discussed in subsection 3.1. In line with the LCA studies, the reference scenario and alternative scenarios are established in the goal and scope definition, and primary and secondary data are collected in the inventory analysis phase. Calculating and modelling potential environmental performances is conducted in the impact assessment and interpretation phases, and a sensitivity analysis is conducted along with a discussion of the results.

The references of each LCA study are conventional materials. The reference year is based on data availability during inventory collection. Different mix designs from literature studies and locally developed mix designs were considered when establishing alternative scenarios. Results from Publications I and II guided the goal and scope definition for Publications III and IV. Scenarios analysed in the different publications were modified after the LCI data collection phase because of the iterative nature of LCA. In the publications, primary data were collected locally from industries and companies. Where primary data are not available, secondary data from literature studies, environmental reports from industries, and LCI databases were applied. The environmental performances for all the geopolymer mix designs were modelled and calculated using an LCA supported product sustainability software, GaBi (Sphera, 2021). A sensitivity analysis was performed to evaluate the influence of materials, energy, allocation, and modelling assumptions of the product system on the LCA results. The publications have been reported in the scientific literature and are described in detail in this section.

3.1 Principles of LCA methodology

LCA addresses environmental performance throughout a product's life cycle from cradle-to-grave (ISO 14040, 2006) and is extensively used for environmental performance assessment. According to ISO 14040 and 14044 standards, the LCA study is conducted in four phases: goal and scope definition, inventory analysis phase, impact assessment phase, and interpretation phase (ISO 14040, 2006). LCA is an iterative method; thus, different stages of the scope may need to be revised to reconcile with the goal of the study (ISO 14040, 2006). Figure 3.1 illustrates the LCA framework.

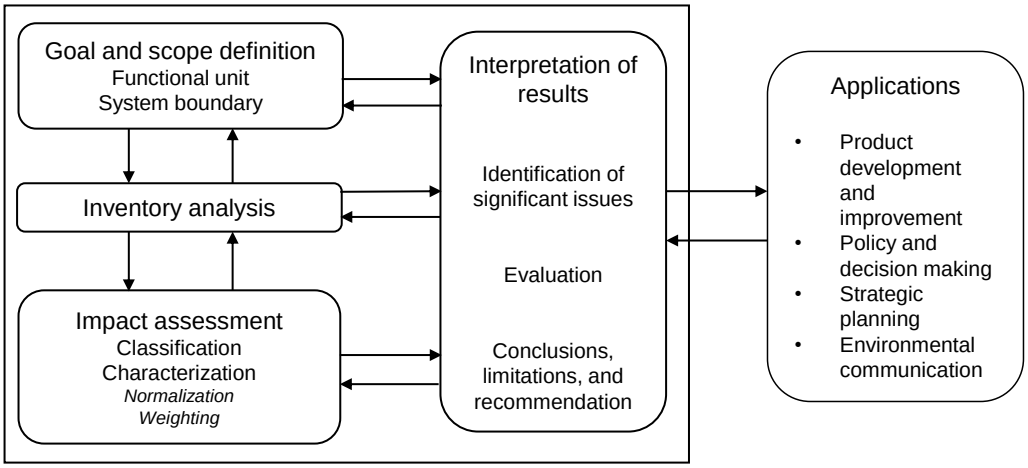

Figure 3.1: Life cycle assessment framework with main the main LCA phases modified from ISO 14040 (2006)

The first phase of LCA is the goal and scope definition phase. The goal defines the purpose of the study and the motives for implementing the study, among other things. The scope defines the product system to be studied, function and functional unit, system boundary, selected impact categories, impact assessment methodology and interpretation, assumptions, limitations of the studied product system, initial data quality requirements, etc. This phase should be adequately completed to ensure that the specifics of the study are consistent and adequately address the stated goal (ISO 14040, 2006). The functional unit and system boundary are pertinent to the goal and scope definition phases and will be discussed further.

The functional unit defines "the quantification of the identified functions of the product and provides a reference to which all inputs and outputs are related which is essential to ensure comparability of LCA results" (ISO 14040, 2006). The functional unit must be coherent with the goal and scope, measurable, and well-defined. The system boundary defines the unit processes contained within the LCA and must also be coherent with the goal of the study. In the scope definition, decisions are made based on the unit processes included in the study and the depth to which they should be studied. In the LCA definition, the environmental performance of products should be assessed throughout its life cycle, from raw material acquisition to end-of-life and recycling, which are the "cradle-to-grave" and "cradle-to-cradle" approaches, respectively. However, it is permitted to remove life cycle stages or processes if they do not drastically alter the total LCA results, but they should be clearly indicated and the implications should be explained (ISO 14044, 2007). The system boundary is described with a process flow diagram illustrating the beginning and end of the unit processes and their interrelationships (ISO 14044, 2007). The elements included in the system boundary depend on the goal and scope definition, intended application, data constraints, and cut-off criteria (ISO 14040, 2006).

Inventory analysis, also known as life cycle inventory (LCI), “involves data collection and calculation procedures to quantify relevant inputs and outputs of a product system” This phase is also iterative and can be resource-intensive because data are collected for each unit process contained in the system boundary (ISO 14044, 2007). Data can be primary and/or secondary and collected from production sites, literature, or calculated. Data can be classified into energy inputs, raw material inputs, ancillary inputs or other physical inputs, products, co-products, wastes, and emissions to air, water, soil, and other environmental aspects. These data should be detailed, referenced, and stated if data quality requirements are not met (ISO 14044, 2007). As the LCI phase advances, one can encounter limitations and new data requirements, necessitating a new change in data collection procedures (ISO 14040, 2006).

The life cycle impact assessment (LCIA) phase evaluates the potential environmental performance related to functional units using LCI results. In this phase, LCI data are associated with environmental impact categories and provide information for the interpretation phase. LCIA is coordinated with other LCA phases and considers the system boundary, LCI data quality, availability of LCI results, and sufficiency of the results to conduct LCIA in conformity with the goal and scope definition (ISO 14044, 2007). The LCIA is limited to environmental issues specified in the goal and scope and comprises obligatory and optional elements (ISO 14040, 2006). The obligatory elements shown in Figure 3.1 include the selection of impact categories, category indicators, characterisation models, assigning LCI results to selected impact categories (classification), and category indicator result calculation (characterisation) (ISO 14044, 2007). The optional elements of LCIA include normalisation and weighting. Normalisation involves calculating the magnitude of the category indicator results relative to the reference information. It can be used to check for inconsistencies and provide information on the relative significance of the indicator results. Normalisation is also required for weighting. Weighting involves converting and possibly aggregating indicator results across impact categories using numerical factors based on value choices (ISO 14044, 2007).

The interpretation phase is where the findings from LCI and LCIA are discussed. The interpretation phase should be consistent with the goal and scope definition, signify potential environmental impacts, identify and evaluate significant issues and their sensitivity to the overall LCA results (ISO 14040, 2006). When identifying significant issues in the interpretation phase, first, the main contributors to the LCIA results regarding the most relevant life cycle phases, processes, or impact categories are determined through contribution analysis. Contribution analysis is a method commonly employed to break down the total LCIA results of a study into individual contributions by quantifying how much a process, phase, or impact category contributes to the total results. This helps in identifying the most significant contributing processes and the elementary flows of a product system. Contribution analysis can be used to identify the need for additional data collection, especially for the most contributing processes, and can also be used for product improvement. Second, some choices made during LCA, such as methodological choices and assumptions, can potentially influence the accuracy of the overall LCA results. Thus,

sensitivity analysis is performed to identify uncertainties of relevant issues among inventory data, impact assessment data, and methodological assumptions and choices to assess their reliability and analyse their sensitivity to the overall LCA results (EC-JRC, 2010).

3.1.1 Environmental impact categories and assessment

The LCIA phase evaluates potential environmental performance through the characterisation of elementary flows through a sequence of causally related impacts to areas of protection (AoPs). LCIA indicators can be categorised into two levels: midpoint and endpoint. Midpoint indicators concentrate on certain environmental problems, while endpoint indicators describe the final impact of environmental problems on the AoPs (EC-JRC, 2010). In LCA studies, impact categories should be selected to cover all environmental issues relevant to the accessed product system. The impact categories may differ depending on the applied impact assessment methodology. However, it is recommended by the International Reference Life Cycle Data System (ILCD) handbook for LCA studies that midpoint impact categories accessed in an LCA study should include human toxicity, radiation, carcinogens, respiratory inorganics, climate change, ozone layer, acidification, eutrophication, ecotoxicity, summer smog, land use, and resource depletion, while AoPs should include human health, natural environment, and natural resources (EC-JRC, 2010). This is illustrated in Figure 3.2. However, since the goal and scope definition of a study and LCI guide the assessment of potential environmental performance categories, there might be some restrictions in employing fully ILCD recommendations.

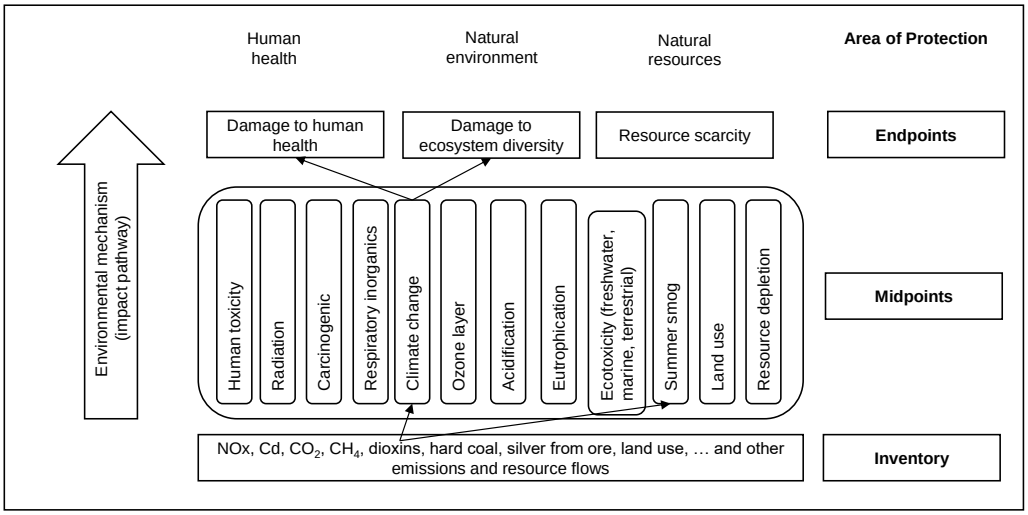

Figure 3.2: Schematic steps from inventory to category endpoints modified from EC-JRC (2010)

3.1.2 Data quality matrix

In this dissertation, the pedigree matrix shown in Table 3.1 was employed to assess the data quality of the LCI data based on five respective data quality indices: reliability, completeness, temporal correlation, geographical correlation, and further technological correlation. These indexes are arranged in order and scored based on five quality levels between 1 and 5, where 1 is excellent and 5 is poor.

Table 3.1: Pedigree matrix with data quality indicators to assess quality of data sources (Weidema et al., 2013)

Indicator score	**1** **Excellent**	**2** **Very good**	**3** **Good**	**4** **Fair**	**5** **Poor**
Reliability	Verified data based on measurements	Verified data partly based on assumptions or non-verified data based on measurements	Non-verified data partly based on qualified estimates	Qualified estimate (e.g., by industrial ex-pert)	Non-qualified estimate
Completeness	Representative data from all sites relevant for the market considered, over an adequate period to even out normal fluctuations	Representative data from >50% of the sites relevant for the market considered, over an adequate period to even out normal fluctuations	Representative data from only some sites (<50%) relevant for the market considered or >50% of sites but from shorter periods	Representative data from only one site relevant for the market considered or some sites but from shorter periods	Representativeness unknown or data from a small number of sites ***and*** from shorter periods
Temporal correlation	Less than 3 years of difference to the dataset period	Less than 6 years of difference to the dataset period	Less than 10 years of difference to the dataset period	Less than 15 years of difference to the dataset period	Age of data unknown or more than 15 years difference to the dataset period
Geographical correlation	Data from area under study	Average data from larger area in which the area under study is included	Data from area with similar production conditions	Data from area with slightly similar production conditions	Data from unknown ***or*** distinctly different area (North America instead of Middle East, OECD-Europe instead of Russia)
Further technological correlation	Data from enterprises, processes and mate-rials under study	Data from processes and materials under study (i.e., identical	Data from processes and materials under study but from	Data on related processes or materials	Data on related processes on laboratory scale ***or*** from different technology

	technology) but from different enterprises	different technology

3.2 Geopolymer binder and fibre reinforced geopolymer composites

3.2.1 Description of study

The environmental performance of geopolymer binder mix design (Publication I) and FRGC mix design (Publication II) were the objects of focus. Publications I and II were the basis of the study for the dissertation, where the key contributing materials to the environmental performance of geopolymers were determined. The results obtained from these publications served as a foundation for Publication III and guided the development of geopolymer mix designs for Publication IV. The mix designs for Publication I were developed in the laboratory, while mix designs for Publication II were collected from the literature, and the environmental performance calculations for Publications I and II were guided by the LCA framework.

The materials used for the development of geopolymer mix design in Publication I include phosphate mine tailings, metakaolin, sodium silicate solution, and NaOH. The mine tailings used were Siilinjärvi phosphate mine tailings waste from Eastern Finland which consist of 65% phlogopite mica, including carbonates, silicates, and apatite. This mine tailings waste cannot be used directly for alkali activation owing to its poor chemical reactivity. Thus, the mine tailings were used with metakaolin, which is a more reactive material. The mine tailings were pre-treated by grinding before the alkali activation. The reference scenario used for comparison in Publication I is PC.

The materials used in the FRGC mix designs in Publication II include CFA, GBFS, NaOH pellets, sodium silicate solution, sand, gravel, steel fibre, glass fibre, and polypropylene fibre. The reference scenario used for comparison in Publication II was PC concrete and steel fibre reinforced PC concrete. Alternative scenarios include different mix designs for steel, glass, and polypropylene FRGCs.

3.2.2 Goal, functional unit, and impact categories

The objective of Publication I is to quantify the environmental performance of different geopolymer binder production from phosphate mine tailings and metakaolin in comparison to PC and identify the most contributing unit processes to their environmental impacts. The functional unit is defined as the environmental performance of 1 kg of geopolymer binder, and the activities involved during its production. For consistent interpretation of results, the functional unit is adapted to include compressive strength by calculating the ratio of each environmental impact category to compressive strength (MPa) (Vieira et al., 2018).

The objective of Publication II is to quantify the environmental performances of different FRGC mix designs in comparison to PC concrete and steel fibre reinforced PC concrete, while also identifying the most contributing unit processes to aid the future development of geopolymers. The functional unit for Publication II is defined as the environmental performance of 1 m^3 of concrete and the activities involved in its production.

The LCAs for Publication I and II were performed with GaBi software (version 8.6.0.20) using the CML 2010 (version 2016) impact assessment method. The environmental impact categories assessed in Publications I and II are detailed in Table 3.2. The impact categories in Publication I are based on associated environmental issues and emissions generated during binder production such as raw material and energy consumption, fuel handling and storage which can be a potential source of soil and groundwater contamination (Chen et al., 2010a; Stajanca and Estokova, 2012).

Table 3.2: Impact categories assessed for the environmental performance in Publication I and II

Area of protection	**HUMAN HEALTH**				**NATURAL ENVIRONMENT**					**NATURAL RESOURCE**
Impact category	GWP	ODP	HTP	POCP	AP	EP	FAETP	MAETP	TETP	ADP_FF
Publication I	✓				✓	✓				✓
Publication II	✓	✓	✓	✓	✓	✓	✓	✓	✓	✓

Global warming potential (GWP 100 years), ozone layer depletion potential (ODP), acidification potential (AP), eutrophication potential (EP), abiotic depletion potential for fossil fuel (ADP_FF), freshwater aquatic ecotoxicity potential (FAETP), human toxicity potential (HTP), marine aquatic ecotoxicity potential (MAETP), photochemical ozone creation potential (POCP), and terrestrial ecotoxicity potential (TETP).

3.2.3 System boundary and scenarios

The LCAs of Publication I and II is limited to the production stage “cradle-to-gate”, and the processes contained in the system boundary are raw material extraction, pre-treatment of waste materials, mixing of constituents, and energy consumption. The use and end-of-life phases are excluded from the system boundary based on the assumption that equivalent impacts are expected from these phases. Heat curing was included in the calculation of the environmental performance of the geopolymer according to the production method reported in the literature. Transportation was omitted because similar distances were assumed for the raw materials. The omitted phases were outside the system boundary, as shown in Figure 3.3, and details of the acronyms used in the figure can be found under Table 3.3.

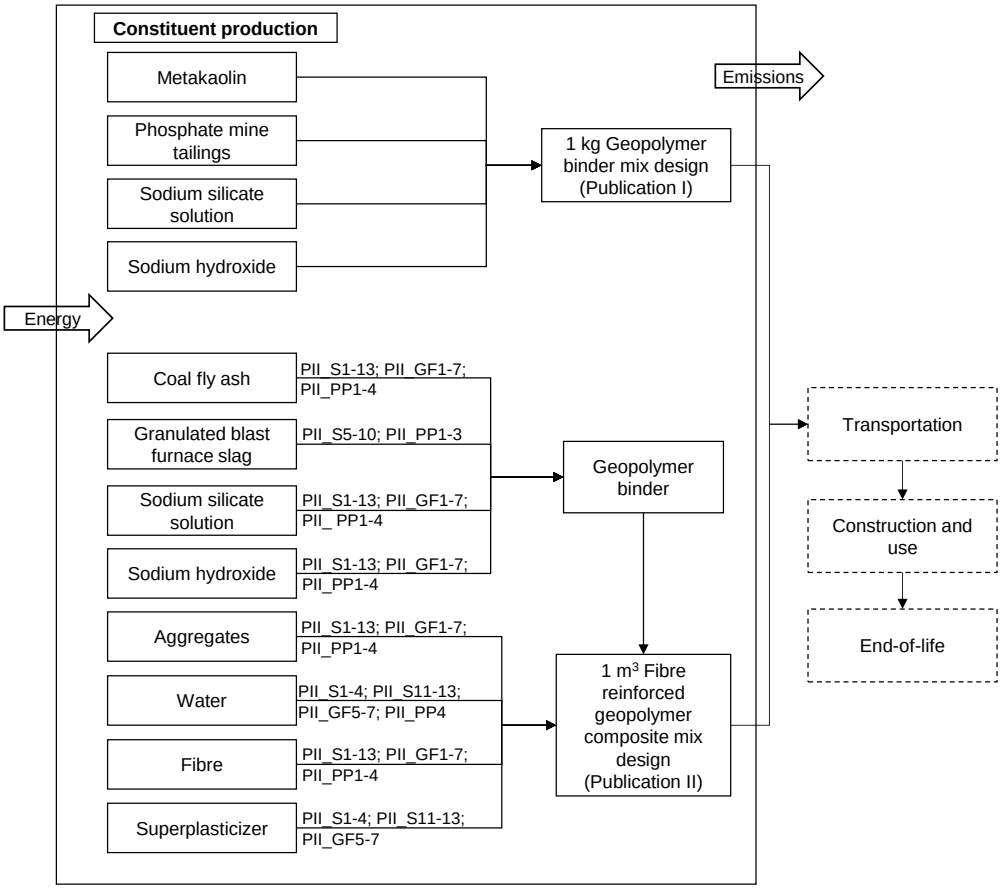

Figure 3.3: System boundary for Publication I and II

The scenarios representing the different mix designs for Publications I and II are shown in Table 3.3. In publication I, the content of metakaolin decreases from 100 g to 0 g and vice versa for phosphate mine tailings. The content of alkali activator remains constant while water content varies between 24 g and 47 g. The scenarios in Publication II are grouped according to reference scenarios and type of fibre reinforcement. Subsequently, the most environmentally optimal mix designs for the respective groups are further analysed.

Table 3.3: Mix designs for geopolymer binder mix design (Publication I) and Fibre reinforced geopolymer composite (Publication II)

	PC	CFA	GBFS	MK	MT	NaOH	Na_2SiO_3	Sand	Gravel	SP	H_2O	Fibre	MPa
Geopolymer binder mix design (g) – Publication I													
PI_PM0/10				100	0	22	33				47		2
PI_PM1/9				90	10	22	33				47		2
PI_PM2/8				80	20	22	33				47		3

PI_PM3/7			70	30	22	33				40		2
PI_PM4/6			60	40	22	33				40		10
PI_PM5/5			50	50	22	33				40		11
PI_PM6/4			40	60	22	33				40		13
PI_PM7/3			30	70	22	33				40		21
PI_PM8/2			20	80	22	33				24		12
PI_PM9/1			10	90	22	33				24		2
PI_PM10/0			0	100	22	33				47		2
Fibre reinforced geopolymer composite mix designs (kg/m^3) – Publication II												
Reference scenarios												
PII_PCC	360						598	1266		192		35
PII_SFRPCC	360						598	1266	4	192	39[s]	39
Alternative scenarios												
Steel fibre reinforced geopolymer composite												
PII_S1		408			16	103	600	1248	10	16	19[s]	38
PII_S2		408			16	103	600	1248	14	16	39[s]	41
PII_S3		408			16	103	600	1248	14	18	58[s]	42
PII_S4		408			16	103	600	1248	16	18	78[s]	43
PII_S5		412	276		57	294	1100[ss]				78[s]	74
PII_S6		412	276		57	294	1100[ss]				117[s]	74
PII_S7		412	276		57	294	1100[ss]				156[s]	82
PII_S8		450	60		24	175	1237[ss]				31[s]	61
PII_S9		450	60		24	175	1237[ss]				63[s]	62
PII_S10		450	60		24	175	1237[ss]				94[s]	62
PII_S11	39	355			14	101	554	1293	12	55	20[s]	42
PII_S12	39	355			14	101	554	1293	12	55	39[s]	43
PII_S13	39	355			14	101	554	1293	12	55	59[s]	47
Glass fibre reinforced geopolymer composite												
PII_GF1		400			18	143	540	1260			13[g]	66
PII_GF2		400			18	143	540	1260			20[g]	60
PII_GF3		400			18	143	540	1260			26[g]	54
PII_GF4		400			18	143	540	1260			33[g]	70
PII_GF5	39	355			14	101	554	1293	12	55	0.27[g]	36
PII_GF6	39	355			14	101	554	1293	12	55	0.54[g]	32
PII_GF7	39	355			14	101	554	1293	12	55	0.80[g]	41
Polypropylene fibre reinforced geopolymer composite												
PII_PP1		450	60		24	175	1237[ss]				4[p]	61
PII_PP2		450	60		24	175	1237[ss]				7[p]	60
PII_PP3		450	60		24	175	1237[ss]				11[p]	60
PII_PP4		369			21	132	581	1171		32	14[p]	39

PI – Publication I, PII – Publication II, [s] steel fibre; [g] glass fibre; [p] polypropylene fibre; [ss] silica sand; H_2O – water; CFA – Coal fly ash; GBFS – granulated blast furnace slag; MK – Metakaolin; MT – Mine tailings; Na_2SiO_3 – sodium silicate; NaOH – sodium hydroxide; PCC – Portland cement concrete; SFRPCC – steel fibre reinforced Portland cement concrete; SP – Superplasticizer; SS – Silica sand; Reference for PCC, SFRPCC, S1 to 4 - Ganesan et al. (2015); Reference for S5 to 7 - Khan et al. (2018); Reference for S8 to 10, PP1 to 3 - Al-mashhadani et al. (2018); Reference for S11 to 13 - Vijai et al. (2012a); Reference for

GF1 to 4 - Nematollahi et al. (2014); Reference for GF6 to GF7 Vijai et al. (2012b); Reference for PP4 - Patil and Patil (2015).

3.2.4 Life cycle inventory

The LCI data used were gathered from local sources and academic literature. To conduct LCA modelling, some unit processes were readily available in the GaBi database, while others had to be created and modelled. The unit processes sourced from the GaBi database include PC, sand, gravel, silica sand, electricity, water, NaOH, glass fibre, and polypropylene fibre. The unit processes unavailable in the GaBi database were modelled based on information from the literature.

The unit process of the sodium silicate solution was modelled following the approach and LCI data from Fawer et al. (1999) as detailed in section 2.2.1 and presented in Figure 3.4. In Publication I, sodium silicate solution with a weight ratio of 3.3, was used in the geopolymer binder, while in Publication II, sodium silicate with a weight ratio of 2.0, was used in the mix designs (Fawer et al., 1999). The phosphate mine tailings unit process was modelled as shown in Figure 3.5, based on the energy needed to grind the tailings in the laboratory, which is 1.25 MJ/kg. The kaolin unit process was available in the GaBi database; however, metakaolin requires calcination. The metakaolin unit process was modelled as shown in Figure 3.6 by including kaolin calcination energy, which is 2.5 MJ/kg of natural gas (Heath et al., 2014; NLK, 2002). The emission inventory data for CFA process was collected from Kawai et al. (2005) and is detailed in Figure 3.7. GGBFS process was modelled according to the data provided by Marceau and VanGeem (2003) for the granulation, drying, crushing, and grinding processes, and this is shown in Figure 3.8. The steel fibre unit process was unavailable in the GaBi database when this study was carried out, so the steel fibre process was modelled based on steel sheet stamping and bending unit processes. Steel sheet stamping and bending are part of the production process for making steel metal parts and were a viable alternative to represent the steel fibre process because they have similar input materials. The unit process for the superplasticizer was modelled according to data from the Environmental Product Declaration (EPD) of the European Federation of Concrete Admixtures Associations Ltd. (EFCA). The system boundary of the superplasticizer was at the production stage (EFCA, 2015). In Publication I, oven curing was required during geopolymer binder production, and the energy consumed was 1.87 MJ/kg at 40 °C for 24 h, while the energy for mixing mix designs was 0.0045 MJ/kg. In Publication II, heat curing was included in the calculations according to the literature requirement during geopolymer composite development, and the energy consumed was estimated to be 2.12 MJ/MPa (Bai et al., 2014). The synthesis conditions for geopolymers were mainly laboratory scale. Thus, energy consumption would most likely be lower when full-scale commercially tested technology is used. To ensure the quality of data interpretation, the LCI data were transferred to GaBi 8.6.0.20.

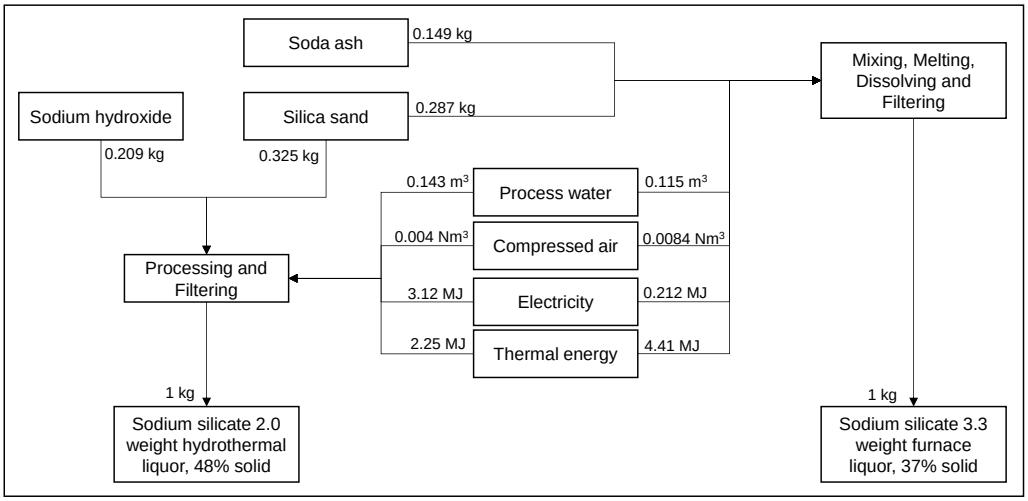

Figure 3.4: Material flow chart to produce sodium silicate hydrothermal and furnace liquor modified from Fawer et al. (1999).

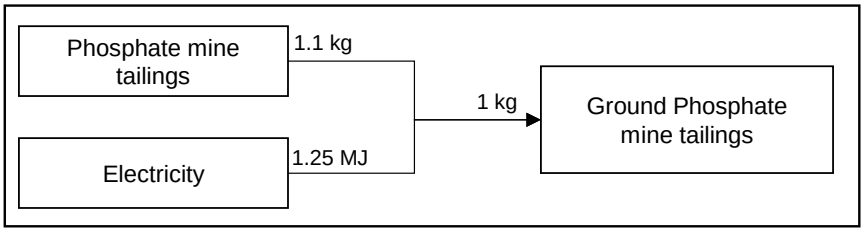

Figure 3.5: Material flow chart of ground of phosphate mine tailings.

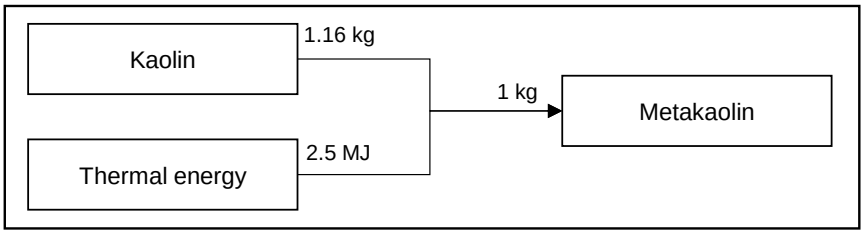

Figure 3.6: Material flow chart for calcination of kaolin to produce metakaolin

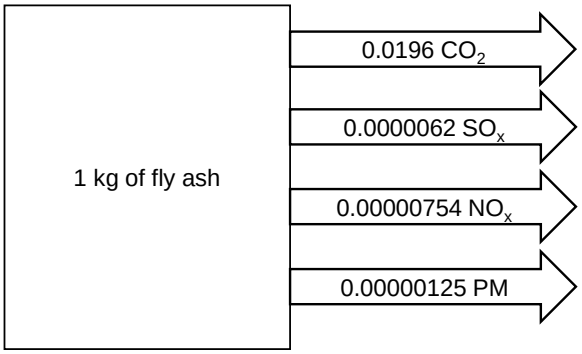

Figure 3.7: Emission inventory data for coal fly ash (Kawai et al., 2005).

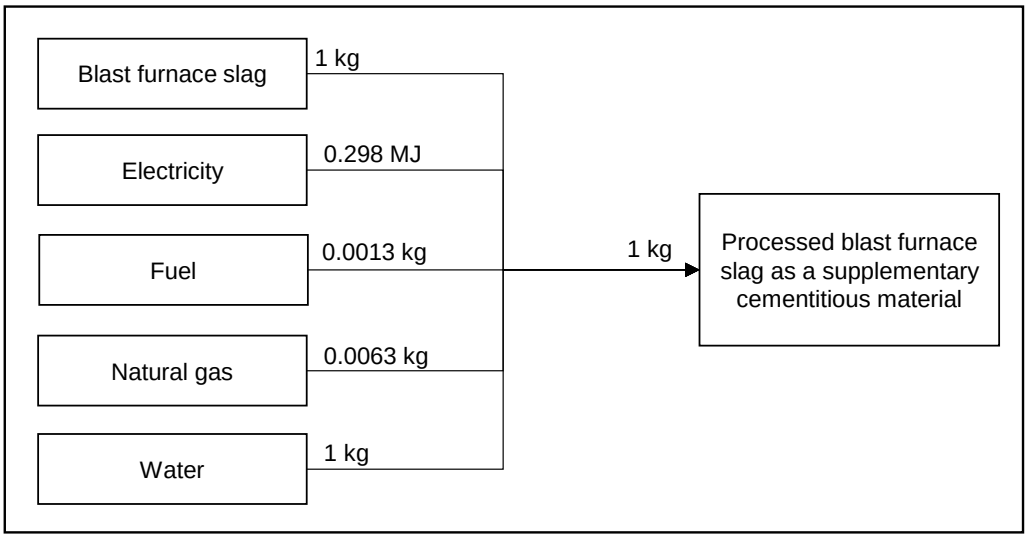

Figure 3.8: Material flow chart for the processing of GGBFS as a supplementary cementitious material.

The geographical scope of this study was Finland; therefore, the Finnish dataset was used when available. However, when data were unavailable, EU-28 datasets were used. The LCI sources for the different material inputs are summarised in Table 3.4.The data quality indexes were obtained from the dataset documentation and the local data were estimated according to the data quality matrix detailed in section 3.1.2.

Table 3.4: Data sources and quality index of LCI dataset for Publication I and II.

Type of data	Source	Description of process	Data quality index (Pedigree matrix)
Polypropylene fibre	GaBi database 2018	EU28: Polypropylene fibre	(3,3,2,4,2)
Steel fibre	GaBi database 2018	Steel sheet stamping and bending	(3,3,2,2,2)
Glass fibre	GaBi database 2018	Glass fibre	(3,3,2,3,3)
Sodium hydroxide	GaBi database 2018	Sodium hydroxide, 100% caustic soda	(3,3,2,2,2)
Sodium silicate	Fawer et al. (1999)	Sodium silicate 2.0, hydrothermal liquor, 48% solid	(2,2,5,1,1)
Sodium silicate	Fawer et al, (1999)	Sodium silicate 3.3, Furnace route, 37% solid	(2,2,5,1,1)
Portland cement	GaBi database 2018	Cement (CEM I) (Publication II)	(3,3,4,4,5)
Portland cement	CEMBUREAU, 2015	CEM I (Publication I)	(1,2,1,1,1)
Sand	GaBi database 2018	Sand 0/2	(3,3,4,3,4)
Gravel	GaBi database 2018	Gravel 2/32	(3,3,2,4,3)
Silica sand	GaBi database 2018	Excavation and processing	(3,3,2,2,2)
Superplasticizer	EFCA, 2015	Superplasticiser	(1,2,1,1,1)
Water	GaBi database 2018	EU-28: Tap water	(3,3,4,4,3)
Electricity	GaBi database 2018	FI: Electricity grid mix	(3,3,4,3,4)
Coal fly ash	Fatec (2020)	Coal fly ash pre-treatment	(1,2,1,1,1)
GGBFS	Marceau and VanGeem (2003)	GGBFS beneficiation	(2,3,5,4,1)
Mine tailings	Laboratory data	Grinding of tailings	(1,2,1,1,1)
Metakaolin	GaBi database 2018, Heath et al. (2014), NLK (2002)	Kaolin Calcination	(3,3,2,3,3)

3.2.5 Sensitivity analysis

From the contribution analysis, sodium silicate was identified to be the major contributor to the geopolymer binder mix designs in Publication I and FRGCs mix designs in Publication II. Sensitivity analysis of sodium silicate was conducted by employing alternative LCI data for sodium silicate to determine its influence on the environmental performance results. The initial LCI data used for sodium silicate in modelling and calculating the environmental performance results were from Fawer et al. (1999), and the energy used in this sodium silicate production was primarily fossil fuels; thus, it is denoted as *Fawer_FF*. The alternative LCI data employed for the sensitivity analysis include: 1) substituting fossil fuel with biogas renewable energy in the sodium silicate production method by Fawer et al. (1999), denoted as *Fawer_RE*; 2) LCI data for sodium silicate production from the best available techniques for the manufacture of large-volume inorganic chemicals (EU, 2007), denoted as *BAT*; and 3) LCI data from the Ecoinvent database, denoted as *Ecoinvent*. These different LCI data for sodium silicate solution production can be found in Table 3.5.

Table 3.5: Process data of the hydrothermal process to produce 2.0 weight ratio sodium silicate liquor 48% solid content.

Inputs per tonne of sodium silicate solution	***Fawer_FF*** **(Fawer et al., 1999)**	***Fawer_RE*** **(Fawer et al., 1999)**	***BAT*** **(EU, 2007)**	***Ecoinvent*** **(Ecoinvent database)**
Raw materials				
Silica sand	325 kg	325 kg	337 kg	676 kg
Sodium hydroxide	209 kg	209 kg	209 kg	435 kg
Auxiliary materials				
Water (steam production)	143 m^3	143 m^3	155 kg	297 kg
Compressed air	4 Nm^3	4 Nm^3		
Additives	0.7 kg	0.7 kg	0.7 kg	
Water consumption				
Process, cooling and washing water			0.77 m^3	0.88 m^3
Energy				
Process energy	5227 MJ	5227 MJ*	589 MJ	906 MJ
Fuel production and delivery	144 MJ	144 MJ	184 MJ	
Total energy consumption	5371 MJ	5371 MJ	773 MJ	906 MJ

* biogas renewable energy

3.3 Waste-derived alkali-silicates for geopolymer mortar

3.3.1 Description of study

Results from Publications I and II demonstrated that the environmental performance of geopolymer materials is highly dependent on the alkali activator (mainly sodium silicate). Sodium silicate is a major contributor to the geopolymer binder and FRGCs with respect to GWP, AP, and ADP (Abdulkareem et al., 2019a; Habert et al., 2011; McGuire et al., 2011). This is mainly because of the high energy required during the production of sodium silicate, as discussed in Section 2.2.1. Improving the environmental performance of geopolymers requires improvements in the development of sodium silicate by exploring alternative production methods from other silica-rich waste materials such as RHA (Tchakouté et al., 2016; Tong et al., 2018) and glass waste (Vinai and Soutsos, 2019). However, most studies on alternative production of alkali-silicates from wastes have focused on the mechanical properties of these waste-derived activated geopolymers and not on their environmental performance. As a result, the results from Publications I and II created the focus of Publication III, which assessed the environmental performance of geopolymer mortars from waste-derived (RHA and glass waste) alkali activated geopolymers in comparison to geopolymers from conventional alkali-silicate.

The production of alkali-silicate from RHA was modelled according to the study by Tong et al. (2018). RHA-derived silicate was produced through the hydrothermal method by milling RHA for 15 min to produce a fine powder which was subsequently dissolved in NaOH solution. This mixture was heated and stirred continuously at 80 °C for 3 h to produce an aqueous solution (two-part mix) with the following composition: NaOH (8.7%), RHA (24%), and water (67.3%). The process is shown in Figure 3.11. Subsequently, an RHA activated geopolymer mortar was produced by blending RHA-derived alkali-silicate, CFA, GBFS, and sand. The mortar was then cured at room temperature.

The production of alkali-silicate from glass waste was modelled according to Vinai and Soutsos (2019). Glass waste was produced through fusion by milling glass waste for 10 min and heating with NaOH powder at 150 °C for 1h to produce a powder activator (one-part mix) with the following composition: NaOH (52%) and glass waste (48%). This process is shown in Figure 3.12. Subsequently, a glass waste-activated geopolymer mortar was produced by mixing glass waste-derived alkali-silicate, CFA, GBFS, and sand. The mortar was then cured at room temperature.

3.3.2 Goal, functional unit, and impact categories

The goal of Publication III is to quantify the potential to improve the environmental performance of one- and two-part geopolymers by utilising chemically modified waste-derived alkali-silicate instead of conventional alkali-silicate. The functional unit is defined as the environmental performance of 1 m^3 geopolymer mortar production with

compressive strengths between 52 and 60 MPa at 28 days. Similar functions and service life were assumed for the assessed scenarios due to similarity in their compressive strengths. The environmental impact categories employed were GWP, AP, ADP_FF, and POCP. These impact categories were chosen based on the major environmental issues associated with PC production (Chen et al., 2010b; Van Den Heede and De Belie, 2012). GaBi 9.1.0.53 software and ReCiPe 2016 v1.1 (midpoint hierarchist timeframe) were used for the environmental performance modelling and impact assessment methods, respectively.

3.3.3 System boundary and scenarios

The system boundary utilised for Publication III is cradle-to-gate and includes raw material production, pre-treatment of waste, mixing of constituents, and energy consumption. Transportation, use phase, and end-of-life phase were excluded from the system boundary as comparable and similar impacts were expected from these phases. The system boundary is illustrated in Figure 3.9.

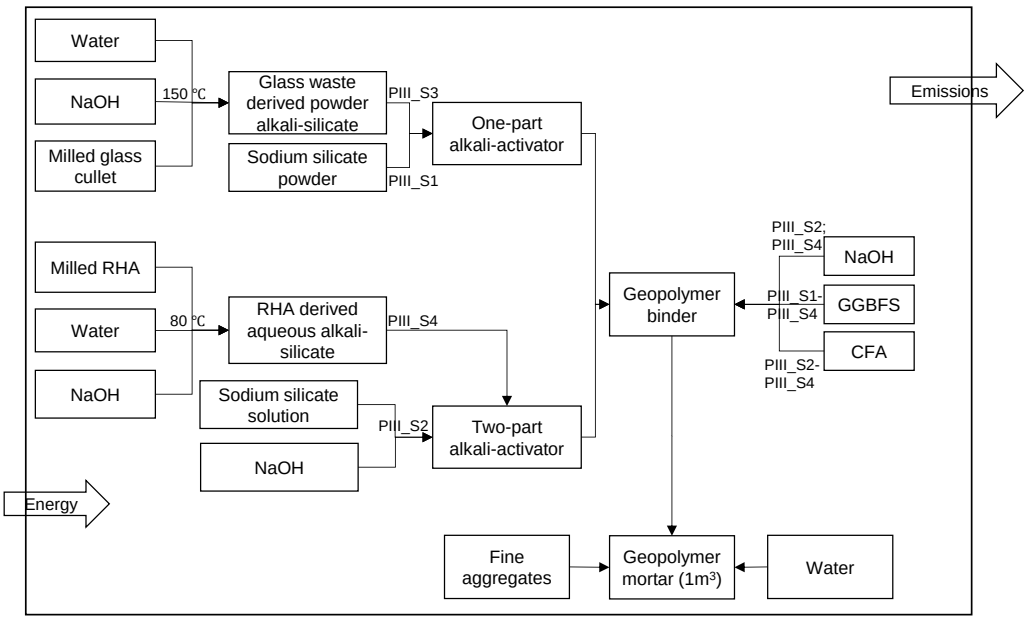

Figure 3.9: System boundary for Publication III

The four scenarios considered in Publication III are as follows.

- PIII_S1 – one-part geopolymer mortar from conventional sodium silicate powder.

- PIII_S2 – two-part geopolymer mortar from conventional aqueous sodium silicate solution.
- PIII_S3 – one-part geopolymer mortar from powder glass-waste-derived alkali-silicate.
- PIII_S4 – two-part geopolymer mortar from aqueous RHA-derived alkali-silicate.

PIII_S1 and PIII_S2 are both reference scenarios. PIII_S1 represents a one-part geopolymer mortar activated using conventional sodium silicate powder, while PIII_S2 represents a two-part geopolymer mortar with aqueous sodium silicate solution and NaOH as activators. PIII_S3 and PIII_S4 are the alternative scenarios considered. PIII_S3 is a one-part geopolymer mortar produced using a chemically modified glass waste powder activator. PIII_S4 represents a two-part geopolymer mortar from a chemically modified RHA aqueous activator. The synthesis conditions for the geopolymers were defined at the laboratory scale. All mortars were cured at room temperature; hence, the energy required for heat curing was avoided. The selected scenarios represent geopolymer mortars with comparable compressive strengths. These scenarios were collected from the literature. Similarities in the system boundaries and quantities of constituents were taken into consideration for consistency during comparison. The scenarios were limited to four because at the time this study was undertaken, there was limited information on waste-derived alkali-activated geopolymers with a strength range within the scope of Publication III. Table 3.6 illustrates the geopolymer mortar mix designs.

Table 3.6: Mix designs for geopolymer mortar scenarios considered in Publication III.

Constituent (kg/m^3)	**PIII_S1** **52 MPa [1]**	**PIII_S2** **58 MPa [2]**	**PIII_S3** **58 MPa [3]**	**PIII_S4** **60 MPa [2]**
Coal fly ash	0	321	313	326
GBFS	373	214	208	217
Sand	1445	1471	1432	1493
Glass-waste-derived activator	0	0	126	0
RHA-derived activator	0	0	0	196
Sodium silicate	109[a]	157[b]	0	0
NaOH pellets	0	26	0	36
Water	241	131	231	99

[1] Yang et al. (2010) [2] Tong et al. (2018); [3] Vinai and Soutsos (2019); [a] sodium silicate powder; [b]sodium silicate solution; WG: waste glass; RHA: rice husk ash

3.3.4 Life cycle inventory

Unit processes for NaOH, sand, electricity, and water were sourced from the GaBi database, while unit processes for sodium silicate solution (Figure 3.4) and sodium silicate powder (Figure 3.10) were sourced from the Ecoinvent 3.4 database. The emission inventory data for CFA was sourced from literature (Kawai et al., 2005) as shown in Figure 3.7. The treatment GGBFS, RHA, and glass waste unit processes was modelled based on literature studies.

Glass waste, RHA, CFA, and GGBFS were considered wastes in Publication III and allocated no environmental burdens from previous processes. Thus, only the environmental impacts during the grinding and treatment of these wastes were considered. RHA-derived aqueous activator processes as shown in Figure 3.11 comprise electricity for milling RHA at 0.04 MJ/kg and 0.74 MJ/kg of electricity to dissolve RHA in NaOH. However, this estimation is more than the actual energy needed for simplification in the analysis (Tong et al., 2018). Glass waste-derived powdered activator as shown in Figure 3.12 comprise electricity for milling glass at 0.18 MJ/kg and 0.072 MJ/kg of electricity required to heat glass powder with NaOH (Vinai and Soutsos, 2019). The GGBFS process was modelled according to the data provided by Marceau and VanGeem (2003) for the granulation, drying, crushing, and grinding processes as shown in Figure 3.8. The synthesis conditions for the geopolymer mortars were defined at the laboratory scale. Even though capital goods can have a significant influence on the total LCA results (Liikanen et al., 2017), the capital goods of trucks, equipment, and buildings were outside the scope of Publication III. Table 3.7 shows the LCI data sources for the different processes for the geopolymer mortar in Publication III. The data quality indexes were obtained from the dataset documentation and the local data were estimated according to the data quality matrix detailed in section 3.1.2.

Table 3.7: Data sources and quality index of LCI dataset for Publication III

Type of data	Source	Description of process	Data quality index (Pedigree matrix)
Sodium hydroxide	GaBi database 2019	EU-28: Sodium hydroxide (caustic soda mix, 100%)	(3,3,2,2,2)
Sodium silicate solution	Ecoinvent 3.4 database	EU-28: Sodium silicate production, hydrothermal liquor, product in 48% solution state	(2,2,5,1,1)
Sodium silicate powder	Ecoinvent 3.4 database	EU-28: Sodium silicate production, spray powder, 80%	(2,2,5,1,1)
Sand	GaBi database 2019	EU-28: Sand 0/2	(3,3,4,3,4)
Water	GaBi database 2019	EU-28: tap water	(3,3,4,4,3)

Electricity	GaBi database 2019	FI: electricity grid mix	(3,3,4,3,4)
Coal fly ash	Fatec (2020)	Coal fly ash pre-treatment	(1,2,1,1,1)
GGBFS	Marceau and VanGeem (2003)	GBFS beneficiation	(2,3,5,4,1)
Glass-waste-derived activator	Vinai and Soutsos (2019)	Chemically modified glass waste activator	(2,4,1,3,1)
RHA-derived activator	Tong et al. (2018)	Chemically modified RHA activator	(2,4,2,3,1)

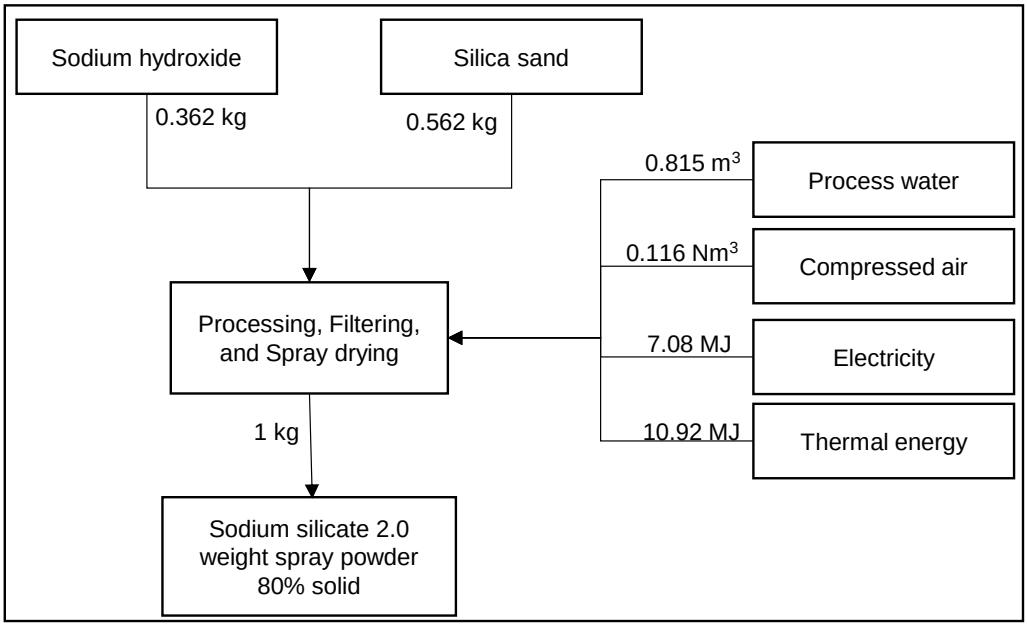

Figure 3.10: Material flow chart to produce sodium silicate spray powder modified from Fawer et al. (1999).

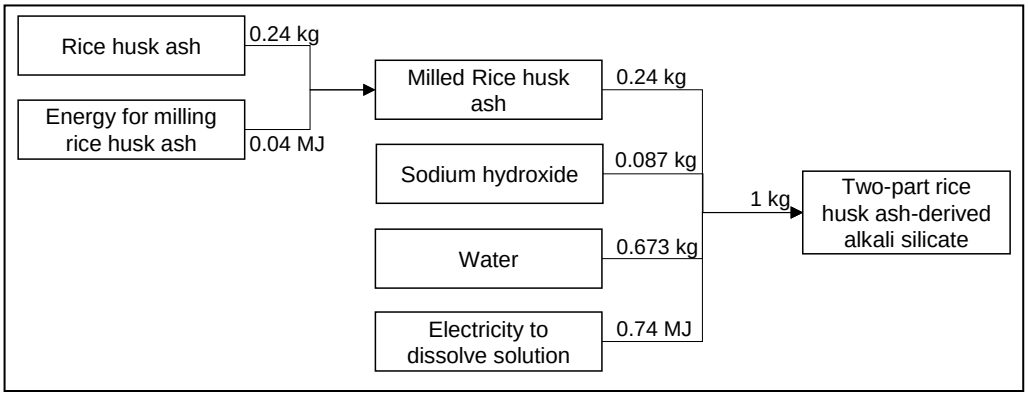

Figure 3.11: Material flow chart to produce aqueous rice husk ash-derived alkali-silicate

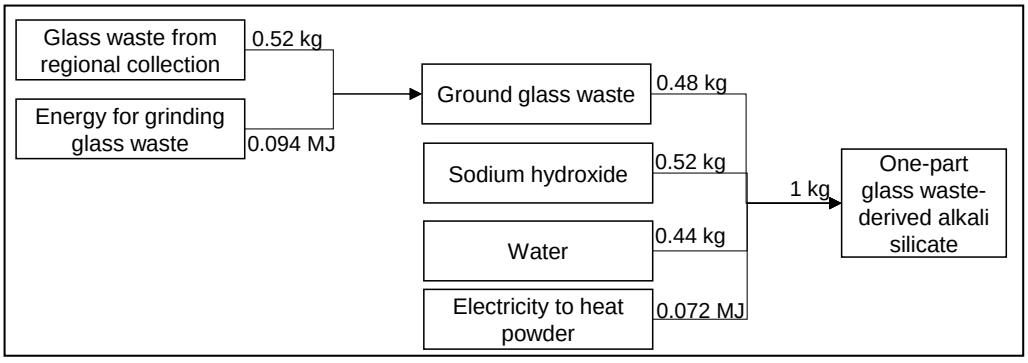

Figure 3.12: Material flow chart to produce powdered glass waste-derived alkali-silicate

3.3.5 **Sensitivity analysis**

Sensitivity analysis was conducted to determine the influence of different NaOH production methods on the environmental performance results obtained from the GaBi database. NaOH was not included in the geopolymerisation of PIII_S1; thus, a sensitivity analysis was conducted between PIII_S2, PIII_S3, and PIII_S4.

The initial NaOH production method used to determine the environmental performance of the geopolymer mortars was EU-28: 100% NaOH from chlorine-alkali electrolysis using a membrane, diaphragm, and amalgam technology mix and is depicted as *EU_NaOH*. This process includes the share of each technology in the mix. The differences between the three technologies lie in the separation technology. In mercury cell electrolysis, the cathode is a stream of mercury at the bottom of the cell. Sodium is reduced on mercury and immediately forms amalgam. The amalgam stream is fed into a converter, where it is mixed with water to form caustic soda and hydrogen and to regenerate the mercury cathode. There are multiple anodes made of graphite, in which

chloride ions are reformed into chlorine gas. Diaphragm cell electrolysis uses an asbestos diaphragm on an iron grid to separate the anode and cathode reaction chambers. The sodium chloride solution is led through the anode chamber through the diaphragm into the cathode chamber. This process uses less energy than the mercury cell process, but the products (caustic soda and chlorine) require extensive concentration and cleaning because they contain sodium chloride and oxygen. Thus, the overall energy consumption is slightly higher than that obtained using the mercury cell process. The membrane separates the reaction chambers and consists of modified polytetrafluoroethylene (Teflon), which is penetrable for sodium ions but not water molecules. The main advantages of this process are its energy efficiency, the purity of the product caustic soda (virtually free of chloride), and the fact that it does not involve dangerous substances such as asbestos or mercury. However, it does require a relatively pure salt as the input (Sphera, 2021).

The alternative NaOH production methods used for sensitivity analysis include RER (Europe) 100% NaOH from brine solution depicted as *RER_NaOH*, and DE (Germany) 100% NaOH using the technology mix as described above and denoted as *DE_NaOH*. While *DE_NaOH* represents German data, *EU_NaOH* represents the EU-28 data. In *RER_NaOH*, NaOH is a by-product of chlorine production by electrolysis, where an electric current is passed through a brine solution.

Additionally, in the initial calculations, RHA, GBFS, and CFA were assumed to have no allocated emissions from their main processes as they were considered waste materials and only emissions from the beneficiation processes were considered for the materials. Thus, sensitivity analysis was conducted to determine the effect of mass-based allocation on the environmental performance results. Also, glass cullet (treatment of glass waste from unsorted public collection) sourced from Ecoinvent database, was included for glass waste.

Mass allocation of RHA was calculated based on emissions from production of rice (non-basmati) sourced from the Ecoinvent database. As discussed in Section 2.2.3 when rice paddy is husked, 20% of rice husk is produced. Subsequently, 18-22% of the dry content by weight of RHA is produced from rice husks. Hence, 4% of the emissions were allocated to RHA from rice (non-basmati) production. Furthermore, mass allocation of GBFS and CFA were calculated based on emissions from pig iron production and electricity production from hard coal, respectively. Data from 2019 shows that 3.5 million tonnes of steel (which is a main product of pig iron) was produced in Finland (World Steel Association, 2020). Also, the world steel association estimated blast furnace slag to be 275 kg/tonne of crude steel. Thus 962 thousand tonnes of blast furnace slag production was estimated for 2019. Hence 22% of emissions are allocated to blast furnace slag as a by-product of pig iron production. This mass allocation correlates with GBFS mass allocation percentage found in literature studies between 19% and 20% (Chen et al., 2010c; Saade et al., 2015). Additionally, data from Finalnd in 2019 shows that 279 thousand tonnes of CFA was produced and 2.3 million tonnes of hard coal was consumed as fuel to generate electrcity. Thus, 10% of emissions are allocated to CFA from electricity produced form hard coal. This mass allocation also correlates with CFA mass

allocation emissions found in literature studies between 9% and 12% (Chen et al., 2010c; Seto et al., 2017).

The mass allocation is calculated using Equation 3.1, where C_m is the mass allocation coefficient and m is the mass of quantities. For instance in the case of CFA, the mass allocation C_m is calculated by dividing the mass of CFA produced by the sum of the mass of CFA produced and hard coal consumed as fuel to generate electricity. Additionally, to determine the environmental impacts of CFA and blast furnace slag, the secondary processes (grinding, granulation etc.) the material goes through are added to the allocated emissions from the primary process of production of the material. The environmental impacts for CFA, GGBFS, RHA and waste glass can be seen in Table 3.8.

$$C_m = m_{by\ product} \div (m_{by\ product} + m_{main\ product}) \quad (3.1)$$

Table 3.8: Environmental impact of glass cullet, rice husk ash, coal fly ash, and blast furnace slag.

	Global warming potential kg CO_2 eq.	**Abiotic depletion potential for fossil fuel** kg oil eq.	**Acidification potential** kg SO_2 eq.	**Photochemical ozone formation** kg NOx eq.
Glass cullet	0.0164	0.00292	0.0000295	0.0000394
Rice husk ash	0.0824	0.00612	0.0001968	0.0000764
GGBFS	0.3765	0.1332	0.0011	0.0010
Coal fly ash	0.1275	0.0367	0.0003	0.0002

GGBFS-ground granulated blast furnace slag

3.4 Geopolymer product case study – low-height noise barrier

3.4.1 Description of study

The results from Publications I and II guided the development of different geopolymer composite mix designs to produce a low-height noise barrier (LHNB), which is the object of focus in Publication IV. The main purpose of an LHNB is to reduce the noise generated during railway traffic. LHNBs are a type of noise barrier with a nominal height between 85 cm and 110 cm above the rail surface and are gradually becoming prevalent in railway tracks (Figure 3.13) (Vahtera, 2011). They can be designed using different materials, such as traditional concrete, steel and aluminium etc. (Bendtsen, 2010). Railway traffic noise has more sound energy at high frequencies, and its reduction is essential for a higher quality of life. LHNBs are situated close to the rail track to dampen the impact of the rolling noise from the rail-wheel collision, and their efficacy is determined by the insertion loss, which evaluates the sound pressure before and after incorporating the

LHNB (Valdebenito and Dahmen, 2013). LHNBs differ from regular noise barriers in terms of location, height, urban visibility, and construction costs. They do not obscure views from the train windows and have been built for testing purposes in Finland. Owing to changing track geometry, LHNB is designed on a case-by-case basis and must meet at least the Finnish A3 category for sound absorption which is 8-11 dB (Vahtera, 2011).

Figure 3.13: Low-height noise barrier (85 cm height) in trial use in Finland (Liikennevirasto, 2017)

Acoustic and non-acoustic performances of a LHNB can depreciate over the duration of its working life due to exposure to different environmental conditions and other factors. Due to this, the service life of a noise barrier can be defined as the duration it functions trouble-free with no visible change in insertion loss or appearance (Morgan et al., 2001). Desirable service life for PC concrete noise barrier is averagely 40 years (Environmental Protection Department Highways Department, 2003; Parker, 2006). On the other hand, there is limited information on service life estimation for geopolymer composite noise barriers. Amorim Júnior et al. (2021) investigated durability and service life of metakaolin-based geopolymer based on Fick's second diffusion law with respect to chloride penetration. The service life was estimated to be 12-13 years and 39-45 years, respectively, using the age influence coefficient 0.4 and 0.6. However, the author stated the service life prediction is used prospectively due to lack of good accuracy.

Arenas et al. (2017) investigated noise properties of fly ash-based geopolymers and found the sound absorption of fly ash-based geopolymers is similar to commercial products. The study highlighted that sound absorption coefficient is dependent on ratio of aggregates to binder and not on the type of binder, activating solution ratio, and/or aggregates so far, the size distribution of the aggregates is alike. The study further highlights that sound absorption of a material depends on the thickness of a specimen, and a 120 mm thickness of material is appropriate for road traffic noise barriers. The Finnish standard thickness for concrete noise barrier is at least 100 mm (Liikennevirasto, 2017).

Publication IV investigates the LCA of LHNBs developed from traditional concrete and geopolymer composites by either casting or additive manufacturing (AM). AM is a technology for building three-dimensional (3D) elements from a 3D computer-aided design model. The advantages of 3D fabrication include more flexibility, increased innovations, faster construction, risk mitigation, high material resource efficiency, and cost-effectiveness (Huang et al., 2017). 3D printing has the advantage of manufacturing customised products while maintaining similar performance and functions. However, the environmental performance of AM is still debated. While some consider AM as a sustainable solution because of the near-zero waste achieved during building, others consider AM to be wasteful, as it is reported to consume an estimated 100 times higher specific energy than traditional manufacturing (Liu et al., 2018; Výtisk et al., 2019).

To prepare the pilot-scale geopolymer composite LHNB, an activation reagent was prepared by weighing the solution reagents and then blending for a few minutes. The solution was left to dissolve completely and cooled. The dry ingredients were also weighed and mixed. Then, the activation reagent was poured into the dry mixture, stirred, and subsequently poured into moulds or in a 3D printer with continuous mixing. Air bubbles were removed using a vibrator after casting. The products were cured at room temperature for 7 days and shielded with a plastic film cover. Excess casting and other pieces were disposed with normal aggregate waste (APILA Group, 2020). This manufacturing method applies to all scenarios examined in Publication IV. These prototypes are predefined designs, and the objective is to analyse their environmental performance based on different materials, construction systems, compressive strengths, and service lives.

According to preliminary product requirements, LHNB must consist of two parts: a top of the barrier and foundation module (Vahtera, 2011). For the precast LHNB, the modules were cast indoors and then transported to the construction site. The height of each LHNB was 90 cm, and each was placed on a steel slab rising 10 cm above the ground surface, making the total height of the LHNB 1 m. The steel slab was not included in this study because it was the same for all scenarios. As shown in Figure 3.14, the weight of one module is 330 kg, and for a 20 m long LHNB, 45 modules were attached with stainless steel rebar welded to the caps screwed into the lifting anchors of the modules. The thickness of the casted LHNB is 150 mm which is a suitable thickness for the Finnish standard concrete thickness which is at least 100 mm for a noise barrier (Liikennevirasto,

2017). The specific mass of the LHNB scenarios is comparable with a safety marginal inclusive in the design.

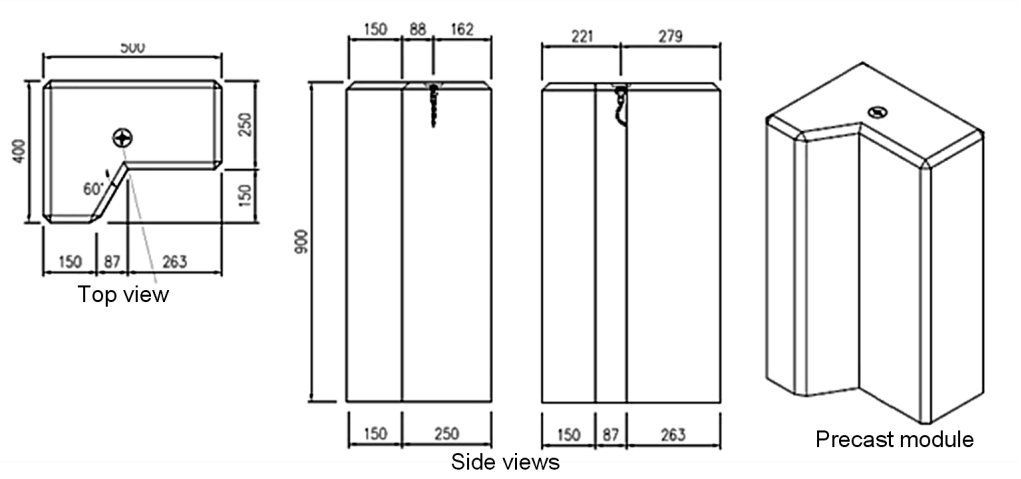

Figure 3.14: Pilot precast LHNB module for the UIR project (Concept design by Design Reform ltd, 2020)

For the AM LHNB, the modules were printed in a factory and transported to the site for assembly. The modules are hollow in structure, stacked, and laid next to each other, and filled with 58 litres of crushed aggregate per module. The weight and height of one module for the 3D printed LHNB is 57 kg and 45 cm, respectively. Two layers were used to reach a height of 90 cm, and each was placed on a steel slab rising 10 cm above the ground surface, making the total height of the barrier 1 m. For a 20 m long LHNB, 90 modules were used. The thickness of the AM LHNB is 295 mm which is also suitable for Finnish standard for noise barrier thickness as mentioned above. The visual details are shown in Figure 3.15.

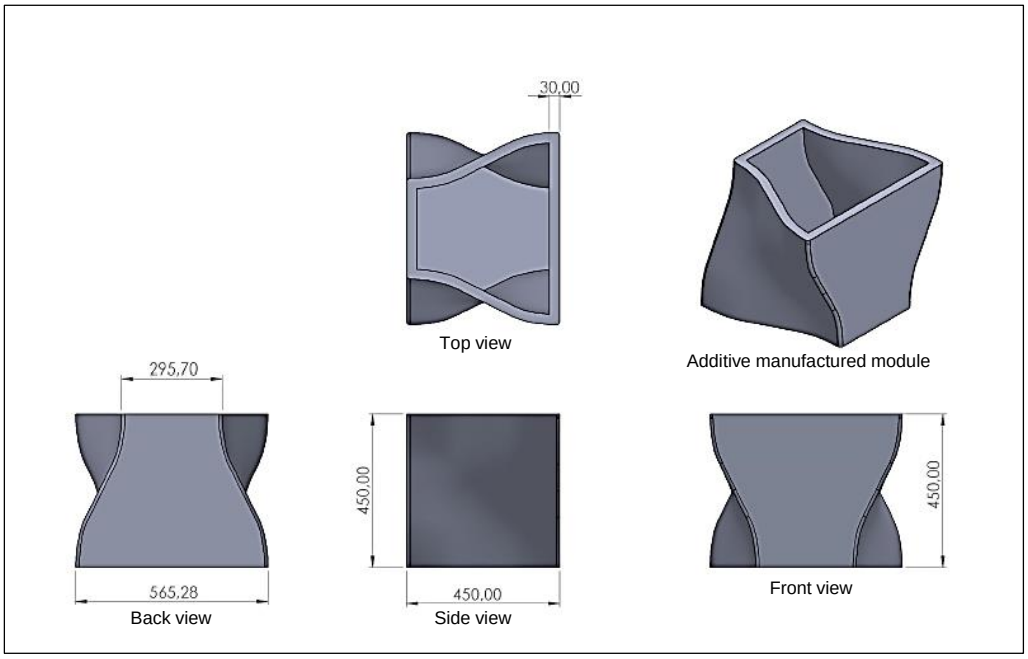

Figure 3.15: Pilot additive manufactured LHNB module for the UIR project (Concept design by Design Reform ltd, 2020).

3.4.2 **Goal, functional unit, and impact categories**

The goals of Publication IV are to quantify the environmental performance of an LHNB made from either PC concrete or geopolymer, identify hotspots, and evaluate the impact of product system changes on the environmental performance. The principal function of the pilot LHNB is to protect neighbouring residents from excessive noise produced by railway traffic. The functional unit is 20 m LHNB with 10 dB absorption capacity. The LHNB is situated in the railway track of the city of Lappeenranta in Finland, where it will be in full operation. Five different LHNB mix designs are analysed as will be discussed further in section 3.4.3. Although, the LHNBs have the same function, differences in mix designs will influence their durability and service life and this will further influence the effectiveness of their function. Also, there is limited studies on the parameters needed to calculate service life of the geopolymer composites. Thus, 40 years of service life is assumed for all scenarios in this paper. However, sensitivity analysis is conducted for service life (10-40 years) of the geopolymer LHNB scenarios. In this regard, the functional unit is adapted to include compressive strength and service life to yield a more consistent interpretation and assessment of results (Marinković et al., 2021; Vieira et al., 2018). This is achieved by applying two indicators. The first indicator is defined as the ratio of environmental impact category to 28 days compressive strength (MPa) of a 20 m long LHNB as shown in Equation 3.2. The second indicator is defined as the ratio of

environmental impact category to 28 days compressive strength (MPa) and service life (years) of a 20 m long LHNB as shown in Equation 3.3 (Müller et al., 2019; Vieira et al., 2018).

$$Indicator_1 = \frac{Environmental\ impact\ category}{Compressive\ strength{*}20m} \quad (3.2)$$

$$Indicator_2 = \frac{Environmental\ impact\ category}{Compressive\ strength{*}20m{*}years} \quad (3.3)$$

The impact categories chosen are similar to the major environmental issues associated with raw material and energy consumption, air, water, and land emissions during concrete production, including GWP, ADP_FF, POCP, and AP (Chen et al., 2010b; Kikuchi and Kuroda, 2011; Zhang et al., 2006). GaBi 9.2.0.58 and ReCiPe 2016 v1.1 (midpoint hierarchist timeframe) were used for the environmental performance and impact assessment methods, respectively.

3.4.3 System boundary and scenarios

The system boundary, as shown in Figure 3.16 comprise all life cycle stages from cradle to grave of a LHNB. Processes include raw material extraction, secondary materials, construction, transportation, and utilities (energy). The materials used to manufacture the LHNB include PC, water, alkali activator, precursors, and fine and coarse aggregates. Transportation of materials required for construction of the LHNB was included in the environmental performance analysis. When the LHNB depreciates and can no longer fulfil its function, the LHNB modules are demolished, crushed, and landfilled. Carbonation is also taken into consideration to determine potential CO_2 savings that can be achieved during the use and end-of-life phases. Capital equipment is excluded unless they are already incorporated into the unit processes of the background system. The primary data of the product system were provided by the developers (APILA Group, 2020) of the LHNB mix designs.

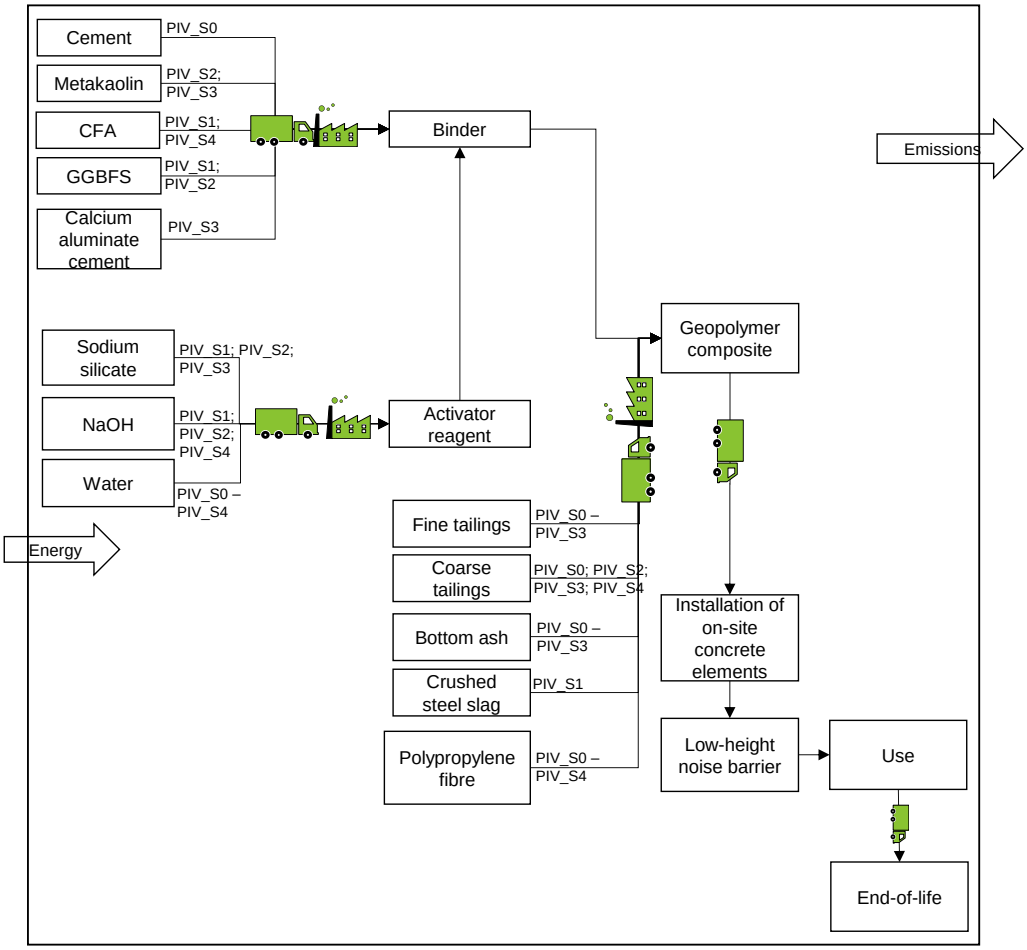

Figure 3.16: System boundary for Publication IV

Different mix-deigns in Publication IV were developed for precast and AM LHNB, as described in the five scenarios below.

- PIV_S0 – Precast PC concrete LHNB
- PIV_S1 – Precast geopolymer composite LHNB
- PIV_S2 – Precast geopolymer composite LHNB
- PIV_S3 – AM geopolymer composite LHNB
- PIV_S4 – AM geopolymer composite LHNB

PIV_S0 represents the reference scenario and uses a PC as a binder. PIV_S1 and PIV_S2 describe two different precast geopolymer composite mix designs, while PIV_S3 and PIV_S4 illustrate two different AM geopolymer composite mix designs, as summarised

in Table 3.9. The precursors used in PIV_S1 and PIV_S4 were mainly CFA and GGBFS, while the precursors for PIV_S2 combined GGBFS and metakaolin, and the precursor for PIV_S3 combined calcium aluminate cement and metakaolin. The fine aggregates were made up of fine tailings in all scenarios except PIV_S4, in which milled bio fly ash was used. Coarse tailings and bottom ash were used in PIV_S0, PIV_S2, and PIV_S3, respectively, as coarse aggregates, while PIV_S1 contained bottom ash and crushed steel slag. Other materials include water and polypropylene fibres. These scenarios show that there are significant proportions of local bio fly ashes, tailings, and steel slags in the mix designs.

Table 3.9: Mix designs for Publication IV (APILA Group, 2020)

Constituent	**PIV_S0** **32 MPa**	**PIV_S1** **20 MPa**	**PIV_S2** **25 MPa**	**PIV_S3** **29 MPa**	**PIV_S4** **13 MPa**
Portland cement	27%				
Calcium aluminate cement				4%	
Activator		10%	15%	19%	0.3%
Waste precursor (CFA and GBFS)		25%	4%		37%
Metakaolin			9%	13%	
Fine aggregates	9%	13%	19%	13%	17%
Coarse aggregates	52%	45%	48%	43%	30%
Water	12%	6%	4%	6%	16%
Polypropylene fibre	0.14%	0.14%	0.14%		

3.4.4 Life cycle inventory

The LCI unit processes for NaOH, polypropylene fibre, transportation, PC, electricity, and water were sourced from GaBi database. The LCI unit processes for sodium silicate solution (Figure 3.4) and calcium aluminate cement were sourced from the Ecoinvent 3.4 database and Environmental Product Declaration by Cimsa Cimento (CIMSA, 2015). The kaolin unit process is available in the GaBi database; however, metakaolin requires calcination. The metakaolin unit process (Figure 3.6) was created by including kaolin calcination energy which is 2.5 MJ/kg of natural gas (Heath et al., 2014; NLK, 2002). The GGBFS process was modelled according to the data provided by Marceau and VanGeem (2003) for the granulation, drying, crushing, and grinding processes (Figure 3.8). 0.11 MJ/kg was needed for pre-treatment of CFA from internal communication with Fatec (2020). The energy consumption for processing tailings and crushed steel slag was

0.011 MJ/kg and 0.063 MJ/kg, respectively, while the energy consumption for processing bio fly ash was 0.045 MJ/kg. These data were sourced from local companies. The electricity requirement for 3D printing was estimated to be 7 MJ/t (Jäppinen, 2017) while the data for precast was estimated to be 2.16 MJ/t (Tahvanainen, 2020). It is assumed that limited maintenance and repair activities are required during the use phase of the LHNB. Table 3.10 shows the LCI data sources for the different processes for the geopolymer mortar in Publication IV while Table 3.11 shows the transportation distances of the different materials. The data quality indexes were obtained from the dataset documentation and the local data were estimated according to the data quality matrix detailed in section 3.1.2.

Table 3.10: Data sources and quality index of LCI dataset for Publication IV

Type of data	Source	Description of process	Data quality index (Pedigree matrix)
Sodium hydroxide	GaBi database 2019	EU-28: Sodium hydroxide (caustic soda mix, 100%)	(3,3,2,2,2)
Sodium silicate solution	Ecoinvent 3.4 database	EU-28: Sodium silicate production, hydrothermal liquor, product in 37% solution state	(2,2,5,1,1)
Portland cement	GaBi database 2019	Portland cement (CEM I)	(3,3,4,4,5)
Metakaolin	GaBi database 2018, Heath et al. (2014), NLK (2002)	Kaolin Calcination	(3,3,2,3,3)
Water	GaBi database 2019–	EU-28: tap water	(3,3,4,4,3)
Electricity	GaBi database 2019	FI: electricity grid mix	(3,3,4,3,4)
GBFS	Marceau and VanGeem, (2003)	GBFS beneficiation	(2,3,5,4,1)
Coal fly ash	Fatec (2020)	Coal fly ash pre-treatment	(1,2,1,1,1)
Tailings	Locally sourced	Grinding of tailings	(1,2,1,1,1)
CAC	CIMSA (2015)	Cimsa Cemento	(2,2,1,4,2)
Steel slag	Locally sourced	Crushed steel slag	(1,2,1,1,1)
Crushed stone	GaBi database 2019	DE: crushed stone 16/32	(3,3,2,3,2)
Transportation	GaBi database 2018	Truck-trailer, Euro 5, 34-40t gross weight / 27t payload capacity	(3,3,2,2,2)
Diesel	GaBi database 2018	Diesel mix at refinery	(3,3,2,3,3)

Polypropylene fibre	GaBi database 2019	EU-28: Polypropylene fibres	(3,3,2,4,2)

Table 3.11: Transportation of different materials from point of source to construction facility.

	PIV_S0 (km)	**PIV_S1** (km)	**PIV_S2** (km)	**PIV_S3** (km)	**PIV_S4** (km)
Sodium hydroxide	15	15	15	264	264
Sodium silicate	15	15	15	1233	0
Tailings	238	238	238	38	38
GBFS	174	174	174	427	427
Coarse aggregate	274	274	274	2.4	2.4
Milled bio fly ash	279	279	279	5.9	5.9
Metakaolin	13	13	13	271	271
Polypropylene fibre	174	174	174	0	0
Portland cement	48	48	48	240	240
Coal fly ash	435	435	435	275	275
Landfill location	152	152	152	140	140
Crushed steel slag	224	224	224	36	36

3.4.5 **Sensitivity analysis**

Sensitivity analysis is applied to evaluate the influence of modelling assumptions and choices in a product system (EC-JRC, 2010). As discussed in section 3.4.2, service life was assumed to be 40 years for all the LHNB mix designs because the desirable service life for PC concrete noise barrier is averagely 40 years. However, due to material differences in the mix designs of the LHNB scenarios, sensitivity analysis was conducted for the geopolymer composite (PIV_S1-PIV_S4) in range 10 years to 40 years to determine the influence of changes in service life on the environmental performance of the geopolymer composite LHNB scenarios.

3.5 Carbonation methodology

As discussed in Section 2.5, carbonation needs to be considered in the emission calculation of concrete. In Publication IV, carbonation is taken into consideration to determine potential CO_2 savings that can be achieved during the use and end-of-life phases. A report by Stripple et al. (2018) detailed the carbonation reaction steps and documented three different CO_2 uptake calculation methodologies based on complexity and accuracy. These different methods are related to the annual CO_2 uptake. In the study, the simplified methodology presented by Stripple et al. (2018) was used to calculate the CO_2 uptake in the LHNB use and end-of-life phases.

For the use stage, two alternative CO_2 uptake calculations are provided to handle uncertainty.

- Alternative A: annual CO_2 uptake for the use stage is estimated as "0.2 multiplied by the reported emission from calcination of consumed cement clinker"
- Alternative B: annual CO_2 uptake for the use stage is estimated as "0.15 multiplied by the reported emission from calcination of consumed cement clinker"

For the end-of-life (demolishing, crushing, and storage),

- Annual CO_2 uptake is estimated as "(0.02) multiplied by the reported emission from calcination of consumed cement clinker"

Alternatively, if the amount of annual concrete recycling is known and the amount of annual crushed concrete used as secondary raw material is also known, the CO_2 uptake in the end-of-life and secondary use phases can be individually calculated as 10 kg CO_2/m^3 concrete (Stripple et al., 2018).

4 Results and discussion

4.1 Geopolymer binder and fibre reinforced geopolymer composites

4.1.1 Contribution analysis for geopolymer binder

The potential application of the geopolymer binder mix design in Publication I is as a substitute for PC; thus, the environmental performance results of the mix designs are compared to PC CEM I, as reported by CEMBUREAU (2015a). To begin with, the geopolymer binder mix designs have a better environmental performance when compared to CEM I in AP, EP, and GWP except in ADP_FF where the environmental performance is worse. Among the geopolymer binder mix designs, PI_PM10/0 exhibited the best environmental performance across the four impact categories. This is due to the lack of metakaolin in its mix design. On the other hand, PI_PM0/10 had the worst environmental performance across the four impact categories owing to the 100% metakaolin precursor in its mix design, except in AP, where PI_PM8/2 and PI_PM9/1 had the worst environmental performance. This is due to the extra metakaolin included with mine tailings in the precursor mix. The geopolymer binder mix designs have a compressive strength between 2 and 21 MPa as shown in Table 3.3. A low compressive strength (2–3 MPa) was obtained from the mix designs PI_PM0/10-PI_PM3/7, PI_PM9/1, and PI_PM10/0, as the mix designs were not optimal for alkali activation of metakaolin. However, the variation of mine tailings and metakaolin in the mix designs PI_PM4/6 – PI_PM8/2 showed a profound effect on their compressive strength in the range of 10–21 MPa, with PI_PM7/3 having the highest compressive strength of 21 MPa.

In addition to having the highest compressive strength, PI_PM7/3 had better environmental performance than PI_PM0/10-PI_PM6/4, owing to the lower amounts of metakaolin in its mix design. These results indicate that although PI_PM10/0 had the best environmental performance in geopolymer binder mix designs, its low compressive strength makes it less ideal for construction purposes (>10 MPa is required for construction purposes), but it is suitable for landfill purposes in the solidification and stabilisation of hazardous waste (>0.35 MPa is required for landfill purposes) (Xia et al., 2019). On the other hand, PI_PM6/4 and PI_PM7/3 with compressive strengths of 13 and 21 MPa, respectively, are better suited for construction purposes.

Furthermore, when compared to CEM I, PI_PM7/3 was 51%, 22%, and 19% more environmentally favourable in GWP, EP, and AP, respectively. In contrast, in ADP_FF, PI_PM7/3 was 54% more environmentally unfavourable than CEM I. This is because of the energy intensity in the production of NaOH and sodium silicate.

To further interpret the results, sodium silicate, NaOH, electricity (for mixing and curing), and metakaolin are the main contributors to the environmental impact categories in PI_PM7/3, contributing 31%, 25%, 20%, and 19%, respectively, to GWP. In AP, sodium silicate, NaOH, and electricity contributed 39%, 25%, and 25%, respectively. In EP,

sodium silicate, NaOH, and electricity contributed 43%, 25%, and 19%, respectively. Lastly, sodium silicate, NaOH, electricity, and metakaolin contributed 29%, 24%, 17%, and 25%, respectively, to ADP_FF. The contribution analysis of the phosphate mine tailings and metakaolin geopolymer binder mix designs (Publication I) to the impact categories ADP_FF, AP, EP, and GWP are presented in Figure 4.1.

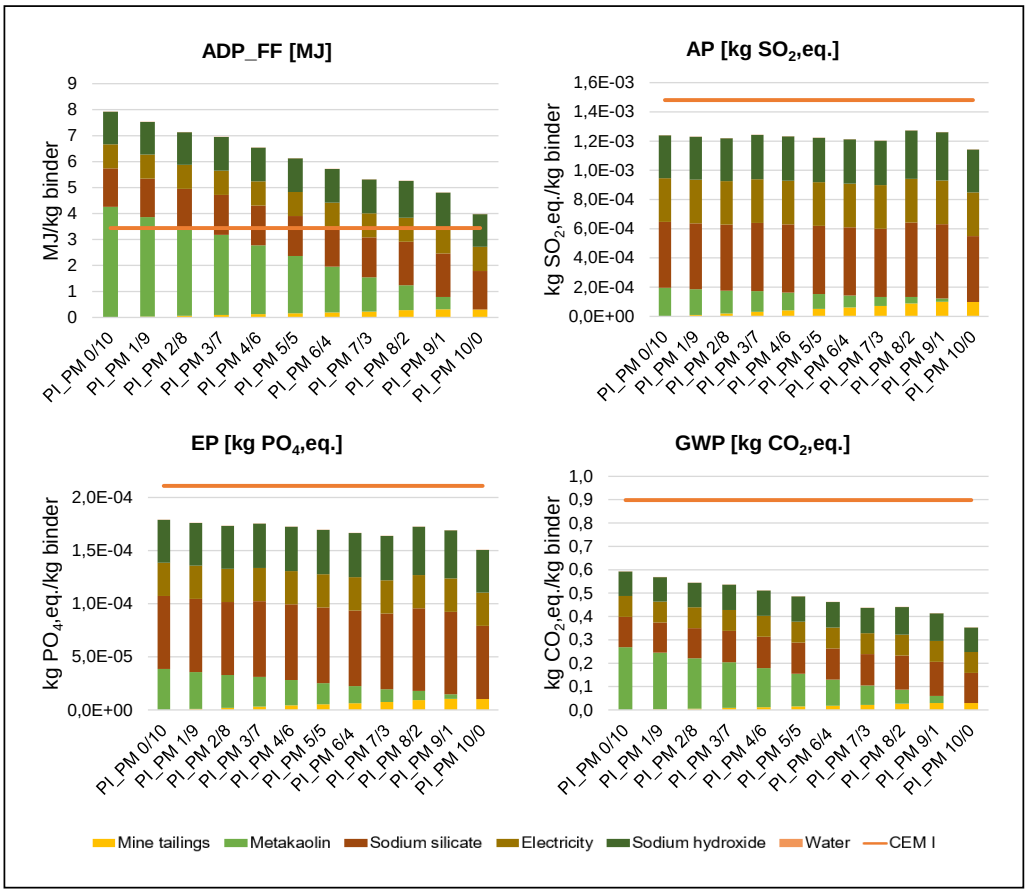

Figure 4.1: Contribution analysis for geopolymer binder

Conversely, for a more consistent interpretation and assessment of results the compressive strengths of the different mix designs are adapted to the environmental performance analysis by calculating the ratio of each environmental impact category to 7 days compressive strength (MPa) (Vieira et al., 2018). For PC CEM I, the 7 days compressive strength is ≥16 MPa (BS-EN 197-1, 2011) while the 7 days compressive strength of the geopolymer binders can be found in Table 3.3. The results of adapting the compressive strength in the analysis shows that PI_PM7/3 had the best environmental performance among the rest of the geopolymer binder mix designs in the assessed environmental impact categories. Also, PI_PM7/3 had better environmental performance

when compared to PC CEM I with 38% lower emissions in AP, 41% lower emissions in EP, and 63% lower emissions in GWP except for in ADP_FF where it had 18% worse environmental performance. The worse mix designs when the compressive strength is adapted to the environmental performance results are PI_PM0/10, PI_PM1/9, PI_PM9/1, and PI_PM10/0. When the results in Figure 4.2 are compared to the earlier results in Figure 4.1, PI_PM0/10 still had a worse environmental performance not just among the geopolymer binders but including comparison with PC CEM I, while PI_PM10/0 which initially had the best environmental performance (Figure 4.1) is now seen with a worse environmental performance (Figure 4.2). PI_PM7/3 which was initially the second-best mix design among the geopolymer binders is now the overall best mix design. These results show how the adaptation of compressive strengths in the environmental performance calculation can influence the assessment of results and improve the consistency in the interpretation of results.

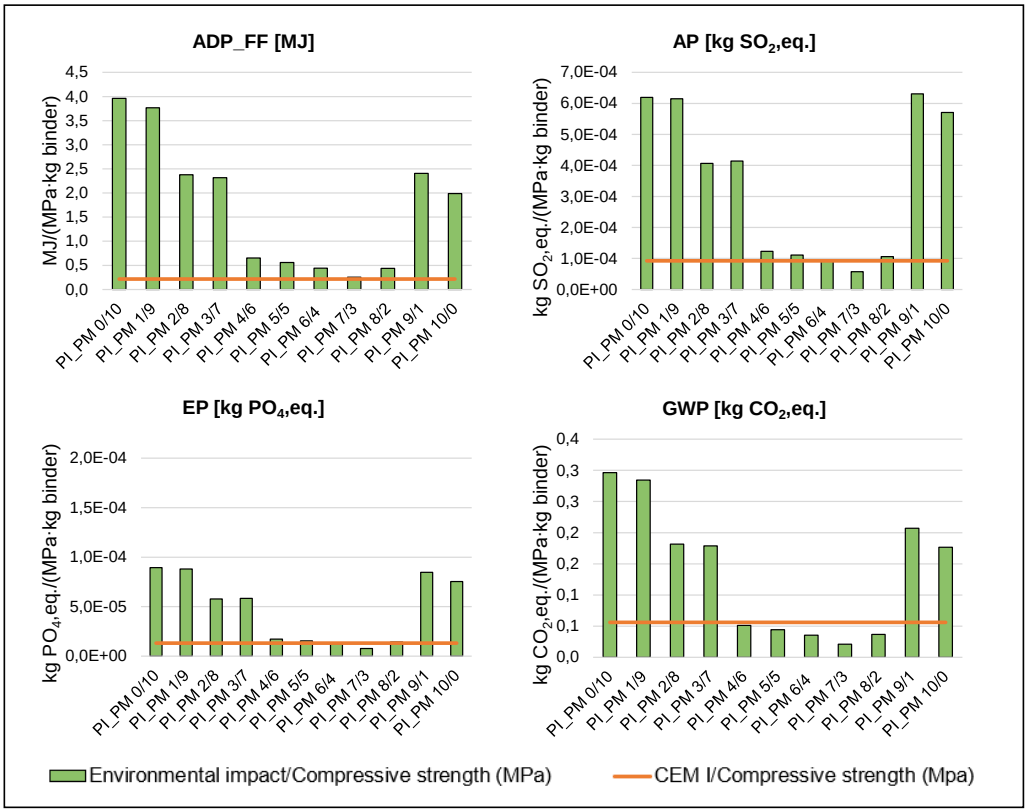

Figure 4.2: Environmental performance of geopolymer binders and PC CEM I with respect to compressive strength at 7 days

4.1.2 Contribution analysis for fibre reinforced geopolymer composites

In addition to assessing the environmental performance of geopolymer binder mix designs (Publication I), the environmental performance of several mix designs (Table 3.3) of FRGCs (Publication II) were assessed. Firstly, the normalised results for all FRGC mix designs were obtained using the CML 01-2016 methodology. Then, the weighted results using the same CML 01-2016 methodology were obtained to determine the most environmentally optimal mix designs of each FRGC group. In addition, the normalised and weighted results for PC concrete and steel fibre reinforced PC concrete reference scenarios were obtained. The weighted results show that PII_S1, PII_GF5, and PII_PP4 were the most environmentally optimal mix designs for the steel, glass, and polypropylene FRGC groups, respectively. In addition, the most relevant environmental impact categories were assessed, and they are ADP_FF, AP, GWP, HTP, and MAETP. This is illustrated in Figure 4.3 where the normalized results for all the environmental impact categories are in the primary axis and the weighted results is in the secondary axis.

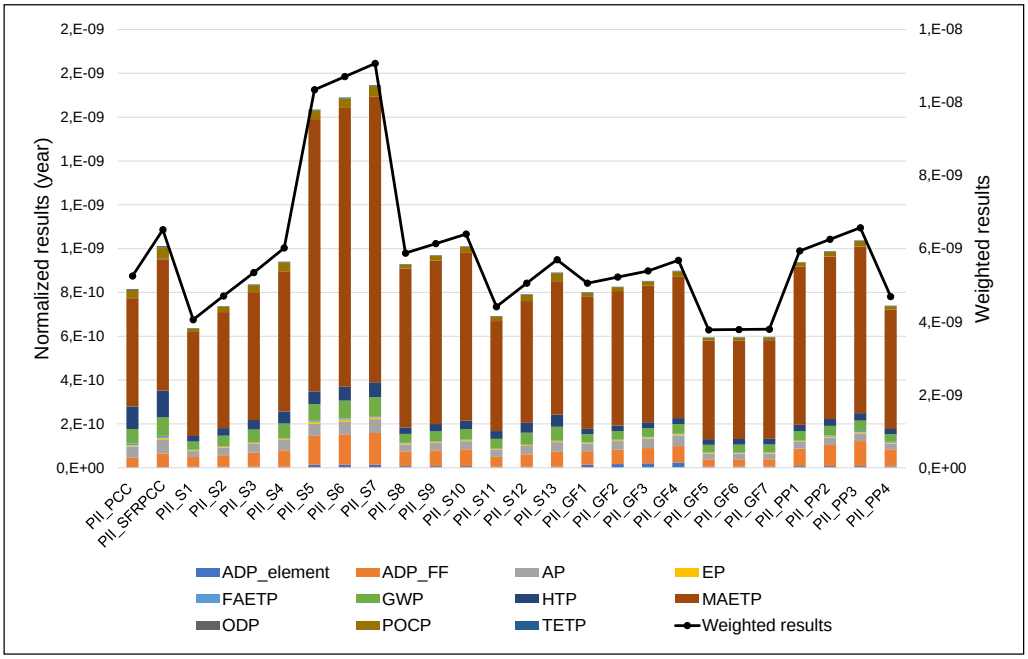

Figure 4.3: Normalized and weighted results for the FRGC mix designs.

Among the most environmentally optimal mix designs, PII_GF5 had the best environmental performance. Although PII_GF5 included 39 kg of cement in its mix design, this does not influence the result owing to having the lowest amount of sodium silicate (101 kg) in all the assessed mix designs. Similarly, PII_S1 had a low amount of sodium silicate (103 kg) in its mix design; however, the environmental impact of steel fibre made it environmentally unfavourable when compared to PII_GF5. PII_PP4 was

environmentally unfavourable when compared to the PII_S1 and PII_GF5 in ADP_FF and MAETP, due to the higher amounts of sodium silicate (132 kg) and additional impacts from polypropylene fibre. Also, the compressive strength of PII_PC, PII_SFRPCC, PII_S1, PII_G5, and PII_PP4 is 35 MPa, 39.5 MPa, 38 MPa, 36 MPa, and 39 MPa, respectively. The compressive strengths are comparable which makes for a consistent analysis and interpretation of results.

Subsequently, after determining the most optimal mix designs (PII_S1, PII_GF5, PII_PP4), their contributions to the ADP_FF, AP, GWP, HTP, and MAETP impact categories were assessed. When compared to PC concrete, PII_GF5, PII_S1, and PII_PP4 had 49-52%, 45-50%, and 75-77% better environmental performance in the impact categories AP, GWP, and HTP, respectively. For MAETP, PII_S1 and PII_GF5 had 4% and 9%, respectively, better environmental performance than PC concrete, while PII_PP4 has 11% worse environmental performance. For ADP_FF, PII_S1, PII_GF5, and PII_PP4 had 49%, 27%, and 97%, respectively, worse environmental performance when compared to PC concrete. This is mainly due to the energy consumed during the production of sodium silicate, NaOH, and the respective fibres. Additionally, when compared to steel fibre reinforced PC concrete, PII_GF5, PII_S1, and PII_PP4 had 59-62%, 58-61%, 79-81%, and 9-25% better environmental performance for AP, GWP, HTP, and MAETP, respectively. For ADP_FF, PII_S1, and PII_GF5 had 13% and 26%, respectively, better environmental performance than steel fibre reinforced PC concrete, while PII_PP4 had 16% worse environmental performance.

A comparison of the FRGCs to PC concrete and steel fibre reinforced PC concrete was conducted to observe the differences made to the environmental performance results due to inclusion of steel fibre to PC concrete. Although the difference between the compressive strengths of PC concrete and steel fibre reinforced PC concrete is 4 MPa, as seen in Table 3.3, the difference in environmental performance results shows that steel fibre reinforced PC concrete has 71%, 26%, 30%, 18%, and 22% worse environmental performance when compared to PC concrete for ADP_FF, AP, GWP, HTP, and MAETP, respectively. This shows the influence of steel fibres on environmental performance results.

Contribution analyses show that PC production in PC concrete, and PC production and steel fibre in steel fibre reinforced PC concrete are the major contributing materials to ADP_FF, AP, GWP, HTP, and MAETP. Sodium silicate was the major contributor to PII_GF5, PII_S1, and PII_PP4 for ADP_FF, AP, GWP, HTP, and MAETP. Other major contributing materials for ADP_FF include steel fibre and superplasticizer in PII_S1, superplasticizer and NaOH in PII_GF5, and polypropylene fibre in PII_PP4. For AP, other major contributing materials include steel fibre in PII_S1, cement, and NaOH in PII_GF5, polypropylene fibre, and NaOH in PII_PP4. For GWP, the other contributing materials include steel fibre and superplasticizer in PII_S1, cement, superplasticizer, and NaOH in PII_GF5, polypropylene fibre, and NaOH in PII_PP4, while in HTP, steel fibre in PII_S1, cement in PII_GF5, polypropylene fibre, and NaOH in PII_PP4. Lastly, other major contributing materials to MAETP include steel fibre in PII_S1 and cement in

PII_GF5. Figure 4.4 shows the contribution analysis of these scenarios to the respective impact categories.

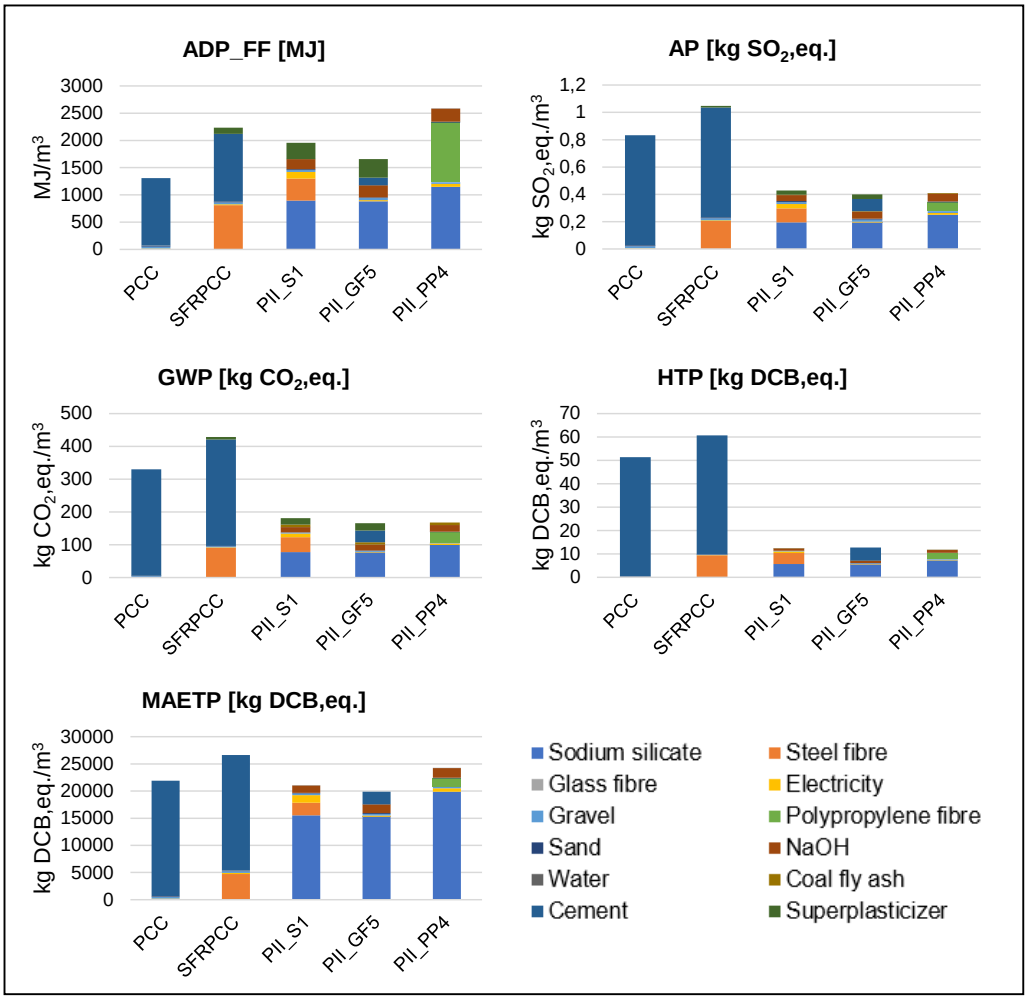

Figure 4.4: Contribution analysis of PC concrete, steel fibre reinforced PC concrete, and steel, glass, and polypropylene fibre reinforced geopolymer composites.

4.1.3 Sensitivity analysis on sodium silicate

From the overall results in the previous section, sodium silicate has a significant influence on the environmental performance of FRGCs. Hence, a sensitivity analysis was conducted on sodium silicate. As mentioned in Section 3.2.5, alternative LCI data for sodium silicate were employed in the sensitivity analysis, and from the obtained results, LCI data from BAT showed the best performance, while Ecoinvent had the worst environmental performance for ADP_FF, AP, GWP, HTP, and MAETP, as shown in

Figure 4.5. When comparing the LCI data of Fawer_FF and BAT, although the quantity of raw materials is very close, the total energy consumed in the production of sodium silicate (hydrothermal route) using Fawer_FF is 6.95 times more than that in BAT. This is due to the use of improved process control in the mixing and filtering steps of the production process, thereby maintaining a lower energy consumption (EU, 2007). With this range in energy consumption between Fawer_FF and BAT, substituting fossil fuels in Fawer_FF with biogas in Fawer_RE showed a considerable decrease in emissions in all impact categories except for AP. Although Fawer_RE has better environmental performance than Fawer_FF, it is still not as good as BAT. This is still because of the higher energy consumption in Fawer than in BAT. In addition, Ecoinvent showed a significant increase in the AP and HTP. This is because the Ecoinvent process consumes twice the amount of NaOH and silica sand during the production of sodium silicate. This sensitivity analysis shows that the manufacturing method of sodium silicate has a significant impact on the overall environmental performance of geopolymer composites.

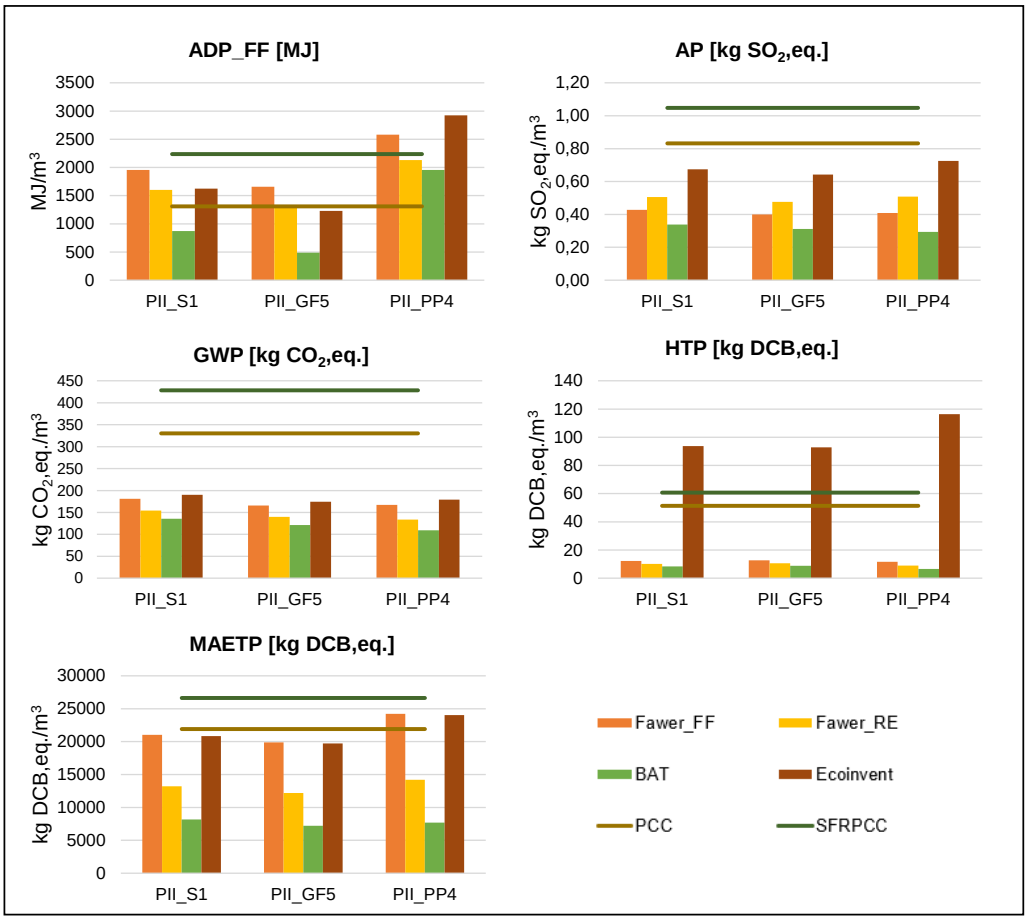

Figure 4.5: Sensitivity analysis of sodium silicate in the FRGC

4.2 Waste-derived alkali-silicates for geopolymer mortar

In the previous section, sodium silicate was identified as a major contributor to the environmental performance of geopolymers. Consequently, the environmental performance of alternative production of alkali-silicate from silica-rich waste materials (RHA and glass waste), as discussed in Section 3.3, was determined.

4.2.1 Contribution analysis

PIII_S1 and PIII_S2 represent one- and two-part geopolymer mortars from conventional sodium silicate powder and sodium silicate solution, respectively, while PIII_S3 and PIII_S4 represent one- and two-part geopolymer mortar from chemically modified glass waste and RHA alkali-silicates, respectively. This is discussed in more detail in Section 3.3.3 The compressive strength of PIII_S1, PIII_S2, PIII_S3, and PIII_S4 is 52 MPa, 58 MPa, 58 MPa, and 60 MPa, respectively. The compressive strengths are in similar range, which makes for a consistent analysis and interpretation of results.

Comparing the one-part geopolymer mortars, PIII_S3 had 62%, 61%, 75%, and 52% better environmental performance than PIII_S1 with regards to GWP, ADP_FF, AP, and POCP, respectively. Comparing the two-part geopolymer mortars regarding GWP, ADP_FF, AP, and POCP, PIII_S4 had 67%, 53%, 84%, and 64% better environmental performance than PIII_S2. Thus, PIII_S3 and PIII_S4 have the best environmental performances in all the four impact categories, indicating that using chemically modified waste-derived alkali-silicate for geopolymer mortars is a more environmentally favourable option than conventional sodium silicate. The results also indicate that PIII_S3 had a slightly better environmental performance than PIII_S4. This is because PIII_S3 does not require additional NaOH during geopolymer activation, whereas PIII_S4 requires additional NaOH during geopolymer activation. However, NaOH constantly appears in all the scenarios, as it is used together with sodium silicate as an activator in PIII_S1, PIII_S2, and PIII_S4, and it is necessary in the chemical modification of glass waste and RHA into alkali-silicates. Hence, a sensitivity analysis was conducted on NaOH and this is discussed in the next section.

The main contributor to the environmental impacts of PIII_S1, PIII_S2, PIII_S3, and PIII_S4 is the respective alkali activator for each mix design namely, sodium silicate powder in PIII_S1, sodium silicate solution and NaOH in PIII_S2, glass waste alkali-silicate in PIII_S3, and RHA alkali-silicate in PIII_S4. This is illustrated in Figure 4.6.

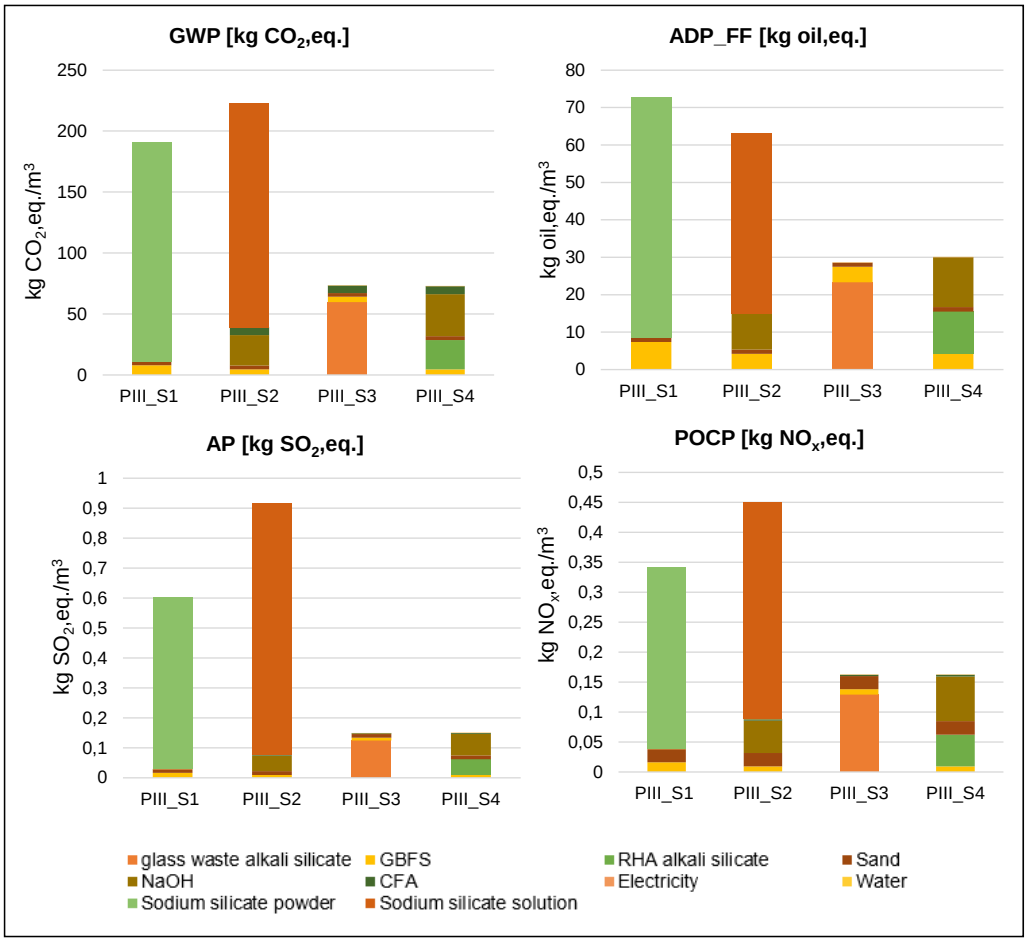

Figure 4.6: Contribution analysis for geopolymer mortars from waste-derived alkali-silicate in comparison to geopolymer mortars from conventional sodium silicate.

4.2.2 Sensitivity analysis on sodium hydroxide

Sensitivity analysis was limited to the influence of NaOH on the environmental performance of geopolymer mortar, as sensitivity analysis on sodium silicate has been explored in Section 4.1.3. The results of the sensitivity analysis, as shown in Figure 4.7 indicated that when compared to EU_NaOH, RER_NaOH has 6–125% worse environmental performance for GWP and AP, whereas for ADP_FF and POCP, there was a slight, 1-5%, better environmental performance. Subsequently, when compared to EU_NaOH, DE_NaOH showed 3-24% better environmental performance for ADP_FF, AP, and POCP, however it showed a 5-20% worse environmental performance for GWP. This indicates that DE_NaOH is a better option of LCI data for NaOH.

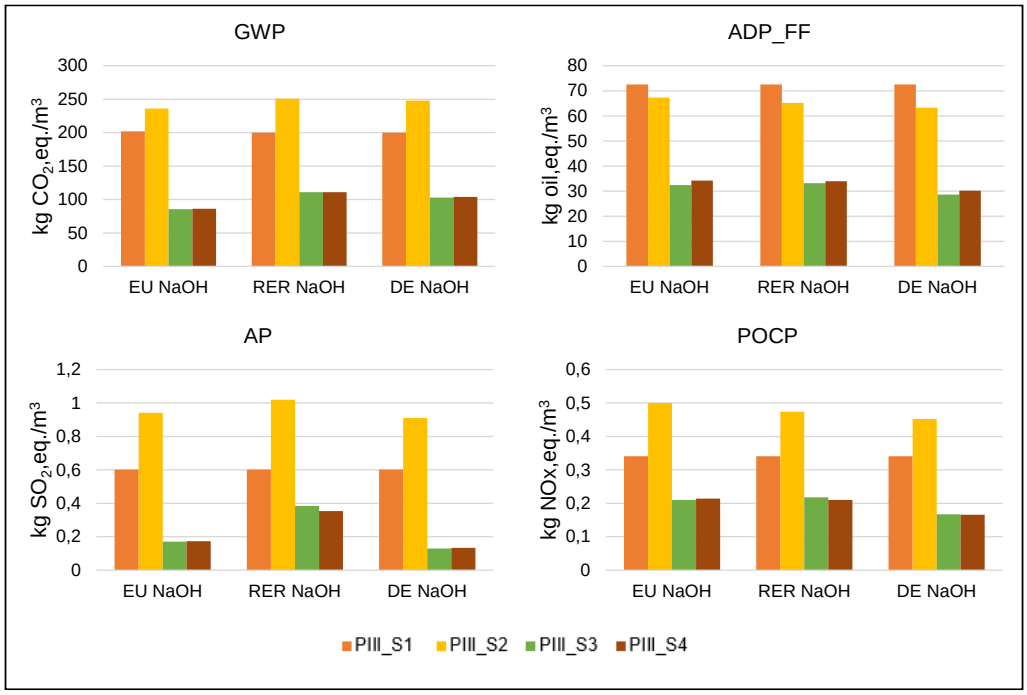

Figure 4.7: Sensitivity analysis of NaOH on geopolymer mortar.

4.2.3 Sensitivity analysis on allocation

Introducing emissions for glass cullet (treatment of glass waste from unsorted public collection) in glass waste did not significantly affect the environmental performance results of PIII_S3 as between 1%-2% increased emissions were observed for GWP, ADP_FF, AP, and POCP. Regarding allocating 4% emissions from rice (non-basmati) production to RHA, 19%, 4%, 25%, and 7% increased emissions were observed in GWP, ADP_FF, AP, and POCP, respectively, for PIII_S4. The results are shown in Figure 4.8. PIII_S3 and PIII_S4 are geopolymer mortar scenarios with chemically modified glass waste and RHA alkali-silicates.

Furthermore, with regards to mass allocation of emissions to CFA, the three scenarios (PIII_S2, PIII_S3, and PIII_S4) with CFA content were analysed and results show 15%-41% increased emissions in GWP, 17%-35% increased emissions in ADP_FF, 85-51% increased emissions in AP, and 10%-23% increased emissions in POCP. Regarding mass allocation of emissions to GGBFS, all scenarios (PIII_S1, PIII_S2, PIII_S3, and PIII_S4) with GGBFS content were analysed. Results show 32%-89% increased emissions in GWP, 36%-73% increased emissions in ADP_FF, 25%-151% increased emissions in AP, and 41%-97% increased emissions in POCP. These results are detailed in Table 4.1.

Overall, integrating glass cullets emissions and allocated emissions of RHA, CFA, GGBFS in PIII_S1-PIII_S4 show 47%-149% increased emissions in GWP, 54%-110% increased emissions in ADP_FF, 33%- 225% increased emissions in AP, and 50%-124% increased emissions in POCP, as shown in Table 4.2. Nonetheless, comparing one- and two-part geopolymer mortar from chemically modified glass waste (PIII_S3) and RHA alkali-silicate (PIII_S4) to one- and two-part geopolymer mortars from conventional sodium silicate powder (PIII_S1) and sodium silicate solution (PIII_S2), show that PIII_S3 has 42%, 43%, 54% and 39% reduced emissions in GWP, ADP_FF, AP, and POCP when compared to PIII_S1, and PIII_S4 shows 38%, 30%, 59%, and 36% reduced emissions in GWP, ADP_FF, AP, and POCP when compared to PIII_S2.

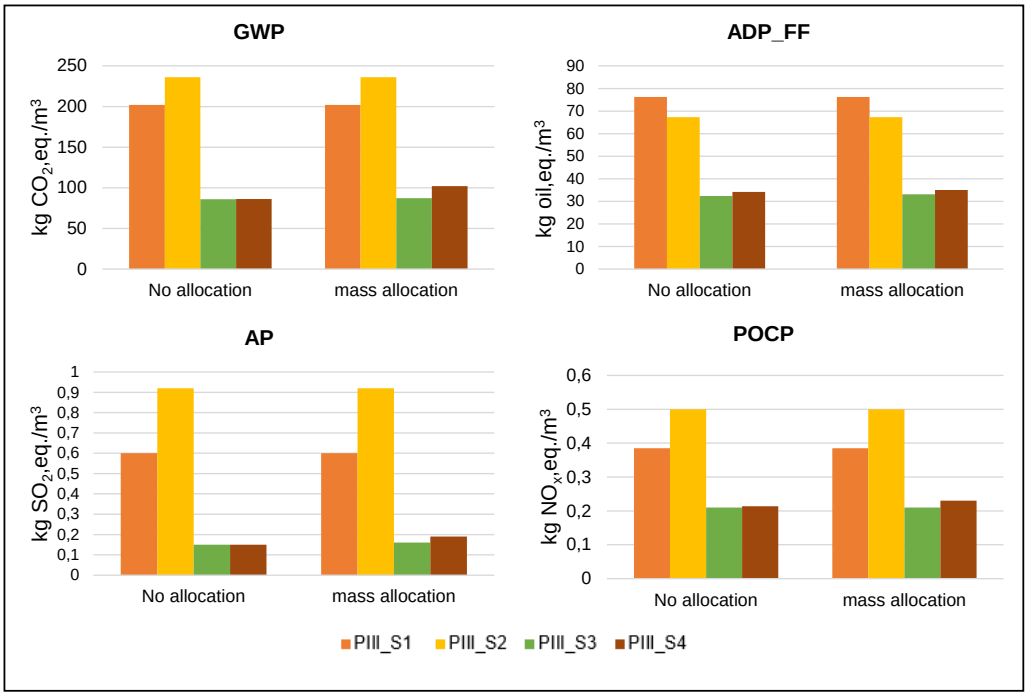

Figure 4.8: Sensitivity analysis on mass allocated emissions on RHA and glass cullet emissions.

Table 4.1: Sensitivity analysis of mass allocation of CFA and GGBFS geopolymer mortars

GWP	**PIII_S1**	**PIII_S2**	**PIII_S3**	**PIII_S4**
No allocation	202	236	86	86
Mass allocation for CFA	202	271	120	121
Mass allocation for GGBFS	335	312	160	163
ADP_FF	**PIII_S1**	**PIII_S2**	**PIII_S3**	**PIII_S4**

No allocation	76	67	32	34
Mass allocation for CFA	76	79	44	46
Mass allocation for GGBFS	119	92	56	59
AP	**PIII_S1**	**PIII_S2**	**PIII_S3**	**PIII_S4**
No allocation	0.60	0.92	0.15	0.15
Mass allocation for CFA	0.6	1.00	0.23	0.23
Mass allocation for GGBFS	1.00	1.15	0.37	0.39
POCP	**PIII_S1**	**PIII_S2**	**PIII_S3**	**PIII_S4**
No allocation	0.39	0.50	0.21	0.21
Mass allocation for CFA	0.39	0.55	0.26	0.26
Mass allocation for GGBFS	0.74	0.70	0.41	0.42

Table 4.2: Sensitivity analysis results of geopolymer mortars based on allocated emissions of RHA, CFA, GGBFS, and glass cullet emissions.

GWP	**PIII_S1**	**PIII_S2**	**PIII_S3**	**PIII_S4**
No allocation	202	236	86	86
Mass allocation	335	347	195	215
ADP_FF	**PIII_S1**	**PIII_S2**	**PIII_S3**	**PIII_S4**
No allocation	76	67	32	34
Mass allocation	119	103	68	72
AP	**PIII_S1**	**PIII_S2**	**PIII_S3**	**PIII_S4**
No allocation	0.60	0.92	0.15	0.15
Mass allocation	1.00	1.23	0.46	0.50
POCP	**PIII_S1**	**PIII_S2**	**PIII_S3**	**PIII_S4**
No allocation	0.39	0.50	0.21	0.21
Mass allocation	0.74	0.75	0.46	0.48

GWP-global warming potential, ADP_FF-abiotic depletion potential (fossil fuel), AP-acidification potential, POCP-photochemical ozone creation potential.

4.3 Geopolymer product case study – low-height noise barrier

4.3.1 Contribution analysis

Four different geopolymer composite mix designs (PIV_S1, PIV_S2, PIV_S3, PIV_S4) with different amounts of alkali activator, precursors, and aggregates are compared against a reference PC scenario PIV_S0. The precursors and aggregates are mainly from by-products and wastes, while the amount of alkali activator varied between 0.3-19%. The LCIA results generated are based on the environmental assessment of the different LHNB scenarios (Table 3.9). The environmental performance results illustrate the environmental impacts of the LHNB in their different life cycle phases.

In the production phase, with respect to GWP, PIV_S1, PIV_S2, PIV_S3, and PIV_S4 had 44%, 7%, 32% and 96% lower global warming effects respectively, when compared to PIV_S0. With respect to ADP_FF, PIV_S1, PIV_S2, and PIV_S3 have 33%, 123% and 36% increased oil extraction respectively while PIV_S4 has 87% decrease, respectively, when compared to PIV_S0. With respect to POCP, PIV_S1, PIV_S2, PIV_S3, and PIV_S4 had 41%, 17%, 47% and 94% lower formation of photochemical oxidants, when compared to PIV_S0. Finally, with respect to AP, PIV_S1, PIV_S2, and PIV_S3 have respectively, 10%, 62%, and 27% potential increase in atmospheric deposition of acidifying compounds while PIV_S4 has 96% decrease when compared to PIV_S0. Still in the production phase, regarding GWP, cement is the most significant contributing material in PIV_S0 (90%). In PIV_S1, alkali activator and transportation were the most significant contributor at 80% and 16% respectively. In PIV_S2, alkali activator and metakaolin were the significant contributors at 70% and 19% respectively. Regarding PIV_S3, sodium silicate, metakaolin and calcium aluminate cement contributed 59%, 19% and 13% respectively. While in PIV_S4, transportation, aggregates, and alkali activator were the most significant contributor at 39%, 38%, and 11%. With respect to ADP_FF, cement (70%) and transportation (21%) mostly contributed to PIV_S0. Alkali activator and transportation contributed 73% and 16% respectively, to PIV_S1. In PIV_S2 and PIV_S3, alkali activator contributed 61% each and metakaolin contributed 24% and 29% to the scenarios, respectively. In PIV_S4, transportation and aggregates contributed 33% each. With respect to POCP, cement and transportation contributed 84% and 15% respectively to PIV_S0. Alkali activator and transportation are the most significant contributors to PIV_S1 at 70% and 27% respectively, PIV_S2 at 71% and 17% respectively, and PIV_S3 at 69% and 14% respectively. In PIV_S4, transportation and aggregates had 93% and 19% contribution, respectively. Finally, with respect to AP, cement (91%) is also the most significant contributing material in PIV_S0. Alkali activator is the most significant contributing material in PIV_S1 (90%), PIV_S2 (91%), and PIV_S3 (75%). In PIV_S4, transportation and aggregates contributed 45% and 26%, respectively. Other materials had minimal contribution lower than 10%. The contribution of the respective input materials and energy to respective impact categories in the production phase can be found in Figure 4.9.

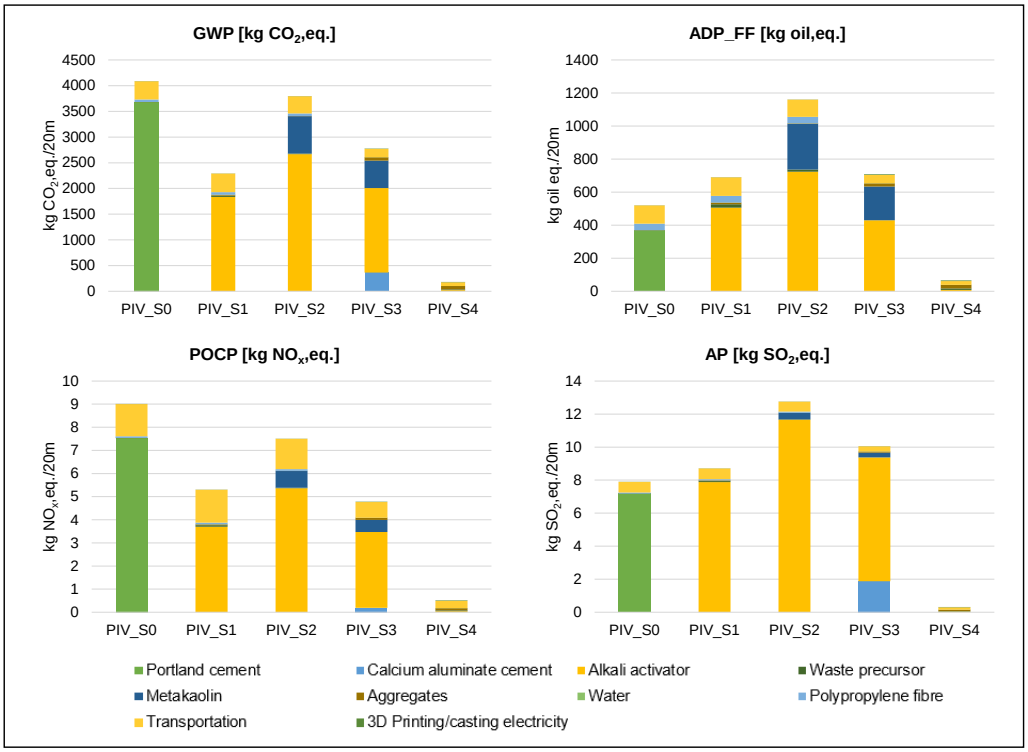

Figure 4.9: Contribution analysis in the production phase of the low-height noise barrier scenarios.

In the use phase, carbonation as discussed in section 3.5 is considered, and alternative B is used to calculate the annual CO_2 uptake for more conservative results. Calcination emission from cement is estimated to be approximately 49% (Stripple et al., 2018). For the geopolymer scenarios which have no cement content, CO_2 uptake is not calculated. This is because of the limited data availability for the CO_2 uptake of CFA and GGBFS. Although, CO_2 uptake for GGBFS has been estimated to be 35 kg CO_2/ton, it is recommended to include these additions when advanced CO_2 uptake methodology is applied. Since, simplified CO_2 uptake methodology is applied in this study, CO_2 uptake for scenarios with cement content (PIV_S0 and PIV_S3) are the only ones considered. Since minimal to no-maintenance and repair activities are expected during the usage of the LHNB, the emissions in the use phase are limited to activities leading to carbonation and CO_2 uptake. Thus, annual CO_2 uptake for PIV_S0 and PIV_S3 is estimated to be 270 and 27 kg CO_2 eq./20m, respectively.

In the end-of-life phase, LHNB are demolished and transported to landfill. Emissions from demolition, crushing, and landfill are comparable for all the scenarios since the weights of the LHNB are equivalent. Annual CO_2 uptake is also considered in the end-of-life phase and estimated to be 36 and 4 kg CO_2 eq./20m for PIV_S0 and PIV_S3, respectively.

For the overall LCA results including the production, use and end-of-life phases, PIV_S2 has the highest GWP emissions, with 0.35% increase above PIV_S0, while PIV_S1, PIV_S3 and PIV_S4 have 37%, 26% and 89% lower GWP emissions compared to PIV_S0. With respect to ADP_FF, PIV_S1, PIV_S2, and PIV_S3 have 28%, 107% and 31% increased oil consumption respectively, while PIV_S1 has 76% decrease in oil consumption compared to PIV_S0. With respect to POCP, PIV_S1, PIV_S2, PIV_S3, and PIV_S4 have 36%, 15%, 41%, and 83% lower potential of formation of photochemical oxidants when compared to PIV_S0. With respect to AP, PIV_S1, PIV_S2, and PIV_S3 have 9%, 54%, 24%, respectively, potential increase in atmospheric deposition of acidifying compounds while PIV_S4 has 85% decrease, when compared to PIV_S0.

Figure 4.10 shows the overall LCA results of the LHNB scenarios and on the secondary axis is the 28 days compressive strength of PIV_S0, PIV_S1, PIV_S2, PIV_S3, and PIV_S4 at 32 MPa, 20 MPa, 25 MPa, 29 MPa, and 13 MPa, respectively.

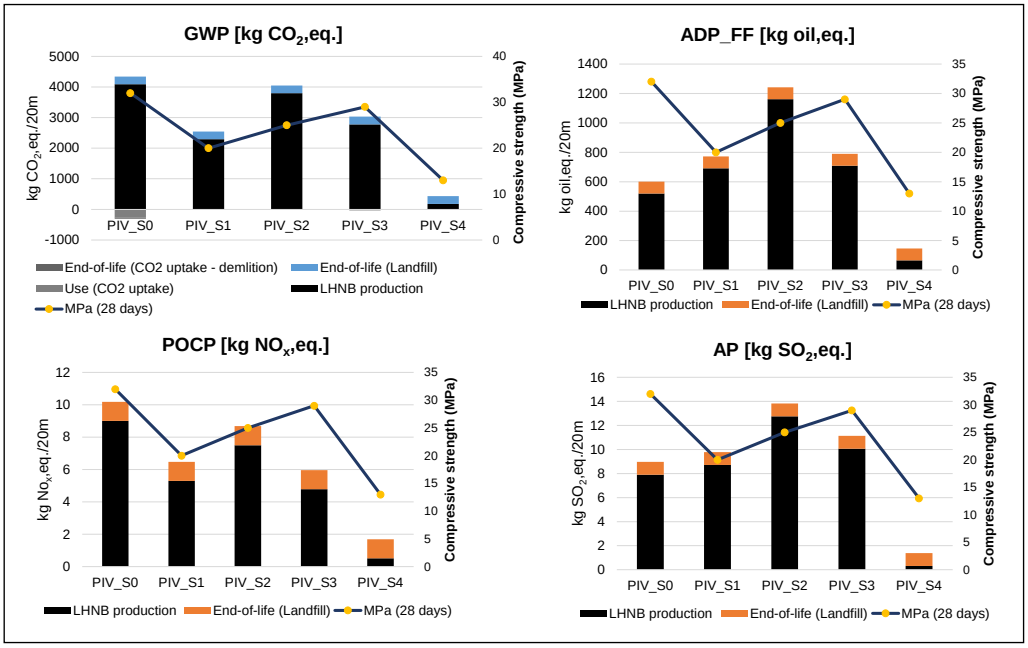

Figure 4.10: Overall LCA results of the low-height noise barrier scenarios

Due to the observable differences in the compressive strengths of the LHNB mix designs, a more consistent interpretation and assessment of results will require the environmental performance results be calculated with respect to compressive strength and service life using *Indicator*$_1$ (Equation 3.2) and *Indicator*$_2$ (Equation 3.3) respectively, as discussed in section 3.4.2. When *Indicator*$_1$ is used to assess the environmental performance of the LHNB scenarios with respect to compressive strength as shown in Figure 4.11, PIV_S2

has the highest emissions followed by PIV_S1 in the respective environmental impact categories, while PIV_S4 has the best environmental performance with this indicator only that it has a significant lower compressive strength compared to the rest.

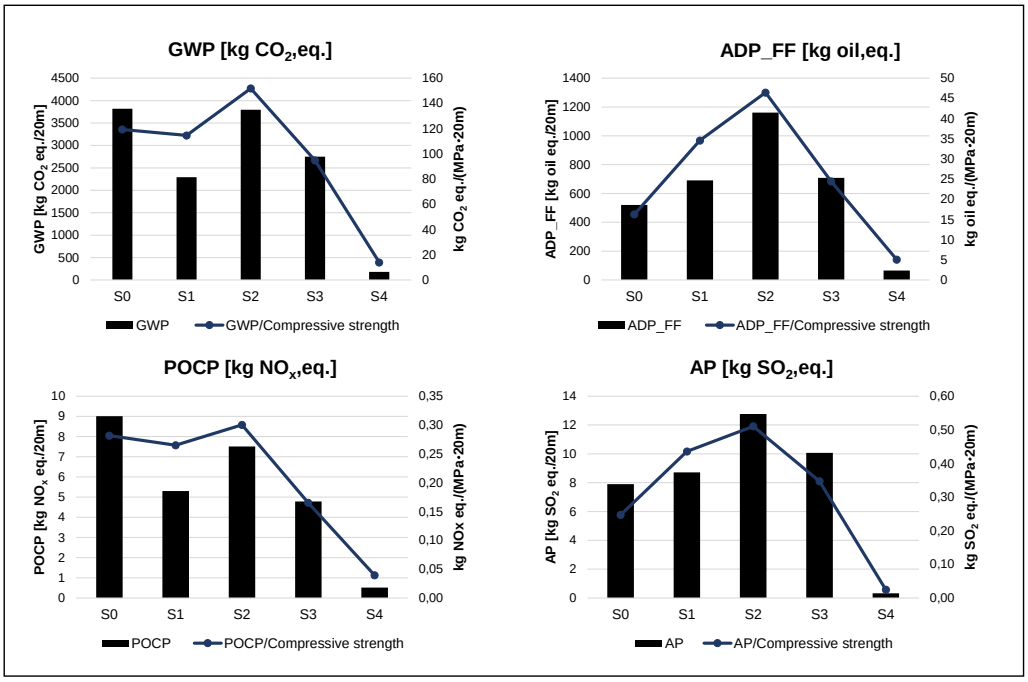

Figure 4.11: LCA results with respect to compressive strength of the LHNB scenarios

For additional consistent interpretation of results, *Indicator*$_2$ is used to assess the environmental performance of the LHNB scenarios with respect to compressive strength and service life as shown in Figure 4.12. Similarly, as above-mentioned, PIV_S2 is the worst scenario with this indicator followed by PIV_S1 while PIV_S4 has the best environmental performance.

These differences in results obtained in Figure 4.10, Figure 4.11, and Figure 4.12, shows the significance of including compressive strength and service life for a more consistent interpretation of results. The limitation to this analysis is assumption of 40 years of service life for all the LHNB scenarios. As a result, a sensitivity analysis was conducted and is detailed in the next section.

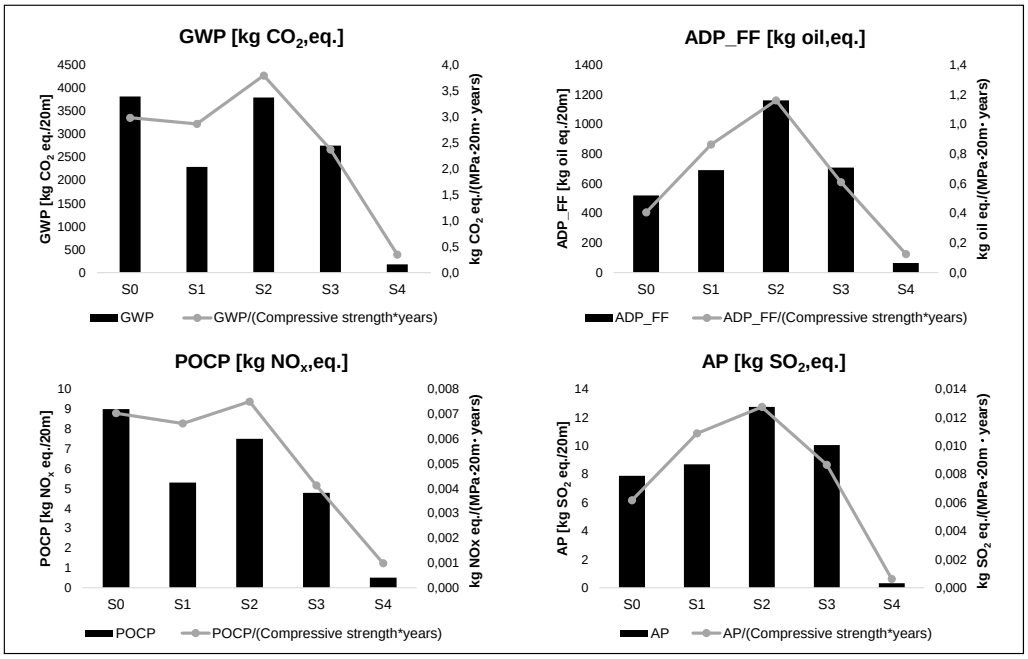

Figure 4.12: LCA results with respect to service life of the LHNB scenarios

Overall, the assessment carried out shows that the production stage is the most significant life cycle phase. The major environmental problem associated with the reference scenario (PIV_S0) is due to cement production which has been known to be a major environmental pollutant (Andrew, 2018b; Crossin and Carre, 2012). Most of the environmental impacts from the production phase of the geopolymer composites LHNB (PIV_S1-PIV_S4) originated from alkali activator. This dissertation has also shown alkali activator from silica-rich chemically modified waste products such as rice husk ash and waste glass are more environmentally friendly than conventional alkali-silicate without compromising on their mechanical properties.

Furthermore, transportation emissions were significant during production of PIV_S4. Transportation emissions is of importance due to environmental burden from long distance transportation of materials. Thus, most of the materials are transported only within regional scale (averagely 200 km).

PIV_S4 illustrates improvement potential in developing LHNB from 83% weight-% of industrial side streams and maximizing the efficient use of resources using AM construction method. The integration of AM in geopolymer makes it a superior and sustainable alternative to precast PC concrete (Yao et al., 2020) due to increased flexibility. This is also highlighted in this study comparing PIV_S2 and PIV_S3. Although, both mix designs are comparable, PIV_S2 had worse environmental performance than PIV_S3, as the later was constructed through AM, with a unique hollow

shape resulting in flexible LHNB development and lesser material consumption. Whereas PIV_S2 was produced using the traditional construction method resulting in more material consumption. Additionally, environmental desirability of AM from carbon and energy viewpoint, varies depending on how the printing is executed (Saade et al., 2020). Besides the potential environmental performance of AM, other uniqueness include complexity-achievement and reduced hazardous exposure of workers etc. (Saade et al., 2020). Conversely, the shift to AM can lead to loss of jobs due to less manpower needed. There is still an open question on AM revolutionizing traditional construction, however, it can be said that AM will transform construction to highly sophisticated structures with improved environmental performance.

4.3.2 Sensitivity analysis on service life

The LHNB scenarios are made up of different mix designs with different materials which results in different compressive strength (Figure 4.10) which can also influence the service life of the LHNB scenarios. PC concrete noise barrier has a standard service life of 40 years but there is an uncertainty on the service life of the geopolymer composites LHNB scenarios. Thus, a sensitivity analysis is conducted to determine how changes in the service life (10 to 40 years) of the geopolymer composite LHNB scenarios influence the LCA results. Service life PC concrete LHNB (PIV_S0) remains constant.

The results in Figure 4.13 show that with regards GWP, PIV_S4 has the best environmental performance with lower GWP emissions than PIV_S0 at the different years while the environmental performance of PIV_S1 and PIV_S3 becomes equal to PIV_S0 at 35 years and 30 years of service life respectively. With respect to AP, only PIV_S4 has better environmental performance than PIV_S0 whether it last 10 years or 40 years while with respect to ADP_FF, PIV_S4 has equal environmental performance to PIV_S0 at 12 years. With respect to POCP, environmental performance of PIV_S1 and PIV_S2 becomes equal to PIV_S0 at 40 years of service life. Any year less will make them less environmentally favourable while PIV_S3 becomes environmental favourable to PIV_S0 at 25 years of service life and PIV_S4 remains environmentally favourable than PIV_S0 at the different years.

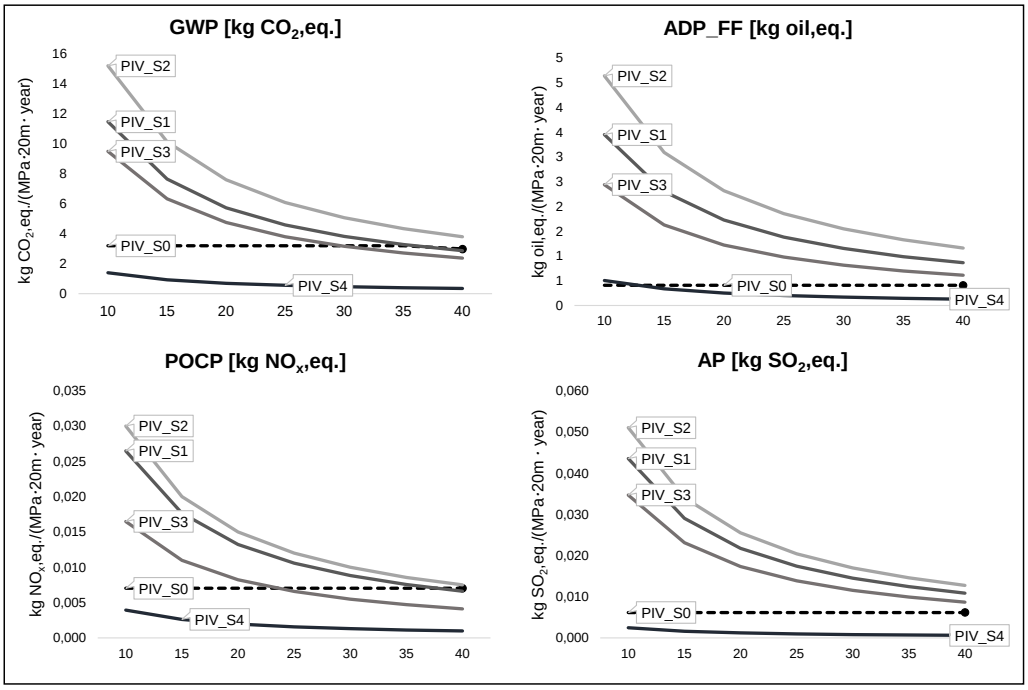

Figure 4.13: LCA results with respect to changing service life (10 to 40 years) of the geopolymer composite LHNB scenarios

4.4 General discussion

Based on the main objective of this dissertation and the collective results, this dissertation supports the often-emphasised view that geopolymer binders and composites can be considered as low-carbon alternatives to PC and PC concrete. The LCA of the geopolymer mix designs demonstrated the possibility of developing geopolymers from industrial by-products and waste and the possibility of substituting alkali activators with waste-derived activators (Abdulkareem et al., 2021a, 2021b). However, it is not self-evident that geopolymer composites are more environmentally friendly than PC concrete, as some mix designs have considerably higher environmental impacts than PC concrete. Thus, in the development of geopolymer composite mix designs, it is very important to consider the role of alkali activators in environmental performance. This can make the mix design development more challenging as it is vital that the geopolymer composites still meet the mechanical properties for the purpose they will be used.

The environmental sustainability of geopolymers largely depends on the locally available materials, to reduce the carbon footprint produced during the transportation of materials. However, the local availability of some precursors such as CFA, which is the most used precursor in geopolymer composite development, is in decline. For instance, 348 thousand tonnes of CFA were produced in Finland in 2017 (LUKE, 2017), and this

will decline further as Finland plans to ban coal combustion by 2029 (Hukkanen, 2019). In addition, the EU have seen reductions in the availability of CFA due to targets to stop coal combustion for energy production. As seen in Figure 4.14, there was a decline in the inland production and combustion of hard coal in EU-27 countries from 1990 to 2019: from 277 and 390 million tonnes, respectively, in 1990, to 65 and 176 million in 2019 (Eurostat, 2020b).

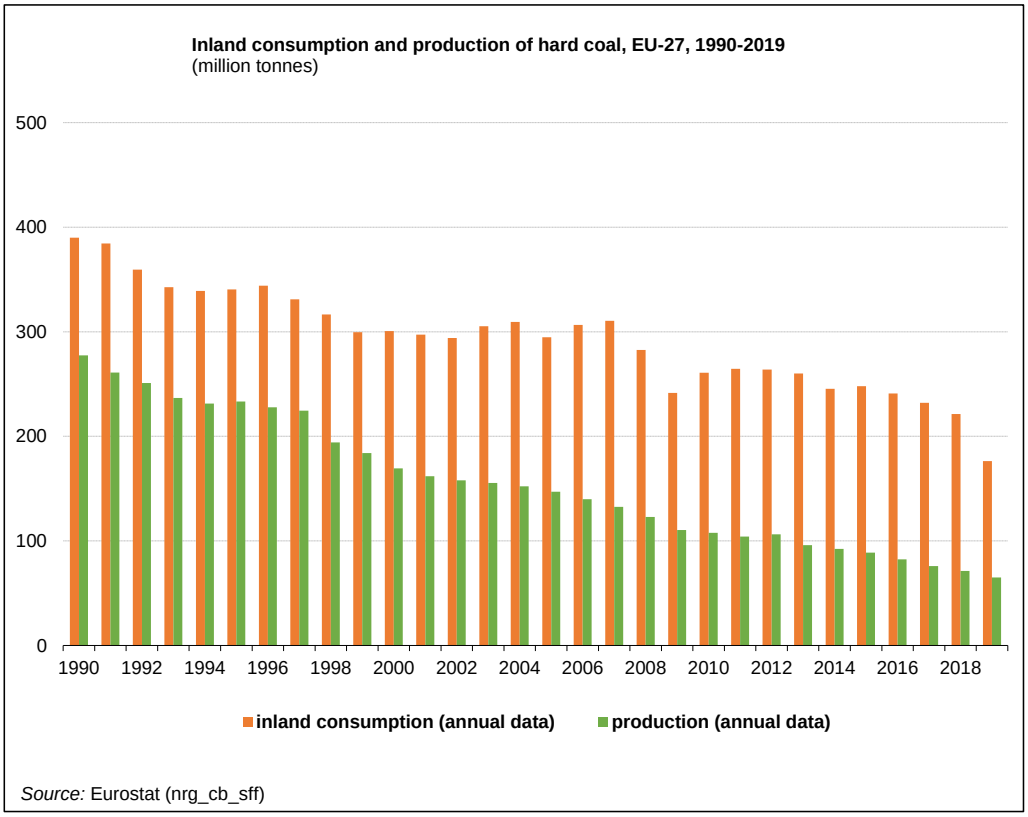

Figure 4.14: Inland consumption and production of hard coal, EU-27, 1990–2019 (Eurostat, 2020b).

On the other hand, the only blast furnace plant in Finland will be replaced with an arc furnace between 2030 and 2040 (SSAB, 2021), leading to no blast furnace slag production in Finland. The production of blast furnace slag was consistent from 2000 to 2016, according to the European Association representing metallurgical slag producers and processors, as shown in Figure 4.15, however, there was a 22% reduction in production from 2016 to 2018.

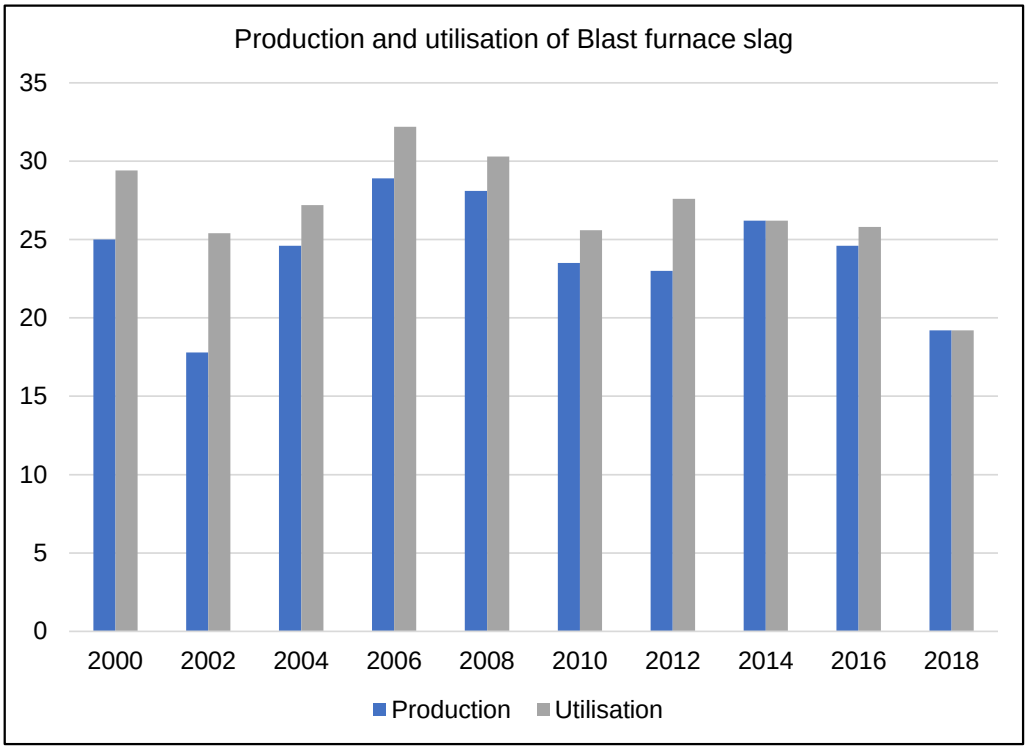

Figure 4.15: Production and utilisation of blast furnace slag in Europe (Euroslag, 2019).

Furthermore, CFA and GBFS are already competitive materials due to their use in other industries, mainly the cement and concrete industry, with 76 thousand tonnes of CFA and 113 thousand tonnes of GBFS consumed in Finland's cement industry in 2019 (Finnsementti Oy, 2020). This raises doubts about the future availability of these precursors. Alternative sources of both precursors can be imported from neighbouring countries that still actively combust coal and use blast furnaces and/or recovering CFAs that have been stockpiled. However, the implication of importation is an increase in costs due to processing and transportation, and increased transportation emissions. Other implications include dependency on other countries and impacts on the quality of CFA due to production processes and storage. This is also related to stockpiled CFA, where energy is required for recovery (Alberici et al., 2017). Alternatively, CFA production is increasing in China, with approximately 3 billion tonnes of CFA underutilised (Luo et al., 2021). Therefore, there is a possibility of the production of geopolymer composites in China. However, this will defeat the purpose of producing locally produced geopolymers. These concerns raise questions over the environmental and economic implications of the long-term production of geopolymers and their future sustainability.

Another alternative to combating the limited availability of these precursors is to consider other local industrial wastes with pozzolanic properties as supplementary cementitious

materials. Studies have been conducted to develop geopolymer binders using phosphate mine tailings and metakaolin as precursors, such as in the initial study included in this dissertation (Niu et al., 2020). Other potential precursors include paper sludge ash (Adesanya et al., 2018; Antunes Boca Santa et al., 2013; Frías et al., 2015), sewage sludge ash (Istuque et al., 2019), and bottom coal ash (Antunes Boca Santa et al., 2013; Ul Haq et al., 2014). This opens the possibilities of developing different suitable geopolymer composite mix designs for different countries based on the local availability of precursors, as the supply of industrial wastes is critical in the overall adoption of geopolymers. Exploring potential local precursors is an important direction for the future development of geopolymers and a better option than the transportation of precursors from different parts of the world.

5 Conclusions

The primary aim of this dissertation is to compare the environmental performance of geopolymer materials to conventional materials to support decision-making in the development of environmentally sustainable construction materials. The first sub-objective that helped fulfil this aim was to identify the most important factors contributing to the environmental performance of geopolymers that could be considered in future development by quantifying the environmental performance of different geopolymer binders and composite mix designs.

In the analysis of geopolymer binders (Publication I) and fibre reinforced geopolymer composites (FRGCs) (Publication II), LCAs of different mix designs were conducted, with PC (CEM I) as the reference scenario for geopolymer binders in Publication I, and PC concrete and steel fibre reinforced PC concrete as reference scenarios for the FRGCs in Publication II. Results from Publication I shows that the binder with the best environmental performance had 0.02 kg CO_2, eq./(MPa·kg) compared to the CEM I binder which had 0.1 kg CO_2, eq./(MPa·kg). The results from Publication I and II indicated that the alkali activator (sodium silicate) is the major contributor to the environmental impact of mix designs. Other major contributing materials include metakaolin and NaOH for the geopolymer binder and including steel and polypropylene fibre for the FRGCs. However, these other contributing materials are not used consistently in geopolymer development, apart from NaOH which is used to a lesser extent when compared to sodium silicate as an alkali activator. Furthermore, the mix designs with the best environmental performance among the FRGCs were steel fibre reinforced geopolymer composites (PII_S1) with 181 kg CO_2, eq./m^3, glass fibre reinforced geopolymer composites (PII_GF5) with 166 kg CO_2, eq./m^3 and polypropylene fibre reinforced geopolymer composites (PII_PP4) with 167 kg CO_2, eq./m^3. These mix designs have 4%-6% sodium silicate and 1% NaOH in their mix designs. PII_GF5 also included 2% PC in its mix design. By selecting these mix designs, 45% and 50% reductions in GWP can be achieved from PII_S1, PII_GF5 and PII_PP4, respectively, when compared to using PC concrete (330 kg CO_2, eq./m^3), and 58% and 61% reduction in GWP can be achieved from PII_S1 PII_GF5 and PII_PP4, respectively, when compared to using steel fibre reinforced PC concrete (429 kg CO_2, eq./m^3). Sensitivity analysis was conducted to determine the effects of employing alternative sodium silicate LCI data on FRGCs. The analysis reveals that the type of LCI data employed for sodium silicate can significantly influence the overall environmental performance results positively and negatively.

Based on the above results, the possibility of reducing the environmental impacts of sodium silicate alkali activator by substituting it with waste-derived alkali-silicate was studied. Thus, the second objective of this dissertation was to quantify the potential to improve the environmental performance of geopolymers by utilising chemically modified waste-derived alkali-silicates (from silica-rich waste materials such as glass waste and RHA) instead of conventional alkali-silicates. Powder alkali-silicate was produced from chemically modified glass waste (PIII_S3), while an aqueous alkali-silicate was produced

from chemically modified RHA (PIII_S4). By substituting geopolymer from conventional sodium silicate powder with geopolymer from glass waste alkali-silicate, GWP reduction will be 62% and by substituting geopolymer from conventional sodium silicate solution with geopolymer from RHA alkali-silicate, GWP reduction will be 67%. The GWP results for PIII_S1, PIII_S2, PIII_S3, and PIII_S4 are 202, 236, 86, and 86 kg CO_2, eq./m^3, respectively. Although the mix designs in which the results are based were from literature studies and, quantitatively, the results are only valid for the respective studies, these environmental performance results still help guide the development of geopolymers in general. A sensitivity analysis was conducted to determine the effect of employing alternative NaOH production methods in geopolymer development. The results show that the type of production process can slightly impact the environmental performance of geopolymers. Additionally, the influence of mass-based allocated emissions for RHA, CFA, and GGBFS were considered, in addition to considering treatment of glass waste from unsorted public collection. The GWP results was 335, 347, 195, and 215 kg CO_2, eq./m^3, respectively for PIII_S1, PIII_S2, PIII_S3, and PIII_S4. Thus, mass allocation showed 47%-149% increased emissions when compared to no allocation. Nonetheless, comparing one- and two-part geopolymer mortar from chemically modified glass waste (PIII_S3) and RHA alkali-silicate (PIII_S4) to one- and two-part geopolymer mortars from conventional sodium silicate powder (PIII_S1) and sodium silicate solution (PIII_S2), show that PIII_S3 has 42% reduced emissions in GWP when compared to PIII_S1, and PIII_S4 shows 38% reduced emissions in GWP when compared to PIII_S2.

The results from the above studies supported decision-making and guided the development of geopolymer composite mix designs in a project involving LUT universities and partners. These geopolymer composite mix designs were developed to reduce environmental impacts by minimising the use of alkali activators and natural precursors, such as metakaolin, in the mix design. To further determine the environmental impact of the use and end-of-life phases of these geopolymer composites, a pilot case study product was required. The case study product was an LHNB, for which an LCA study was carried out. Hence, the final sub-objective was to quantify and compare the environmental performance of an LHNB made from PC concrete or geopolymer composites, identify hotspots, and evaluate the impact of product system changes on the performance. Due to differences in the compressive strength of the different mix designs (PIV_S0-PIV_S4), compressive strength at 28 days and an estimated service life (40 years) were used as indicators to assess the environmental performance of the LHNB. The main results from the mix design point of view show the possibility of developing a geopolymer composite LHNB from 83% weight-% of industrial wastes and by-products, and 0.3% weight-% of alkali activator with GWP of 0.8 kg CO_2, eq./(MPa·20m·years). The overall LCA results shows GWP reduction of 73% was achieved when compared to the reference scenario (PIV_S0) with GWP of 3.2 kg CO_2, eq./(MPa·20m·years). From the perspective of the life-cycle phases, 270 and 27 kg CO_2 eq./20m of CO_2 uptake can be achieved in the use phase of PIV_S0 and PIV_S3 which are the only scenarios with cement content, while in the end-of-life phase, 36 and 4 kg CO_2 eq./20m CO_2 uptake can be achieved in PIV_S0 and PIV_S3. Additive manufacturing integration in the

geopolymers created a sustainable advantage. Regarding product system changes, sensitivity analysis was carried out by varying the service life from 10-40 years for the geopolymer LHNB. This is due to differences in compressive strengths which can lead to differences in service life. Results of sensitivity analysis shows that PIV_S4 had the best environmental performance overall at the different years when compared to PIV_S0, PIV_S1, PIV_S2 and PIV_S3.

In conclusion, this dissertation explored the environmental sustainability of geopolymer composites using LCA methodology. The dissertation also examined the influence of different materials and production processes on the LCA results and was conducted to guide and support decision-making in the development of geopolymer composites for sustainable construction. Generally, suitable material availability will determine the composition and the amount of PC concrete that can be locally substituted with geopolymer composites. However, based on the results from this dissertation, we are now in a position to reduce the contribution of PC production to global CO_2 emissions, by substituting with more environmentally sustainable geopolymer composites, bringing us closer to the goal of EU climate target in GHG emissions reduction.

References

Abdulkareem, M., Havukainen, J., Horttanainen, M., 2019. How environmentally sustainable are fibre reinforced alkali-activated concretes? J. Clean. Prod. 236. https://doi.org/10.1016/j.jclepro.2019.07.076

Abdulkareem, M., Havukainen, J., Nuortila-Jokinen, J., Horttanainen, M., 2021a. Environmental and economic perspective of waste-derived activators on alkali-activated mortars. J. Clean. Prod. 280, 124651. https://doi.org/10.1016/j.jclepro.2020.124651

Abdulkareem, M., Havukainen, J., Nuortila-Jokinen, J., Horttanainen, M., 2021b. Life cycle assessment of a low-height noise barrier for railway traffic noise. J. Clean. Prod. 323, 129169. https://doi.org/10.1016/j.jclepro.2021.129169

Adesanya, E., Ohenoja, K., Luukkonen, T., Kinnunen, P., Illikainen, M., 2018. One-part geopolymer cement from slag and pretreated paper sludge. J. Clean. Prod. 185, 168–175. https://doi.org/10.1016/j.jclepro.2018.03.007

Al-mashhadani, M.M., Canpolat, O., Aygörmez, Y., Uysal, M., Erdem, S., 2018. Mechanical and microstructural characterization of fiber reinforced fly ash based geopolymer composites. Constr. Build. Mater. 167, 505–513. https://doi.org/10.1016/j.conbuildmat.2018.02.061

Alberici, S., De Beer, J., Van Der Hoorn, I., Staats, M., 2017. Fly ash and blast furnace slag for cement manufacturing. BEIS Res. Pap. no. 19 35, 35.

Alomayri, T., 2017a. Effect of glass microfibre addition on the mechanical performances of fly ash-based geopolymer composites. J. Asian Ceram. Soc. 5, 334–340. https://doi.org/10.1016/J.JASCER.2017.06.007

Alomayri, T., 2017b. The microstructural and mechanical properties of geopolymer composites containing glass microfibres. Ceram. Int. 43, 4576–4582. https://doi.org/10.1016/j.ceramint.2016.12.118

Alomayri, T., Low, I.M., 2013. Synthesis and characterization of mechanical properties in cotton fiber-reinforced geopolymer composites. J. Asian Ceram. Soc. 1, 30–34. https://doi.org/10.1016/j.jascer.2013.01.002

Amorim Júnior, N.S., Andrade Neto, J.S., Santana, H.A., Cilla, M.S., Ribeiro, D. V., 2021. Durability and service life analysis of metakaolin-based geopolymer concretes with respect to chloride penetration using chloride migration test and corrosion potential. Constr. Build. Mater. 287, 122970. https://doi.org/10.1016/J.CONBUILDMAT.2021.122970

Andersson, R., Stripple, H., Gustafsson, T., Ljungkrantz, C., 2019. Carbonation as a

method to improve climate performance for cement based material. Cem. Concr. Res. 124, 105819. https://doi.org/10.1016/j.cemconres.2019.105819

Andrew, R.M., 2018a. Global CO2 emissions from cement production. Earth Syst. Sci. Data 10, 195–217. https://doi.org/10.5194/essd-10-195-2018

Andrew, R.M., 2018b. Global CO 2 emissions from cement production. Earth Syst. Sci. Data 105194, 195–21710.

Antunes Boca Santa, R.A., Bernardin, A.M., Riella, H.G., Kuhnen, N.C., 2013. Geopolymer synthetized from bottom coal ash and calcined paper sludge. J. Clean. Prod. 57, 302–307. https://doi.org/10.1016/j.jclepro.2013.05.017

APILA Group, 2020. Apila Group [WWW Document]. URL https://www.apilagroup.fi/en/ (accessed 11.10.20).

Arenas, C., Luna-Galiano, Y., Leiva, C., Vilches, L.F., Arroyo, F., Villegas, R., Fernández-Pereira, C., 2017. Development of a fly ash-based geopolymeric concrete with construction and demolition wastes as aggregates in acoustic barriers. Constr. Build. Mater. 134, 433–442. https://doi.org/10.1016/j.conbuildmat.2016.12.119

Bai, C.:, Shi, Y., Fabian, S., Li, K.T. V, Xu, H., 2014. Microwave Curing Techniques for Manufacturing Alkali-activated Fly Ash. Paper presented at the 34th Annual Cement and Concrete Science Conference.

Bajpai, R., Choudhary, K., Srivastava, A., Sangwan, K.S., Singh, M., 2020. Environmental impact assessment of fly ash and silica fume based geopolymer concrete. J. Clean. Prod. 254, 120147. https://doi.org/10.1016/j.jclepro.2020.120147

Bendtsen, H., 2010. Noise Barrier Design: Danish and Some European Examples.

BS-EN 197-1, 2011. Cement Part 1: Composition, specifications and conformity criteria for common cements, BSI Standards Publication.

BS-EN197-1:, 2011. Cement Part 1: Composition, Specifications and Conformity Criteria for Common Cements. Br. Stand. 50.

CEMBUREAU, 2019. 2019 Activity Report.

CEMBUREAU, 2015a. Environmental Product Declaration (EPD) Portland Cement (CEM I) produced in Europe.

CEMBUREAU, 2015b. Environmental Product Declaration (EPD) Portland-composite cement (CEM II). https://doi.org/10.4324/9781315270326-75

CEMBUREAU, 2015c. Environmental Product Declaration (EPD) Blast furnace cement

(CEM III). https://doi.org/10.4324/9781315270326-75

Chen, C., Habert, G., Bouzidi, Y., Jullien, A., 2010a. Environmental impact of cement production: detail of the different processes and cement plant variability evaluation. J. Clean. Prod. 18, 478–485. https://doi.org/10.1016/j.jclepro.2009.12.014

Chen, C., Habert, G., Bouzidi, Y., Jullien, A., 2010b. Environmental impact of cement production: detail of the different processes and cement plant variability evaluation. J. Clean. Prod. 18, 478–485. https://doi.org/10.1016/j.jclepro.2009.12.014

Chen, C., Habert, G., Bouzidi, Y., Jullien, A., Ventura, A., 2010c. LCA allocation procedure used as an incitative method for waste recycling: An application to mineral additions in concrete. Resour. Conserv. Recycl. 54, 1231–1240. https://doi.org/10.1016/j.resconrec.2010.04.001

CIMSA, 2015. Environmental Product Declaration - Çimsa Çimento San. Ve Tic. A.Ş.

Crossin, E., Carre, A., 2012. Comparative Life Cycle Assessment of Concrete blends.

Davidovits, J., 2015. False Values on CO2 Emission for Geopolymer Cement/Concrete published in Scientific Papers, Technical Paper #24, Geopolymer Institute Library, www.geopolymer.org.

Davidovits, J., 1994. Properties of Geopolymer cements, Alkaline Cements and Concretes.

Duxson, P., Provis, J.L., 2008. Designing precursors for geopolymer cements. J. Am. Ceram. Soc. 91, 3864–3869. https://doi.org/10.1111/j.1551-2916.2008.02787.x

EC-JRC, 2010. International reference Life Cycle Data system (ILCD) handbook - General guide for Life Cycle Assessment - Detailed guidance, International Reference Life Cycle Data System (ILCD) Handbook -- General guide for Life Cycle Assessment -- Detailed guidance. Luxembourg. https://doi.org/10.2788/38479

ECOBA, 2016. ecoba European Coal Combustion Products Association Production [WWW Document]. URL http://www.ecoba.com/ecobaccpprod.html (accessed 3.16.21).

EFCA European Federation of Concrete Admixtures Asssociations Ltd. [WWW Document], 2015. . EPD-EFC-20150091-IAG1-EN. URL http://www.efca.info/efca-publications/environmental/ (accessed 9.3.18).

Environmental Protection Department Highways Department, 2003. Guidelines On Design of Noise Barriers.

EU, 2014. Production of Chlor-Alkali.

EU, 2007. Reference Docunent on Best Available Techniques for the Manufacture of Large Volume Inorganic Chemicals -Solids and Others Industry. Eur. Comm. BREF-LVI, 1–711.

Euromines, 2019. Production by mineral | Euromines [WWW Document]. URL http://www.euromines.org/mining-europe/production-mineral#Kaolin (accessed 4.5.21).

European Parliament and Council, 2008. Directive 2008/98/EC of the European Parliament and of the Council of 19 November 2008 on waste and repealing certain directives, Official Journal of the European Union. https://doi.org/2008/98/EC.; 32008L0098

Euroslag, 2019. Iron and steel mining slags (ferrous slags) Statistics 2018 [WWW Document]. URL https://www.euroslag.com/products/statistics/statistics-2018/ (accessed 4.5.21).

Eurostat, 2020a. Waste statistics - Statistics Explained. 08.12.2020.

Eurostat, 2020b. Coal production and consumption statistics [WWW Document]. URL https://ec.europa.eu/eurostat/statistics-explained/index.php?title=Coal_production_and_consumption_statistics (accessed 5.25.21).

Fatec, 2020. Fatec Oy [WWW Document]. URL http://www.fatec.fi/en.html (accessed 5.12.21).

Fawer, M., Concannon, M., Rieber, W., 1999. Life cycle inventories for the production of sodium silicates. Int. J. Life Cycle Assess. 4, 207–212. https://doi.org/10.1007/BF02979498

Finnsementti Oy, 2020. Ympäristöraportti 2020.

Frías, M., Rodríguez, O., Sánchez De Rojas, M.I., 2015. Paper sludge, an environmentally sound alternative source of MK-based cementitious materials. A review. Constr. Build. Mater. https://doi.org/10.1016/j.conbuildmat.2014.10.007

Gagg, C.R., 2014. Cement and concrete as an engineering material: An historic appraisal and case study analysis. Eng. Fail. Anal. 40, 114–140. https://doi.org/10.1016/J.ENGFAILANAL.2014.02.004

Ganesan, N., Abraham, R., Deepa Raj, S., 2015. Durability characteristics of steel fibre reinforced geopolymer concrete. Constr. Build. Mater. 93, 471–476. https://doi.org/10.1016/j.conbuildmat.2015.06.014

Ghosh, R., 2013. A Review Study on Precipitated Silica and Activated Carbon from Rice Husk. J. Chem. Eng. Process Technol. 04. https://doi.org/10.4172/2157-7048.1000156

Glass Alliance Europe, 2019. Glass industries - Glass Alliance Europe [WWW Document]. URL https://www.glassallianceeurope.eu/en/industries (accessed 5.10.21).

Gursel, A.P., Maryman, H., Ostertag, C., 2016. A life-cycle approach to environmental, mechanical, and durability properties of "green" concrete mixes with rice husk ash. J. Clean. Prod. 112, 823–836. https://doi.org/10.1016/J.JCLEPRO.2015.06.029

Habert, G., D'Espinose De Lacaillerie, J.B., Roussel, N., 2011. An environmental evaluation of geopolymer based concrete production: Reviewing current research trends. J. Clean. Prod. 19, 1229–1238. https://doi.org/10.1016/j.jclepro.2011.03.012

Hasnaoui, A., Ghorbel, E., Wardeh, G., 2019. Optimization approach of granulated blast furnace slag and metakaolin based geopolymer mortars. Constr. Build. Mater. 198, 10–26. https://doi.org/10.1016/J.CONBUILDMAT.2018.11.251

Heath, A., Paine, K., McManus, M., 2014. Minimising the global warming potential of clay based geopolymers. J. Clean. Prod. 78, 75–83. https://doi.org/10.1016/j.jclepro.2014.04.046

Huang, R., Riddle, M.E., Graziano, D., Das, S., Nimbalkar, S., Cresko, J., Masanet, E., 2017. Environmental and Economic Implications of Distributed Additive Manufacturing: The Case of Injection Mold Tooling. J. Ind. Ecol. 21, S130–S143. https://doi.org/10.1111/jiec.12641

Hukkanen, V., 2019. Suomi haluaa olla ykkösten joukossa kivihiilestä luopujana – Puola, Kiina, Kreikka rakentavat samaan aikaan lisää hiilivoimaa | Yle Uutiset | yle.fi. Yle.

ISO 14040, 2006. Management environnemental - Life cycle assessment - Principles and framework, IS0 International Organization for Standardization.

ISO 14044, 2007. Environmental Management. Life Cycle Assessment. Requirements and Guidelines. IS0 Int. Organ. Stand. 3, 16.

Istuque, D.B., Soriano, L., Akasaki, J.L., Melges, J.L.P., Borrachero, M.V., Monzó, J., Payá, J., Tashima, M.M., 2019. Effect of sewage sludge ash on mechanical and microstructural properties of geopolymers based on metakaolin. Constr. Build. Mater. 203, 95–103. https://doi.org/10.1016/J.CONBUILDMAT.2019.01.093

Jäppinen, P., 2017. Electricity consumption for 3D printing.

Kawai, K., Sugiyama, T., Kobayashi, K., Sano, S., 2005. Inventory data and case studies

for environmental performance evaluation of concrete structure construction. J. Adv. Concr. Technol. 3, 435–456. https://doi.org/10.3151/jact.3.435

Keawthun, M., Krachodnok, S., Chaisena, A., 2014. Conversion of waste glasses into sodium silicate solutions. Int. J. Chem. Sci. 12, 83–91.

Khan, M.Z.N., Hao, Y., Hao, H., Shaikh, F.U.A., 2018. Mechanical properties of ambient cured high strength hybrid steel and synthetic fibers reinforced geopolymer composites. Cem. Concr. Compos. 85, 133–152. https://doi.org/10.1016/j.cemconcomp.2017.10.011

Kikuchi, T., Kuroda, Y., 2011. Carbon dioxide uptake in demolished and crushed concrete. J. Adv. Concr. Technol. 9, 115–124. https://doi.org/10.3151/jact.9.115

Liikanen, M., Havukainen, J., Hupponen, M., Horttanainen, M., 2017. Influence of different factors in the life cycle assessment of mixed municipal solid waste management systems – A comparison of case studies in Finland and China. J. Clean. Prod. 154, 389–400. https://doi.org/10.1016/J.JCLEPRO.2017.04.023

Liikennevirasto, 2017. Radan matalan meluesteen tuotevaatimukset (in Finnish). Liikennevirasto.

Liu, X., Li, Z., Chen, H., Yang, L., Tian, Y., Wang, Z., 2016. Rice husk ash as a renewable source for synthesis of sodium metasilicate crystal and its characterization. Res. Chem. Intermed. 42, 3887–3903. https://doi.org/10.1007/s11164-015-2251-7

Liu, Z., Jiang, Q., Cong, W., Li, T., Zhang, H.-C., 2018. Comparative study for environmental performances of traditional manufacturing and directed energy deposition processes. Int. J. Environ. Sci. Technol. 15, 2273–2282. https://doi.org/10.1007/s13762-017-1622-6

LUKE, 2017. Biomass atlas [WWW Document]. URL https://biomassa-atlas.luke.fi/?lang=en (accessed 4.26.21).

Luo, Y., Wu, Y., Ma, S., Zheng, S., Zhang, Y., Chu, P.K., 2021. Utilization of coal fly ash in China: a mini-review on challenges and future directions. Environ. Sci. Pollut. Res. 28, 18727–18740. https://doi.org/10.1007/s11356-020-08864-4

Luukkonen, T., Abdollahnejad, Z., Yliniemi, J., Kinnunen, P., Illikainen, M., 2018. One-part alkali-activated materials: A review. Cem. Concr. Res. 103, 21–34. https://doi.org/10.1016/j.cemconres.2017.10.001

Ma, X., Zhou, B., Gao, W., Qu, Y., Wang, L., Wang, Z., Zhu, Y., 2012. A recyclable method for production of pure silica from rice hull ash. Powder Technol. 217, 497–501. https://doi.org/10.1016/J.POWTEC.2011.11.009

Marceau, M., VanGeem, M.G., 2003. Life Cycle Inventory of Slag Cement Manufacturing Process CTL Project No. 312012.

Marinković, S., Carević, V., Dragaš, J., 2021. The role of service life in Life Cycle Assessment of concrete structures. J. Clean. Prod. 290, 125610. https://doi.org/10.1016/J.JCLEPRO.2020.125610

McGuire, E.M., Provis, J.L., Duxson, P., Crawford, R., 2011. Geopolymer concrete: Is there an alternative and viable technology in the concrete sector which reduces carbon emissions?, in: Concrete 2011. p. CD-ROM Proceedings.

Mellado, A., Catalán, C., Bouzón, N., Borrachero, M. V., Monzó, J.M., Payá, J., 2014. Carbon footprint of geopolymeric mortar: Study of the contribution of the alkaline activating solution and assessment of an alternative route. RSC Adv. 4, 23846–23852. https://doi.org/10.1039/c4ra03375b

Meryman, H., 2009. The Emergence of Rice Husk Ash — A Complimentary Cementing Material with Untapped Global Potential, in: Structures Congress 2009. American Society of Civil Engineers, Reston, VA, pp. 1–10. https://doi.org/10.1061/41031(341)274

Mohseni, E., 2018. Assessment of Na2SiO3to NaOH ratio impact on the performance of polypropylene fiber-reinforced geopolymer composites. Constr. Build. Mater. 186, 904–911. https://doi.org/10.1016/j.conbuildmat.2018.08.032

Morgan, S.M., Kay, D.H., Bodapati, S.N., 2001. Study of Noise Barrier Life-Cycle Costing. J. Transp. Eng. 127, 230–236. https://doi.org/10.1061/(ASCE)0733-947X(2001)127:3(230)

Müller, H.S., Moffatt, J.S., Haist, M., Vogel, M., 2019. A New Generation of Sustainable Structural Concretes-Design Approach and Material Properties, in: IOP Conference Series: Earth and Environmental Science. p. 012002. https://doi.org/10.1088/1755-1315/290/1/012002

Nematollahi, B., Sanjayan, J., Chai, J.X.H., Lu, T.M., 2014. Properties of Fresh and Hardened Glass Fiber Reinforced Fly Ash Based Geopolymer Concrete. Key Eng. Mater. 594–595, 629–633. https://doi.org/10.4028/www.scientific.net/KEM.594-595.629

Nematollahi, B., Sanjayan, J., Qiu, J., Yang, E.H., 2017. High ductile behavior of a polyethylene fiber-reinforced one-part geopolymer composite: A micromechanics-based investigation. Arch. Civ. Mech. Eng. 17, 555–563. https://doi.org/10.1016/j.acme.2016.12.005

Nematollahi, B., Sanjayan, J., Shaikh, F.U.A., 2015. Synthesis of heat and ambient cured one-part geopolymer mixes with different grades of sodium silicate. Ceram. Int. 41,

5696–5704. https://doi.org/10.1016/j.ceramint.2014.12.154

Niu, H., Abdulkareem, M., Sreenivasan, H., Kantola, A.M., Havukainen, J., Horttanainen, M., Telkki, V.V., Kinnunen, P., Illikainen, M., 2020. Recycling mica and carbonate-rich mine tailings in alkali-activated composites: A synergy with metakaolin. Miner. Eng. 157, 106535. https://doi.org/10.1016/j.mineng.2020.106535

NLK, 2002. Ecosmart concrete project: Metakaolin Pre-feasibility study, Report EA2860. Vancouver, British Columbia.

Parker, G., 2006. Effective noise barrier design and specification. 1st Australas. Acoust. Soc. Conf. 2006, Acoust. 2006 Noise Prog. 349–353.

Passuello, A., Rodríguez, E.D., Hirt, E., Longhi, M., Bernal, S.A., Provis, J.L., Kirchheim, A.P., 2017. Evaluation of the potential improvement in the environmental footprint of geopolymers using waste-derived activators. J. Clean. Prod. 166, 680–689. https://doi.org/10.1016/j.jclepro.2017.08.007

Patil, S.S., Patil, A.A., 2015. Properties of Polypropylene Fiber Reinforced Geopolymer Concrete 5, 2909–2912.

Provis, J.L., 2018. Alkali-activated materials. Cem. Concr. Res. https://doi.org/10.1016/j.cemconres.2017.02.009

Rai, A., Joshi, Y.P., 2014. Applications and Properties of Fibre Reinforced Concrete. J. Eng. Res. Appl. 4, 123–131.

Ranjbar, N., Mehrali, Mehdi, Behnia, A., Javadi Pordsari, A., Mehrali, Mohammad, Alengaram, U.J., Jumaat, M.Z., 2016. A Comprehensive Study of the Polypropylene Fiber Reinforced Fly Ash Based Geopolymer. PLoS One 11, e0147546. https://doi.org/10.1371/journal.pone.0147546

Saade, M.R.M., Silva, M.G. Da, Gomes, V., 2015. Appropriateness of environmental impact distribution methods to model blast furnace slag recycling in cement making. Resour. Conserv. Recycl. 99, 40–47. https://doi.org/10.1016/j.resconrec.2015.03.011

Saade, M.R.M., Yahia, A., Amor, B., 2020. How has LCA been applied to 3D printing? A systematic literature review and recommendations for future studies. J. Clean. Prod. 244, 118803. https://doi.org/10.1016/j.jclepro.2019.118803

Salas, D.A., Ramirez, A.D., Ulloa, N., Baykara, H., Boero, A.J., 2018. Life cycle assessment of geopolymer concrete. Constr. Build. Mater. 190, 170–177. https://doi.org/10.1016/j.conbuildmat.2018.09.123

Sandanayake, M., Gunasekara, C., Law, D., Zhang, G., Setunge, S., 2018. Greenhouse gas emissions of different fly ash based geopolymer concretes in building construction. J. Clean. Prod. 204, 399–408. https://doi.org/10.1016/j.jclepro.2018.08.311

Sedira, N., Castro-Gomes, J., Kastiukas, G., Zhou, X., Vargas, A., 2017. A review on mineral waste for chemical-activated binders: Mineralogical and chemical characteristics. Min. Sci. https://doi.org/10.5277/msc172402

Seto, K.E., Churchill, C.J., Panesar, D.K., 2017. Influence of fly ash allocation approaches on the life cycle assessment of cement-based materials. J. Clean. Prod. 157, 65–75. https://doi.org/10.1016/j.jclepro.2017.04.093

Sphera, 2021. What is GaBi Software [WWW Document]. URL http://www.gabi-software.com/overview/what-is-gabi-software/ (accessed 4.1.21).

SPhera, 2021. Life Cycle Impact Assessment (LCIA) methods [WWW Document]. URL http://www.gabi-software.com/finland/support/gabi/gabi-5-lcia-documentation/life-cycle-impact-assessment-lcia-methods/ (accessed 4.1.21).

SSAB, 2021. Ensimmäinen fossiilivapaissa teräksissä HYBRIT-teknologian avulla [WWW Document]. URL https://www.ssab.fi/ssab-konserni/kestava-kehitys/kestavat-toiminnot/hybrit (accessed 5.1.21).

Stajanca, M., Estokova, A., 2012. Environmental Impacts of Cement Production. Tech. Univ. Kosice, Civ. Eng. Fac. Inst. Archit. Eng. 296–302.

Stripple, H., Ljungkrantz, C., Gustafsson, T., Andersson, R., 2018. CO 2 uptake in cement-containing products Background and calculation models for IPCC implementation Commissioned by Cementa AB and IVL research foundation.

Tahvanainen, T., 2020. Electricity consumption of casting.

Tchakouté, H.K., Rüscher, C.H., Hinsch, M., Djobo, J.N.Y., Kamseu, E., Leonelli, C., 2017. Utilization of sodium waterglass from sugar cane bagasse ash as a new alternative hardener for producing metakaolin-based geopolymer cement. Geochemistry 77, 257–266. https://doi.org/10.1016/J.CHEMER.2017.04.003

Tchakouté, H.K., Rüscher, C.H., Kong, S., Kamseu, E., Leonelli, C., 2016. Comparison of metakaolin-based geopolymer cements from commercial sodium waterglass and sodium waterglass from rice husk ash. J. Sol-Gel Sci. Technol. 78, 492–506. https://doi.org/10.1007/s10971-016-3983-6

Teh, S.H., Wiedmann, T., Castel, A., de Burgh, J., 2017. Hybrid life cycle assessment of greenhouse gas emissions from cement, concrete and geopolymer concrete in Australia. J. Clean. Prod. 152, 312–320.

https://doi.org/10.1016/j.jclepro.2017.03.122

Tong, K.T., Vinai, R., Soutsos, M.N., 2018. Use of Vietnamese rice husk ash for the production of sodium silicate as the activator for alkali-activated binders. J. Clean. Prod. 201, 272–286. https://doi.org/10.1016/J.JCLEPRO.2018.08.025

Ul Haq, E., Kunjalukkal Padmanabhan, S., Licciulli, A., 2014. Synthesis and characteristics of fly ash and bottom ash based geopolymers-A comparative study. Ceram. Int. 40, 2965–2971. https://doi.org/10.1016/j.ceramint.2013.10.012

Vahtera, E., 2011. Raidemelun vaimennuskyky matalien meluesteiden tuotevaatimuksena (in Finnish).

Valdebenito, M.J., Dahmen, J., 2013. Life Cycle Assessment Screening: Environmental Impacts of a Novel Vegetative Sound Structure Authors.

Van Den Heede, P., De Belie, N., 2012. Environmental impact and life cycle assessment (LCA) of traditional and "green" concretes: Literature review and theoretical calculations. Cem. Concr. Compos. 34, 431–442. https://doi.org/10.1016/j.cemconcomp.2012.01.004

Vieira, D.R., Calmon, J.L., Zulcão, R., Coelho, F.Z., 2018. Consideration of strength and service life in cradle-to-gate life cycle assessment of self-compacting concrete in a maritime area: a study in the Brazilian context. Environ. Dev. Sustain. 20, 1849–1871. https://doi.org/10.1007/s10668-017-9970-4

Vijai, K., Kumutha, R., Vishnuram, B.G., 2012a. Effect Of Inclusion Of Steel Fibres On The Properties Of Geopolymer Concrete Composites 13, 381–389.

Vijai, K., Kumutha, R., Vishnuram, B.G., 2012b. Properties Of Glass Fibre Reinforced Geopolymer Concrete Composites. Asian J. Civ. Eng. (Building Housing) 13, 511–520.

Vinai, R., Soutsos, M., 2019. Production of sodium silicate powder from waste glass cullet for alkali activation of alternative binders. Cem. Concr. Res. 116, 45–56. https://doi.org/10.1016/j.cemconres.2018.11.008

Výtisk, J., Kočí, V., Honus, S., Vrtek, M., 2019. Current options in the life cycle assessment of additive manufacturing products. Open Eng. 9, 674–682. https://doi.org/10.1515/eng-2019-0073

Weidema, B.P., Bauer, C., Hischier, R., Mutel, C., Nemecek, T., Reinhard, J., Vadenbo, C.O., Wernet, G., 2013. Overview and methodology. Data quality guideline for the ecoinvent database version 3.

Weil, M., Gasafi, E., Buchwald, A., Dombrowski, K., Buchwald, A., 2005. Sustainable

Design of Geopolymers - Integration of Economic and Environmental Aspects in the Early Stages of Material Development. 11th Annu. Int. Sustain. Dev. Res. Conf. 279–283.

Wescott, R.F., Mcnulty, M.W., Vangeem, M.G., Gajda, J., 2010. Prospects for Expanding the Use of Supplementary Cementitious Materials in California.

World Steel Association, 2020. 2020 World steel in figures, 2020 World steel in figures.

Wu, K., Zhang, D., 2018. Cement-Based Composite Materials, in: Composite Materials Engineering, Volume 2. Springer Singapore, Singapore, pp. 489–529. https://doi.org/10.1007/978-981-10-5690-1_4

Xia, M., Muhammad, F., Zeng, L., Li, S., Huang, X., Jiao, B., Shiau, Y.C., Li, D., 2019. Solidification/stabilization of lead-zinc smelting slag in composite based geopolymer. J. Clean. Prod. 209, 1206–1215. https://doi.org/10.1016/j.jclepro.2018.10.265

Yang, K.-H., Song, J.-K., Lee, J.-S., 2010. Properties of alkali-activated mortar and concrete using lightweight aggregates. Mater. Struct. 43, 403–416. https://doi.org/10.1617/s11527-009-9499-6

Yao, Y., Hu, M., Di Maio, F., Cucurachi, S., 2020. Life cycle assessment of 3D printing geo-polymer concrete: An ex-ante study. J. Ind. Ecol. 24, 116–127. https://doi.org/10.1111/jiec.12930

Zhang, Z., Wu, X., Yang, X., Zhu, Y., 2006. BEPAS - A life cycle building environmental performance assessment model. Build. Environ. 41, 669–675. https://doi.org/10.1016/j.buildenv.2005.02.028

Zhuang, X.Y., Chen, L., Komarneni, S., Zhou, C.H., Tong, D.S., Yang, H.M., Yu, W.H., Wang, H., 2016. Fly ash-based geopolymer: clean production, properties and applications. J. Clean. Prod. 125, 253–267. https://doi.org/10.1016/J.JCLEPRO.2016.03.019

Publication I

Niu, H., Abdulkareem, M., Sreenivasan, H., Kantola, A.M., Havukainen, J., Horttanainen, M., Telkki, V.V., Kinnunen, P., and Illikainen, M.
Recycling mica and carbonate-rich mine tailings in alkali-activated composites: A synergy with metakaolin.

Reprinted with permission from
Journal of Minerals Engineering
Vol. 157, pp. 106535, 2020

Minerals Engineering 157 (2020) 106535

Contents lists available at ScienceDirect

Minerals Engineering

journal homepage: www.elsevier.com/locate/mineng

Recycling mica and carbonate-rich mine tailings in alkali-activated composites: A synergy with metakaolin

He Niu[a], Mariam Abdulkareem[b], Harisankar Sreenivasan[a], Anu M. Kantola[c], Jouni Havukainen[b], Mika Horttanainen[b], Ville-Veikko Telkki[c], Paivo Kinnunen[a,*], Mirja Illikainen[a]

[a] Fibre and Particle Engineering Research Unit, University of Oulu, P.O. Box 4300, FI-90570 Oulu, Finland
[b] Lappeenranta-Lahti University of Technology, School of Energy Systems, Department of Sustainability Science, P.O. Box 20, FI-53851 Lappeenranta, Finland
[c] NMR Research Unit, Faculty of Science, University of Oulu, P.O. Box 3000, FI-90014 Oulu, Finland

ARTICLE INFO

Keywords:
Mine tailings
Metakaolin
Geopolymers
Gel chemistry
Life cycle assessment
Zeolite
Mechanochemical activation

ABSTRACT

The main objective of this paper was to investigate the alkali activation of mine tailings (MT) after mechanochemical activation and the effect of metakaolin (MK) addition. Finnish mica-rich tailings from a phosphate mine were studied as precursors for alkali-activated materials (AAM) with a potential application as a substitute for ordinary Portland cement (OPC). The principal physical properties (water absorption, apparent porosity and unconfined compressive strength) were measured for samples containing 30% to 70% tailings. Zeolite phases such as natrolite and cancrinite were observed and the formation of C-(N)-A-S-H[1] and N-A-S-H gels was identified by XRD, DRIFT, FESEM-EDS and NMR technologies. A life cycle assessment (LCA) was conducted on specimens in comparison to OPC. This work indicated that phosphate MT can be recycled through alkali activation with lower CO_2 emission compared to all-metakaolin geopolymers and that the binder phase formed at the most promising tailings contents (60– 70%) was C-(N)-A-S-H gel.

1. Introduction

Greenhouse gas emissions are a global issue and the leading cause of the global climate change. One tonne of Portland cement manufactured produces approximately one tonne of carbon dioxide (Hasanbeigi et al., 2010). Therefore, developing materials with lower CO_2 emission as alternative to the traditional Portland cement is important. Alkali-activated materials (AAM) are cementitious binders that have been investigated for several decades with respect to their excellent performances and mechanical properties, refractory, and acid resistance (Bakharev, 2005; Duxson et al., 2007; Novais et al., 2018; Vickers et al., 2015). AAM can contribute to reduce the carbon footprint, especially when waste materials, such as fly ash, slag, waste rocks and mine tailings are utilised (Kinnunen et al., 2018; MacKenzie et al., 2007; Maragkos et al., 2009; Rattanasak and Chindaprasirt, 2009).

AAM are produced from solid precursors under alkaline conditions, which involves both a high-calcium system and low-calcium system (geopolymer), containing C-(A)-S-H gel and N-A-S-H gel, respectively (Provis, 2013). Moreover, the coexistence of both cementitious binder gels; that is, C-(N)-A-S-H is possible. (Yip et al., 2005) The compatibility of C-S-H and N-A-S-H systems has been found to be highly susceptible to the threshold value of OH^- concentration, which also influences the gel formation sequences (Alonso and Palomo, 2001a; Alonso and Palomo, 2001b). Calcium addition has also been used to modify the N-A-S-H gels, forming (N,C)-A-S-H gels under high pH conditions (> 12) (García-Lodeiro et al., 2010). The product phase of sodium-silicate activation of Ca-containing aluminosilicate precursors consists of amorphous C-A-S-H gel along with C-(N)-A-S-H gel (Myers et al., 2015).

MT are currently underutilised industrial side streams, with potential to be used as a secondary raw material in AAM. The usual disposal of phosphate MT is done by transporting them to storage impoundments (Kauppila et al., 2013). The storage of tailings poses an environmental risk and cost money and energy for construction and maintenance. Therefore, the reprocessing and remediation of mining waste is an interesting alternative. The Siilinjärvi phosphate MT (Eastern Finland) consists of 65% phlogopite mica (2:1-layer lattice aluminosilicate) in addition to carbonates, silicates and apatite (O'Brien et al., 2015). It cannot be directly used for alkali activation due to its poor chemical reactivity. Furthermore, the gel formation of MT-based geopolymer is a complex issue as it depends on the specific minerals presenting in the tailings and has been little explored so far. Since MT are not highly reactive precursors, they have been mostly used in

* Corresponding author.
E-mail address: Paivo.Kinnunen@oulu.fi (P. Kinnunen).
[1] C-CaO, N-Na_2O, A-Al_2O_3, S-SiO_2, H-H_2O.

https://doi.org/10.1016/j.mineng.2020.106535
Received 30 March 2020; Received in revised form 11 June 2020; Accepted 29 June 2020

conjunction with reactive raw materials, such as metallurgical slag. Thermal analysis was successfully conducted on the tailings-slag geopolymers, indicating both C-S-H and C-A-S-H gels decomposition and recrystallisation (Ye et al., 2014a). Zhang et al. (Zhang, 2013) summarised that waste materials such as hematite tailings, gold MT, copper MT can be used for producing geopolymer bricks, among which the coexistence of $CaCO_3$ and N-A-S-H gel systems was achieved by introducing cement kiln dust for alkali activation (Ahmari and Zhang, 2013). These studies shed the light on the gel formation in tailings-based geopolymers and on how to guide the gel development in tailings-based geopolymers.

Pre-treatment is often necessary for MT before utilisation. S. Moukannaa et al. (Moukannaa et al., 2019, 2018) studied the heat treatment and alkaline fusion on phosphate MT, and they also investigated the alkali activation of such pre-treated tailings with fly ash and MK. Although that study carried out the recycling of phosphate MT, which consisted mainly of fluorapatite and quartz, and therefore the findings are not relevant to the utilisation of mica and carbonate-rich side streams in our study. In addition, high-temperature pre-treatments can be energy and time consuming compared to mechanochemical treatment, which is a more efficient and greener method (Boldyreva, 2013). Mechanochemical activation, especially intensive grinding, can generate internal stress, induced by shear force and impact between particles and grinding media. In our previous research, the amorphisation of phlogopite-bearing phosphate MT by mechanochemical activation was observed (Niu et al., 2020). Alkaline reactivity tests demonstrated that mechanochemical activation improved reactivity seen as increased silicon and aluminium dissolution rates in alkaline media. Mechanochemical activation has been conducted on different precursors, such as kaolin (Balczár et al., 2016), fly ash (Mucsi et al., 2015), natural minerals (MacKenzie et al., 2007) and vanadium MT (Wei et al., 2017) for the purpose of alkali activation; however, the effect of mechanochemical activation on mica-rich phosphate MT has not been studied.

Therefore, the aim of this work was to alkali-activate mechanochemical activated phosphate MT with various tailings/MK mass ratios and to investigate the mechanism of gel formation in this complex multi-mineral system. Thus, it might be possible to guide the utilisation of mine tailings as secondary materials for construction and building application. Life cycle assessment of the end-products was conducted and compared to similar construction materials based on ordinary Portland cement (OPC).

2. Materials and methods

The metakaolin (MK; MetaMax, Aquaminerals Finland Ltd) was purchased from BASF (Germany) and the phosphate MT were obtained from Siilinjärvi phosphate mining site (yearly production:10 Mt/a; Stock: 280 Mt), Finland, which mainly consists of phlogopite (64%), dolomite (6%), calcite (14%) and tremolite (1.4%). The chemical compositions of both MK and MT are provided in

Table 1. The sodium hydroxide (VWR Chemicals, > 97%) and sodium silicate solution (VWR Chemicals, SiO_2: 26.8%, Na_2O: 8.2%) were used as alkali activator. Twelve M NaOH solution was prepared before experiments and left overnight to cool down.

The MT were subjected to mechanochemical activation (Vibratory disc mill; Retsch RS 200) before alkali-activation according to our previous research. It indicated that 4-min ground raw tailings obtained a D50 of 7.22 μm and a BET surface area of 6.9745 ± 0.0210 m^2/g. In addition, it also generated around 40% of amorphous phase according to Rietveld refinement. The X-ray diffraction and DRIFT were also conducted on both precursors as provided in Fig. A1. The typical DRIFT bands of MK are shown in Fig. A1a, after which Table 1 provides the positions and assigned bands of MT. It should be noted that the shift of dolomite and calcite bands is significantly attributed to the pre-treatment and the Mg/Ca ratio in the initial composition. For instance, the bands in the range of 2600 to 2500 cm^{-1} can be assigned to the combination of ν_1 and ν_2 modes, which is in line with the previous studies (Gunasekaran and Anbalagan, n.d.; Nguyen et al., 1991). The morphologies of MK and mechanically activated MT are shown in Fig. A2 using scanning electron microscope (FESEM, Zeiss). The particle shape of MT is normally irregular as MK.

Table 2
Experimental mix design for alkali-activated materials.*

Sample name	PMT (Phosphate tailings)/wt %	MK (Metakaolin)/ wt%	H_2O/Na	Na/Al	Si/Al	Liquid/ solid
PM 0/10	0	100	4.31	0.59	1.31	0.45
PM 1/9	10	90	4.29	0.65	1.39	0.45
PM 2/8	20	80	4.07	0.72	1.49	0.45
PM 3/7	30	70	3.70	0.8	1.62	0.35
PM 4/6	40	60	3.69	0.9	1.77	0.35
PM 5/5	50	50	3.67	1.03	1.97	0.35
PM 6/4	60	40	3.65	1.2	2.24	0.35
PM 7/3	70	30	3.64	1.44	2.60	0.35
PM 8/2	80	20	2.54	1.79	3.14	0.3
PM 9/1	90	10	2.53	2.37	4.03	0.3
PM 10/0	100	0	4.07	3.47	5.72	0.40

* The calculated ratios are based on the assumption of fully reacted reactants.

2.1. Preparation of alkali-activated samples

The alkali-activation was subjected to the binary mixture of mechanochemically activated phosphate MT and MK. The mix design is given in Table 2. The mass ratio of sodium silicate solution and sodium hydroxide solution was fixed at 1.4 for all samples, which is based on the PM 5/5 where Na/Al and Si/Al ratios are 1 and 2 respectively. The liquid to solid ratio was variable due to the rheological properties of the slurry; however, the samples named through PM 3/7 to PM 7/3 had a constant liquid/solid mass ratio of 0.35. It requires a higher liquid/solid ratio from PM 0/10 to PM 2/8, while a lower ratio was applied for PM 8/2 to PM 9/1. Two precursors were dry-mixed for 5 min before alkali-activation. The slurry was thoroughly blended by a high shear mixer at 1000 rpm for 5 min; thereafter, it was shaped by using Polyethylene moulds with dimensions of 20 mm in height and 25 mm in diameter. The vibrating machine (Vortex-Genie 2, Prolab Oy) was used to remove all air bubbles. The samples were demoulded after curing at 40 °C for 24 h and then continuously cured in a sealed plastic bag for 7 days.

2.2. Sample characterisation

Physical properties, such as apparent porosity and water absorption were tested according to the standard EN-1936: 2006 (EN, 2007). After the preliminary UCS test of all the samples, subsequent

Table 1
Chemical composition of the raw materials by XRF analysis.

Sample	SiO_2	Al_2O_3	CaO	MgO	K_2O	Fe_2O_3	P_2O_5	TiO_2	MnO	Others	L.O.I.
PMT	32.99	7.09	12.92	17.27	5.53	7.99	0.95	0.27	0.12	0.86	14.01
MK	53	44.5	–	–	0.1	0.4	–	1.4	–	–	0.3

characterisations were conducted on five samples in particular through PM 3/7 to PM 7/3, since they were synthesised under the same L/S ratio. The 7-day cured samples were crushed into pieces and mounted for scanning electron microscopy (SEM). Apart from the SEM analysis, the fragments were ground manually using pestle and mortar and submerged in isopropanol to remove the loosely bound water, thereby ceasing the alkali activation. The resulted powders were subsequently stored in a desiccator until measurement.

X-ray diffraction analysis was subjected to a Rigaku SmartLab 4.5 kW, with the equipment parameters of Co source (40 kV and 135 mA) K_α ($K_{\alpha1}$ = 1.78892 Å; $K_{\alpha2}$ = 1.79278 Å; $K_{\alpha1}/K_{\alpha2}$ = 0.5), scan rate of 3°/min and 0.02°/step. The phase identification was conducted using the PDXL2 Software Suite with integrated PDF-4 (2019) database. Chemical characterisation of hardened samples was performed by using diffuse reflectance infrared Fourier transform (DRIFT). The spectra were collected using a Bruker Vertex 80v spectrometer (USA) with a range of 400 to 4,000 cm^{-1}, and 40 scans were taken at a resolution of 1 cm^{-1} for each sample. The morphology of AAM was characterised with Zeiss ULTRA plus FESEM, with an acceleration voltage of 5 kV. FESEM-EDS (Energy Dispersive X-ray Spectroscopy) analysis was conducted using FESEM with an acceleration voltage of 15 kV and beam current of 120 × 10^{-8} A. The polished cross-sections of PM samples were subjected to at least 50 points analysis under the magnification of ×3000 and the working distance was 6 to 8 mm. UCS was performed with the Zwick Roell 100 kN machine with a loading force of 3 mm/min until failure. Soaking tests were performed by immersing three hardened samples in deionised water (DI-water) for 24 h with a sample/water mass ratio of 1/3 for each batch, after which the liquid and the solid were subjected to the inductively coupled plasma-optical emission spectroscopy (ICP-OES) and UCS, respectively.

The ^{27}Al and ^{29}Si NMR spectra were obtained on a Bruker Advance III 300 spectrometer operating at 78.24 MHz for ^{27}Al and 59.65 MHz for ^{29}Si. For the purpose of conducting MAS experiments, the samples were packed into 7 mm zirconia rotors, then rotated with a frequency of 7 kHz. For ^{27}Al, 2048 scans were accumulated with a repetition rate of 2 s, and for ^{29}Si the corresponding parameters were 8192 scans and 3 s. Neither proton decoupling nor cross polarisation was used. The chemical shifts were referenced to $Al(NO_3)_3$ and TMS (tetramethylsilane), for which the reference shifts were set to zero ppm.

2.3. Life cycle assessment (LCA)

LCA is a method for assessing and evaluating potential environmental impacts of a product or system. It is performed in four phases: (1) goal and scope definition, (2) inventory phase, (3) impact assessment phase, and (4) interpretation phase (EN ISO 14040, 2006). This method has been applied in assessing the environmental impacts of numerous materials, including AAM (Abdulkareem et al., 2019; Passuello et al., 2017; Petrillo et al., 2016). The goal of the study is to estimate and compare impacts generated from developing alkali-activated binder from phosphate MT and MK in comparison to OPC. The study framework considers the four processes of cradle-to-gate alkali-activated binder formulations, including raw material production, waste beneficiation, mixing of constituents and associated emissions and energy consumptions. The functional unit is the production of 1 kg of binder. Excluded processes from this study include transportation as it is assumed all raw materials considered in this study are locally produced and have similar transportation distances. The use phase and end-of-life phase are also excluded from this study as it is assumed that comparable and similar impacts are expected from these phases.

The LCA study was performed using the Centrum voor Milieukunde Leiden (CML) 2016 method (Thinkstep, 2019). CML 2016 indicators provide information on the environmental issues associated with inputs and outputs of the product system (EN ISO 14040, 2006). This assessment principally focuses on global warming potential (GWP), acidification potential (AP), eutrophication potential (EP) and abiotic depletion potential (ADP fossil) impact categories. These impact categories are relevant for assessment of emissions generated during the production of binders (Chen et al., 2010a, Van Den Heede and De Belie, 2012), which is the central issue of this study. Moreover, the characterisation method for these impacts are better established than for the toxicity impacts, where both lack of reliable data and methodological uncertainty reduce their reliability (Merrild et al., 2012). The LCA modelling was performed using the GaBi LCA modelling software (version 8.6.0.20).

2.4. Life cycle inventory

Life cycle inventory (LCI) is the phase where all unit processes included in the system boundary are quantified. LCI data of the different processes considered in this study are listed in Appendix B. Data sources for Life cycle inventory Table B1. The data were collected from GaBi database, scientific literature and environmental reports from industrial organisations. Unit processes such as sodium hydroxide, water and electricity were sourced from the GaBi database. The unit process of sodium silicate solution was modelled following the approach and LCI data from (Fawer et al., 1999). This solution is produced by dissolving sodium silicate lumps in water at an elevated temperature and pressure to yield a solution with 37% of total solids which is thereafter filtered (Fawer et al., 1999). Data for energy production were adapted to the Finnish context, and geographical scope of this study was limited to Finland, thus, a Finnish dataset was used. Where dataset for Finland is unavailable, the EU-28 dataset was used. For the baseline study, CEM I as reported by (CEMBUREAU, 2015) was used as a basis of comparison. It composed about 92.5% clinker as main constituent and minor additional constituents. Environmental impacts of capital goods such as trucks, equipment, buildings were not taken into account in this study.

Oven curing is required for alkali-activated binder during production is essential for initiating chemical reaction of the binder at first instance. The energy consumed during curing in the lab was 1.87 MJ/kg at 40°C for 24 h. Mixing of the ingredients consumed 0.0045 MJ/kg and grinding of phosphate tailings consumed 1.25 MJ/kg in the lab. Kaolin as reported from the GaBi database was already dried and milled. However, to produce metakaolin, kaolin had to be calcined, consuming 2.5 MJ/kg of natural gas (Heath et al., 2014; NLK, 2002). The synthesis conditions for the alkali-activated binders are defined at laboratory scale. Thus, energy consumption is lower when full scale commercially tested technology is used.

3. Results and discussion

3.1. Physical properties

The 7-day UCS of alkali-activated binders are shown in Fig. 1a. The variation of MK amount had a profound impact on the mechanical properties of tailings-metakaolin based geopolymers. It should be noted that the mix design here is not optimal for the alkali-activation of MK, thereby the solely MK-based geopolymer obtained a rather low UCS. With lower amounts of substitution of MK by MT from 0% to 30%, the UCS of each sample does not change considerably. When the proportion of MT continuously increases, the growth of UCS can be seen until it reaches 70%, at which point it gains the highest UCS of more than 20 MPa. Thereafter, the UCS diminishes with the incremental MT content. The mix design of samples containing 30–70% MT was otherwise identical; therefore, the following characterisations were conducted on these specimens. The samples were specially dubbed as 'PM samples' in the following part of this article. Fig. 1b demonstrates the variation of PM samples for water absorption and apparent porosity. It is obvious that apparent porosity and water absorption substantially decreased from PM 6/4 to PM 7/3, indicating the formation of highly dense binder regarding to the Si/Al ratio close to 2.6. The apparent porosity has a good correlation with their strength results; that is, the

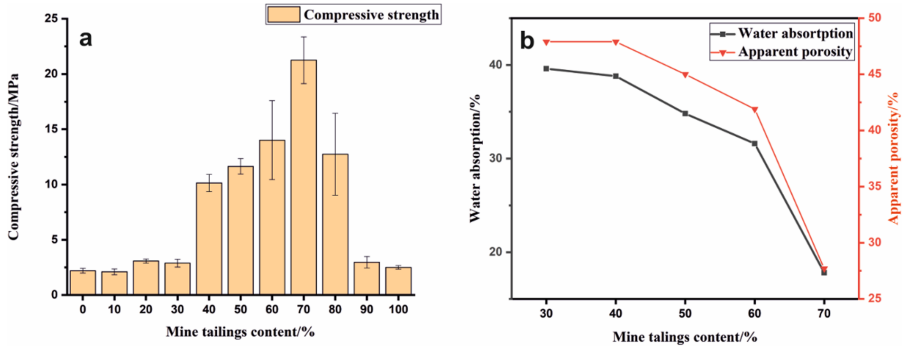

Fig. 1. (a) Compressive strength of tailings-metakaolin based geopolymers after 7 days of curing, (b) water absorption and apparent porosity of tailings-metakaolin based geopolymers after 7 days of curing.

increasing UCS varies with decreasing apparent porosity and water absorption. Since the mould has a fractionally thinner dimension, the measured compressive strength might be slightly lower than the genuine one.

3.2. XRD and DRIFT

The diffractograms of PM samples are presented in Fig. 2, in which XRD intensity was normalised by the strongest reflection of each sample in order to compare the relative intensities. The main crystalline phases of PM samples originate from MT, of which the mineralogical components include phlogopite (ICDD, PDF-4 #04-012-5381), calcite (ICDD, PDF-4 #04-012-0489), dolomite (ICDD, PDF-4 #04-015-9848), and tremolite (ICDD, PDF-4 #04-013-2249). A new phase conspicuously appeared in PM 3/7, PM 4/6 and PM 5/5 according to XRD pattern, which is ascribed to the reflection of vermiculite (ICDD, PDF-4 #04-017-7291). Vermiculite is structurally analogous to phlogopite and has both balanced cations (Mg^{2+}, Ca^{2+} and Na^{+}) and water filling its interlayer. It should be mentioned that the K^{+} becomes loosely bonded in the interlayer during mechanochemical activation. Thus, this transformation results from the cation exchange by smaller Na^{+} during the alkali activation. The formation of vermiculite can be seen from PM 3/7 to PM 5/5, whilst it disappears once zeolite such as natrolite was formed. It is possible to conclude that vermiculite might be the intermediate phase in favour of the generation of zeolites, that is, zeolitisation of vermiculite (Johnson and Worrall, 2007). The peak of quartz at around 29°/2θ corresponds to the trend of decreasing amount of raw metakaolin from PM 3/7 to PM 7/3. A new carbonate mineral, gaylussite, was formed by reacting amorphised MT (containing intermediate calcium of 14.75%) with alkali activator in PM 5/5. As for PM 6/4, a crystalline zeolite, natrolite, appeared alkali activation. Another crystalline phase, cancrinite, shows in the XRD pattern of PM 7/3, nucleating from gels and acting as the microaggregates embedded in the binder matrix (Ye et al., 2014b).

Fig. 3 shows DRIFT spectra of tailings-metakaolin based geopolymers, in which the band alternations prove the occurrence of geopolymerisation. The partial disappearance of in-plane vibration in Al–O–Si band at 665 cm^{-1} (see Table A1) indicates the decomposition of tetrahedral layers in amorphous phlogopite and suggested that mechanochemical activated MT participated in the alkali activation. In addition, the weakened band at 720 cm^{-1} of MK during alkali activation is assigned to symmetric Al–O–Si stretching vibration (Mo et al., 2014). The frequency at 780 to 790 cm^{-1} appearing demonstrated the quartz in the original MK (Fernández-Jiménez and Palomo, 2005). The original Si–O–T band of MK in the region of 1300 cm^{-1} no longer existed in any of the PM samples due to the dissolution in alkali activator; therefore, the new band appeared at 1200 cm^{-1} in PM 3/7, representing the Si–OH stretching vibrations in the resulting geopolymers (Mo et al., 2014). Furthermore, this band (dash line) progressively shifted to a lower frequency with the incremental content of MT,

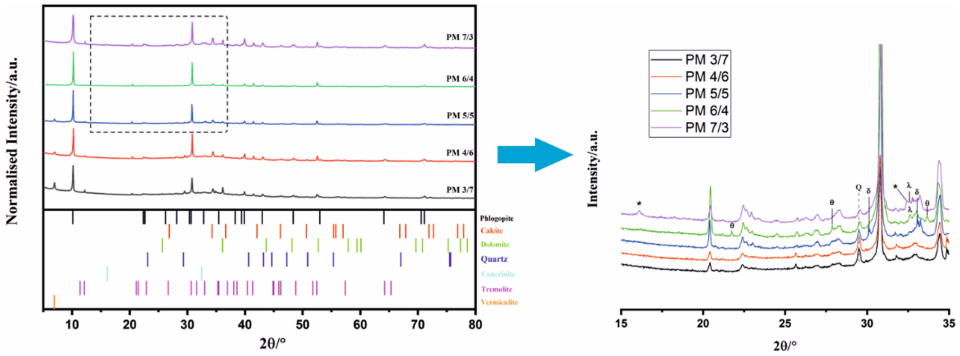

Fig. 2. X-ray diffraction patterns of tailings-metakaolin based geopolymer samples. δ: gaylussite (PDF# 04-010-3621); θ: natrolite (PDF#04-011-7181); λ: sodium calcium carbonate (PDF#04-02102551); *: cancrinite (PDF#04-015-7815); Q: Quartz (PDF#04-007-2627).

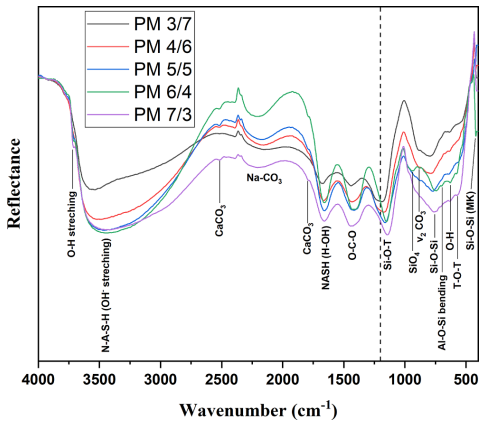

Fig. 3. DRIFT spectra of the tailings-metakaolin based geopolymer samples.

showing that more polycondensation occurred. Another evidence is the bending band of Si–O shifting to a lower frequencies (700 cm^{-1}), which was also characterised as the formation of geopolymers (Palomo and Glasser, 1992). Two distinct broad bands were situated at approximately 3450 cm^{-1} and 1650 cm^{-1}, representing the O–H stretching band and O–H bending band, respectively, which indicates the occurrence of polycondensation (Chindaprasirt et al., 2009). It is interesting that the sharpest O–H stretching (3711 cm^{-1}) for the trioctahedral group ($Mg_3(OH)$) practically disappeared, compared to that of raw tailings (see Table A1). This observation can be interpreted to mean that the crystal phlogopite degradation likely occurred during the alkali activation. The presence of the band at approximately 1460 cm^{-1} in all PM samples has been ascribed to sodium carbonate (Gadsden, 1975). Another significant band between 2000 to 2200 cm^{-1} was assigned to the stretching vibration of the functional group of Na_2CO_3; that is, carbonate minerals, generated by reacting alkali activator with amorphous MT (Bouaissi, 2019). The hint of the formation of cancrinite can be found by the following assignments: 879 cm^{-1} for C-O bend (CO_3^{2-}) and 1400 cm^{-1} for C–O stretch (CO_3^{2-}), which is in line with the results of previous studies (Król et al., 2018; Mozgawa, 2001; Ye et al., 2014b). Once combined with the results of XRD, the study indicated that there was no crystalline cancrinite in PM 6/4, and the new carbonate mineral was assigned to sodium calcium carbonate (Fig. 2). Furthermore, the weak bands at 736 cm^{-1} and 759 cm^{-1} could be attributed to the formation of T-O bonds in the interconnected tetrahedra in PM 6/4. The formation of single four ring (S4R) was in accordance with the previous study which stated that the band range of 720–760 cm^{-1} is assigned to the formation of natrolite zeolite (four-membered rings) (Fernández-Jiménez and Palomo, 2005; Mozgawa, 2001). The new peak appeared at 760 cm^{-1} in the spectrum of PM 7/3 which is assigned to ν_4 Si-O which was found in other blended gel system of C-S-H and N-A-S-H (García-Lodeiro et al., 2008).

3.3. SEM and EDS

The transformation from phlogopite into vermiculite was observed in PM 3/7 and PM 4/6 (Fig. 4), in which the morphology resembled the light weight aggregates (expanded vermiculite) implanted in cement matrix (Mladenovič et al., 2004). The formation of vermiculite partially resulted from the expended interlayer of phlogopite by mechanochemical activation; however, it differed from the vermiculite with Mg^{2+} and H_2O filling in interlayers (Smith Aitken, 1965). Since the mechanochemically activated MT can release more K^+ ions during the alkaline activation, it can be replaced by smaller Na^+ ions by cation exchange forming Na^+–H_2O interlayers. From the morphology of PM 3/7, original particles are entrained in the matrix suggesting a lack of dissolution in PM 3/7. While dissolved particles from MT generate more binder gels in PM 4/6 (fewer original particles compared to PM 3/7), it can be postulated that the polycondensation practically stopped after MK dissolution. The Si/Al ratio for PM 3/7 and PM 4/6 was 1.62 and 1.77, respectively. According to the research by Oelkers et al. (Oelkers and Gislason, 2001), easily dissolved aluminate units can be adsorbed on reactant surfaces, thereby decreasing the dissolution of silicate units. This unbalanced dissolution leads to a lack of formation of geopolymeric linkages. Accompanied with large residues of unreacted MT, the resulting materials exhibits rather poor mechanical strength.

The gel morphology of PM 5/5 exhibited distinctly different features compared with PM 3/7 and PM 4/6, where the calcium-rich gel, sodium-deficient matrix (light grey), displayed a clear boundary with the sodium-rich (darker grey) one according to the elemental mappings (Fig. 5). The calcium-rich gel had unreacted calcite (i.e. crystalline calcite) particles embedded, in which amorphous calcite was the source of calcium for the generation of C-A-S-H binder. When alkali activators were introduced, amorphous calcite can react with sodium hydroxide, generating calcium species $Ca(OH)_2$ (neutral) and $Na_2Ca(CO_3)_2{\cdot}5H_2O$ (gaylussite) (Valentini et al., 2018). The presence of gaylussite was confirmed by using XRD and DRIFT analyses (Fig. 2 and Fig. 3). The monomeric units of Si and Al tetrahedra were dissolved from MK into alkaline activator, forming N-A-S-H and C-(N)-A-S-H gels. Ca-rich species are prone to react with Ca-bearing species; thereafter, reaction with Si and Al species occurs. Thus, this phenomenon explains how amorphous calcite dissolution favours the generation of C-(N)-A-S-H binder, whilst Na-rich regions displayed pronounced propensity towards N-A-S-H gel. Additionally, at which alkaline concentration is higher than 10 M, the N-A-S-H gel becomes the main product, whilst C-S-H gel is the secondary phase when calcium hydroxide exists (Alonso and Palomo, 2001a). Consequently, amorphous carbonate minerals (calcite, dolomite) can react with the alkaline activator to generate more dissolved calcium ions; these calcium ions are incorporated in amorphous alkaline aluminosilicate hydrates. The dissolution of calcium ions led to the formation of a halo in the Ca mapping around the crystalline calcite particles. It can be interpreted that the boundary between the two gels formed a gaylussite ring (bright green in the Ca map), which resulted from the high aqueous pH in N-A-S-H gel impeding the dissolution of Ca cation. This gaylussite ring prevented the interaction between C-(N)-A-S-H and N-A-S-H gels, decreasing the compatibility of these gels which in turn led to undesirable mechanical properties.

The scanning electron miscroscopy (SEM) image of PM 6/4 (Fig. 6) reveals the crystallisation of the zeolite phase among gel binders. The main substances, natrolite and C-(N)-A-S-H phases, formed in the final product after alkali activation. The bundles of fibres or fan-like crystals in PM 6/4 have been ascribed to the formation of natrolite zeolite, which was produced by breaking the T-O bonds of chemically reactive precursors and regeopolymerisation (Huang et al., 2016; Slaty et al., 2015). The energy dispersive spectra of these two phases are provided in Fig. 6 (P1 and P2). The nucleation of natrolite has been hypothesised as arising from the presence of NaOH, MK, activated MT and the curing conditions as depicted below (El Hafid and Hajjaji, 2015).

$$\begin{aligned} Precursors\ (calcite, dolomite) + Alkali\ activator &\xrightarrow{initial\ stage,\ 40\,^{\circ}C} Gaylussite \\ &+ Aluminosilicate\ species \\ &\xrightarrow{final\ stage,\ 40\,^{\circ}C} Natrolite + C-(N)-A-S-H \end{aligned}$$

There is some evidence to suggest that natrolite is likely formed on the vermiculite where the reflections of vermiculite vanished in XRD pattern (Fig. 2). Therefore, it is reasonable to assume that the natrolite crystallised from the aluminosilicate tetrahedral layers with the supplementation of MK and alkali activator.

In the image of PM 7/3, the tailings-metakaolin based geopolymers

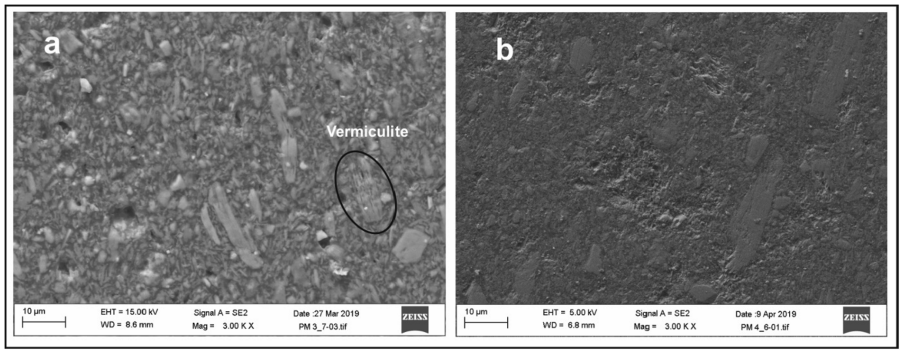

Fig. 4. SEM images of a) PM 3/7 and b) PM 4/6.

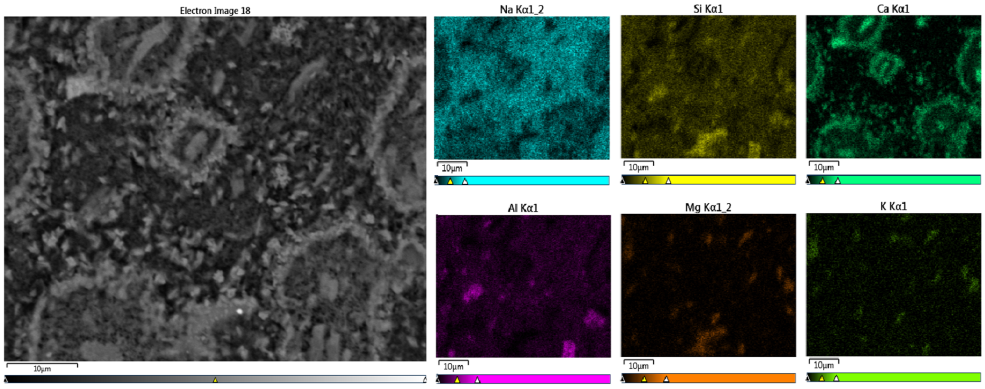

Fig. 5. FESEM back-scattered electron (BSE) images and elemental maps for the PM 5/5.

consisted of densely geopolymeric matrix (Fig. 7). The Mg- and K-bearing particles in mapping images represented unreacted MT (phlogopite) due to its poor alkali reactivity and structural stability. This result is also in line with its lowest apparent porosity. It should be noted that the formation of zeolite-like products results from the alkalinity and composition of raw materials (Criado et al., 2007). Unlike chemically reactive raw materials (calcinated materials), the inert MT precursor must be first pre-treated in order to supply more soluble aluminosilicate phases. In this work, the pre-treatment was still insufficient for the alkali activation, unless the supplement of MK for the inadequate aluminium content in phosphate MT. The morphology in the SEM image contained column-shaped grains, which has been assigned to the formation of C-(N)-A-S-H phase (Chen et al., 2010b). The generation of C-(N)-A-S-H gel is believed to occur at the expense of N-A-S-H phase through the ion exchange mechanism; in addition, PM 7/3 possessed the highest calcium content. This phenomenon was ascribed to the assumption proposed by I. Garcia-Lodeiro (Garcia-Lodeiro et al., 2011). Nevertheless, it slightly differed from this case regarding to the effect of pH, as the pH was 12.67 (> 12) for PM 7/3. The existence of C-(N)-A-S-H was confirmed, which meant that the formation of such gel is depended on not only the ion exchange mechanism but also the alkaline reaction between carbonate minerals (tailings) and MK. Furthermore, it can be hypothesised that the formation of cancrinite is ascribed to the recrystallization from C-(N)-A-S-H gel; however, crystalline cancrinite was not observed in the SEM images probably due to its scale and the complex matrix of C-(N)-A-S-H gel. From the perspective of UCS, PM 7/3 presents a promising UCS compared to other PM samples. Poor mechanical properties have been attributed to the amount of crystalline phase in the resulting samples, in which gel-to-crystal transformation leads to the reduction of mechanical strength due to the occurrence of open porosity and microcracking occurring in this course (Palomo and Glasser, 1992).

The minerology of MT generates complex compositions in the AAM as displayed in the ternary diagrams (Fig. 8). The raw tailings barely contained sodium content, whereas it was rich in calcium. Additionally, the MT had a wider cluster in the $CaO\text{-}Al_2O_3\text{-}SiO_2$ diagram, which is due to calcium-containing minerals such as calcite and dolomite. Thus, the data of raw tailings are not taken into account during chemical analysis in this section. The $Na_2O\text{-}Al_2O_3\text{-}SiO_2$ diagram displayed more clustered EDS data points than those in the $CaO\text{-}Al_2O_3\text{-}SiO_2$ counterpart. PM 3/7 exhibited no correlation with geopolymeric gel formation in both diagrams, thereby showing rather weak UCS. However, PM 4/6 and PM 5/5 generated N-A-S-H and Na-rich C-(N)-A-S-H gel after alkali activation, illustrating the increase of UCS which almost doubled that of PM 3/7. N-A-S-H gel predominantly formed in the $Na_2O\text{-}Al_2O_3\text{-}SiO_2$ system of PM 5/5; these results were consistent with the observation in SEM. The data points of PM 6/4 located in the N-A-S-H gel area which are genuinely assigned to the natrolite, and the Na-rich C-(N)-A-S-H gel which has confirmed in preceding results. With MT content increased to 70%, it promotes the formation of C-(N)-A-S-H gel and the (re)

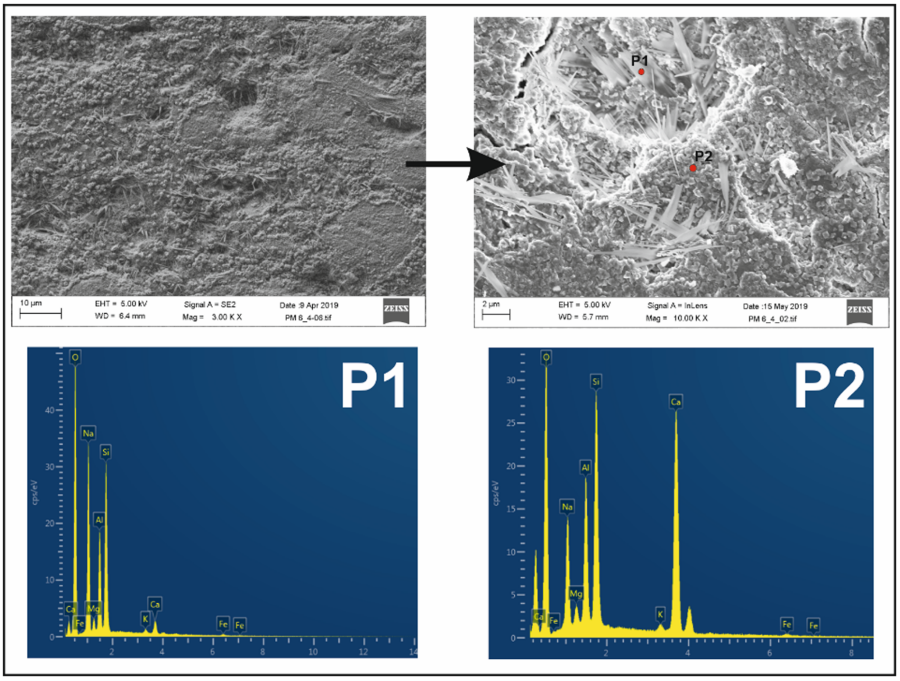

Fig. 6. SEM micrographs of PM 6/4 and energy dispersive spactra of fibrous phase (P1) and gel matrix (P2).

crystallisation of cancrinite is developed. Compared with PM 7/3, PM 5/5 and PM 6/4 predominantly consisted of Na-rich C-(N)-A-S-H gel.

The ternary diagram explicitly illustrated the development of gel formation with the increasing tailings content. At a lower content of sodium ions (Na/Al less than 1), the accumulation of free alumina units occurred, thereby preventing further polycondensation. With the incremental Na/Al ratio, it facilitated the alkali activation; thereafter, it produced not only N-A-S-H gel but also C-(N)-A-S-H gel after the appearance of sodium calcium carbonate and calcium hydroxide.

3.4. ^{29}Si and ^{27}Al MAS NMR

The results of the NMR analysis are shown in Fig. 9. Among all the products, analysis was performed for three samples: PM 3/7, PM 5/5 and PM 7/3 (which have low, medium and high compressive strength, respectively). Among all the reactants, measurements were done only for MK. Measurement of MT was unsuccessful due to its high iron content.

The results of the ^{29}Si NMR analysis are depicted in Fig. 9a. The

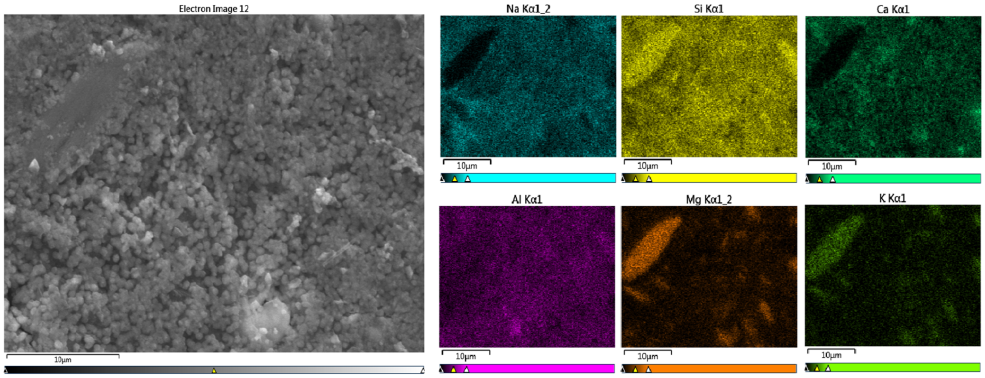

Fig. 7. FESEM secondary electron images and elemental maps for the PM 7/3.

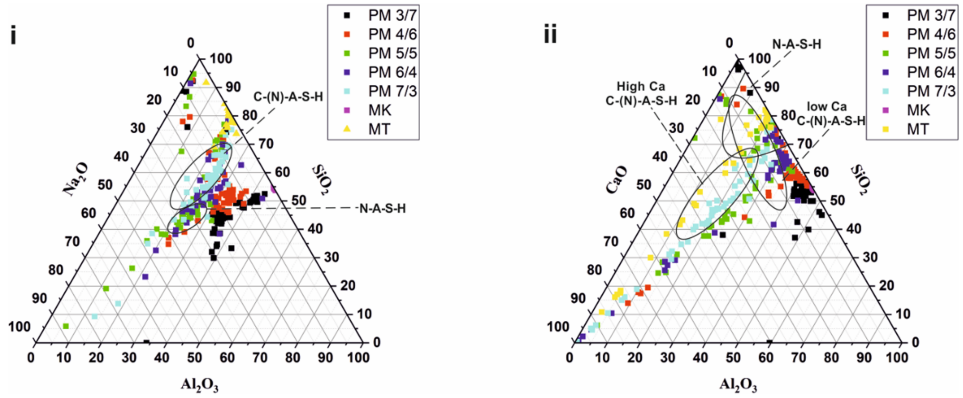

Fig. 8. Projection of alkali-activated materials chemistry onto the i) Na_2O-Al_2O_3-SiO_2 ternary diagram and ii) CaO-Al_2O_3-SiO_2 ternary diagram showing the elemental composition of cured PM samples for 7 days and raw materials. The regions of C-(N)-A-S-H and N-A-S-H were approximately from (Walkley et al., 2016), (Ismail et al., 2014) and (van Deventer et al., 2015).

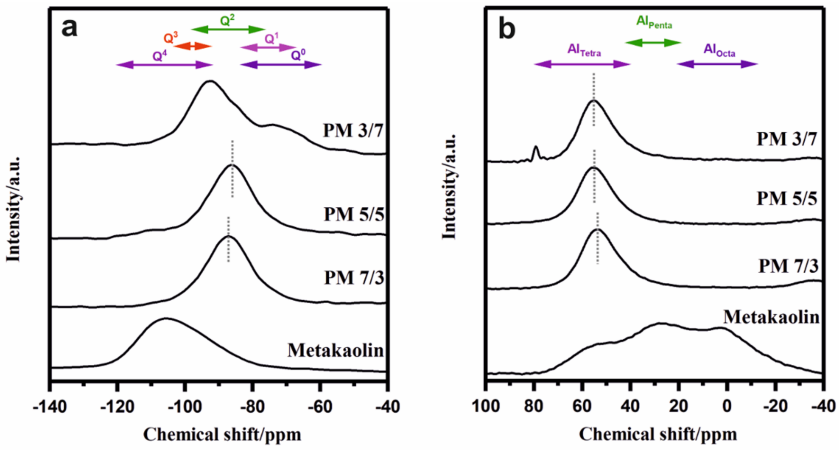

Fig. 9. The results of (a) ^{29}Si NMR and (b) ^{27}Al NMR analysis for products and reactants.

spectrum of MK displayed a broad amorphous component involving mainly Q^4 and Q^3 species. The high strength product, PM 7/3, displayed mainly Q^2 species, which indicated the presence of non-cross-linked C-(N)-A-S-H units. The spectrum of medium strength product PM 5/5 was similar to PM 7/3, except there was a slight shift of the main peak to the right (indicating more non-cross-linked C-(N)-A-S-H phase) and the emergence of a small hump converting Q^4 (indicating N-A-S-H phase) and Q^3 species. In the case of the low-strength sample, PM 3/7, the most dominant feature was a strong peak close to Q^4 (indicating N-A-S-H phase) and Q^3 species. It is possible that Q^3 species formed part of cross-linked C-(N)-A-S-H. Contribution from Q^2 species was a shoulder feature (indicating presence of non-cross-linked C-(N)-A-S-H). Another important feature of this sample is a considerable broad hump covering Q^1 and Q^0 species. This feature indicated the presence of sodium silicate species, which do not contribute to compressive strength like C-(N)-A-S-H. This is one of the reasons for PM3/7 displaying low strength. Both C-(N)-A-S-H and N-A-S-H phase are reported to be formed during alkali activation of clay by-products from phosphate mines (Mabroum et al., 2020).

The results of the ^{27}Al NMR analysis of are depicted in Fig. 9b. MK consists of tetrahedral, pentahedral and octahedral aluminum species. The high-strength product, PM 7/3 consisted tetrahedral aluminum species, which indicated the presence of non-cross-linked C-(N)-A-S-H units. The spectrum of medium strength product PM 5/5 was similar to PM 7/3, except for the slight shift of the tetrahedral peak to the left. In the case of the low strength sample (PM 3/7), a similar tetrahedral component was visible. Notably, C-(N)-A-S-H had tetrahedral aluminum; hence, the spectra of all the products exhibited a similar tetrahedral component. However, there was a small shift of this component towards right as we move from PM 7/3 to PM 3/7. This feature was due to the fact that the chemical shift values of aluminum follows the order: (Al^4 in q^2) > (Al^4 in q^3) > (Al^4 in q^4) (Houston et al., 2009; Myers et al., 2015). The low strength sample PM 3/7 displayed an additional component at approximately 80 ppm which may belong to

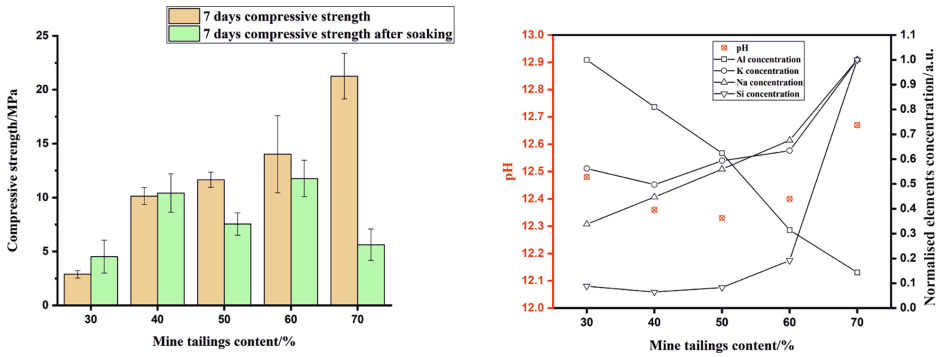

Fig. 10. (a) compressive strength of tailings-metakaolin geopolymer samples after soaking in DI water for 24 h, (b) ICP-OES analysis and pH of the liquid after soaking test.

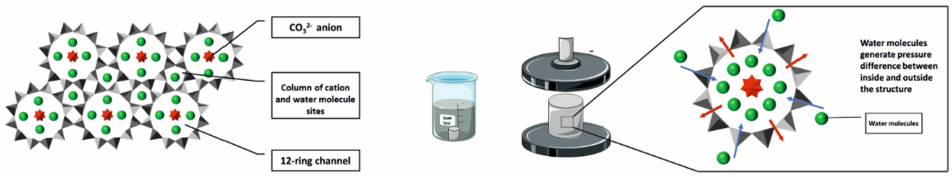

Fig. 11. Schematic structure change of cancrinite after soaking test (aluminosilicate tetrahedra in grey).

low-connectivity aluminate species (Faust and Ribeiro, n.d.; Sagoe-Crentsil and Weng, 2006). Since these species do not contribute to strength-enhancing C-(N)-A-S-H phase, it may contribute towards the low strength of PM 3/7. No octahedral component was detected in any of the products (in spite of having high Mg content), although minor octahedral component corresponding to hydrotalcite is detected in previous study involving alkali activation of clay by-products from phosphate mines (Mabroum et al., 2020).

3.5. Soaking test

The soaking test can affect the UCS of PM samples (Fig. 10), and the decrease of UCS has also been observed in other studies (Boutterin and Davidovits, 2003). There is a synergetic effect between the swelling pressure and regeopolymerization for PM samples. For PM 3/7 and PM 4/6, there is a significant leaching of Al species which means that the geopolymeric reaction was unfulfilled, furthermore, there was less formation of aluminosilicate hydrates indicating a weak and porous matrix. However, dissolvable Al species took part in the re-geopolymerization, which expresses larger effect than swelling repulsion between particles resulting in a higher soaked strength. There is a different situation for PM 5/5, PM 6/4 and PM 7/3, where geopolymerization was achieved thereby the effect of swelling pressure is more conspicuous, leading to a lower strength.

The filtrate was collected and subjected to ICP-OES analysis. The least leaching of sodium concentration in PM 3/7 could be attributed to the strongly bonded sodium cations with negative units such as $Si_4O_8(OH)_6^{4-}$, $SiO(OH)_3^-$ and $SiO_2(OH)_2^{2-}$, forming a rather weak matrix (Panias et al., 2007). Another piece of evidence is the high concentration of Al in solution, indicating a lower amount of aluminium taken part in alkali activation.

As for PM 5/5 and PM 6/4, they consisted of lower amounts of C-(N)-A-S-H gel, revealing the decrease of UCS. It is reasonable to assume that C-(N)-A-S-H gel has higher water-solubility, when compared with N-A-S-H and C-A-S-H gels. Another assumption is that K^+ ions were dissolved from more soluble phases, and this induced capillary force resulting in microcracks within interfaces or grain boundaries.

PM 7/3 had the highest degree of alkali activation and displayed the lowest leaching content of aluminium among all PM samples. Interestingly, it was the sample that was most affected by the 24-h soaking, simultaneously showing the lowest water absorption and porosity (Fig. 1b). These findings might be explained by the presence of cancrinite (Fig. 11). Structural alternation occurred in the cancrinite-like (C-N-A-S-H) gel, in which water can easily penetrate into the cancrinite structure. Cancrinite can be found in nature as a porous mineral, of which the fundamental layers of six-membered rings of SiO_4 and AlO_4 tetrahedra are stacked along the c-axis in an AB-AB sequence (Hackbarth et al., 1999). There are two types of cages within cancrinite structures: 11-hedral cavities and ε-cages along with 12-ring channels as depicted in Fig. 11. The largest discrepancy of UCS in PM 7/3 after soaking might be explained by the structural destabilisation of cancrinite-like (C-N-A-S-H) gel, in which water can easily stab into cancrinite structure. Moreover, the limited space in cages and clogged channels results in the blocking of pore structure, thereby preventing extra water entering. It continues exerting pressure to the porous structure during cage expansion, leading to the low UCS (Liu et al., 2007). Therefore, the weakened alkali-activated structures presented undesirable compressive strength after a 24-h soaking, displaying the lowest water absorption and porosity.

3.6. Life cycle assessment

Fig. 12 shows GWP, AP, EP and ADP (fossil) LCA results for the different alkali-activated binders in comparison to OPC. For the alkali-activated binder (PM 7/3) with the highest UCS (> 20 MPa), excellent performances were shown in impact categories GWP, AP and EP, with 50%, 16% and 18% respectively, lesser emissions than OPC. The significant contributors in these impact categories for PM 7/3 are the

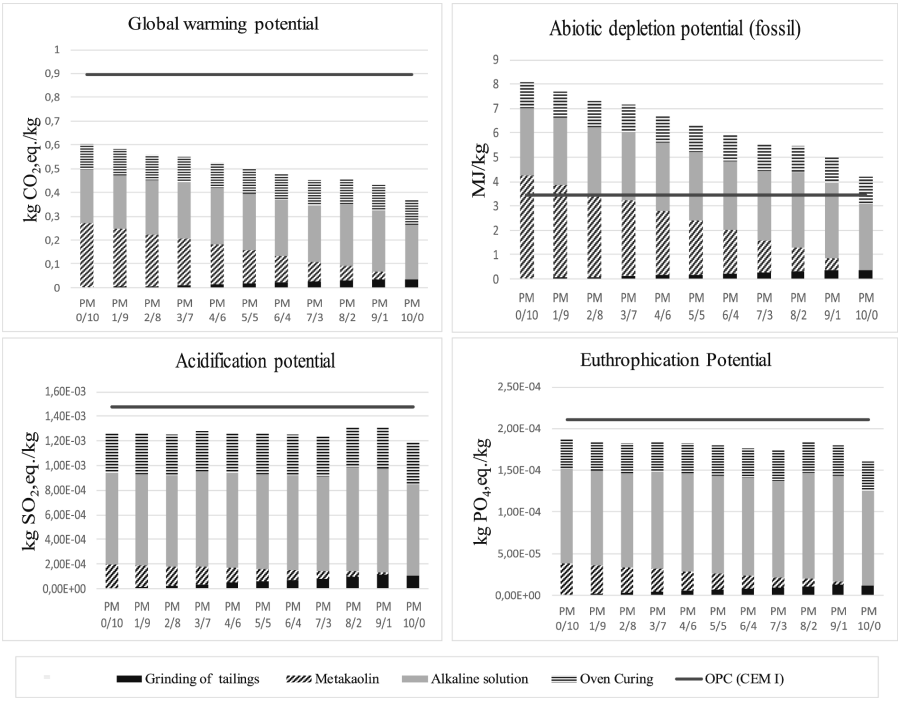

Fig. 12. Life cycle impact assessment results for alkali-activated binder in comparison to CEM I.

alkaline solution (sodium silicate and sodium hydroxide) and curing which account for 52% and 24% respectively for GWP, 62% and 27% respectively for AP, and 67% and 21% for EP. ADP (fossil) showed a significant 61% increase in energy consumption when compared to OPC, with alkaline solution, MK and curing contributing 51%, 24% and 20% respectively. The high amount of energy is associated to energy consumed during production of alkaline solution (Fawer et al., 1999) and in calcining kaolin to MK (Heath et al., 2014). MT beneficiation showed minimal contribution (less than 10%) in all impact categories. This is because only beneficiation impacts were considered, as MT was considered as wastes in this study. Also, MK showed minimal contribution in impact categories AP and EP but a bit higher contribution (19%) in GWP. To reduce the impact of alkaline solution, studies have recommended using silica rich waste materials as a substitute to conventional alkaline solution (Abdulkareem et al., 2019; Passuello et al., 2017). With respect to curing, waste heat can be used for energy thereby increasing the environmental performance of the binder.

As discussed in section 3.1, increasing UCS varies with decreasing apparent porosity and water absorption and when the proportion of MT continuously increases with decrease in MK, the growth of UCS can be seen until it reaches 70% (PM 7/3), at which point it gains the highest UCS > 20 MPa. However, with regards to LCA, continuous increase in MT with decrease in MK leads to a decrease in emissions in GWP, decrease fossil consumption in ADP (fossil) and not much varying effect in AP and EP. This is as a result of MT having lower emissions than MK. It should however be noted that while the UCS of mix designs in this study are considerably lower than that of a standard OPC (32.5 MPa) (BS EN 197–1, 2011). PM 7/3 (> 20 MPa) with 70% MT and 30% MK is closer in strength to OPC. Therefore, improved strength in the mix-design should still amount to lesser emissions compared to OPC.

This LCA study highlights the relevance of using waste materials in the development of alkali-activated binders. Not only are significant impact reductions achieved, but a useful alternative to simply disposing waste residues (which may eventually lead to contamination) is provided.

4. Conclusion

This study investigated the synthesis of AAM using mechanochemically activated phosphate MT with MK as (calcium) aluminosilicate precursors. The geopolymer with the higher content of tailings (60% to 70%) displayed the best mechanical properties (> 20 MPa).

There were two main factors to consider: 1) The mechanochemical activation improves the chemical reactivity of tailings, and 2) the presence of calcium-rich carbonate minerals accelerates the formation of C-(N)-A-S-H binder. The chemical process of alkali-activated phosphate tailings-metakaolin based geopolymers appear to more complicated due to the appearance of the C-(N)-A-S-H binder. New zeolites, such as natrolite (which was fibre-like) and cancrinite (which was column-like) formed.

With the increment of tailings quantity (> 70%), water requirement was lowered due to more favourable particle shape. Although the highest compressive strength was achieved with 70% tailings, water resistance in PM 7/3 still required further improvement. The recycling of MT significantly depends on its chemical and mineralogical composition, and its interactions with alkaline activators.

From the view of circular economy, this study provides a potential method to recycle mine tailings with high added value rather than backfill or impoundment. The manufacturing of tailings-based geopolymers gives huge opportunities for local availability such as

minimizing traffic expense and maximizing sustainability. Particularly, it considerably decreases CO_2 emissions in comparison with OPC. According to the performance of tailings-based geopolymers, such a material displayed promising properties for construction applications, such as brick manufacturing.

CRediT authorship contribution statement

He Niu: Writing - original draft, Conceptualization, Formal analysis. **Mariam Abdulkareem:** Writing - original draft. **Harisankar Sreenivasan:** Writing - original draft. **Anu M. Kantola:** Writing - original draft. **Jouni Havukainen:** Writing - original draft. **Mika Horttanainen:** Writing - original draft. **Ville-Veikko Telkki:** Writing - original draft. **Paivo Kinnunen:** Conceptualization, Supervision, Writing - review & editing. **Mirja Illikainen:** Supervision, Writing - review & editing, Funding acquisition.

Declaration of Competing Interest

The authors declare that they have no known competing financial interests or personal relationships that could have appeared to influence the work reported in this paper.

Acknowledgement

The authors gratefully acknowledge the financial support from the Academy of Finland [grants #292526, #319676 and #326291] and the European Union's EU Framework Programme for Research and Innovation Horizon 2020 [Grant Agreement No 812580 ("SULTAN", https://etn-sultan.eu)]. The authors would like to thank Pasi Juntunen for the assistance in FESEM measurement, Mr. Pekka Tanskanen and Mr. Marcin Selent for their assistance in XRD analysis, Mr. Aki-Petteri Pokka for the assistance in compressive strength measurement. Mr. Jarno Karvonen and Mr. Jani Österlund are acknowledged for their contribution in laboratory experiments. V.-V.T. thanks the Academy of Finland (grants #289649, 294027 and 319216) for the financial support.

Appendix A. . Fundamental information of precursors

See Figs. A1 and A2 Table A1.

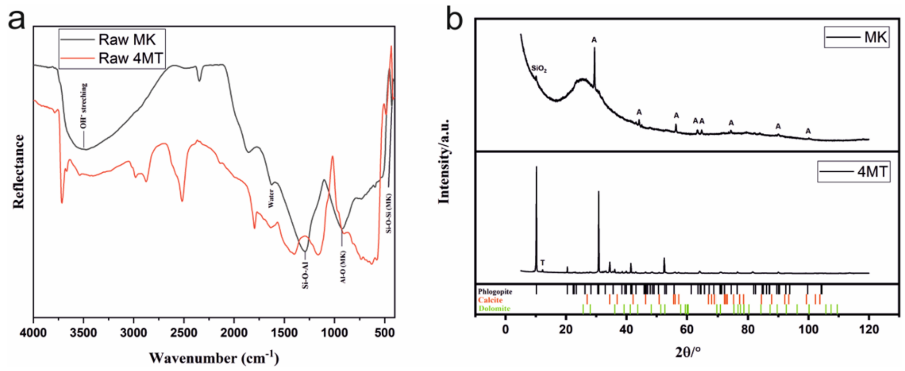

Fig. A1. (a) DRIFT spactra of raw materials (b) XRD patterns of raw materials. quartz (#04-007-2627), A: anatase (#00-064-0803), T: tremolite (#04-013-2249).

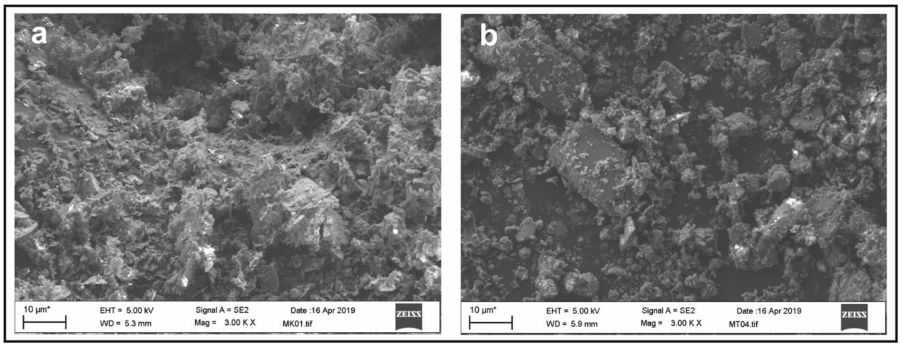

Fig. A2. (a) SEM secondary electron micrographs of metakaolin, (b) SEM secondary electron micrographs of 4-min ground phosphate mine tailings.

Table A1
Description of main bands of 4-min ground phosphate mine tailings.

Wavenumber (cm^{-1})	Band characterization	Reference
3711	OH-stretching vibration (phlogopite)	(Bigham et al., 2001; Farmer, 1974; Schingaro et al., 2013)
3665	OH-stretching vibration Group I (tremolite)	(Najorka and Gottschalk, 2003)
3535	OH-stretching vibration Group III (tremolite)	(Najorka and Gottschalk, 2003)
2979	Carbonate ν_2 overtone (dolomite)	(Messerschmidt, 1985; Nguyen et al., 1991)
2873	Carbonate (calcite)	(Messerschmidt, 1985; Nguyen et al., 1991)
2519	$2\nu_2 + \nu_4$ combination mode (dolomite, calcite)	(Gunasekaran and Anbalagan, n.d.; Nguyen et al., 1991)
1795	Carbonate (calcite)	(Nguyen et al., 1991)
1635	Carbonate ν_3 (apatite)	(Bigham et al., 2001; Rehman and Bonfield, 1997)
1395	C-O Asymmetric stretching ν_3 (dolomite, calcite)	(Clark, n.d.)
1162	Si-O-T (T: Si or Al) (phlogopite)	(Rees et al., 2007)
974	Non-diagnostic Si-O stretching (phlogopite)	(Bigham et al., 2001; Farmer, 1974)
905	Out-of-plane bending ν_2 (dolomite, calcite)	(Farmer, 1974; Rehman and Bonfield, 1997)
823	Apical Al-O bond from AlO_4 (phlogopite)	(Bigham et al., 2001; Farmer, 1974)
732	In-plane bending ν_4 (dolomite, calcite)	(Gunasekaran and Anbalagan, n.d.)
693	Perpendicular vibration (phlogopite)	(Bigham et al., 2001; Farmer, 1974)
665	In-plane vibration of Al-O-Si (phlogopite)	(Bigham et al., 2001; Farmer, 1974)
628	OH vibration (phlogopite)	(Bigham et al., 2001; Farmer, 1974)
579	Asymmetric deformation ν_4 (apatite)	(Veiderma et al., 1998)

Appendix B. . Data sources for Life cycle inventory

See Table B1.

Table B1
Data sources.

Type of data	Source
Sodium hydroxide	GaBi database 2019 (EU-28, sodium hydroxide, 100% caustic soda)
Sodium silicate solution	(Fawer et al., 1999) (sodium silicate 3.3, furnace liquor, 37% solid)
Cement	(CEMBUREAU, 2015) (OPC CEM I)
Metakaolin	Heath et al., 2014; NLK, 2002
Water	GaBi database, 2019 (EU- 28, tap water)
Electricity	GaBi database, 2019 (Finland, electricity grid mix)

References

Abdulkareem, M., Havukainen, J., Horttanainen, M., 2019. How environmentally sustainable are fibre reinforced alkali-activated concretes? J. Clean. Prod. 236. https://doi.org/10.1016/J.JCLEPRO.2019.07.076.

Ahmari, S., Zhang, L., 2013. Utilization of cement kiln dust (CKD) to enhance mine tailings-based geopolymer bricks. Constr. Build. Mater. 40, 1002–1011. https://doi.org/10.1016/j.conbuildmat.2012.11.069.

Alonso, Santiago, Palomo, A., 2001a. Calorimetric study of alkaline activation of calcium hydroxide–metakaolin solid mixtures. Cem. Concr. Res. 31, 25–30. https://doi.org/10.1016/S0008-8846(00)00435-X.

Alonso, S., Palomo, A., 2001b. Alkaline activation of metakaolin and calcium hydroxide mixtures: influence of temperature, activator concentration and solids ratio. Mater. Lett. 47, 55–62. https://doi.org/10.1016/S0167-577X(00)00212-3.

Bakharev, T., 2005. Resistance of geopolymer materials to acid attack. Cem. Concr. Res. 35, 658–670.

Balczár, I., Korim, T., Kovács, A., Makó, É., 2016. Mechanochemical and thermal activation of kaolin for manufacturing geopolymer mortars–Comparative study. Ceram. Int. 42, 15367–15375.

Bigham, J.M., Bhatti, T.M., Vuorinen, A., Tuovinen, O.H., 2001. Dissolution and structural alteration of phlogopite mediated by proton attack and bacterial oxidation of ferrous iron. Hydrometallurgy 59, 301–309. https://doi.org/10.1016/S0304-386X(00)00186-9.

Boldyreva, E., 2013. Mechanochemistry of inorganic and organic systems: what is similar, what is different? Chem. Soc. Rev. 42, 7719. https://doi.org/10.1039/c3cs60052a.

Bouaissi, A., 2019. Mechanical properties and microstructure analysis of FA-GGBS-HMNS based geopolymer concrete. Constr. Build. Mater. 12.

Boutterin, C., Davidovits, J., 2003. Réticulation géopolymérique (LTGS) et matériaux de construction. Géopolymère 1, 79–88.

CEMBUREAU, 2015. Environmental Product Declaration (EPD) Portland Cement (CEM I) produced in Europe.

Chen, C., Habert, G., Bouzidi, Y., Jullien, A., 2010a. Environmental impact of cement production: detail of the different processes and cement plant variability evaluation. J. Clean. Prod. 18, 478–485. https://doi.org/10.1016/j.jclepro.2009.12.014.

Chen, S., Wu, M., Zhang, S., 2010b. Mineral phases and properties of alkali-activated metakaolin-slag hydroceramics for a disposal of simulated highly-alkaline wastes. J. Nucl. Mater. 402, 173–178. https://doi.org/10.1016/j.jnucmat.2010.05.015.

Chindaprasirt, P., Jaturapitakkul, C., Chalee, W., Rattanasak, U., 2009. Comparative study on the characteristics of fly ash and bottom ash geopolymers. Waste Manag. 29, 539–543. https://doi.org/10.1016/j.wasman.2008.06.023.

Clark, R.N., n.d. Spectroscopy of Rocks and Minerals, and Principles of Spectroscopy 64.

Criado, M., Fernández-Jiménez, A., de la Torre, A.G., Aranda, M.A.G., Palomo, A., 2007. An XRD study of the effect of the SiO2/Na2O ratio on the alkali activation of fly ash. Cem. Concr. Res. 37, 671–679. https://doi.org/10.1016/j.cemconres.2007.01.013.

Duxson, P., Provis, J.L., Lukey, G.C., van Deventer, J.S.J., 2007. The role of inorganic polymer technology in the development of 'green concrete'. Cem. Concr. Res. 37, 1590–1597. https://doi.org/10.1016/j.cemconres.2007.08.018.

El Hafid, K., Hajjaji, M., 2015. Effects of the experimental factors on the microstructure and the properties of cured alkali-activated heated clay. Appl. Clay Sci. 116–117, 202–210. https://doi.org/10.1016/j.clay.2015.03.015.

EN ISO 14040, 2006. SFS-EN ISO 14040 ENVIRONMENTAL MANAGEMENT. LIFE CYCLE ASSESSMENT . PRINCIPLES AND FRAME- WORK (ISO 14040 : 2006).

EN, T., 2007. Natural stone test methods-Determination of real density and apparent density, and of total and open porosity. Turk. Stand. Inst. Ank. 13.

Farmer, V.C., 1974. Infrared spectra of minerals. Mineralogical society.

Faust, B.C., Ribeiro, A., n.d. Speciation of aqueous mononuclear Al(III)-hydroxo and other Al (III) complexes at concentrations of geochemical relevance by aluminum-27 nuclear magnetic resonance spectroscopy 11.

Fawer, M., Concannon, M., Rieber, W., 1999. Life cycle inventories for the production of sodium silicates. Int. J. Life Cycle Assess. 4, 207–212. https://doi.org/10.1007/BF02979498.

Fernández-Jiménez, A., Palomo, A., 2005. Mid-infrared spectroscopic studies of alkali-activated fly ash structure. Microporous Mesoporous Mater. 86, 207–214. https://doi.org/10.1016/j.micromeso.2005.05.057.

J.A. Gadsden, Infrared spectra of minerals and related inorganic compounds, 1975.

García-Lodeiro, I., Fernández-Jiménez, A., Blanco, M.T., Palomo, A., 2008. FTIR study of

the sol–gel synthesis of cementitious gels: C-S–H and N–A–S–H. J. Sol-Gel Sci. Technol. 45, 63–72. https://doi.org/10.1007/s10971-007-1643-6.
García-Lodeiro, I., Fernández-Jiménez, A., Palomo, A., Macphee, D.E., 2010. Effect of calcium additions on N-A-S-H cementitious gels. J. Am. Ceram. Soc. https://doi.org/10.1111/j.1551-2916.2010.03668.x.
Garcia-Lodeiro, I., Palomo, A., Fernández-Jiménez, A., Macphee, D.E., 2011. Compatibility studies between N-A-S-H and C-A-S-H gels. Study in the ternary diagram Na_2O–CaO–Al_2O_3–SiO_2–H_2O. Cem. Concr. Res. 41, 923–931. https://doi.org/10.1016/j.cemconres.2011.05.006.
Gunasekaran, S., Anbalagan, G., n.d. Thermal decomposition of natural dolomite 6.
Hackbarth, K., Gesing, T.M., Fechtelkord, M., Stief, F., 1999. Synthesis and crystal structure of carbonate cancrinite $Na_8[AlSiO_4]_6CO_3(H_2O)_{3.4}$, grown under low-temperature hydrothermal conditions. Microporous Mesoporous Mater. 12.
Hasanbeigi, A., Menke, C., Price, L., 2010. The CO_2 abatement cost curve for the Thailand cement industry. J. Clean. Prod. 18, 1509–1518. https://doi.org/10.1016/j.jclepro.2010.06.005.
Heath, A., Paine, K., McManus, M., 2014. Minimising the global warming potential of clay based geopolymers. J. Clean. Prod. 78, 75–83. https://doi.org/10.1016/j.jclepro.2014.04.046.
Houston, J.R., Maxwell, R.S., Carroll, S.A., 2009. Transformation of meta-stable calcium silicate hydrates to tobermorite: reaction kinetics and molecular structure from XRD and NMR spectroscopy. Geochem. Trans. 10, 1. https://doi.org/10.1186/1467-4866-10-1.
Huang, X., Huang, T., Li, S., Muhammad, F., Xu, G., Zhao, Z., Yu, L., Yan, Y., Li, D., Jiao, B., 2016. Immobilization of chromite ore processing residue with alkali-activated blast furnace slag-based geopolymer. Ceram. Int. 42, 9538–9549. https://doi.org/10.1016/j.ceramint.2016.03.033.
Ismail, I., Bernal, S.A., Provis, J.L., San Nicolas, R., Hamdan, S., van Deventer, J.S.J., 2014. Modification of phase evolution in alkali-activated blast furnace slag by the incorporation of fly ash. Cem. Concr. Compos. 45, 125–135. https://doi.org/10.1016/j.cemconcomp.2013.09.006.
Johnson, C.D., Worrall, F., 2007. Novel low density granular adsorbents – properties of a composite matrix from zeolitisation of vermiculite. Chemosphere 68, 1153–1162. https://doi.org/10.1016/j.chemosphere.2007.01.049.
Kauppila, P., Räsänen, M.L., Myllyoja, S., 2013. Best Environmental Practices in Metal Ore Mining (Metallimalmikaivostoiminnan parhaat ympäristökäytännöt).
Kinnunen, P., Ismailov, A., Solismaa, S., Sreenivasan, H., Räisänen, M.-L., Levänen, E., Illikainen, M., 2018. Recycling mine tailings in chemically bonded ceramics – a review. J. Clean. Prod. 174, 634–649. https://doi.org/10.1016/j.jclepro.2017.10.280.
M. Król, P. Rożek, W. Mozgawa, Preparation and Structure of Geopolymer-Based Alkali-Activated Circulating Fuildized Bed Ash Composite for Removing Ni2+ from Wastewater, in: D. Singh, M. Fukushima, Y.-W. Kim, K. Shimamura, N. Imanaka, T. Ohji, J. Amoroso, M. Lanagan (Eds.), Ceram. Trans. Ser., John Wiley & Sons, Inc., Hoboken, NJ, USA, 2018: pp. 147–154. doi:10.1002/9781119494096.ch15.
Liu, Q., Navrotsky, A., Jove-Colon, C.F., Bonhomme, F., 2007. Energetics of cancrinite: effect of salt inclusion. Microporous Mesoporous Mater. 98, 227–233. https://doi.org/10.1016/j.micromeso.2006.09.008.
Mabroum, S., Aboulayt, A., Taha, Y., Benzaazoua, M., Semlal, N., Hakkou, R., 2020. Elaboration of geopolymers based on clays by-products from phosphate mines for construction applications. J. Clean. Prod. 261, 121317. https://doi.org/10.1016/j.jclepro.2020.121317.
MacKenzie, K.J.D., Brew, D.R.M., Fletcher, R.A., Vagana, R., 2007. Formation of aluminosilicate geopolymers from 1:1 layer-lattice minerals pre-treated by various methods: a comparative study. J. Mater. Sci. 42, 4667–4674. https://doi.org/10.1007/s10853-006-0173-x.
Maragkos, I., Giannopoulou, I.P., Panias, D., 2009. Synthesis of ferronickel slag-based geopolymers. Miner. Eng. 22, 196–203. https://doi.org/10.1016/j.mineng.2008.07.003.
Merrild, H., Larsen, A.W., Christensen, T.H., 2012. Assessing recycling versus incineration of key materials in municipal waste: the importance of efficient energy recovery and transport distances. Waste Manage. 32, 1009–1018. https://doi.org/10.1016/J.WASMAN.2011.12.025.
Messerschmidt, R.G., 1985. Complete elimination of specular reflectance in infrared diffuse reflectance measurements. Appl. Spectrosc. 39, 737–739. https://doi.org/10.1366/0003702854250167.
Mladenovič, A., Šuput, J.S., Ducman, V., Škapin, A.S., 2004. Alkali–silica reactivity of some frequently used lightweight aggregates. Cem. Concr. Res. 34, 1809–1816. https://doi.org/10.1016/j.cemconres.2004.01.017.
Mo, B., Zhu, H., Cui, X., He, Y., Gong, S., 2014. Effect of curing temperature on geopolymerization of metakaolin-based geopolymers. Appl. Clay Sci. 99, 144–148. https://doi.org/10.1016/j.clay.2014.06.024.
Moukannaa, S., Loutou, M., Benzaazoua, M., Vitola, L., Alami, J., Hakkou, R., 2018. Recycling of phosphate mine tailings for the production of geopolymers. J. Clean. Prod. 185, 891–903. https://doi.org/10.1016/j.jclepro.2018.03.094.
Moukannaa, S., Nazari, A., Bagheri, A., Loutou, M., Sanjayan, J.G., Hakkou, R., 2019. Alkaline fused phosphate mine tailings for geopolymer mortar synthesis: Thermal stability, mechanical and microstructural properties. J. Non-Cryst. Solids 511, 76–85. https://doi.org/10.1016/j.jnoncrysol.2018.12.031.
Mozgawa, W., 2001. The relation between structure and vibrational spectra of natural zeolites. J. Mol. Struct. 596, 129–137. https://doi.org/10.1016/S0022-2860(01)00741-4.
Mucsi, G., Kumar, S., Csőke, B., Kumar, R., Molnár, Z., Rácz, Á., Mádai, F., Debreczeni, Á., 2015. Control of geopolymer properties by grinding of land filled fly ash. Int. J. Miner. Process. 143, 50–58. https://doi.org/10.1016/j.minpro.2015.08.010.
Myers, R.J., Bernal, S.A., Gehman, J.D., van Deventer, J.S.J., Provis, J.L., 2015. The role of Al in cross-linking of alkali-activated slag cements. J. Am. Ceram. Soc. 98, 996–1004. https://doi.org/10.1111/jace.13360.
Najorka, J., Gottschalk, M., 2003. Crystal chemistry of tremolite-tschermakite solid solutions. Phys. Chem. Miner. 30, 108–124. https://doi.org/10.1007/s00269-002-0291-1.
Nguyen, T., Janik, L., Raupach, M., 1991. Diffuse reflectance infrared fourier transform (DRIFT) spectroscopy in soil studies. Soil Res. 29, 49. https://doi.org/10.1071/SR9910049.
Niu, H., Kinnunen, P., Sreenivasan, H., Adesanya, E., Illikainen, M., 2020. Structural collapse in phlogopite mica-rich mine tailings induced by mechanochemical treatment and implications to alkali activation potential. Miner. Eng. 151, 106331. https://doi.org/10.1016/j.mineng.2020.106331.
NLK, 2002. Ecosmart concrete project: Metakaolin Pre-feasibility study, Report EA2860. Vancouver, British Columbia.
Novais, R.M., Ascensão, G., Tobaldi, D.M., Seabra, M.P., Labrincha, J.A., 2018. Biomass fly ash geopolymer monoliths for effective methylene blue removal from wastewaters. J. Clean. Prod. 171, 783–794.
O'Brien, H., Heilimo, E., Heino, P., 2015. Chapter 4.3 - The Archean Siilinjärvi Carbonatite Complex, in: Maier, W.D., Lahtinen, R., O'Brien, Hugh (Eds.), Mineral Deposits of Finland. Elsevier, pp. 327–343. https://doi.org/10.1016/B978-0-12-410438-9.00013-3.
Oelkers, E.H., Gislason, S.R., 2001. The mechanism, rates and consequences of basaltic glass dissolution: I. An experimental study of the dissolution rates of basaltic glass as a function of aqueous Al, Si and oxalic acid concentration at 25°C and pH = 3 and 11. Geochim. Cosmochim. Acta 65, 3671–3681. https://doi.org/10.1016/S0016-7037(01)00664-0.
Palomo, A., Glasser, F., 1992. Chemically-bonded cementitious materials based on metakaolin. Br. Ceram. Trans. J. 91, 107–112.
Panias, D., Giannopoulou, I.P., Perraki, T., 2007. Effect of synthesis parameters on the mechanical properties of fly ash-based geopolymers. Colloids Surf. Physicochem. Eng. Asp. 301, 246–254. https://doi.org/10.1016/j.colsurfa.2006.12.064.
Passuello, A., Rodríguez, E.D., Hirt, E., Longhi, M., Bernal, S.A., Provis, J.L., Kirchheim, A.P., 2017. Evaluation of the potential improvement in the environmental footprint of geopolymers using waste-derived activators. J. Clean. Prod. 166, 680–689. https://doi.org/10.1016/j.jclepro.2017.08.007.
Petrillo, A., Cioffi, R., De Felice, F., Colangelo, F., Borrelli, C., 2016. An environmental evaluation: a comparison between geopolymer and OPC concrete paving blocks manufacturing process in italy. Environ. Prog. Sustain. Energy 35, 1699–1708. https://doi.org/10.1002/ep.12421.
Provis, J., 2013. Alkali activated materials: state-of-the-art report, RILEM TC 224-AAM. Springer, New York.
Rattanasak, U., Chindaprasirt, P., 2009. Influence of NaOH solution on the synthesis of fly ash geopolymer. Miner. Eng. 22, 1073–1078. https://doi.org/10.1016/j.mineng.2009.03.022.
Rees, C.A., Provis, J.L., Lukey, G.C., van Deventer, J.S.J., 2007. In situ ATR-FTIR study of the early stages of fly ash geopolymer gel formation. Langmuir 23, 9076–9082. https://doi.org/10.1021/la701185g.
Rehman, I., Bonfield, W., 1997. Characterization of hydroxyapatite and carbonated apatite by photo acoustic FTIR spectroscopy. J. Mater. Sci. Mater. Med. 8, 1–4. https://doi.org/10.1023/A:1018570213546.
Sagoe-Crentsil, K., Weng, L., 2006. Dissolution processes, hydrolysis and condensation reactions during geopolymer synthesis: Part II. High Si/Al ratio systems. J. Mater. Sci. 42, 3007–3014. https://doi.org/10.1007/s10853-006-0818-9.
Schingaro, E., Lacalamita, M., Scordari, F., Mesto, E., 2013. 3T-phlogopite from Kasenyi kamafugite (SW Uganda): EPMA, XPS, FTIR, and SCXRD study. Am. Mineral. 98, 709–717. https://doi.org/10.2138/am.2013.4283.
Slaty, F., Khoury, H., Rahier, H., Wastiels, J., 2015. Durability of alkali activated cement produced from kaolinitic clay. Appl. Clay Sci. 104, 229–237. https://doi.org/10.1016/j.clay.2014.11.037.
Smith Aitken, W.W., 1965. An occurrence of phlogopite and its transformation to vermiculite by weathering. Mineral. Mag. J. Mineral. Soc. 35, 151–164. https://doi.org/10.1180/minmag.1965.035.269.18.
Thinkstep, 2019. Description of the CML 2001 method [WWW Document]. URL http://www.gabi-software.com/support/gabi/gabi-lcia-documentation/cml-2001/ (accessed 6.30.19).
Valentini, L., Contessi, S., Dalconi, M.C., Zorzi, F., Garbin, E., 2018. Alkali-activated calcined smectite clay blended with waste calcium carbonate as a low-carbon binder. J. Clean. Prod. 184, 41–49. https://doi.org/10.1016/j.jclepro.2018.02.249.
Van Den Heede, P., De Belie, N., 2012. Environmental impact and life cycle assessment (LCA) of traditional and "green" concretes: Literature review and theoretical calculations. Cem. Concr. Compos. 34, 431–442. https://doi.org/10.1016/j.cemconcomp.2012.01.004.
van Deventer, J.S.J., San Nicolas, R., Ismail, I., Bernal, S.A., Brice, D.G., Provis, J.L., 2015. Microstructure and durability of alkali-activated materials as key parameters for standardization. J. Sustain. Cem.-Based Mater. 4, 116–128. https://doi.org/10.1080/21650373.2014.979265.
Veiderma, M., Knubovets, R., Tõnsuaadu, K., 1998. Structural properties of apatites from Finland studied by FTIR spectroscopy. Bull. Geol. Soc. Finl. 70, 69–75. https://doi.org/10.17741/bgsf/70.1-2.005.
Vickers, L., van Riessen, A., Rickard, W.D.A., 2015. Fire-Resistant Geopolymers, SpringerBriefs in Materials. Springer Singapore, Singapore. https://doi.org/10.1007/978-981-287-311-8.
Walkley, B., San Nicolas, R., Sani, M.-A., Rees, G.J., Hanna, J.V., van Deventer, J.S.J., Provis, J.L., 2016. Phase evolution of C-(N)-A-S-H/N-A-S-H gel blends investigated via alkali-activation of synthetic calcium aluminosilicate precursors. Cem. Concr. Res. 89, 120–135. https://doi.org/10.1016/j.cemconres.2016.08.010.
Wei, B., Zhang, Y., Bao, S., 2017. Preparation of geopolymers from vanadium tailings by

mechanical activation. Constr. Build. Mater. 145, 236–242. https://doi.org/10.1016/j.conbuildmat.2017.03.234.
Ye, J., Zhang, W., Shi, D., 2014a. Effect of elevated temperature on the properties of geopolymer synthesized from calcined ore-dressing tailing of bauxite and ground-granulated blast furnace slag. Constr. Build. Mater. 69, 41–48. https://doi.org/10.1016/j.conbuildmat.2014.07.002.
Ye, N., Yang, J., Ke, X., Zhu, J., Li, Y., Xiang, C., Wang, H., Li, L., Xiao, B., 2014b. Synthesis and characterization of geopolymer from bayer red mud with thermal pre-treatment. J. Am. Ceram. Soc. 97, 1652–1660. https://doi.org/10.1111/jace.12840.
Yip, C.K., Lukey, G.C., van Deventer, J.S.J., 2005. The coexistence of geopolymeric gel and calcium silicate hydrate at the early stage of alkaline activation. Cem. Concr. Res. 35, 1688–1697. https://doi.org/10.1016/j.cemconres.2004.10.042.
Zhang, L., 2013. Production of bricks from waste materials – a review. Constr. Build. Mater. 47, 643–655. https://doi.org/10.1016/j.conbuildmat.2013.05.043.

Publication II

Abdulkareem, M., Havukainen, J., and Horttanainen, M.
How environmentally sustainable are fibre reinforced alkali-activated concretes?

Reprinted with permission from
Journal of Cleaner Production
Vol. 236, pp. 117601, 2019

Journal of Cleaner Production 236 (2019) 117601

Contents lists available at ScienceDirect

Journal of Cleaner Production

journal homepage: www.elsevier.com/locate/jclepro

How environmentally sustainable are fibre reinforced alkali-activated concretes?

Mariam Abdulkareem*, Jouni Havukainen, Mika Horttanainen

Lappeenranta-Lahti University of Technology, School of Energy Systems, Department of Sustainability Science, P.O.Box 20, FI-53851, Lappeenranta, Finland

ARTICLE INFO

Article history:
Received 15 January 2019
Received in revised form
20 May 2019
Accepted 9 July 2019
Available online 11 July 2019

Handling Editor. Zhen Leng

Keywords:
Fibre reinforced alkali-activated concretes
Conventional concrete
Life cycle assessment
Sensitivity analysis
Contribution analysis
Environmental sustainability

ABSTRACT

Alkali-activated concretes have been receiving increasingly attention as they are identified to be key components towards achieving sustainable construction in future. A detailed comparative environmental assessment study of different mix-designs of fibre reinforced alkali-activated concretes (FRAAC), conventional concrete (CC) and steel fibre reinforced conventional concrete (SFRCC), was conducted using Life cycle assessment (LCA) methodology. LCA study was conducted to determine the environmental performance of the different FRAACs when compared to CC and SFRCC, and also to identify the most important contributing factors to their environmental burdens. Results from the contribution analysis conducted indicated that sodium silicate solution was the major contributing material in the different FRAACs mix-designs. This is because, in addition to the high amount of energy required in the production of sodium silicate solution, high quantities of the solution is required in the development of the alkali-activated concretes. Furthermore, sensitivity analysis conducted indicated that there is a high variability in the environmental assessment results when different life cycle inventory (LCI) data sources of sodium silicate solution are used. Thus, amount of constituents and source of LCI data used, can hugely influence the overall results of the LCA study. As a result, constituent materials required in the development of FRAACs (especially ones which result in higher environmental burdens in FRAACs e.g. sodium silicate) should be cautiously utilised. Alternatively, they can be substituted with materials of lower environmental impacts where applicable, while ensuring the mechanical properties of the alkali-activated concretes are not compromised upon.

1. Introduction

The distinctive properties of concrete in terms of its availability, usability, and price, among other benefits, makes it the most commonly used construction material (Petrillo et al., 2016). Thus, making cement in high demand, as it is the principal binder material used in concrete production (Mehta, 2002). With the excellent properties of concrete comes the drawbacks, and it is considered one of the highest causes of environmental impacts due to factors such as increasingly production of concrete, emissions of CO_2 from calcination of limestone and a high energy consumption during cement production (Mehta, 2002; Turner and Collins, 2013). On a global scale, the construction industry depletes about two-fifths of raw stone, sand, and gravel, one-fourth of virgin wood, 16% of water, and 40% of energy annually; making the industry one of the largest exploiters of the earth's natural resources (Dixit et al., 2010).

According to the European Cement Association, an estimation of 4.7 billion tonnes of cement was produced globally in 2016 (CEMBUREAU, 2017). In 2016, greenhouse gas (GHG) emissions of CO_2 production was estimated to be 1.45 ± 0.2 Gt $CO_{2,\ eq.}$ contributing about 8% of global GHG emissions (Andrew, 2018). The CO_2 emissions usually result from two processes in cement production. The first process is the chemical reaction process required in the production of clinker during the thermal decomposing of $CaCO_3$ to CaO to produce cement; while the second process is emissions derived from combustion of fossil fuels to generate energy for heating raw materials needed in cement production (Andrew, 2018). Other environmental burdens besides CO_2 emissions, also emanate during cement and concrete production such as loss of agricultural land, resource extraction, usage of potable water to wash aggregates and to suppress dust, noise and vehicle pollution, dust emissions, water pollution, and landscape degradation (Zainudeen and Jeyamathn, 2004). Nonetheless, it should be noted that if cement were produced on a lesser scale at a reduced consumption, the environmental burdens would be reduced (Mehta,

* Corresponding author.
E-mail address: mariam.abdulkareem@lut.fi (M. Abdulkareem).

https://doi.org/10.1016/j.jclepro.2019.07.076

2002). As such, durability and lastingness of buildings and other construction products, will lead to a lesser need for virgin materials and resource extraction.

The concern for a more sustainable environment has led to increased research in alternative ways of reducing environmental burdens caused by cement production and by large, concrete production. This has led to possibilities of fusing methods such as material recycling in the concrete industry. This is achieved by recycling waste products from one industry to be used as raw materials in another industry (Mehta, 2002). Traditionally, many industries use the conventional linear economic model 'take-make-consume-throw away' (Brennan et al., 2014), which makes many industrial side-streams landfilled. The advent of sustainable development has led to more recycling and reusing of waste products. Thus, in some concrete industries, some industrial side-streams are recycled and reused as supplementary cementitious materials (SCMs) as a partial replacement for cement. Some additional trends in introducing sustainability to concrete industry also include the use of alkali-activated binders as a substitute to cement.

Alkali-activated binders are synthesized by reacting an alkali silicate/alkali hydroxide solution with an aluminosilicate powder and water (Singh et al., 2015). SCMs with a high Si/Al (aluminosilicate) ratio can be used as source materials. Aluminosilicate SCMs that have demonstrated good results include but are not limited to coal fly ash, granulated blast furnace slag (GBFS), natural pozzolans and calcined clay (Provis, 2017). A comprehensive knowledge of these SCMs' chemical compositions must be carried out to determine the potential of the source materials (Mehta and Siddique, 2016). Aluminosilicate precursors differ from region to region making it very versatile and locally adaptable. They differ in terms of availability, reactivity, cost and value. Thus, not making them a standardised material with respect to Portland cement. When considering developing alkali-activated binders for construction purposes, one key factor that should be taken into account is the local availability (minimised transportation) of suitable raw materials to enhance its sustainability prospects (Provis, 2017).

Barriers to utilisation of SCMs include inconsistency in compositions of materials. This is because the properties of SCMs can vary significantly over time, for example in the case of coal fly ash, they vary from plant to plant due to factors such as type of coal combusted, source of coal, and mixing of fly ash with other particles or materials during post-production phase (Wescott et al., 2010). Other barriers include; market barriers - as SCMs are yet to have widespread market acceptance. In addition, availability of supply for SCMs in the long-term is of great concern because the growth of coal plants for instance, might be hindered due to advent of renewable energy, stringent environmental regulations, and incorporation of sustainable measures to industries (Bouzoubaà and Fournier, 2005; Wescott et al., 2010).

Alkali-Activated binders (AABs) can be produced using two main pathways namely; one-part mix (dry powder with water) (Duxson and Provis, 2008; Luukkonen et al., 2018) and two-part mix (using liquid activator) (Duxson et al., 2007). The two-part mix is the most common and the focus of this study. However, one-part mix may be more scalable in future due to less difficulty in handling and transporting when compared to liquid activators (Luukkonen et al., 2018).

Alkali-activated concretes (AACs) is produced by a mixture of AAB with fine and coarse aggregates, and water. They can be quite brittle, and this makes them sensitive to cracking, thereby forming micro-cracks when loaded which eventually leads to macro-cracks, deterioration and failures, making them unable to withstand additional load (Al-mashhadani et al., 2018; Ganesan et al., 2015). As a result of this drawback, the durability of AACs are undermined. To overcome this limitation and to enhance its ductility, toughness and limit the tendency of cracking, AACs are reinforced with fibres (Alomayri, 2017a). The fibres transmit stress between fibre and matrix through the interfacial bond by crossing the paths of potential cracks (Alomayri, 2017a). The use of Fibre-Reinforced Alkali-Activated Concrete (FRAAC) has attracted much attention among researchers due to the superior physical and mechanical properties that can be achieved (Alomayri, 2017a) as compared to ordinary AAC. However, it should be noted that the characteristics of fibre reinforced concrete depend on many factors such as size, type, elastic properties etc. (Ganesan et al., 2015). Thus, the type of fibre used as well as the pattern of dispersion of fibres in the alkali-activated matrix can affect the mechanical properties. As a result, the type and form of fibre, surface and matrix properties have to be taken into consideration (Alomayri et al., 2013).

There have been different studies carried out on the influence of the fibres on concretes (Al-mashhadani et al., 2018; Alrefaei and Dai, 2018; Assaedi et al., 2017; Behera et al., 2018; Bhutta et al., 2017; Mohseni, 2018; Shaikh et al., 2018). Polyvinyl alcohol micro-fibres as reinforcement in concrete composites have shown to significantly increase ductility which led to increase in toughness and energy absorption of the concrete (Hamoush et al., 2010). A study by Alomayri (2017b) showed that the inclusion of glass micro-fibre as reinforcement material in AAC enhanced the post cracking response of the geopolymer composite (Alomayri, 2017b). Flexural strength and modulus properties and toughness were also enhanced. The increased toughness increased the energy absorption properties of the concrete (Alomayri, 2017b). Steel reinforcement in AAC has shown to improve strength, crack resistance, energy absorption, impact resistance, ductility and modulus of elasticity while decreasing brittleness (Ganesan et al., 2015).

Furthermore, there have been studies comparing environmental performance of conventional concretes to AACs (Davidovits, 2015; Habert et al., 2011; Marinković et al., 2017; McLellan et al., 2011; Ouellet-Plamondon and Habert, 2015; Passuello et al., 2017; Petrillo et al., 2016; Teixeira et al., 2016; Van Den Heede and De Belie, 2012; Yang et al., 2013). Habert et al. (2011) concluded that with respect to global warming, AAC had a slightly lower impact than Ordinary Portland Cement (OPC) concrete. Also, the study revealed that AAC had higher environmental impact than OPC conrete in other impact categories majorly due to the presence of sodium silicate in AAC. McLellan et al. (2011) estimated a 44–64% improvement of greenhouse gas emissions of AAC over OPC. Yang et al. (2013) estimated that CO_2 reduction rate of AAC with respect to OPC concrete was in the range of 55–75%. However, the CO_2 reduction depended on the type, concentration and dosage of alkali activators. The environmental performance results of these studies conflict and vary because of differences in aspects such as different system boundaries, functional units, inventory data etc. Thus, it will be difficult to compare these results. However, most importantly, these studies shed light to different contributing factors to the environmental burdens of AACs.

Environmental performance of different FRAACs has substantially been less investigated. One of the few papers that features environmental performance of FRAACs is by Ohno and Li (2018). The results of the study showed that the significant contributors to the embodied energy and global warming intensity are the alkaline activator and polyvinyl alcohol (PVA) fibre. In addition, it was stated from the results that FRAAC had greater total energy consumption than conventional concrete due to the addition of PVA fibre. However, FRAAC had a lower global warming impact in comparison to conventional concrete (Ohno and Li, 2018).

Although, FRAACs seem promising for construction purposes in the efforts to reuse waste, to lower CO_2 emissions and generally achieve environmental improvements in the concrete industry, there is still a need for a comprehensive environmental assessment

done on FRAACs to determine if it they are a more environmentally sustainable alternative with respect to conventional concrete. Due to the lack of in depth studies on the environmental performance of FRAACs, this paper will be focussing on comparing the environment performance of different FRAACs with respect to conventional concrete in addition to identifying the most important factors contributing to their environmental burdens.

2. Materials and method

According to ISO 14040:2006, "Life cycle assessment (LCA) addresses the environmental aspects and potential environmental impacts throughout a product's life cycle from raw material acquisition through production, use, end-of-life treatment, recycling, and final disposal" (EN ISO 14040, 2006). The method utilised in this study follow the phases of LCA, which are: (1) goal and scope definition, (2) inventory phase, (3) impact assessment phase, and (4) interpretation phase. Besides these four compulsory phases, other optional steps include classification, characterisation, normalisation, grouping, and weighting. To establish confidence in LCA results, some evaluation procedures such as completeness check, consistency check and sensitivity check, are recommended (EN ISO 14040, 2006).

The different materials considered in this study include materials such as cement, sand, gravel and water for the conventional Concrete (CC) mix-design while SFRCC has included in it steel fibre. For the FRAACs, the major input materials are fly ash, sodium hydroxide pellets, sodium silicate solution, sand, gravel, steel fibre, glass fibre and polypropylene fibre; where sodium hydroxide and sodium silicate are used as activators.

Steel fibres used as reinforcement in concrete demonstrates properties such as shrinkage control of concrete, temperature resistance, high fatigue strength resistance to impact, erosion and abrasion resistance to splitting (Rai and Joshi, 2014). The degree of improvement gained by steel fibres in concrete depends on concrete mix and age, fibre content and volume fraction and fibre geometry and orientation. They have been generally known to improve compressive, tensile, flexural fatigue and impact strength (Rai and Joshi, 2014). Steel fibre reinforced concrete can be applied when constructing new pavements and in the repair of existing pavements. It can also be applied in hydraulic structures, industrial floors, tunnel linings, shotcrete linings, refractory concrete, and precast application and in structural applications (Behbahani et al., 2013).

Inclusion of glass fibres to concrete results in improved tensile and impact strength of the concrete. Due to ability of glass fibre to get brittle with time, alkali resistant glass fibre have been introduced to help combat the drawbacks of the former (Rai and Joshi, 2014). Glass fibre concretes are mainly applied as architectural precast concrete and in exterior building façade panels. They can also be applied in building renovation works, water and drainage works, bridge and tunnel lining panels, acoustic barriers and screens (Rai and Joshi, 2014).

Polypropylene (PP) fibre reinforced concrete leads to increased impact resistance, increased tensile strength and energy absorption (Jain et al., 2011). Polypropylene fibre reinforced concrete have been applied in structural applications such as foundation piles, piers, highways, industrial floors, bridge decks, facing panels, heavyweight coating for underwater pipes and floatation units for walkways (Najimi et al., 2009). They are also applied for controlling shrinkage and temperature cracking, rigid pavement. Due to the usefulness of PP fibre reinforced concrete in controlling shrinkage and fine cracks, it can also be applied in structural applications such as airports and industrial floors (Najimi et al., 2009). From these studies, it can be seen that these fibre reinforced concretes (steel, glass and polypropylene) can be implemented in similar structural applications.

2.1. Goal and scope definition

The object of analysis in this study is fibre-reinforced alkali-activated concrete (FRAAC) and the overall goal of this study is to perform an environmental assessment of different types and mix-designs of FRAACs in comparison to conventional concrete (CC) and steel fibre reinforced conventional concrete (SFRCC). This is required to determine the environmental performance of the FRAACs, estimate and compare the impacts of the different concretes while also identifying the main factors contributing to their environmental burdens that could be taken into account in future development.

In accordance to the goal of the study, the system boundary was determined as shown in Fig. 1. Heat Curing was included in the

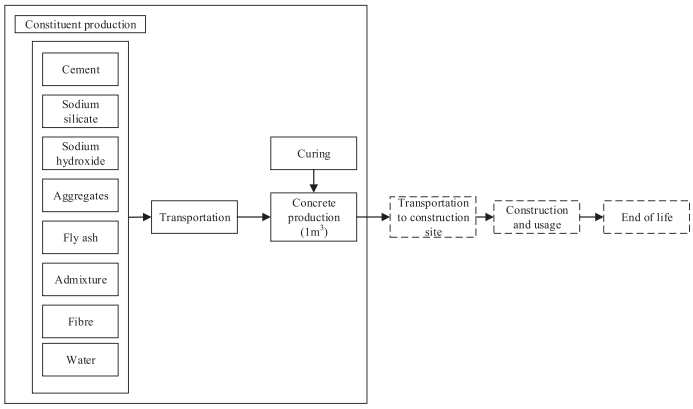

Fig. 1. LCA system boundary illustrating production of 1 m^3 Concrete.

concrete production phase for some of the FRAACs. Transportation of raw materials to concrete production site was omitted from the assessment since similar distances was assumed for transportation of the raw materials and similar impacts were expected. In addition, similar applications and impacts were expected from the Use phase, hence, omitted from the assessment. The End-of-life phase was also omitted from assessment as it was assumed that the End-of-life phase (where part of the waste is recycled and part is disposed in landfill) of the different concrete mixes are comparable. The omitted phases are outside the system boundary as shown in Fig. 1.

Since this study is primarily focussed on concrete production, the unit processes will be limited to the production stage as shown in Fig. 1. Based on the system boundary, the unit processes illustrated are associated with the different raw material constituents used in the production of CC, SFRCC and FRAAC. The functional unit of this study is defined as the environmental impact generated due to the activities involved in the production of 1 m^3 of concrete. As a result of these different concrete mix-designs having the possibility of multiple specific applications in structural engineering, thus, a singular function cannot be selected (Habert et al., 2011; Passuello et al., 2017).

2.2. Life cycle inventory (LCI)

2.2.1. Data collection

This is the phase where material inputs (e.g. energy) and outputs (e.g. emissions) within the system boundary are quantified (Teixeira et al., 2016). A detailed literature review was conducted to obtain mix-designs of concrete and FRAACs and these are presented in Table 1.

The mix-designs are grouped as follows:

- Conventional concrete (CC)
- Steel fibre reinforced conventional concrete (SFRCC)
- Steel fibre reinforced alkali-activated concrete (SFRAAC)
- Glass fibre reinforced alkali-activated concrete (GFRAAC)
- Polypropylene fibre reinforced alkali-activated concrete (PPFRAAC)

Conventional concrete acts as the reference scenario. Steel fibre reinforced conventional concrete was included in the assessment to observe how steel fibre influences the strength of the concrete and also see how it compares in terms of environmental performance with the FRAACs. The different mix-designs were collected as directly reported from different literature studies (analysed and tested).

The FRAACs mix-designs were grouped according to the type of fibre reinforcement (steel fibre, glass fibre and polypropylene fibre) as shown in Table 1. Each group have in them different quantities of constituent materials to observe how varied quantities of these materials affects the strength of the concrete. All FRAAC mix-designs as shown in Table 1 are analysed to determine the mix-design that is most environmentally optimal, which will be further analysed in section 3. The result of the environmental assessment of all mix-designs in Table 1 can be found in the supplementary material.

Table 1
Mix-designs for conventional concrete, steel fibre reinforced conventional concrete and fibre reinforced alkali-activated concretes.

	Cement kg/m^3	Fly ash kg/m^3	GBFS kg/m^3	NaOH pellets kg/m^3	Na_2SiO_3 solution kg/m^3	Sand kg/m^3	Silica sand kg/m^3	Gravel kg/m^3	Super-plasticizer kg/m^3	Water kg/m^3	steel fibre kg/m^3	glass fibre kg/m^3	PP fibre kg/m^3	Comp. Strength MPa	REF
Conventional concrete															
CC	360					598		1266		192				35	[1]
SFRCC	360					598		1266	4	192	38.64			39.5	[1]
Steel fibre reinforced alkali-activated concrete															
S_1		408		16.4	103	600		1248	10.2	16	19.32			38.4	[1]
S_2		408		16.4	103	600		1248	14.5	16	38.64			41.2	[1]
S_3		408		16.4	103	600		1248	14.5	18	57.95			42.5	[1]
S_4		408		16.4	103	600		1248	16	18	78.28			43.8	[1]
S_5		412	276	56.51	294.3		1100				78			74	[2]
S_6		412	276	56.51	294.3		1100				117			74	[2]
S_7		412	276	56.51	294.3		1100				156			82	[2]
S_8		450	60	24	175		1237.5				31.4			61.67	[3]
S_9		450	60	24	175		1237.5				62.8			61.97	[3]
S_10		450	60	24	175		1237.5				94.2			62.52	[3]
S_11	39.43	354.87		14.38	101.39	554.4		1293.4	11.83	55.18	19.63			42.44	[4]
S_12	39.43	354.87		14.38	101.39	554.4		1293.4	11.83	55.18	39.25			43.09	[4]
S_13	39.43	354.87		14.38	101.39	554.4		1293.4	11.83	55.18	58.88			47.46	[4]
Glass fibre reinforced alkali-activated concrete															
GF_1		400		18.27	143	540		1260				13,3		66	[5]
GF_2		400		18.27	143	540		1260				19.9		60	[5]
GF_3		400		18.27	143	540		1260				26.5		54	[5]
GF_4		400		18.27	143	540		1260				33.1		70	[5]
GF_5	39.43	354.87		14.38	101.39	554.4		1293.4	11.83	55.18		0.268		35.97	[6]
GF_6	39.43	354.87		14.38	101.39	554.4		1293.4	11.83	55.18		0.536		32.08	[6]
GF_7	39.43	354.87		14.38	101.39	554.4		1293.4	11.83	55.18		0.804		40.73	[6]
Polypropylene fibre reinforced alkali-activated concrete															
PP_1		450	60	24	175		1237.5						3.64	60.97	[3]
PP_2		450	60	24	175		1237.5						7.28	60.44	[3]
PP_3		450	60	24	175		1237.5						10.92	59.78	[3]
PP_4		368.91		21.3	132.14	581.03		1171.29		31.9			14.19	39.21	[7]

CC- conventional concrete; SFRCC – steel fibre reinforced conventional concrete; GBFS – granulated blast furnace slag; NaOH – sodium hydroxide; Na_2SiO_3 – sodium silicate: PP – polypropylene.
[1] Ganesan et al. (2015), [2] Khan et al. (2018), [3] Al-mashhadani et al., 2018, [4] Vijai et al. (2012a), [5] Nematollahi et al. (2014), [6] Vijai et al. (2012b), [7] Patil and Patil (2015)..

2.2.2. Data sources

The data utilised in this study were gathered from published literature and the LCA modelling was carried out using GaBi software system LCA tool. The Gabi database, which PE International, has provided and checked for consistency, are primarily concerned with material and energy flow required in the production process of a material. GaBi professional database with extensions 2018 served as the main data sources for collecting the LCI of some materials utilised in this study such as cement, sand, gravel, silica sand, transportation, electricity, water, sodium hydroxide, glass fibres and polypropylene fibres.

Life cycle inventory (LCI) for sodium silicate solution was not available in the GaBi database. Hence, it was sourced from the article Life cycle inventories for the production of sodium silicates (Fawer et al., 1999). Sodium silicate with weight ratio of 2.0 was used in this study and it is produced by hydrothermally dissolving silica sand in sodium hydroxide solution (Fawer et al., 1999). Fly ash is considered to have a very small environmental footprint because fly ash mostly does not require beneficiation. (Lemay, 2017; Marceau et al., 2007). Thus, only transportation impacts will be attributed to fly ash. For steel fibres, there is no direct LCA information in the Gabi database and due to insufficient LCA data on steel fibre from literature, the material will be modelled based on the unit process steel sheet stamping and bending. Steel sheet stamping and bending is a part production in making steel metal parts and since it has similar input material as required in making steel fibres, the unit process was adopted. Thus, the impacts associated with 1 kg of steel sheet stamping and bending will for now be assumed to equal 1 kg of steel fibre. Inventory data for the admixture used (superplasticizer) was also not available in GaBi database, but was otherwise sourced from the environmental product declaration (EPD) owned by the European Federation of Concrete Admixtures Associations Ltd. (EFCA). The base materials for the superplasticizer contain lignosulphonate, naphthalene sulphonate, melamine sulphonate, polycarboxylate, additives and water. The result of the LCA of the superplasticizer was selected from the product with the highest environmental impact for a worst-case scenario and is limited to the production stage (cradle to gate). There were no allocations applied for production and the data quality was considered to be good (EFCA, 2015).

The LCI sources for the different material inputs are summarised in Table 2. In general, LCI for this study was made using a combination of information from different sources (Gabi, EPD and literature). The inventory data gotten from literature were transferred to the GaBi software version of 8.6.0.20 to ensure quality of data interpretation.

Table 2
Sources of LCI datasets.

Type of data	Source
Polypropylene fibre	GaBi database 2018
Steel fibre	GaBi database 2018 (steel sheet stamping and bending)
Glass fibre	GaBi database 2018
Sodium hydroxide	GaBi database 2018 (sodium hydroxide, 100% caustic soda)
Sodium silicate	Fawer et al. (1999); (sodium silicate 2.0, hydrothermal liquor, 48% solid)
Sand	GaBi database 2018 (sand 0/2)
Gravel	GaBi database 2018 (gravel 2/32)
Silica sand	GaBi database 2018 (excavation and processing)
Superplasticizer	EFCA (2015)
Water	GaBi database 2018 (tap water)
Electricity	GaBi database 2018 (electricity grid mix)
Transportation	GaBi database 2018 (truck-trailer, Euro 5, 34-40t gross weight/27t payload capacity)
Cement	GaBi database 2018 (Portland cement CEM I)
Diesel	GaBi database 2018 (diesel mix at refinery)

2.3. Life cycle impact assessment (LCIA)

The impact assessment categories used in this study in assigning LCI results to specific environmental issues, are namely; global warming potential (GWP 100 years), ozone layer depletion potential (ODP), acidification potential (AP), eutrophication potential (EP), abiotic depletion potential (ADP elements), abiotic depletion potential (ADP fossil), freshwater aquatic ecotoxicity potential (FAETP), human toxicity potential (HTP), marine aquatic ecotoxicity potential (MAETP), photochemical Ozone Creation Potential (POCP) and terrestrial ecotoxicity potential (TETP). These indicators are according to Centrum voor Milieukunde Leiden (CML) 2015 indicators and provide information on the environmental issues associated with inputs and outputs of the product system (EN ISO 14040, 2006). The CML impact assessment method is a widely adopted method due to its robustness, and limiting uncertainties by restricting quantitative modelling to the early stages in the cause-effect chain, when compared to other impact assessment methods (Turk et al., 2015; Deviatkin et al., 2016).

2.3.1. Normalisation

Normalisation is an optional step used in the "calculation of the magnitude of the category indicator results relative to some reference information" (EN ISO 14040, 2006). There are difficulties associated with comparing and ranking impact categories, especially when they have different standardisations. As a result, normalisation is applied to help compare different impact category indicators (Aymard and Botta-Genoulaz, 2017). Normalised impact is the impact of the studied system (in a certain category) divided by the estimated environmental impact of a reference region (Aymard and Botta-Genoulaz, 2017). Equation (1) illustrates how normalisation is calculated.

$$N_i = S_i / R_i \quad (1)$$

where, i is the impact category, N_i is the normalised impact for a specific impact category, S_i is the characterised impact of the impact category i of the system under study, and R_i is the estimated environmental impact of a reference region. The normalisation values R_i, used in this study is the global equivalents from CML 01−2015 (including biogenic carbon) sourced from GaBi software and are shown in Table 3 below.

Table 3
Global equivalents reference values for estimated environmental impact of each impact category from GaBi software.

Impact category	R_i
Abiotic depletion potential (ADP elements) - kg Sb eq.	3.61E8
Abiotic depletion potential (ADP fossil) - MJ	3.8E14
Acidification potential (AP) - kg SO2 eq.	2.39E11
Eutrophication potential (EP) - kg Phosphate eq.	1.58E11
Freshwater aquatic ecotoxicity potential (FAETP) - kg DCB eq.	2.36E12
Global warming potential (GWP 100 years) - kg CO2 eq.	4.18E13
Human toxicity potential (HTP) - kg DCB eq.	2.58E12
Marine aquatic ecotoxicity potential (MAETP) - kg DCB eq.	1.94E14
Ozone layer depletion potential (ODP) - kg R11 eq.	2.27E8
Photochemical ozone creation potential (POCP) - kg Ethene eq.	3.68E10
Terrestrial ecotoxicity potential (TETP) - kg DCB eq.	1.09E12

2.3.2. Contribution analysis

To get started with interpretation of results, it is essential to identify the key processes that contribute the most to the LCA results (Ciroth et al., 2017) by decomposing the total LCA results into individual process contributions (Liikanen et al., 2017). Once these key processes have been identified, further checks such as sensitivity analysis can be conducted to evaluate the overall robustness of the LCA study (Zampori et al., 2016). The benefits of contribution analysis includes focussing on processes to improve environmental performance of the system of study (Zampori et al., 2016).

2.3.3. Sensitivity analysis

Sensitivity analysis "is a procedure to determine how changes in data and methodological choices affect the results of the LCIA" (EN ISO 14040, 2006). There are two reasons for conducting sensitivity analysis; 1) Sensitivity analysis is conducted to identify the key parameters influencing the system and how they change under different systems conditions (Guo and Murphy, 2012). 2) Sensitivity analysis can be used to study how uncertainty in a model output can be apportioned to different sources of uncertainty in a model input. In this study, the sensitivity analysis will be carried out to determine how the system changes under different conditions.

3. Results and discussion

As presented in section 2.2.1, the data collected (Table 1) were analysed to determine the most environmentally optimal mix-design for each respective group of the FRAACs (SFRAAC, GFRAAC and PPFRAAC) and this was carried out using GaBi software tool. Details of the results can be found in the supplementary material. S_1, PP_4, and GF_5 were the most environmentally optimal mix-design in each group of the different FRAACs. For meaningful comparisons during analysis, it was also ensured that these chosen mix-designs were based on having equivalent compressive strength of 38 ± 2 MPa at 28 days. Furthermore, it was ensured that the chosen mix-designs had equivalent amounts of constituent materials except in the quantities of fibres, where the amount varied a bit. These careful considerations were put in place for ease of environmental performance comparison and most importantly to actualise the main goal of the study.

These mix-designs (S_1, PP_4 and GF_5) as shown in Table 4 will represent the different scenarios analysed with respect to CC and SFRCC to establish their environmental performance.

The LCIA results of these scenarios were generated and normalisation (as explained in 2.3.1) was carried out. The normalised results as illustrated in Fig. 2, cannot be summed up because they

Table 4
Chosen mix-designs representing the different scenarios analysed in this study.

Scenarios	Cement kg/m^3	Fly ash kg/m^3	NaOH pellets kg/m^3	Na_2SiO_3 solution kg/m^3	Sand kg/m^3	Gravel kg/m^3	Super-plasticizer kg/m^3	Water kg/m^3	steel fibre kg/m^3	glass fibre kg/m^3	PP fibre kg/m^3
CC	360				598	1266		192			
SFRCC	360				598	1266	4	192	38.64		
S_1		408	16.4	103	600	1248	10.2	16	19.32		
PP_4		368.91	21.3	132.14	581.03	1171.29		31.9			14.19
GF_5	39.43	354.87	14.38	101.39	554.4	1293.4	11.83	55.18		0.268	

CC – conventional concrete, SFRCC - Steel fibre reinforced conventional concrete, S_1 - Steel fibre reinforced alkali-activated concrete, PP_1 - Polypropylene fibre reinforced alkali-activated concrete, GF_5 - Glass fibre reinforced alkali-activated concrete.

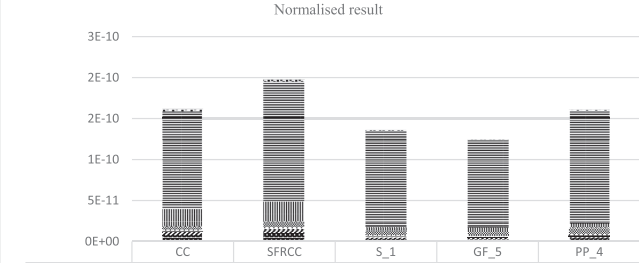

	CC	SFRCC	S_1	GF_5	PP_4
TETP	4E-13	5E-13	2E-13	2E-13	2E-13
POCP	2E-12	3E-12	7E-13	5E-13	7E-13
MAETP	1E-10	1E-10	1E-10	1E-10	1E-10
HTP	2E-11	2E-11	5E-12	5E-12	5E-12
FAETP	8E-13	8E-13	2E-13	2E-13	4E-13
ADP (fossil)	4E-12	6E-12	5E-12	4E-12	8E-12
ADP (elements)	1E-12	1E-12	2E-12	2E-12	3E-12
ODP	7E-14	7E-14	2E-18	8E-15	2E-18
EP	7E-13	8E-13	5E-13	5E-13	5E-13
AP	4E-12	5E-12	2E-12	2E-12	2E-12
GWP	8E-12	1E-11	4E-12	4E-12	4E-12

Fig. 2. Normalised results of the studies scenarios.

are shares of global impact of different impact categories. Thus, the graph is a way to visualise the normalised impacts and the importance of the different impact categories as compared to one another.

All three FRAACs S_1, GF_5 and PP_4 had decreased emissions of 16%, 23% and 0.8% respectively, when compared to CC, and decreased emissions of 32%, 37% and 19%, respectively, when compared to SFRCC (see supplementary information for weighted results). From these results and from the quantities of the different constituent materials as shown in Table 4, it can be seen that GF_5 was the most environmentally sustainable among the FRAACs despite having a small amount of cement (39.43 kg/m^3) in its mix-design. However, the low amount of sodium silicate (101.39 kg/m^3) and sodium hydroxide (14.38 kg/m^3) compensated for the inclusion of cement. PP_4 was the least environmentally sustainable among the FRAACs as a result of having the highest amount of sodium silicate (132.14 kg/m^3) and sodium hydroxide (21.3 kg/m^3).

3.1. Contribution analysis

As discussed in section 2.3.2, contribution analysis is to identify the processes significantly contributing to the LCA results. Thus, the total result is decomposed into individual process contributions. The contribution analysis will be based on MAETP, HTP, ADP (fossil), GWP and AP environmental impact categories, since they are the most relevant impact categories in this study (Fig. 2).

Sodium silicate was the highest contributor to these impact categories followed by steel fibre and sodium hydroxide. Steel fibre had the highest process contribution in the category of fibres. However, the amount of steel fibre used (19.32 kg/m^3), was 1.4

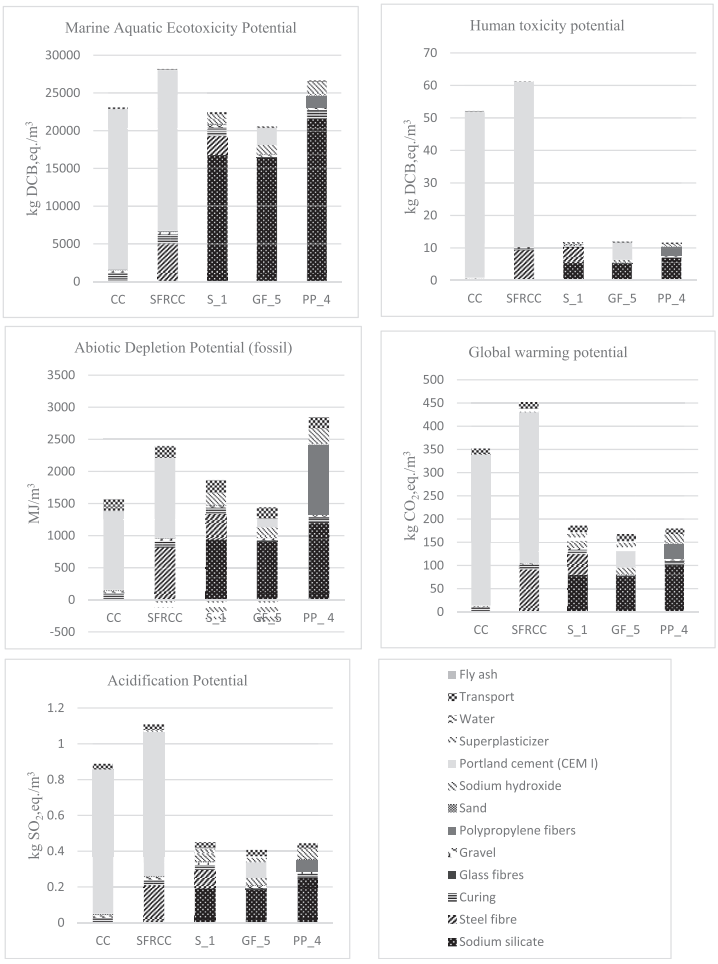

Fig. 3. Contribution of the different processes to MAETP, HTP, ADP (fossil), GWP and AP for the studied scenarios.

times the amount of polypropylene fibre (14.19 kg/m^3) and 72 times the amount of glass fibre (0.268 kg). This has an effect on the overall results based on the differences in fibre quantities. Nevertheless, comparing 1 kg of steel fibres to glass and polypropylene fibres shows steel fibres have a higher environmental impact (see supplementary material). Therefore, factors such as the amount of steel fibre used in comparison to other fibres to actualise similar strength of material, can increase the environmental impact of the alkali-activated concrete.

For sodium silicate, as much as it was the process with the highest contribution, it was observed that a higher quantity of sodium silicate was used (between 101.39 and 132.14 kg/m^3) when compared to sodium hydroxide (between 14.38 and 21.3 kg/m^3) in making the alkali solution. Therefore, the quantity of sodium silicate used in the development of FRAAC (in addition to sodium silicate having a higher environmental impact when compared to other constituent materials except for some of the fibres and sodium hydroxide) made it the process with the highest burden. Thus, quantities of constituent materials especially the alkali activators used can make the FRAAC more or less environmentally sustainable than CC or SFRCC.

Heat curing, transportation (diesel and truck), sand (0/2), fly ash, gravel and water had minimal contribution (less than 10%) to the respective impact categories. Fly ash is considered to have a very small environmental footprint because fly ash mostly does not require beneficiation. (Lemay, 2017; Marceau et al., 2007). Thus, only transportation impacts was attributed to fly ash. Curing is essential for initiating chemical reaction of alkali-activated concretes at first instance. The FRAACs required curing except GF_5. CC and SFRCC also did not require curing. Curing consumed 86.4 MJ (Bai et al., 2014) of electricity for 24 h at 85 °C. Transportation was constant for all the different mix-designs, as it is assumed the different concrete types were locally produced within a distance of 100 km between raw material production and concrete production. In situations of higher distances, impacts related to transportation will also increase.

GF_5 had the lowest overall process contributions to the impact categories as a result of having the least amount of constituent materials and also did not consume extra energy needed for curing.

With respect to GWP, GF_5, S_1 and PP_4 are 52%, 47% and 49% respectively, lower than CC, and 63% and 58% and 60% lower than SFRCC. With respect to MAETP, GF_5 and S_1 are 11% and 3% respectively, lower than CC, and 27% and 20% lower than SFRCC, while PP_4 is 15% higher than CC and 6% lower and SFRCC. With respect to HTP, GF_5, S_1 and PP_4 are 76%, 77% and 78% respectively, lower than CC, and both GF_5 and S_1 are 80% lower than SFRCC while PP_4 is 81% lower than SFRCC. With respect to ADP (fossil), GF_5 and S_1 are 29% and 0.4% respectively, lower than CC and 51% and 31% lower than SFRCC, while PP_4 is 80% and 26% higher than CC and SFRCC respectively. Finally, with respect to AP, GF_5, S_1 and PP_4 are 54%, 49% and 50% respectively, lower than CC, and 63%, 59% and 60% lower than SFRCC (see Fig. 3).

Based on these results, the significant contributor to the FRAACs is the sodium silicate which correlates with study by Ohno and Li (2018), which acknowledges alkaline activator (majorly sodium silicate) as significant contributors to embodied energy and global warming intensity. Others studies such as Ouellet-Plamondon and Habert (2014), Passuello et al. (2017) and Turner and Collins (2013), also acknowledges alkali activator as the greatest contributor to the environmental impact of alkali activated concretes. Although, the focus of these studies was on alkali activated concrete without fibre reinforcement.

3.2. Sensitivity analysis

3.2.1. Sodium silicate

The results of research performed so far on LCA of alkali-activated concretes are contradictory. This is mostly the consequence of different LCI data used for alkali activators (Marinković et al., 2017). In this section, the effect of different inventory data for sodium silicate on the overall results is discerned.

For all the impact categories featured in the contribution analysis, sodium silicate was consistently the highest contributor to the different impact categories for the different FRAACs. Thus, sensitivity analysis as described in section 2.3.3 was carried out on sodium silicate solution by collecting LCI data of sodium silicate from two different sources in addition to the reference sodium silicate data (Fawer et al., 1999) used for the main LCIA results. These two additional LCI sources are from Ecoinvent database and best available technique (BAT) for the manufacture of large volume inorganic chemicals (IPPC, 2007). Furthermore, fuel substitution was carried out on the reference sodium silicate data sourced from Fawer et al. (1999) by replacing fossil fuel used in producing sodium silicate with biogas renewable energy (LCI biogas data was sourced from GaBi database).

From Fig. 4, it is seen how using different LCI sources of sodium silicate can influence the overall LCIA results. When the fossil fuel used in producing sodium silicate (Fawer_FE) is substituted with biogas (Fawer_RE), ADP emissions reduced by 23%, 32% and 17% for S_1, GF_5 and PP_4 respectively. Emission reduction between 15% and 20% was observed for GWP. MAETP had a reduction between 40% and 43% and HTP had a reduction between 18% and 25%. Only AP had an increase between the range of 18% and 20%. When comparing BAT to Fawer_FE, ADP (fossil) had a reduction in the range of 23%–44% for the different FRAACs, AP had a reduction between 18% and 40%, GWP had a reduction between 25% and 33%, HTP had a reduction between 30% and 42%, and MAETP had a reduction between 62% and 68%.

Sodium silicate data from Ecoinvent database gave the highest LCIA results. This is because the major raw materials (silica sand and sodium hydroxide) used in production of sodium silicate using the hydrothermal process, was twice higher in Ecoinvent when compared to Fawer_FE (Fawer et al., 1999) and BAT (IPPC, 2007). Besides, energy used in production of sodium silicate using BAT data consumed about 6.9 times less when compared to Fawer_FE and 1.2 times less when compared to Ecoinvent.

It should be noted that BAT result is when sodium silicate is produced with the best available technique and technologies with the best practicable environmental option. To reduce dust emissions, measures such as using fabric filters, electrostatic precipitators, low sulphur fuel, low NO_x burners, adopting primary measures such as reducing air/fuel ratio and reducing combustion air temperature among other factors are taken into consideration to achieve environmental benefits.

These different LCI sources of sodium silicate solution shows how variability in data can significantly change the outcome of LCIA results. If BAT was used as the reference LCI for sodium silicate to determine the normalised LCIA results, the overall results of the different FRAACs would have shown a much higher environmental performance than CC and SFRCC, as compared to when FAWER_FE is used. Conversely, this would have been otherwise if Ecoinvent data was used as the reference LCI data.

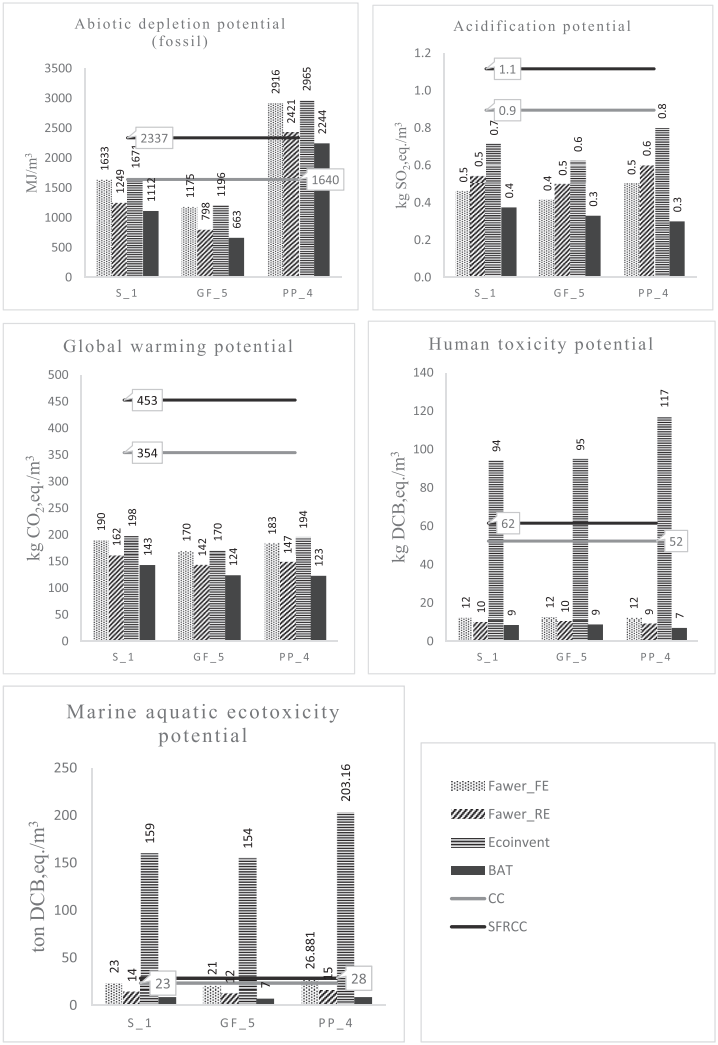

Fig. 4. Sensitivity analysis of sodium silicate. Where; **Fawer_FE** – LCI data for sodium silicate (hydrothermal process) from Fawer et al. (1999) using fossil fuel (Reference scenario); **Fawer_RE** - LCI data for sodium silicate (hydrothermal process) from Fawer et al. (1999) using biogas renewable energy; **Ecoinvent** – LCI data for sodium silicate (hydrothermal process) from Ecoinvent database; **BAT** - LCI data for sodium silicate (hydrothermal process) from best available technique (BAT) for the manufacture of large volume inorganic chemicals (IPPC, 2007).

4. Conclusions

This study used Life Cycle Assessment methodology to carry out a detailed environmental assessment of fibre reinforced alkali-activated concretes (FRAACs) in comparison to conventional concrete (CC) and steel fibre reinforced conventional concrete (SFRCC). This was conducted to estimate and compare the environmental impacts of the different concretes while also identifying the major constituent material behind the environmental burdens that could be taken into account in the future development of FRAACs.

The results showed that the FRAACs studied (GF_5, S_1 and PP_4), had lower environmental impacts than CC and SFRCC in all the impact categories studied except in Abiotic Depletion Potential (fossil) and Marine Aquatic Ecotoxicity Potential where PP_4 was higher than CC and SFRCC. In the contribution analysis, sodium silicate solution was found to be the major contributing factor to

the environmental burden of the different FRAACs. This is as a result of high energy consumption during the production of sodium silicate solution in addition to using a higher quantity of sodium silicate in the production of alkali solution for the development of FRAACs. Due to the heavy effects of sodium silicate solution, sensitivity analysis was carried out to observe how different LCI sources of sodium silicate affected the overall LCIA results. Results of the sensitivity analysis showed that using LCI data from best available technology (BAT) gave the most environmentally optimal results while LCI data from Ecoinvent database was the least optimal.

The study highlights that future research and development of FRAACs should focus on reducing uncertainty of secondary data, by using data from local databases encompassed with site-specific data and data quality information. This can be achieved by collaborative effort of local industries and LCA experts, such that LCA studies can be conducted on primary data related to production processes and this can be implemented in the local database for future use. Furthermore, by taking into account the mix-designs, and the effect, varying quantities of constituent materials (especially the alkali activators) have on the alkali-activated concrete, it is recommended that constituent materials such as sodium silicate should be cautiously used or substituted with a more environmental friendly activator while not compromising on the mechanical properties of the concrete.

Acknowledgements

The authors would like to acknowledge the European Regional Development Fund, European Union through the urban innovative actions initiative for co-financing the Urban Infra Revolution project under the project number UIA02-155.

Appendix A. Supplementary data

Supplementary data to this article can be found online at https://doi.org/10.1016/j.jclepro.2019.07.076.

References

Al-mashhadani, M.M., Canpolat, O., Aygörmez, Y., Uysal, M., Erdem, S., 2018. Mechanical and microstructural characterization of fiber reinforced fly ash based geopolymer composites. Constr. Build. Mater. 167, 505–513. https://doi.org/10.1016/j.conbuildmat.2018.02.061.

Alomayri, T., 2017a. The microstructural and mechanical properties of geopolymer composites containing glass microfibres. Ceram. Int. 43, 4576–4582. https://doi.org/10.1016/j.ceramint.2016.12.118.

Alomayri, T., 2017b. Effect of glass microfibre addition on the mechanical performances of fly ash-based geopolymer composites. J. Asian Ceram. Soc. 5, 334–340. https://doi.org/10.1016/J.JASCER.2017.06.007.

Alomayri, T., Shaikh, F.U.A., Low, I.M., 2013. Characterisation of cotton fibre-reinforced geopolymer composites. Compos. B Eng. 50, 1–6. https://doi.org/10.1016/j.compositesb.2013.01.013.

Alrefaei, Y., Dai, J.G., 2018. Tensile behavior and microstructure of hybrid fiber ambient cured one-part engineered geopolymer composites. Constr. Build. Mater. 184, 419–431. https://doi.org/10.1016/j.conbuildmat.2018.07.012.

Andrew, R.M., 2018. Global CO 2 emissions from cement production. Earth Syst. Sci. Data 10, 195–217. https://doi.org/10.5194/essd-10-195-2018.

Assaedi, H., Shaikh, F.U.A., Low, I.M., 2017. Effect of nanoclay on durability and mechanical properties of flax fabric reinforced geopolymer composites. J. Asian Ceram. Soc. 5, 62–70. https://doi.org/10.1016/j.jascer.2017.01.003.

Aymard, V., Botta-Genoulaz, V., 2017. Normalisation in life-cycle assessment: consequences of new European factors on decision-making. Supply Chain Forum 18, 76–83. https://doi.org/10.1080/16258312.2017.1333385.

Bai, C., Shi, Y., Fabian, S., Li, K.T.V., Xu, H., 2014. Microwave curing techniques for manufacturing alkali-activated fly ash. In: Paper Presented at the 34th Annual Cement and Concrete Science Conference.

Behbahani, H., Nematollahi, B., Farasatpour, M., 2013. Steel Fiber Reinforced Concrete : a Review.

Behera, P., Baheti, V., Militky, J., Louda, P., 2018. Elevated temperature properties of basalt microfibril filled geopolymer composites. Constr. Build. Mater. 163, 850–860. https://doi.org/10.1016/j.conbuildmat.2017.12.152.

Bhutta, A., Borges, P.H.R., Zanotti, C., Farooq, M., Banthia, N., 2017. Flexural behavior of geopolymer composites reinforced with steel and polypropylene macro fibers. Cement Concr. Compos. 80, 31–40. https://doi.org/10.1016/j.cemconcomp.2016.11.014.

Bouzoubaà, N., Fournier, B., 2005. Current situation with the production and use of supplementary cementitious materials (SCMs) in concrete construction in Canada. Can. J. Civ. Eng. 32, 129–143. https://doi.org/10.1139/l04-109.

Brennan, J., Ding, G., Wonschik, C.-R., Vessalas, K., 2014. A closed-loop system of construction and demolition waste recycling. In: Isarc.

CEMBUREAU, 2017. CEMBUREAU Activity Report 2017.

Ciroth, A., Eisfeldt, F., Möller, F., Rodríguez, C., 2017. Hotspots Analysis in LCA Supported by Novel Visualisations Presentation Overview.

Davidovits, J., 2015. Environmental implications of geopolymers [WWW document]. Mater. Today. https://www.materialstoday.com/polymers-soft-materials/features/environmental-implications-of-geopolymers/. (Accessed 13 April 2018).

Deviatkin, I., Kapustina, V., Vasilieva, E., Isyanov, L., Horttanainen, M., 2016. Comparative life cycle assessment of deinking sludge utilization alternatives. J. Clean. Prod. 112, 3232–3243. https://doi.org/10.1016/J.JCLEPRO.2015.10.022.

Dixit, M.K., Fernández-Solís, J.L., Lavy, S., Culp, C.H., 2010. Identification of parameters for embodied energy measurement: a literature review. Energy Build. 42, 1238–1247. https://doi.org/10.1016/j.enbuild.2010.02.016.

Duxson, P., Fernández-Jiménez, A., Provis, J.L., Lukey, G.C., Palomo, A., Van Deventer, J.S.J., 2007. Geopolymer technology: the current state of the art. J. Mater. Sci. 42, 2917–2933. https://doi.org/10.1007/s10853-006-0637-z.

Duxson, P., Provis, J.L., 2008. Designing precursors for geopolymer cements. J. Am. Ceram. Soc. 91, 3864–3869. https://doi.org/10.1111/j.1551-2916.2008.02787.x.

EFCA, 2015. European federation of concrete admixtures asssociations Ltd. [WWW document]. EPD-EFC-20150091-IAG1-EN. http://www.efca.info/efca-publications/environmental/. (Accessed 9 March 2018).

EN ISO 14040, 2006. Environmental Management -Life Cycle Assessment -Principles and Framework Management Environnemental. IS0 International Organization for Standardization.

Fawer, M., Concannon, M., Rieber, W., 1999. Life cycle inventories for the production of sodium silicates. Int. J. Life Cycle Assess. 4, 207–212. https://doi.org/10.1007/BF02979498.

Ganesan, N., Abraham, R., Deepa Raj, S., 2015. Durability characteristics of steel fibre reinforced geopolymer concrete. Constr. Build. Mater. 93, 471–476. https://doi.org/10.1016/J.CONBUILDMAT.2015.06.014.

Guo, M., Murphy, R.J., 2012. LCA data quality: sensitivity and uncertainty analysis. Sci. Total Environ. 435–436, 230–243. https://doi.org/10.1016/j.scitotenv.2012.07.006.

Habert, G., D'Espinose De Lacaillerie, J.B., Roussel, N., 2011. An environmental evaluation of geopolymer based concrete production: reviewing current research trends. J. Clean. Prod. 19, 1229–1238. https://doi.org/10.1016/j.jclepro.2011.03.012.

Hamoush, S., Abu-Lebdeh, T., Cummins, T., 2010. Deflection behavior of concrete beams reinforced with PVA micro-fibers. Constr. Build. Mater. 24, 2285–2293. https://doi.org/10.1016/J.CONBUILDMAT.2010.04.027.

IPPC, 2007. Integrated Pollution Prevention and Control Reference Document on Best Available Techniques for the Manufacture of Large Volume. Inorganic Chemicals-Solids and Others industry.

Jain, R., Gupta, R., Khare, M.G., Dharmadhikari, A.A., 2011. Use of polypropylene fibre reinforced concrete as a construction material for rigid pavements. Indian Concr. J. C 45–53.

Khan, M.Z.N., Hao, Y., Hao, H., Shaikh, F.U.A., 2018. Mechanical properties of ambient cured high strength hybrid steel and synthetic fibers reinforced geopolymer composites. Cement Concr. Compos. 85, 133–152. https://doi.org/10.1016/j.cemconcomp.2017.10.011.

Lemay, L., 2017. Coal combustion products in green building. Coal Combust. Prod. 395–414. https://doi.org/10.1016/B978-0-08-100945-1.00017-4.

Liikanen, M., Havukainen, J., Hupponen, M., Horttanainen, M., 2017. Influence of different factors in the life cycle assessment of mixed municipal solid waste management systems – a comparison of case studies in Finland and China. J. Clean. Prod. 154, 389–400. https://doi.org/10.1016/J.JCLEPRO.2017.04.023.

Luukkonen, T., Abdollahnejad, Z., Yliniemi, J., Kinnunen, P., Illikainen, M., 2018. One-part alkali-activated materials: a review. Cement Concr. Res. 103, 21–34. https://doi.org/10.1016/j.cemconres.2017.10.001.

Marceau, M.L., Nisbet, M.A., Vangeem, M.G., 2007. Life Cycle Inventory of Portland Cement Concrete.

Marinković, S., Dragaš, J., Ignjatović, I., Tošić, N., 2017. Environmental assessment of green concretes for structural use. J. Clean. Prod. 154, 633–649. https://doi.org/10.1016/j.jclepro.2017.04.015.

McLellan, B.C., Williams, R.P., Lay, J., van Riessen, A., Corder, G.D., 2011. Costs and carbon emissions for geopolymer pastes in comparison to ordinary portland cement. J. Clean. Prod. 19, 1080–1090. https://doi.org/10.1016/J.JCLEPRO.2011.02.010.

Mehta, A., Siddique, R., 2016. An overview of geopolymers derived from industrial by-products. Constr. Build. Mater. 127, 183–198. https://doi.org/10.1016/J.CONBUILDMAT.2016.09.136.

Mehta, P.K., 2002. Greening of the concrete industry for sustainable development. Concr. Int. 24, 23–28.

Mohseni, E., 2018. Assessment of Na2SiO3to NaOH ratio impact on the performance of polypropylene fiber-reinforced geopolymer composites. Constr. Build. Mater. 186, 904–911. https://doi.org/10.1016/j.conbuildmat.2018.08.032.

Najimi, M., Farahani, F.M., Pourkhorshidi, A.R., 2009. Effects of Polypropylene Fibers on Physical and Mechanical Properties of Concretes.

Nematollahi, B., Sanjayan, J., Chai, J.X.H., Lu, T.M., 2014. Properties of fresh and hardened glass fiber reinforced fly ash based geopolymer concrete. Key Eng. Mater. 594–595, 629–633. https://doi.org/10.4028/www.scientific.net/KEM.594-595.629.

Ohno, M., Li, V.C., 2018. An integrated design method of Engineered Geopolymer Composite. Cement Concr. Compos. 88, 73–85. https://doi.org/10.1016/j.cemconcomp.2018.02.001.

Ouellet-Plamondon, C., Habert, G., 2015. Life cycle assessment (LCA) of alkali-activated cements and concretes. Handb. Alkali-Activated Cem. Mortars Concr. 663–686. https://doi.org/10.1533/9781782422884.5.663.

Ouellet-Plamondon, C., Habert, G., 2014. Life cycle assessment (LCA) of alkali-activated cements and concretes | Claudiane Ouellet-Plamondon - academia.edu [WWW Document]. http://www.academia.edu/19791159/Life_cycle_assessment_LCA_of_alkali-activated_cements_and_concretes. (Accessed 19 February 2018).

Passuello, A., Rodríguez, E.D., Hirt, E., Longhi, M., Bernal, S.A., Provis, J.L., Kirchheim, A.P., 2017. Evaluation of the potential improvement in the environmental footprint of geopolymers using waste-derived activators. J. Clean. Prod. 166, 680–689. https://doi.org/10.1016/j.jclepro.2017.08.007.

Patil, S.S., Patil, A.A., 2015. Properties of polypropylene fiber. Reinforced Geopolymer Concrete 5, 2909–2912.

Petrillo, A., Cioffi, R., De Felice, F., Colangelo, F., Borrelli, C., 2016. An environmental evaluation: a comparison between geopolymer and OPC concrete paving blocks manufacturing process in Italy. Environ. Prog. Sustain. Energy 35, 1699–1708. https://doi.org/10.1002/ep.12421.

Provis, J.L., 2017. Alkali-activated materials. Cement Concr. Res. 114, 40–48. https://doi.org/10.1016/J.CEMCONRES.2017.02.009.

Rai, A., Joshi, Y.P., 2014. Applications and properties of fibre reinforced concrete. J. Eng. Res. Appl. 4, 123–131.

Shaikh, F.U.A., Fairchild, A., Zammar, R., 2018. Comparative strain and deflection hardening behaviour of polyethylene fibre reinforced ambient air and heat cured geopolymer composites. Constr. Build. Mater. 163, 890–900. https://doi.org/10.1016/j.conbuildmat.2017.12.175.

Singh, B., Ishwarya, G., Gupta, M., Bhattacharyya, S.K., 2015. Geopolymer concrete: a review of some recent developments. Constr. Build. Mater. 85, 78–90. https://doi.org/10.1016/j.conbuildmat.2015.03.036.

Teixeira, E.R., Mateus, R., Camões, A.F., Bragança, L., Branco, F.G., 2016. Comparative environmental life-cycle analysis of concretes using biomass and coal fly ashes as partial cement replacement material. J. Clean. Prod. 112, 2221–2230. https://doi.org/10.1016/J.JCLEPRO.2015.09.124.

Turk, J., Cotič, Z., Mladenovič, A., Šajna, A., 2015. Environmental evaluation of green concretes versus conventional concrete by means of LCA. Waste Manag. 45, 194–205. https://doi.org/10.1016/J.WASMAN.2015.06.035.

Turner, L.K., Collins, F.G., 2013. Carbon dioxide equivalent (CO2-e) emissions: a comparison between geopolymer and OPC cement concrete. Constr. Build. Mater. 43, 125–130. https://doi.org/10.1016/J.CONBUILDMAT.2013.01.023.

Van Den Heede, P., De Belie, N., 2012. Environmental impact and life cycle assessment (LCA) of traditional and "green" concretes: literature review and theoretical calculations. Cement Concr. Compos. 34, 431–442. https://doi.org/10.1016/j.cemconcomp.2012.01.004.

Vijai, K., Kumutha, R., Vishnuram, B.G., 2012a. Effect of inclusion of steel fibres on the properties of geopolymer concrete composites, 13, 381–389.

Vijai, K., Kumutha, R., Vishnuram, B.G., 2012b. Properties of glass fibre Reinforced geopolymer concrete composites. Asian J. Civ. Eng. Building House. 13, 511–520.

Wescott, R.F., Mcnulty, M.W., Vangeem, M.G., Gajda, J., 2010. Prospects for Expanding the Use of Supplementary Cementitious Materials in California.

Yang, K.H., Song, J.K., Song, K. Il, 2013. Assessment of CO 2 reduction of alkali-activated concrete. J. Clean. Prod. 39, 265–272. https://doi.org/10.1016/j.jclepro.2012.08.001.

Zainudeen, N., Jeyamathn, J., 2004. Cement and its effect to the environment : a case study in SriLanka. Dep. Build. Econ. Univ. Moratuwa 1408–1416. https://doi.org/10.1109/7.993240.

Zampori, L., Saouter, E., Schau, E., Cristobal, J., Castellani, V., Sala, S., 2016. Guide for interpreting life cycle assessment result, EUR 28266 EN. https://doi.org/10.2788/171315.

Publication III

Abdulkareem, M., Havukainen, J., Nuortila-Jokinen, J., and Horttanainen, M.
Environmental and economic perspective of waste-derived activators on alkali-activated mortars

Reprinted with permission from
Journal of Cleaner Production
Vol. 280, pp. 124651, 2021

ARTICLE IN PRESS

Journal of Cleaner Production xxx (xxxx) xxx

Contents lists available at ScienceDirect

Journal of Cleaner Production

journal homepage: www.elsevier.com/locate/jclepro

Environmental and economic perspective of waste-derived activators on alkali-activated mortars

Mariam Abdulkareem [a, *], Jouni Havukainen [a], Jutta Nuortila-Jokinen [b], Mika Horttanainen [a]

[a] Lappeenranta-Lahti University of Technology, School of Energy Systems, Department of Sustainability Science, P.O.Box 20, 53851, Lappeenranta, Finland
[b] Lappeenranta-Lahti University of Technology, Research Platform RE-SOURCE, P.O.Box 20, FI-53851, Lappeenranta, Finland

ARTICLE INFO

Article history:
Received 9 January 2020
Received in revised form
13 August 2020
Accepted 11 October 2020
Available online xxx

Handling editor Bin Chen

Keywords:
Waste-derived activator
Waste glass
Rice husk ash
One-part alkali-activated mortar
Two-part alkali-activated mortar
Life cycle assessment

ABSTRACT

Alkali-activated binders have been considered a low carbon alternative to cement and are produced by reacting aluminosilicate precursor with an alkali-activator. However, alkali-activators have been observed to be a major contributor to the environmental burdens of alkali-activated materials regarding various environmental impact categories. Therefore, this study aims to perform an environmental impact assessment using life cycle assessment methodology on alkali-activated mortars produced from chemically modified one- and two-part waste-derived activators (waste glass and rice husk ash) in comparison to conventional one- and two-part alkali-activated mortars, to estimate the influence of activator on environmental impact of mortar. Additionally, a simplified cost analysis of the different mortar compositions was conducted. A sensitivity analysis was performed on the key parameters, and allocating emissions to waste glass and rice husk ash. Results show that waste glass and rice husk ash-derived alkali-activated mortar resulted in up to 62%, 61%, 76% and 56% reduced emission respectively in climate change, fossil depletion, terrestrial acidification and photochemical ozone creation formation when compared to conventional alkali-activated mortar counterpart. Sensitivity analysis indicated that waste glass and rice husk ash are not so sensitive to mass allocation, with a maximum of 5% increased emissions observed in the above-mentioned impact categories. Additionally, sensitivity analysis on sodium hydroxide demonstrated that production from chlorine-alkali electrolysis using technology-mix produced improved environmental performance in comparison to production from brine solution and diaphragm route, respectively. Sensitivity analysis on sodium silicate using an alternative inventory data indicated the emissions can increase regarding one-part or decrease regarding two-part alkali-activated mortars. Results from cost analysis indicated up to 19% cost savings from waste-derived alkali-activated mortar compared to conventional alkali-activated mortar. In conclusion, chemically modified waste-derived activators are a promising alternative in improving environmental performance of alkali-activated materials if their usage also reduces or substitutes the need for conventional alkali-activators.

1. Introduction

Cement production has rapidly grown in recent years with an estimate of 4.7 billion tonnes produced globally in 2016 (CEMBUREAU, 2017), and an estimated contribution between 4% and 8% of global CO_2 emissions (Andrew, 2018). CO_2 emissions from cement production results respectively from thermally decomposing carbonates (mainly limestone) into oxides and CO_2, to produce clinker; and during generation of high amount of energy (from combustion of fossil fuels) needed to heat raw materials (over 1000 °C) (Andrew, 2018). There are different types of cement binders categorized from CEM I – V, containing cement clinker in the range of 5%–100% (BS EN 197-1, 2011) with different percentages of industrial by-products and/or wastes materials such as blast furnace slag, silica fume, pozzolana, fly ash, burnt shale and limestone, to partially replace cement binder for an improved environmental performance among other reasons (CEMBUREAU, 2015a; 2015b; 2015c).

* Corresponding author. Lappeenranta-Lahti University of Technology, School of Energy Systems, Department of Sustainability Science, P.O.Box 20, FI-53851, Lappeenranta, Finland.
E-mail addresses: Mariam.Abdulkareem@lut.fi (M. Abdulkareem), Jouni.Havukainen@lut.fi (J. Havukainen), Jutta.Nuortila-Jokinen@lut.fi (J. Nuortila-Jokinen), Mika.Horttanainen@lut.fi (M. Horttanainen).

https://doi.org/10.1016/j.jclepro.2020.124651

In addition to integrating industrial by-products with clinker for an improved environmental performance of cement, there has been increased research in reducing environmental impact of cement binders through development of alternative types of binders such as alkali-activated binders (AABs) sometimes referred to as geopolymer binders (Provis, 2018). Geopolymers are largely used to describe low calcium alkali-activated aluminosilicate binders, thus, categorized as a sub-group of alkali-activated materials (Heath et al., 2014; Provis, 2018). Davidovits (1994) defined the concept of geopolymers as polycondensation of polymeric aluminosilicates and alkali-silicates, yielding three-dimensional polymeric frameworks. They do not require very high temperatures during production, thus, reducing high fuel consumption (Davidovits, 2015). By and large, AABs are produced by reacting solid aluminosilicate raw materials (precursor) with an alkali-activator to form a hardened binder (Tong et al., 2018; Vinai and Soutsos, 2019). These aluminosilicate precursors can be in the form of virgin raw materials such as metakaolin, or in the form of industrial side-streams with a high Si/Al ratio such as coal fly ash (CFA) and granulated blast furnace slag (GBFS), which have demonstrated good results in production of AABs (Provis, 2018).

AABs can be produced in two pathways namely one-part and two-part pathways (Luukkonen et al., 2018a).

- Two-part AABs as depicted in Fig. 1 are more conventional and are produced by reacting solid aluminosilicate precursor with a concentrated aqueous solution of alkali silicate and hydroxide, and water. They are mainly suitable for precast applications (Luukkonen et al., 2018a). However, with respect to large scale production of two-part AABs, impracticalities of handling large amounts of corrosive, viscous and hazardous alkali solutions led to increased research in the development of one-part AAB (Luukkonen et al., 2018a).
- One-part AAB as depicted in Fig. 2 is produced by reacting solid aluminosilicate precursor with solid alkali silicate, thereby producing a dry mixture binder similarly to cement. One-part AABs are more suited for in situ applications where handling of viscous alkali solutions can be more challenging, making them more scalable in future as it is similar to cement in terms of usage and packaging (Luukkonen et al., 2018a; Provis, 2018).

AABs (especially one-part AABs) can be a potential alternative to Ordinary Portland cement (OPC). Although, they are not likely to fully replace OPC, they can serve as a supplementary binder to OPC thereby reducing CO_2 emissions from the cement industry (Luukkonen et al., 2018a). Some advantages of AABs over OPC include but are not limited to high resistance against acids, high temperature resistance, high strength and high durability (Weil et al., 2005). However, these advantages also depend strongly on mixture composition of materials, curing time and temperature (Weil et al., 2005). Besides, alkali-activated materials provide means of reusing and recycling waste materials as secondary raw

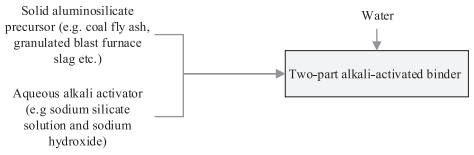

Fig. 1. Two-part alkali-activated binder.

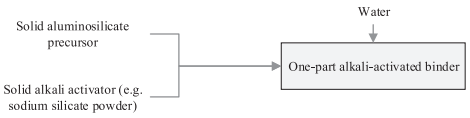

Fig. 2. One-part alkali-activated binder.

materials, to avoid problems of waste disposal and associated environmental burdens. To further promote alkali-activated materials as a feasible and beneficial option, precursors and activators should be locally available to minimise transportation costs and emissions. The downside of AABs is not having a standardised approach when compared to OPC, thus, not making it a solution suitable for all circumstances (Provis, 2018). Additionally, they can be susceptible to cracking, failures and deterioration as a result of their brittleness. This can however be overcome by reinforcement with fibres or other suitable materials (Alomayri, 2017).

The environmental sustainability of alkali-activated materials is highly dependent on alkali-activators (commonly used are sodium hydroxide and sodium silicate). More information on production of these chemicals can be found in the supplementary material. Sodium silicate as an activator is known to produce a more compact and dense material with higher mechanical strength in comparison to hydroxide-activated materials. Thus, a higher quantity of sodium silicate is used when both chemicals are used as activators (Mohseni, 2018; Nematollahi et al., 2015). However, sodium silicate has also been observed to be a major contributor to the environmental burdens of alkali-activated materials regarding various impact categories such as global warming potential (GWP), acidification potential (AP), abiotic depletion potential (ADP), toxicity potentials etc. (Abdulkareem et al., 2019a; Habert et al., 2011; McGuire et al., 2011). These emissions are mainly as a result of the high energy consumption required during their production (Fawer et al., 1999). Furthermore, a study carried out by Abdulkareem et al. (2019b) comparing the environmental assessment of one-part and two-part alkali-activated mortars (AAMs) demonstrated that one-part AAM had higher environmental impact when compared to its two-part counterpart mainly as a result of the additional energy required to produce sodium silicate powder which is required in the production of one-part AAM (Abdulkareem et al., 2019b). Although, the powder activator is a more desirable option when compared to the aqueous activator regarding handling and use, it is however not desirable due to its higher environmental burdens.

In a bid to develop activators with reduced environmental impacts, while retaining high mechanical properties of alkali-activated materials, there has been increased research in the production of sodium silicate from other silica rich waste materials such as rice husk ash (Tchakouté et al., 2016; Tong et al., 2018), sugarcane bagasse ash (Norsuraya et al., 2016; Tchakouté et al., 2017), waste glass (Passuello et al., 2017; Vinai and Soutsos, 2019) and silica fume (Bajza et al., 1998; Rouseková et al., 1997) etc. Most of these studies are however focused on the mechanical properties of alkali-activated materials from these waste derived activators (chemically modified by caustic solution) and not on the environmental impacts. As a result, this study will focus on environmental impact assessment of waste-derived AAMs in comparison to conventional AAMs, to estimate and compare their environmental performance. In addition, a simplified cost analysis of these different mortar compositions will be conducted to assess their economic sustainability.

2. Materials and method

2.1. Materials

2.1.1. Waste glass (WG) cullet

Glass production has large similarities with sodium silicate production as it involves reaction of silica sand and soda ash at a temperature of more than 1100 °C (EU, 2007). Thus, making silicon dioxide the main component of glass. WG cullet is a potential source of silicate with amorphous silica content of 70–75% (Vinai and Soutsos, 2019). Glass production is quite extensive which means that there is a high amount of WG available for open and closed-loop recycling. However, composition, colour and contamination of WG can reduce the amount of glass that can be reused in closed-loop recycling of glass (Vinai and Soutsos, 2019). Over 12 million tons of glass bottles and jars are collected and recycled in Europe with an average glass recycling rate of 74% (FEVE, 2019).

Alkali-activator from WG can be produced using hydrothermal or fusion methods. Hydrothermal method involves heating of WG in an alkaline solution while fusion method involves heating WG and NaOH powder at a very high temperature. Hydrothermal method produces aqueous alkali-activator while fusion methods produce powder alkali-activator (Vinai and Soutsos, 2019). Hence, making possible production of one-part waste-derived alkali activator. The environmental impacts of producing powder activator from WG cullet using the fusion method was assessed following the production process reported by Vinai and Soutsos (2019). WG cullet was milled by means of Retsch PM 400 ball mill for 10 min and then reacted with NaOH powder by heating in an electric furnace at 150 °C for 1 h. The mass proportion of WG cullet and NaOH was 48% and 52% respectively. The advantage of this procedure is that it produces a powder activator as opposed to a liquid activator. Mortar produced from WG-derived activator is prepared by mixing required amounts of sand, CFA, GBFS and activator. The mixtures were cured at room temperature (Vinai and Soutsos, 2019). From this mixture, a one-part waste-derived AAM is produced.

2.1.2. Rice husk ash

Rice husk ash (RHA) is an agricultural waste material resulting from combustion of rice husk, which is a residual stream from the pod of rice grains (Gursel et al., 2016). Rice husk is generated while milling paddy and has a number of applications such as in fertilizer and substrate, raw material for brick production and renewable energy source from biomass etc. (Tong et al., 2018). Gasification or controlled burning of rice husks in kilns or power plants is an effective way of disposing rice husks thereby producing high quality RHA suitable as a supplementary cementitious material (SCM) (Gursel et al., 2016; Meryman, 2009). RHA is rich in silica, approximately 90%, similarly to glass (Norsuraya et al., 2016; Tong et al., 2018) and has been considered a potential source of silicates for alkali-activated binders (Ghosh, 2013; Kamseu et al., 2017; Liu et al., 2016; Ma et al., 2012; Tong et al., 2018). Temperature and duration of combustion process are important during combustion of rice husk, as shorter duration and higher temperatures are expected to maximize the amorphous content of RHA and induce formation of crystalline SiO_2. The RHA share of rice husk is 18–22% of dry content by weight. Market availability of amorphous RHA with silica content of about 95% makes industrial production of silicate from RHA possible (Tong et al., 2018).

The environmental impacts of producing alkali-activator from RHA using the hydrothermal method was assessed following the production process reported by Tong et al. (2018). RHA was milled for 15 min by means of Retsch PM400 to produce a fine RHA powder. RHA powder was dissolved in a NaOH solution, heated and kept under magnetic stirring. The composition of the solution is NaOH (8.7%), RHA (24%) and water (67.3%) in mass (Gursel et al., 2016; Tong et al., 2018). To produce alkali-activated mortar from RHA-derived activator, fly ash and GBFS were blended manually and sand was subsequently added to the mix. Afterward, the activator was added to the mix and subsequently cured at room temperature (Tong et al., 2018). From this mixture, a two-part waste-derived AAM is produced.

2.2. Life cycle assessment methodology

Life cycle assessment (LCA) addresses "environment aspects and potential environmental impacts throughout a products' life cycle from raw material acquisition through production, use, end-of-life treatment, recycling and final disposal" (EN ISO 14040, 2006; EN ISO 14044, 2006). LCA framework is actualised in four phases which are: goal and scope definition, life cycle inventory (LCI) phase, life cycle impact assessment (LCIA) phase and interpretation phase. Additionally, to establish confidence in LCA results, it is recommended to conduct assessment procedures such as sensitivity analysis, consistency check and completeness (EN ISO 14040, 2006).

2.2.1. Goal and scope of study

The goal of this study is to estimate and compare environmental impacts of chemically modified waste-derived alkali-activated mortar (one- and two-part) in comparison to conventional alkali-activated mortars (one- and two-part), to estimate the influence of activator on environmental impact of mortar. The results are compared to assess if waste-derived activators improve environmental performance of AAMs. In addition, a simplified cost analysis was carried to compare the cost of these different mortars to assess their economic sustainability. The functional unit is defined as the environmental burdens generated due to the activities involved in the production of 1 m^3 of AAM with compressive strengths between 52 MPa–60 MPa at 28 days. It is assumed that the scenarios will have similar applications with similar service life.

The system boundary (Fig. 3) utilized in this study contains the main production steps of cradle-to-gate AAM including raw material production, waste treatment and mixing of constituents in which the associated emissions and energy consumptions are calculated. Transportation is excluded from this study as it is assumed all raw materials considered have similar transportation distances. The use phase and end-of-life phase are also excluded from this study as it is assumed that comparable and similar impacts are expected from these phases.

2.2.2. Scenario description

Four scenarios were considered in this study namely.

- S1 – one-part mortar (conventional powder activator)
- S2 – two-part mortar (conventional aqueous activator)
- S3 – one-part mortar (WG-NaOH derived powder activator)
- S4 – two-part mortar (RHA-NaOH derived aqueous activator)

S1 and S2 represents reference scenarios for conventional alkali-activators in the production of one-part and two-part AAM respectively. S3 and S4 represent scenarios derived from chemically modified WG and RHA alkali-activators to produce one-part and two-part AAMs respectively. The synthesis conditions for the AAMs are defined at laboratory scale. Table 1 illustrates mix proportions of these scenarios. All mortars have similar quantities of constituents and equivalent magnitude of compressive strengths at 28 days to aid comparison. All mortars were cured at room temperature, hence, avoiding energy required for thermal curing. WG and RHA are considered as wastes in this study and allocated no

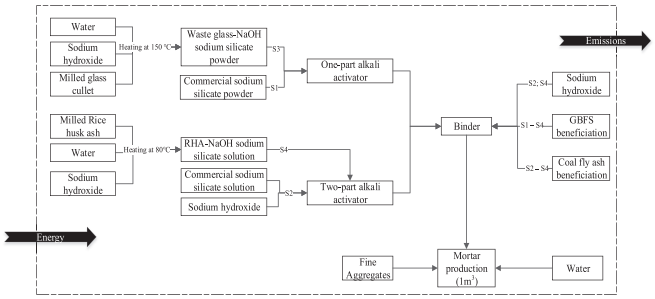

Fig. 3. System boundary depicting production of alkali-activated mortar.

Table 1
Mix proportions of mortars.

Constituent (kg/m^3)	S1 52 MPa [a]	S2 58 MPa [b]	S3 58 MPa [c]	S4 60 MPa [b]
Coal fly ash	0	321	313	326
GBFS	373	214	208	217
Sand	1445	1471	1432	1493
WG-NaOH powder	0	0	126	0
RHA-NaOH solution	0	0	0	196
Sodium silicate	109[d]	157[e]	0	0
Sodium hydroxide pellets	0	26	0	36
Water	241	131	231	99

WG – waste glass.RHA – Rice husk ash. NaOH - Sodium hydroxide. GBFS - Granulated blast furnace slag.
[a] Yang et al. (2010).
[b] Tong et al. (2018).
[c] Vinai and Soutsos (2019).
[d] Sodium silicate powder.
[e] Sodium silicate solution.

environmental burdens based on the EU directive that states "a substance is considered as by-product and not waste if it fulfils certain criteria which are 1) further use of the substance is certain; 2) the substance can be used directly without any further processing other than normal industrial practice; 3) the substance is produced as an integral part of a production process; 4) further use is lawful (European Parliament and Council, 2008)". As a result, only impacts incurred during treatment of WG and RHA will be considered.

Selected scenarios focus on AAM recipes with comparable compressive strength. Data for these scenarios were collected from literature studies. It was ensured that these data were closely related with respect to system boundaries and masses of substances to ease comparison and consistency. Additional scenarios were not taken into consideration as there are limited information on waste-derived AAMs with comparable compressive strength within the scope of this study. For instance, one-part RHA-NaOH derived mortar studied by Luukkonen et al. (2018b), obtained a compressive strength of 32 MPa at 28 days which is high enough, however, not as high as compressive strength of mortars in the scope of this study. Also, Puertas and Torres-Carrasco (2014) and Torres-Carrasco and Puertas (2015) carried out a study on two-part WG-derived activator focusing on paste preparation and not mortar, which is out of scope of this study. Thus, the limitations of this study include the limited number of scenarios for waste-derived AAMs.

2.2.3. Inventory analysis

Life cycle inventory (LCI) is the phase where inputs and outputs as well as produced emission of all unit processes included in the system boundary are quantified. LCI data for processes such as NaOH, sand, electricity and water were sourced from GaBi database. LCI for sodium silicate solution and sodium silicate powder were sourced from Ecoinvent database while LCI for CFA, GBFS, RHA and WG were collected from literature. Table 2 shows data sources for the different processes considered in this study. In this study, pedigree matrix (see supplementary material for more details) is applied to assess the quality of data utilized in this study. Data sources are evaluated based on five independent characteristics namely, reliability, completeness, temporal correlation, geographical correlation, and further technological correlation. Each independent characteristic is scored between 1 and 5 based on 5 quality levels (Weidema et al., 2013).

RHA beneficiation process include electricity for milling (0.0432 MJ/kg) and electricity of 0.74 MJ/kg to dissolve RHA in NaOH by heating at 80 °C for 3 h (Tong et al., 2018). Due to simplifications in the analysis of heat required to dissolved RHA in NaOH, the estimated energy is more than actual energy needed (Tong et al., 2018). WG cullet beneficiation include electricity consumption for milling glass (0.18 MJ/kg) (Vinai and Soutsos, 2019). Electricity required to heat glass powder with NaOH was 0.072 MJ/kg. This value is according to technical specifications obtained for industrial ovens with required capacity (Vinai and Soutsos, 2019). The synthesis conditions for some of the alkali-activated mortars are defined at laboratory scale. Thus, energy consumed might be more conservative when compared to industrial scale production. For GBFS and CFA, they are assumed to come into the system boundary with no environmental burdens, since they are considered wastes. However, GBFS which is used as a supplementary cementitious material (SCM), goes through the processes of

Table 2
Data sources with data quality indexes.

Type of data	Source	Data quality indexes Pedigree matrix
Sodium hydroxide	GaBi database 2019 – EU-28: Sodium hydroxide (caustic soda mix, 100%)	(3,3,2,2,2)
Sodium silicate solution	Ecoinvent database – EU-28: Sodium silicate production, hydrothermal liquor, product in 48% solution state	(2,2,5,1,1)
Sodium silicate powder	Ecoinvent database – EU-28: Sodium silicate production, spray powder, 80%	(2,2,5,1,1)
Sand	GaBi database 2019 – EU-28: Sand 0/2	(3,3,4,3,4)
Water	GaBi database 2019 – EU-28: tap water	(3,3,4,4,3)
Electricity	GaBi database 2019 – FI: electricity grid mix	(3,3,4,3,4)
Coal fly ash	Coal fly ash beneficiation (Kawai et al., 2005)	(4,4,5,5,2)
GBFS	GBFS beneficiation (Marceau and VanGeem, 2003)	(2,3,5,4,1)
Waste glass	Waste glass beneficiation (Vinai and Soutsos, 2019)	(2,4,1,3,1)
Rice husk ash	Rice husk ash beneficiation (Tong et al., 2018)	(2,4,2,3,1)

GBFS – granulated blast furnace slag.

granulation, drying, crushing and grinding (Marceau et al., 2007). Thus, materials and energy required to process GBFS were modelled according to data from Marceau and VanGeem (2003). With respect to CFA, emission associated with treatment process was adopted from Kawai et al. (2005). Environmental impacts of capital good such as trucks, equipment, buildings were not considered in this study. Although, capital goods can have a significant influence on the total results (Liikanen et al., 2017), however, scope of this study is limited to materials and energy needed to produce alkali-activated mortars.

2.2.4. Life cycle impact assessment

The environmental impact categories that will be employed in assigning LCI results to specific environmental issues will be based on four impact categories: climate change, terrestrial acidification, fossil depletion and Photochemical ozone creation (POC) (human health). This is because, cement binder production is associated with environmental issues such as consumption of energy, raw materials and emissions to air, land, and water. Also, fuel handling and storage can be a potential source of soil and groundwater contamination (Stajanca and Estokova, 2012). The associated impact categories to these environmental issues will therefore be relevant for assessment of emissions from binder and mortar production processes (Chen et al., 2010; Van Den Heede and De Belie, 2012). Results of other environmental impact categories (fine particulate matter formation, freshwater consumption, freshwater ecotoxicity, freshwater eutrophication; human toxicity, ionizing radiation, land use, marine ecotoxicity, metal depletion, stratospheric ozone depletion, terrestrial ecotoxicity) are given in the supplementary material. Environmental performance modelling was conducted using GaBi 9.1.0.53 software and selected method was ReCiPe 2016 v1.1 (midpoint hierarchist time-frame) method (Thinkstep, 2019). ReCiPe indicators provide information on the environmental issues associated with inputs and outputs of the product system (EN ISO 14040, 2006). It is a widely adopted method due to its robustness (Hischier et al., 2010).

2.2.5. Sensitivity analysis

Sensitivity analysis "is a procedure to determine how changes in data and methodological choices affect life cycle assessment results" (EN ISO 14040, 2006). Sensitivity analysis is conducted to 1) identify key parameters or factors influencing a product system and the effect of different conditions on the product system 2) study uncertainty in a model input and apportioning of different sources of uncertainty in a model input (Guo and Murphy, 2012). For this study, sensitivity analysis will be based on the first option of how different factors influence a product system.

3. Results

3.1. Environmental assessment of mortars

The results generated as presented in Fig. 4 are based on the environmental assessment of mix proportions of different mortars (Table 1). They illustrate the studied environmental impacts and contribution of different input materials and energy to respective impact categories. Here, S3 and S4 are compared to S1 and S2 (see section 2.2.2 for a detailed description of scenarios).

As seen in Fig. 4, the most contributing materials to S1 and S2 are sodium silicate powder and sodium silicate solution respectively. While WG-NaOH activator contribute the most to S3 and RHA-NaOH activator and sodium hydroxide are the most contributing materials to S4. All the other materials had minimal contribution of less than 10% in the respective impact categories, except for S3 and S4 where GBFS contributed 14% in fossil depletion impact category and in photochemical ozone creation (POC) formation where sand contribute 14% to S4. Overall, chemically modified waste-derived mortars in S3 and S4 have shown to have lower impacts than conventional mortars in S1 and S2. This is because of substituting conventional activator with waste-derived activator. This is also in agreement with other reported studies (Heath et al., 2014; McLellan et al., 2011; Passuello et al., 2017; Tong et al., 2018).

As seen in Fig. 4, with respect to climate change (excluding biogenic carbon), S3 and S4 both had 62% lower emissions when compared to S1; 58% and 59% reduced emissions when compared to S2 respectively leading to a potential reduction in greenhouse gases thereby reducing global mean temperature. This is a result of WG-NaOH and RHA-NaOH as alkali-activators respectively in S3 and S4. Environmental impact of the waste-derived activators mainly come from the treatment process and reaction of the wastes with NaOH to produced sodium silicate. NaOH is the major contributor to the waste-derived activators, contributing 98% of emissions in WG-NaOH activator and 69% emissions in RHA-NaOH activator. More information of environmental assessment of the activators can be found in the supplementary material.

In the fossil depletion impact category, S3 had reduced fossil fuel extraction by 61% and 53% respectively, when compared to S1 and S2. While S4 had reduced fossil fuel extraction by 59% and 51% respectively, when compared to S1 and S2. High fossil fuel extraction from S1 and S2 are as a result of sodium silicate powder and sodium silicate solution consuming 1 MJ/kg and 0.6 MJ/kg of fossil fuel respectively, during production (Fawer et al., 1999). Fossil depletion of WG-NaOH and RHA-NaOH mainly comes from sodium hydroxide used during the reaction process to produce alkali-activator signifying lower fossil fuel extraction.

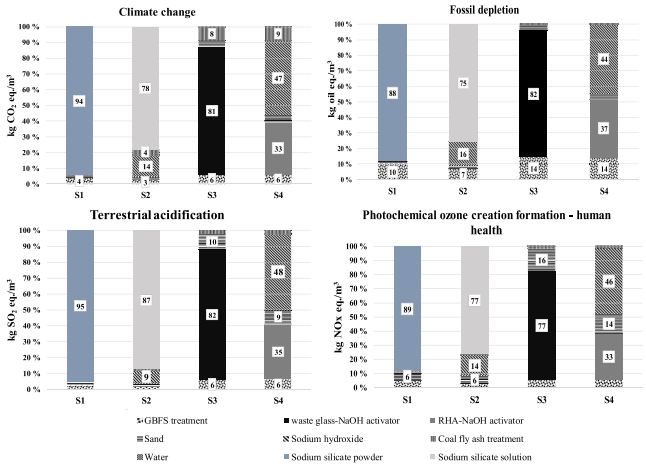

Fig. 4. LCIA results for the different scenarios.

With respect to terrestrial acidification, S3 and S4 had 75% lower emissions respectively when compared to S1 and S2, thereby reducing potential acidity of plant species. While, with respect to POC, S3 and S4 had reduced POC by 51% and 52% respectively when compared S1, and reduced POC by 56% and 57% respectively, when compared to S2, reducing ozone creations leading to reduced frequency and severity of respiratory diseases in human health. As discussed in earlier impact categories, the major contributors are the activators and the avoided burden gained from using waste materials thereby lowering emissions from S3 and S4. Results showing all impact categories can be found in the supplementary material. This shows that waste-derived activators can completely substitute conventional alkali-activators while also producing materials of equivalent strengths. This is also in line with other reported studies (Passuello et al., 2017). Furthermore, this construes the fact that majority of environmental impacts from alkali-activated materials are associated with the type of alkali-activator used (Abdulkareem et al., 2019a, 2019b) and a waste-derived activator can significantly increase their environmental performance.

3.2. Sensitivity analysis

Sensitivity analysis is conducted on the key parameters influencing the system. Based on the results, sodium silicate and NaOH are the major contributing materials to the environmental burdens of AAMs. Consequently, sensitivity analysis will be performed on these chemicals. Additionally, influence of allocation is determined for WG and RHA respectively.

3.2.1. Sensitivity analysis on sodium hydroxide using different production methods

High amounts of sodium hydroxide are required to chemically modify waste glass (S3) and RHA (S4) to produce alkali-activators. Also, additional sodium hydroxide is required in the development of aqueous alkali-activated mortar in S2 and S4 (see Table 1). Thus, the sensitivity analysis was mainly between S2, S3 and S4, using different production methods. The main production method used in this study for sodium hydroxide is "EU NaOH from chlorine-alkali electrolysis, 100% NaOH, using membrane, diaphragm and amalgam technology mix". The alternative production methods used for sensitivity analysis include "RER NaOH from brine solution, 100% NaOH" and "DE NaOH using diaphragm route, 100% NaOH". These are all collected from GaBi database. More information on the emission factors of these different LCI can be found in the supplementary material.

The highest impact was observed in *RER NaOH* in all impact categories, while *EU NaOH* had the least emissions. It can be deduced that producing sodium hydroxide from brine solution (RER NaOH) and diaphragm route (DE NaOH) respectively, caused more environmental impacts compared to using a technology mix of membrane, diaphragm and amalgam production method (EU NaOH) (Fig. 5). To further reduce the environmental footprints of sodium hydroxide, more efficient production processes can be practiced which in overall improves the environmental footprint of alkali-activated materials.

3.2.2. Sensitivity analysis on sodium silicate using different LCI data

Sodium silicate is a significant contributing material to the overall LCA results. Sodium silicate powder and sodium silicate solution was utilized in S1 and S2, respectively. As a result, sensitivity analysis in this section was mainly between S1 and S2, using different LCI data. The original LCI data used is from Ecoinvent database while the alternative LCI data employed is from Fawer et al. (1999).

With respect to climate change and POC, Fawer et al. (1999) exhibited higher impacts when compared to Ecoinvent in S1, at an estimate of 48% and 71% respectively. However, results were contrariwise for S2 with decreased emissions at 13% and 12% respectively. In fossil depletion category, higher environmental impact was observed in Fawer when compared to Ecoinvent for both S1 and S2 at 63% and 3% respectively, while results were the other way round with respect to terrestrial acidification with decreased emissions of 15% and 51% respectively. These results as shown in Fig. 6, show the interconnectedness of LCI data from both

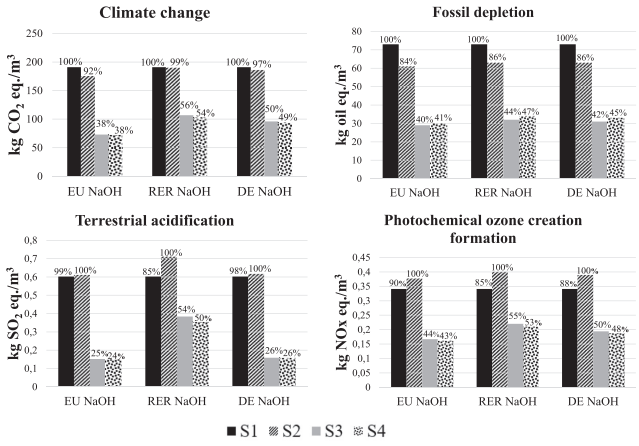

Fig. 5. Sensitivity analysis using different production methods for sodium hydroxide.

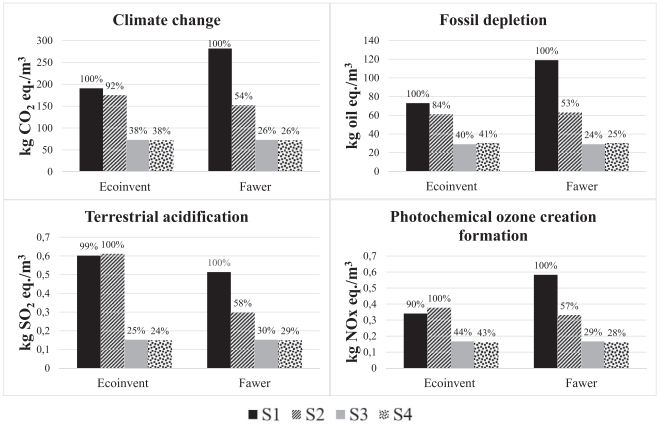

Fig. 6. Sensitivity analysis using alternative LCI data sources for sodium silicate.

Fawer et al. (1999) and Ecoinvent database. Conversely, a study carried out by European Commission on best available techniques (BAT) for manufacture of inorganic chemicals (EU, 2007), detailing inputs and outputs on sodium silicate solution, demonstrated that between 33% and 67% reduced environmental impact can be actualised for the studied impact categories when compared to Fawer et al. (1999) and Ecoinvent database (see supplementary material). This is because of reduced energy consumption and usage of more efficient technologies as document by BAT (EU, 2007). However, the study did not have detailed information for sodium silicate powder. Nonetheless, it can be assumed that reduced emissions are also achieved.

3.2.3. Sensitivity analysis on waste glass and RHA

Waste glass (WG) and RHA were assumed to be waste in this study and only associated emissions from the treatment processes were considered. Based on this assumption, a sensitivity analysis was performed to determine how mass allocation of these waste materials influence overall results of the study. Data for WG and rice were collected from Ecoinvent. Allocation of RHA was estimated from rice (non-basmati) production. As discussed earlier, RHA share in rice husk is 18–22% of dry content by weight while 20% of rice husk is generated from rice paddy, which makes it approximately 4% of RHA from rice paddy. Thus, an estimate of 4% of emissions from production of rice (non-basmati) is allocated to RHA (more details can be found in the supplementary material). Fig. 7 presents the influence of allocating emissions to WG and RHA.

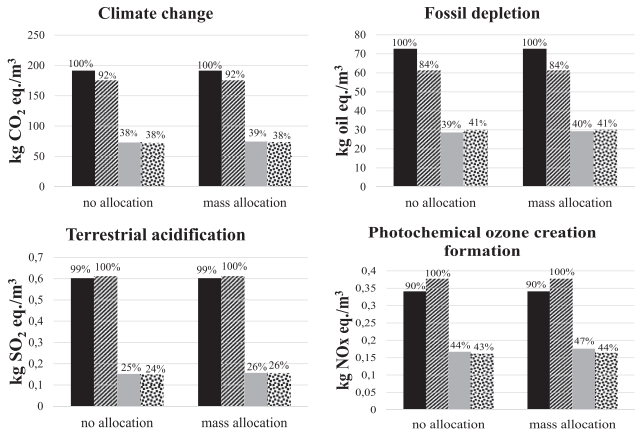

Fig. 7. Sensitivity analysis based on mass allocation of RHA and waste glass.

Scenarios S3 and S4 are particularly focused on since they contain these respective wastes materials. According to Fig. 7, it can be seen that WG and RHA are not so sensitive to the allocation procedure in all the analyzed impact categories, thus, overall, making S3 and S4 a more environmentally friendly option than S1 and S2.

3.3. Cost analysis of mortars

To determine the viability of the AAMs considered in this study, financial cost comparison is required. Thus, this study examines a simplified cost of materials needed to generate the cost of a given formulation of mortar. Sodium silicate provides a significant reactive part of silica in combination with NaOH to produce conventional alkali-activator. From data available on industrial trading websites (alibaba, 2019), conventional sodium silicate powder and solution was estimated to cost an average of 414 €/ton and 203 €/ton respectively. NaOH pellets was estimated to cost an average 414 €/ton. The cost associated with production of the waste-derived alkali-activator are as follows:

a) Cost of one-part WG-NaOH alkali-activator: Based on European statistics, material price for recyclates such as waste glass is 55 €/ton (eurostat, 2019). Thus, considering the mass proportion of WG needed for alkali-activator production, cost of WG was estimated to be 29 €/ton of activator. Additionally, based on mass proportion of NaOH pellet required to chemically modify WG powder, cost of NaOH pellets was estimated to be 199 €/ton of activator. Since it is assumed in this study that all wastes are locally available, negligible transportation costs have been considered. Electricity required for milling glass cullet to glass powder is estimated to be 50 kWh/ton (Vinai and Soutsos, 2019). Thus, 26 kWh/ton is estimated for milling of glass cullet. With market price of electricity for Finland estimated to be 0.064 €/kWh as of 2018, 1.7 €/ton is required to mill glass and energy cost for producing alkali powder from waste glass has been estimated to be 38 €/ton. In total 268 €/ton has been estimated to produce powder alkali-activator from WG, of which 74% of the cost is a result of cost of NaOH.

b) Cost of two-part RHA-NaOH alkali-activator: Price of RHA was collected from industrial trading sites (alibaba, 2019). Considering the required mass proportion for RHA required for alkali-activator production, average cost of RHA required for activator is 16 €/ton. Considering mass proportion of NaOH pellet required to chemically modify RHA, cost of NaOH pellet was estimated to be 36 €/ton of activator. Market price for electricity in Finland was estimated 0.064 €/kWh as at 2018, thus, electricity cost for producing alkali-activator from RHA has been estimated to be 14 €/ton. In total, 69 €/ton has been estimated to produce aqueous alkali-activator of which 52% of the cost is as a result of NaOH.

Prices of CFA and GBFS were collected from industrial trading sites with an average price of 35 €/ton and 43 €/ton respectively (alibaba, 2019). Price of water and sand were based on Finnish market prices, at an average price of 5 €/ton and 8 €/ton, respectively. Based on mass proportion of the different input materials,

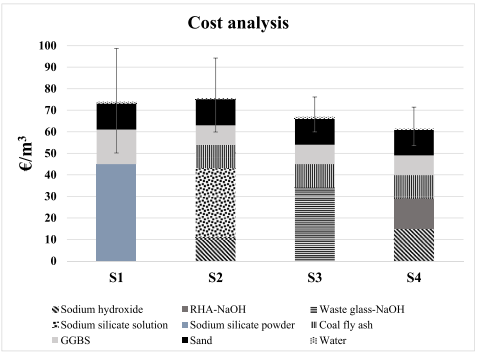

Fig. 8. Simplified cost analysis for the different alkali-activated mortars.

cost of the different mortars was calculated as presented in Fig. 8. Error bars were used to depict the price range of the different mortars. S3 and S4 AAM are slightly cheaper than S1 and S2 AAM, however, there is also possibility of S1 and S2 been cheaper if the lower values of the error bars are considered. These prices may vary quite much because there are no standardised prices for waste materials (RHA, CFA and GBFS) as compared to OPC. With industrially produced AAMs and standardised prices, cheaper price of production can be achieved.

4. Discussion and perspectives

Alkali-activated mortars are considered a low carbon alternative to cement mortars. However, producing a more compact and dense material with higher mechanical strength highly depends on the quantity of alkali-activator. Alkali-activators have also been highlighted as the most contributing material to the environmental impact of alkali-activated materials, with many studies recommending using waste-derived alkali-activators as a substitute to conventional alkali-activators. Furthermore, reduced emissions from sodium silicate can be achieved when fossil fuels are replaced with renewable energy (Abdulkareem et al., 2019a). Despite this been a sustainable alternative in producing alkali-activator, virgin raw materials are still consumed and a high energy consumption in production. WG and RHA have high volumes globally, containing significant shares of silicon oxide which is one of the major elements required in developing alkali-activators. Hence, producing alkali-activator from these waste materials, will mean avoidance of virgin materials consumption and enhancing circularity of wastes.

It should be noted RHA is predominantly produced in rainfed upland regions where rice is grown and incinerated. Therefore, RHA might not be as available in some countries. On the other hand, other silica rich agro-wastes such as straw can be used to replace RHA for countries where rice is not locally produced. WG is available almost everywhere, but its production is more distributed regionally where only large cities produce significant amounts. Therefore, collection from larger areas to the place of utilisation will be needed. Furthermore, material availability and quality of industrial side-streams such as CFA and GBFS, are crucial to the development of AAMs. These industrial side-streams are dependent on production quantity and method of production which can lead to variability in their chemical compositions (Provis, 2018). GBFS is increasingly used in the cement industry, which can reduce its availability for alkali-activated materials. Also, the adoption of renewable energy will limit the availability of CFA, which is a product of energy production from coal combustion. Consequently, research can investigate more materials that do not require much beneficiation (grinding, granulating, and high temperature processes) and has zero to low conventional value for sustainable material productions. Thus, further studies will investigate the scale of supply and demand of these materials and their proposed application.

To further increase the environmental sustainability of waste-derived activators and industrial side-streams, it is important, they are locally available. However, this usually is not the case, and in some instances, raw materials must be transported from one region to another. Transportation implies added cost in production and additional emissions. Depending on where the waste is sourced and where it is produced, transportation burdens might lower net environmental and economic benefits of using wastes. Additionally, increased environmental performance can be actualised by utilising waste heat or renewable energy in the production of waste-derived alkali-activators and beneficiation processes of side-streams.

5. Conclusions

This study highlights the relevance of using waste-based activators to produce alkali-activated mortars in developing environmentally friendly materials. This study lays emphasis on one-part (powder) WG-derived alkali-activated mortar and two-part (aqueous) RHA-derived alkali-activated mortar. In addition, a simplified cost analysis was carried to compare the cost of these different mortars to assess their economic sustainability. Conclusions from this study include:

- Waste glass and rice husk ash derived alkali-activated mortar resulted in up to 62%, 61%, 76% and 56% lower emissions respectively, in all the four studied impact categories (climate change, fossil depletion, terrestrial acidification and photochemical ozone creation formation) when compared to conventional one- and two-part alkali-activated mortar. Additionally, one-part WG-derived alkali-activated mortar without additional sodium hydroxide during mortar production, exhibits possibility of producing mortar almost completely from side-streams (waste glass, fly ash and granulated blast furnace slag) while maintaining equivalent compressive strength as conventional alkali-activated mortars.
- Waste glass and rice husk ash demonstrated little sensitivity to mass allocation procedure, with increased emissions from 0.2% to 5% in the above-mentioned impact categories, thus, making the waste-derived alkali-activated mortar a more environmentally friendly option.
- Sodium hydroxide was consistent in this study in chemically modifying waste glass and RHA to produce alkali-activators and in the development of aqueous alkali-activated mortar. Thus, a sensitivity analysis was carried out on sodium hydroxide using data from different production methods. The default production method used in this study is “EU-28 sodium hydroxide from technology-mix” while the alternative production method for sensitivity analysis includes “RER sodium hydroxide from brine solution” and “DE sodium hydroxide using diaphragm route”. Results illustrated that increased emissions between 1% and 153% was observed from the alternative production routes. Thus, sodium hydroxide production from technology-mix, demonstrated improved environmental performance than sodium hydroxide from brine solution and diaphragm route, respectively. However, with continuous improvement in the emissions profile of the chlor-alkali industry, lower emissions can be expected when assessing sodium hydroxide production in future.
- Sensitivity analysis on sodium silicate using an alternative LCI data (Fawer et al., 1999) showed that with respect to S1, 48%, 63%, and 71% increased impact was observed respectively, for climate change, fossil depletion, and POC and 15% reduced impact in acidification category. With respect to S2, between 12% and 51% of reduced impact is observed for all impact categories except fossil depletion which had a 3% increase. This is all realised when alternative LCI data is compared to the original LCI data.
- With respect to costs of producing waste-derived alkali-activated mortars, analysis show that, a range of 9%–19% of cost savings can be achieved from using waste-derived alkali-activated mortars compared to its conventional counterpart. Additionally, local availability of primary and secondary raw materials needed for production of alkali-activated materials will impact positively on the total cost of production.

It can be concluded that significant environmental impact reductions are not only achieved from waste-derived alkali-activated

mortars, but also provides a useful alternative to utilising waste residues. This study is based on literature studies and quantitatively the results are valid only for those. We can however generalize quite safely that usage of waste glass or rice husk ash as an activator reduces environmental impacts of alkali-activated mortars if their usage also reduces or substitutes the need for conventional alkali-activators in alkali-activated mortars.

CRediT authorship contribution statement

Mariam Abdulkareem: Conceptualization, Data curation, Formal analysis, Investigation, Methodology, Software, Visualization, Writing - original draft, Writing - review & editing. **Jouni Havukainen:** Conceptualization, Data curation, Funding acquisition, Investigation, Methodology, Project administration, Resources, Supervision, Validation, Writing - review & editing. **Jutta Nuortila-Jokinen:** Conceptualization, Funding acquisition, Project administration, Resources, Visualization. **Mika Horttanainen:** Conceptualization, Funding acquisition, Methodology, Resources, Supervision, Validation, Visualization, Writing - review & editing.

Declaration of competing interest

The authors declare that they have no known competing financial interests or personal relationships that could have appeared to influence the work reported in this paper.

Acknowledgements

The authors would like to acknowledge the European Regional Development Fund, through the urban innovative actions initiative for co-financing the Urban Infra Revolution project under the project number UIA02-155.

Appendix A. Supplementary data

Supplementary data to this article can be found online at https://doi.org/10.1016/j.jclepro.2020.124651.

References

Abdulkareem, M., Havukainen, J., Horttanainen, M., 2019a. How environmentally sustainable are fibre reinforced alkali-activated concretes? J. Clean. Prod. 236 https://doi.org/10.1016/J.JCLEPRO.2019.07.076.

Abdulkareem, M., Havukainen, J., Horttanainen, M., 2019b. Environmental assessment of alkali-activated mortars using different activators. In: 17th International Waste Management and Landfill Symposium. CISA publisher, Italy.

alibaba, 2019. Sodium silicate-sodium silicate manufacturers, suppliers and exporters on Alibaba.comSilicate [WWW Document]. https://www.alibaba.com/trade/search?fsb=y&IndexArea=product_en&CatId=&SearchText=sodium+silicate&viewtype=&tab=, 11.28.19.

Alomayri, T., 2017. The microstructural and mechanical properties of geopolymer composites containing glass microfibres. Ceram. Int. 43, 4576–4582. https://doi.org/10.1016/j.ceramint.2016.12.118.

Andrew, R.M., 2018. Global CO 2 emissions from cement production. Earth Syst. Sci. Data 10, 195–217. https://doi.org/10.5194/essd-10-195-2018.

Bajza, A., Rouseková, I., Živica, V., 1998. Silica fume–sodium hydroxide binding systems. Cem. Concr. Res. 28, 13–18. https://doi.org/10.1016/S0008-8846(97)00192-0.

CEMBUREAU, 2015a. Environmental Product Declaration (EPD) Portland Cement (CEM I) Produced in Europe.

CEMBUREAU, 2015b. Environmental Product Declaration (EPD) Portland-composite Cement (CEM II). https://doi.org/10.4324/9781315270326-75.

CEMBUREAU, 2015c. Environmental Product Declaration (EPD) Blast Furnace Cement (CEM III). https://doi.org/10.4324/9781315270326-75.

Chen, C., Habert, G., Bouzidi, Y., Jullien, A., 2010. Environmental impact of cement production: detail of the different processes and cement plant variability evaluation. J. Clean. Prod. 18, 478–485. https://doi.org/10.1016/j.jclepro.2009.12.014.

Davidovits, J., 2015. False Values on CO2 Emission for Geopolymer Cement/Concrete Published in Scientific Papers (No. 24).

Davidovits, J., 1994. PROPERTIES OF GEOPOLYMER CEMENTS joseph. Alkaline Cem. Concr 131–149.

EN I, SO 14040, 2006. SFS-EN ISO 14040 ENVIRONMENTAL MANAGEMENT. LIFE CYCLE ASSESSMENT . PRINCIPLES AND FRAME- WORK (ISO 14040: 2006).

EN ISO 14044, 2006. ISO 14044 – Environmental Management — Life Cycle Assessment — Requirements and Guidelines, ISO 14044. https://doi.org/10.1007/s11367-011-0297-3.

EU, 2007. Reference docunent on best available techniques for the manufacture of large volume inorganic chemicals -solids and others industry. Eur. Comm. BREF-LVI, 1–711.

European Parliament and Council, 2008. Directive 2008/98/EC of the European Parliament and of the Council of 19 November 2008 on Waste and Repealing Certain Directives. Official Journal of the European Union doi.org/2008/98/EC.; 32008L0098.

eurostat, 2019. Material Prices for Recyclates - Eurostat [WWW Document]. https://ec.europa.eu/eurostat/web/waste/prices-for-recyclates, 11.7.19.

Fawer, M., Concannon, M., Rieber, W., 1999. Life cycle inventories for the production of sodium silicates. Int. J. Life Cycle Assess. 4, 207–212. https://doi.org/10.1007/BF02979498.

FEVE, 2019. Statistics - FEVE. The European Container Glass Federation [WWW Document]. https://feve.org/about-glass/statistics/, 11.27.19.

Ghosh, R., 2013. A review study on precipitated silica and activated carbon from rice husk. J. Chem. Eng. Process Technol. 4 (4), 1–7. https://doi.org/10.4172/2157-7048.1000156.

Guo, M., Murphy, R.J., 2012. LCA data quality: sensitivity and uncertainty analysis. Sci. Total Environ. 435–436, 230–243. https://doi.org/10.1016/j.scitotenv.2012.07.006.

Gursel, A.P., Maryman, H., Ostertag, C., 2016. A life-cycle approach to environmental, mechanical, and durability properties of “green” concrete mixes with rice husk ash. J. Clean. Prod. 112, 823–836. https://doi.org/10.1016/J.JCLEPRO.2015.06.029.

Habert, G., D'Espinose De Lacaillerie, J.B., Roussel, N., 2011. An environmental evaluation of geopolymer based concrete production: reviewing current research trends. J. Clean. Prod. 19, 1229–1238. https://doi.org/10.1016/j.jclepro.2011.03.012.

Heath, A., Paine, K., McManus, M., 2014. Minimising the global warming potential of clay based geopolymers. J. Clean. Prod. 78, 75–83. https://doi.org/10.1016/j.jclepro.2014.04.046.

Hischier, R., Editors, B.W., Althaus, H., Bauer, C., Doka, G., Dones, R., Frischknecht, R., Hellweg, S., Humbert, S., Jungbluth, N., Köllner, T., Loerincik, Y., Margni, M., Nemecek, T., 2010. Implementation of Life Cycle Impact Assessment Methods. Ecoinvent report.

Kamseu, E., Beleuk à Moungam, L.M., Cannio, M., Billong, N., Chaysuwan, D., Melo, U.C., Leonelli, C., 2017. Substitution of sodium silicate with rice husk ash-NaOH solution in metakaolin based geopolymer cement concerning reduction in global warming. J. Clean. Prod. 142, 3050–3060. https://doi.org/10.1016/J.JCLEPRO.2016.10.164.

Kawai, K., Sugiyama, T., Kobayashi, K., Sano, S., 2005. Inventory data and case studies for environmental performance evaluation of concrete structure construction. J. Adv. Concr. Technol. 3, 435–456. https://doi.org/10.3151/jact.3.435.

Liikanen, M., Havukainen, J., Hupponen, M., Horttanainen, M., 2017. Influence of different factors in the life cycle assessment of mixed municipal solid waste management systems – a comparison of case studies in Finland and China. J. Clean. Prod. 154, 389–400. https://doi.org/10.1016/J.JCLEPRO.2017.04.023.

Liu, X., Li, Z., Chen, H., Yang, L., Tian, Y., Wang, Z., 2016. Rice husk ash as a renewable source for synthesis of sodium metasilicate crystal and its characterization. Res. Chem. Intermed. 42, 3887–3903. https://doi.org/10.1007/s11164-015-2251-7.

Luukkonen, T., Abdollahnejad, Z., Yliniemi, J., Kinnunen, P., Illikainen, M., 2018a. One-part alkali-activated materials: a review. Cem. Concr. Res. 103, 21–34. https://doi.org/10.1016/j.cemconres.2017.10.001.

Luukkonen, T., Abdollahnejad, Z., Yliniemi, J., Kinnunen, P., Illikainen, M., 2018b. Comparison of alkali and silica sources in one-part alkali-activated blast furnace slag mortar. J. Clean. Prod. 187, 171–179. https://doi.org/10.1016/J.JCLEPRO.2018.03.202.

Ma, X., Zhou, B., Gao, W., Qu, Y., Wang, L., Wang, Z., Zhu, Y., 2012. A recyclable method for production of pure silica from rice hull ash. Powder Technol. 217, 497–501. https://doi.org/10.1016/J.POWTEC.2011.11.009.

Marceau, M., VanGeem, M.G., 2003. Life Cycle Inventory of Slag Cement Manufacturing Process CTL Project No, p. 312012.

Marceau, M.L., Nisbet, M.A., Vangeem, M.G., 2007. Life Cycle Inventory of Portland Cement Concrete.

McGuire, E.M., Provis, J.L., Duxson, P., Crawford, R., 2011. Geopolymer concrete: is there an alternative and viable technology in the concrete sector which reduces carbon emissions?. In: Concrete 2011. CD-ROM Proceedings.

McLellan, B.C., Williams, R.P., Lay, J., van Riessen, A., Corder, G.D., 2011. Costs and carbon emissions for geopolymer pastes in comparison to ordinary portland cement. J. Clean. Prod. 19, 1080–1090. https://doi.org/10.1016/J.JCLEPRO.2011.02.010.

Meryman, H., 2009. The emergence of rice husk ash — a complimentary cementing material with untapped global potential. In: Structures Congress 2009. American Society of Civil Engineers, Reston, VA, pp. 1–10. https://doi.org/10.1061/41031(341)274.

Mohseni, E., 2018. Assessment of Na2SiO3to NaOH ratio impact on the performance of polypropylene fiber-reinforced geopolymer composites. Constr. Build. Mater. 186, 904–911. https://doi.org/10.1016/j.conbuildmat.2018.08.032.

Nematollahi, B., Sanjayan, J., Shaikh, F.U.A., 2015. Synthesis of heat and ambient cured one-part geopolymer mixes with different grades of sodium silicate.

Ceram. Int. 41, 5696–5704. https://doi.org/10.1016/j.ceramint.2014.12.154.
Norsuraya, S., Fazlena, H., Norhasyimi, R., 2016. Sugarcane bagasse as a renewable source of silica to synthesize santa barbara amorphous-15 (SBA-15). Procedia Eng 148, 839–846. https://doi.org/10.1016/j.proeng.2016.06.627.
Passuello, A., Rodríguez, E.D., Hirt, E., Longhi, M., Bernal, S.A., Provis, J.L., Kirchheim, A.P., 2017. Evaluation of the potential improvement in the environmental footprint of geopolymers using waste-derived activators. J. Clean. Prod. 166, 680–689. https://doi.org/10.1016/j.jclepro.2017.08.007.
Provis, J.L., 2018. Alkali-activated materials. Cem. Concr. Res. 114, 40–48. https://doi.org/10.1016/j.cemconres.2017.02.009.
Puertas, F., Torres-Carrasco, M., 2014. Use of glass waste as an activator in the preparation of alkali-activated slag. Mechanical strength and paste characterisation. Cem. Concr. Res. 57, 95–104. https://doi.org/10.1016/J.CEMCONRES.2013.12.005.
Rouseková, I., Bajza, A., Živica, V., 1997. Silica fume-basic blast furnace slag systems activated by an alkali silica fume activator. Cem. Concr. Res. 27, 1825–1828. https://doi.org/10.1016/S0008-8846(97)00191-9.
Stajanca, M., Estokova, A., 2012. Environmental impacts of cement production. Tech. Univ. Kosice, Civ. Eng. Fac. Inst. Archit. Eng. 296–302.
Tchakouté, H.K., Rüscher, C.H., Hinsch, M., Djobo, J.N.Y., Kamseu, E., Leonelli, C., 2017. Utilization of sodium waterglass from sugar cane bagasse ash as a new alternative hardener for producing metakaolin-based geopolymer cement. Geochemistry 77, 257–266. https://doi.org/10.1016/J.CHEMER.2017.04.003.
Tchakouté, H.K., Rüscher, C.H., Kong, S., Kamseu, E., Leonelli, C., 2016. Comparison of metakaolin-based geopolymer cements from commercial sodium waterglass and sodium waterglass from rice husk ash. J. Sol. Gel Sci. Technol. 78, 492–506. https://doi.org/10.1007/s10971-016-3983-6.
Thinkstep, 2019. Description of the CML 2001 method [WWW Document]. http://www.gabi-software.com/support/gabi/gabi-lcia-documentation/cml-2001/, 6.30.19.
Tong, K.T., Vinai, R., Soutsos, M.N., 2018. Use of Vietnamese rice husk ash for the production of sodium silicate as the activator for alkali-activated binders. J. Clean. Prod. 201, 272–286. https://doi.org/10.1016/J.JCLEPRO.2018.08.025.
Torres-Carrasco, M., Puertas, F., 2015. Waste glass in the geopolymer preparation. Mechanical and microstructural characterisation. J. Clean. Prod. 90, 397–408. https://doi.org/10.1016/J.JCLEPRO.2014.11.074.
Van Den Heede, P., De Belie, N., 2012. Environmental impact and life cycle assessment (LCA) of traditional and "green" concretes: literature review and theoretical calculations. Cem. Concr. Compos. 34, 431–442. https://doi.org/10.1016/j.cemconcomp.2012.01.004.
Vinai, R., Soutsos, M., 2019. Production of sodium silicate powder from waste glass cullet for alkali activation of alternative binders. Cem. Concr. Res. 116, 45–56. https://doi.org/10.1016/J.CEMCONRES.2018.11.008.
Weidema, B.P., Bauer, C., Hischier, R., Mutel, C., Nemecek, T., Reinhard, J., Vadenbo, C.O., Wernet, G., 2013. Overview and Methodology. Data Quality Guideline for the Ecoinvent Database Version 3.
Weil, M., Gasafi, E., Buchwald, A., Dombrowski, K., Buchwald, A., 2005. Sustainable design of geopolymers - integration of economic and environmental aspects in the early stages of material development. Sustain. Dev. 279–283.
Yang, K.-H., Song, J.-K., Lee, J.-S., 2010. Properties of alkali-activated mortar and concrete using lightweight aggregates. Mater. Struct. 43, 403–416. https://doi.org/10.1617/s11527-009-9499-6.
CEMBUREAU Activity Report, 2017.

Publication IV

Abdulkareem, M., Havukainen, J., Nuortila-Jokinen, J., and Horttanainen, M.
Life cycle assessment of a low-height noise barrier for railway traffic noise

Reprinted with permission from
Journal of Cleaner Production
Vol. 323, pp. 129169, 2021

Journal of Cleaner Production 323 (2021) 129169

Contents lists available at ScienceDirect

Journal of Cleaner Production

journal homepage: www.elsevier.com/locate/jclepro

Life cycle assessment of a low-height noise barrier for railway traffic noise

Mariam Abdulkareem [a,*], Jouni Havukainen [a], Jutta Nuortila-Jokinen [b], Mika Horttanainen [a]

[a] Lappeenranta-Lahti University of Technology, School of Energy Systems, Department of Sustainability Science, P.O.Box 20, FI, 53851, Lappeenranta, Finland
[b] Lappeenranta-Lahti University of Technology, Research Platform RE-SOURCE, P.O.Box 20, FI, 53851, Lappeenranta, Finland

ARTICLE INFO

Handling editor: Yutao Wang

Keywords:
Low-height noise barrier
Geopolymer composite
Life cycle assessment
Additive manufacturing
Service life
Compressive strength

ABSTRACT

Life cycle assessment (LCA) methodology was applied to assess five locally developed mix designs for a 20 m low-height noise barrier (LHNB) categorized as: precast Portland cement concrete (S0-baseline scenario), two precast geopolymer composites (S1; S2), and two additive-manufactured geopolymer composites (S3; S4). The objective of the study is to carry out a LCA study of the mix designs, to identify environmental hotspots and evaluate the influence of durability and service life on the LCA results. Environmental impact categories assessed are global warming potential (GWP), fossil depletion, photochemical ozone formation, and acidification. Results show that when a fixed service life of 40 years is chosen for all mix designs, S4 is the most environmentally sustainable with 73% reduced GWP when compared to S0. When sensitivity analysis was used to determine the effect of varying service life (10–40 years) on S1–S4; S4 shows equivalent to better environmental performance than S0. Carbonation was considered and result shows up to 8% of CO_2 uptake can be achieved. In conclusion, S4 depicts solutions and concepts that result in environmental improvement potentials for a LHNB from geopolymer composites. The results from this study supported decision-making and guided in the development a 20 m LHNB from 83% industrial side-streams and 0.3% alkali activator maintaining a 10 dB absorption capacity.

1. Introduction

Railway traffic noise, has become a recurrent but much underrated pollutant in modern-day environments and can cause negative effects such as communication interference, effects on social conduct, sleep disturbance, and hearing and concentration loss for neighboring residents (Valdebenito and Dahmen, 2013). Railway traffic noise arise from different sources, most significant is the amount of contact between the rail and the train wheel due to irregularities that cause vibration producing noise known as rolling or traffic noise (Vahtera, 2011). This can be disturbing if noise levels in the vicinity is low. Noise is measured in decibels (dB) on a logarithmic scale. However, for the human ears to respond to the frequency range involved, it is measured using an A-weighted scale (dBA) (Transport Roads and Maritime Services, 2016).

Railway traffic noise has more sound energy at high frequencies and its reduction is essential for a higher quality of life. The noise can be combated by preventing noise generation at source through various technical solutions or by incorporating noise abatement measures such as noise barriers. Noise barriers can be developed using different approaches such as Portland cement concrete, (PCC), steel and aluminum etc. (Bendtsen, 2010). For railway tracks, low-height noise barrier (LHNB) is becoming popular. LHNB as shown in Fig. 1 are a type of noise barrier with a nominal height between 85 cm and 110 cm above the rail surface (Vahtera, 2011). LHNB are sited close to the rail track to dampen the impact of the rolling noise from the rail-wheel collision and their efficacy is determined by the insertion loss, which evaluates the sound pressure before and after incorporating the LHNB (Valdebenito and Dahmen, 2013). LHNB differ from regular noise barriers with regards to location, altitude, urban visibility, and construction costs. They do not obscure views from the train windows and have so far been built for testing purposes in Finland. LHNB are designed on a case-by-case basis due to changing track geometry and must meet at least the Finnish A3 category for sound absorption which is 8–11 dB (Liikennevirasto, 2017; Vahtera, 2011). Despite all these considerations in developing efficient LHNB, their environmental sustainability remains an open question.

While some studies have addressed the acoustic and non- acoustic aspects of LHNB and generally noise barriers (Bendtsen, 2010; Transport Roads and Maritime Services, 2016; Vanhooreweder et al., 2017), and fewer studies have focused on sustainable materials in development of noise barriers (Abbas et al., 2011; Arenas et al., 2017; Asdrubali, 2006;

* Corresponding author.
E-mail addresses: Mariam.Abdulkareem@lut.fi (M. Abdulkareem), Jouni.Havukainen@lut.fi (J. Havukainen), Jutta.Nuortila-Jokinen@lut.fi (J. Nuortila-Jokinen), Mika.Horttanainen@lut.fi (M. Horttanainen).

https://doi.org/10.1016/j.jclepro.2021.129169
Received 2 January 2021; Received in revised form 20 September 2021; Accepted 23 September 2021
Available online 25 September 2021

Louise Rose Joynt, 2005; Oltean-dumbrava and Richards, 2016), there has been very limited research on their life cycle assessment (LCA). A study on environmental assessment of noise barriers by Valdebenito and Dahmen (2013), documented environmental performance of a sound structure comparing a vegetative sound structure and PCC noise barrier. The environmental assessment performed was limited to the production phase and did not include the use and end-of-life phases. The assessment of potential environmental impacts of noise barriers cannot be based on the evaluation of any single phase of the technology, but from raw material extraction, via construction, service life of the final products as well as end-of-life.

LHNB and generally noise barriers are traditionally produced from PCC for their simple design and construction (Abbas et al., 2011). Environmental sustainability of PCC is highly dependent on cement, which is the key binding material with an estimated 4.1 billion tons of global production in 2016 (CEMBUREAU, 2017). Consequently, there have been variety of studies on improving environmental sustainability of PCC such as using recycled materials during production (Brennan et al., 2014; Marinković et al., 2017; Raut et al., 2011; Turk et al., 2015), substitution with geopolymer composite (Abdulkareem et al., 2019; Habert et al., 2011; Luukkonen et al., 2018; Weil et al., 2009), and employing additive manufacturing in construction (Nematollahi et al., 2017; Panda et al., 2017; Panda and Tan, 2018; Van Damme, 2018).

Geopolymers are generally used to depict low calcium alkali activated aluminosilicate binders and are produced by reacting solid aluminosilicate raw materials (precursor) with an alkali activator to form a hardened binder. These precursors can be in the form of natural raw materials such as metakaolin, or as industrial side-streams with a high Si/Al ratio such as coal fly ash (CFA) and granulated blast furnace slag (GBFS) (Davidovits, 1994; Provis, 2018). Integrating industrial by-products in the production of geopolymer composites by reusing and recycling waste materials as secondary raw materials, helps to avoid problems of waste disposal and associated environmental burdens.

Additionally, additive manufacturing is a technology for building three-dimensional (3D) elements from a 3D computer-aided design model. Advantages of 3D fabrications include more flexibility, increased innovations, faster construction, risk mitigation, high material resource efficiency, and cost effectiveness (Huang et al., 2017). 3D printing has an advantage of manufacturing customized products, while maintaining similar performance and functions. However, environmental performance of AM is still debated. While some consider AM as a sustainable solution due to the near zero waste achieved during building, other consider AM as not less wasteful, as it is reported to consume an estimated 100 times higher specific energy than traditional manufacturing (Liu et al., 2018; Výtisk et al., 2019).

In this paper, we investigate life cycle assessment (LCA) study of a pilot scale low-height noise barrier (LHNB) made from Portland cement concrete (PCC) and geopolymer composites. For piloting purposes of new materials and structures, these kinds of low-height structures are suitable due to lower material consumption and manufacturing effort when compared to high structures. Also, there is less manual work when the manufacturing has not been developed in full scale. The LHNB prototypes are predefined designs, and the objective is to analyze their environmental performance based on different mix designs, life cycle phases, and construction techniques using LCA methodology.

2. Materials and method

Life cycle assessment (LCA) methodology is a standardized and established to quantify environmental performance and potential impacts of a product or service throughout its life cycle from extraction of raw materials to its end-of-life phase (EN ISO, 14040, 2006; EN ISO 14044, 2006). A product interacts with the environment in several ways all through the different life cycle phases, with each phase demonstrating a different environmental strain. As a systematic approach, LCA consists of four major phases which are addressed in different sections of this article: goal and scope definition (section 2.1); inventory analysis (section 2.2); impact assessment (section 2.3); and interpretation phase (section 3) (see Fig. S1 in the supplementary material).

This LCA study analyses five different LHNB scenarios, a reference LHNB scenario using precast PCC and four alternative LHNB geopolymer composites scenarios using precast and additive manufacturing construction methods. The geopolymer composites LHNB scenarios are developed mainly from wastes materials and industrial by-products such as coal fly ash (CFA), granulated blast furnace slag, bottom ash, bio ash, crushed steel slag, fine and coarse tailings. These are described in detail in section 2.1.1. The principal function of the LHNB is to protect neighboring residents from excessive noise produced by railway traffic.

Fig. 1. Low-height noise barrier in Finland (Liikennevirasto, 2017).

The pilot LHNB analyzed in this study is 20m in length with a 10 dB absorption capacity. It is situated in the railway track of the city of Lappeenranta in Finland, where it will be in full operation. Acoustic and non-acoustic performances of a LHNB can depreciate over the duration of its working life due to exposure to different environmental conditions and other factors. Due to this, service life of the noise barrier can be defined as the duration it functions trouble-free with no visible change in insertion loss or appearance (Morgan et al., 2001).

Desirable service life for PCC noise barrier is averagely 40 years (Environmental Protection Department Highways Department, 2003; Parker, 2006). On the other hand, there is limited information on service life estimation for geopolymer composite noise barriers. Amorim Júnior et al. (2021) investigated durability and service life of metakaolin-based geopolymer with respect to chloride penetration. The service life of the geopolymer concrete based on Fick's second diffusion law and using the age influence coefficient 0.4 and 0.6 was estimated in the range 12–13 years and 39–45 years, respectively. However, the author stated the service life prediction is used prospectively due to lack of good accuracy. Due to differences in mix designs, the LHNB geopolymer composite scenarios may have different service lives and due to limited studies on the parameters needed to calculate service life of the geopolymer composites, 40 years of service life is assumed for all scenarios in this paper. However, sensitivity analysis for service life (10–40 years) of the geopolymer LHNB scenarios is conducted. When the LHNB depreciates and can no longer fulfill its function, the LHNB modules are demolished, crushed, and landfilled. Carbonation is also taken into consideration to determine potential CO_2 savings that can be achieved during the use and end-of-life phases.

2.1. Goal and scope definition

The goal of this study is to carry out an LCA of five different LHNB mix designs made from either PCC or geopolymer composite and to evaluate the impact of product system changes on their environmental performance. The reasons for carrying out this study is to support decision-making in the development of a LHNB. The functional unit is a 20 m LHNB with 10 dB absorption capacity. Although, the LHNB have the same function, differences in mix designs will influence their durability and service life which will further influence the effectiveness of their function over time. In this regard, the functional unit is adapted to include compressive strength and service life of the concretes to yield a more consistent interpretation and assessment of results (Marinković et al., 2021; Vieira et al., 2018). This is achieved by applying two indicators. The first indicator is defined as the ratio of environmental impact category to compressive strength (MPa) at 28 days of a 20 m long LHNB (Equation (1)). The second indicator is defined as the ratio of environmental impact category to compressive strength (MPa) at 28 days and service life (years) of a 20 m long LHNB (Equation (2)) (Müller et al., 2019; Vieira et al., 2018).

$$Indicator_1 = \frac{Environmental\ \ impact\ \ category}{MPa{\cdot}20m} \quad (1)$$

$$Indicator_2 = \frac{Environmental\ \ impact\ \ category}{MPa{\cdot}20m{\cdot}years} \quad (2)$$

System boundary as shown in Fig. 2 comprise all life cycle stages from cradle to grave. Processes include raw material extraction and secondary material production, construction, transportation, and utilities (energy). Precast and additive manufacturing construction methods are investigated in this study. Transport includes distribution of materials required for construction of the LHNB from suppliers to factory to place of erection. The use stage includes usage of LHNB. At the end-of-life, the LHNB is demolished and landfilled. Capital equipment are excluded unless they are already incorporated in the unit processes of the background system. The primary data of the product system is provided by developers of the LHNB. Where primary data could not be acquired, secondary data were sourced from literature. S0, S1, S2, S3, and S4 as shown in Fig. 2 are the different LHNB scenarios and are further discussed in the next section 2.1.1.

2.1.1. Scenario description

Different mix designs were developed for precast and additive manufactured (AM) LHNB as described in the five scenarios below.

- S0 – Precast PCC
- S1 – Precast geopolymer composite
- S2 – Precast geopolymer composite
- S3 – AM geopolymer composite
- S4 – AM geopolymer composite

S0 represents the reference scenario which all other scenarios are compared against. S1 and S2 describes two different precast geopolymer composite mix designs while S3 and S4 illustrates two different AM geopolymer composite mix designs as shown in Table 1. The materials

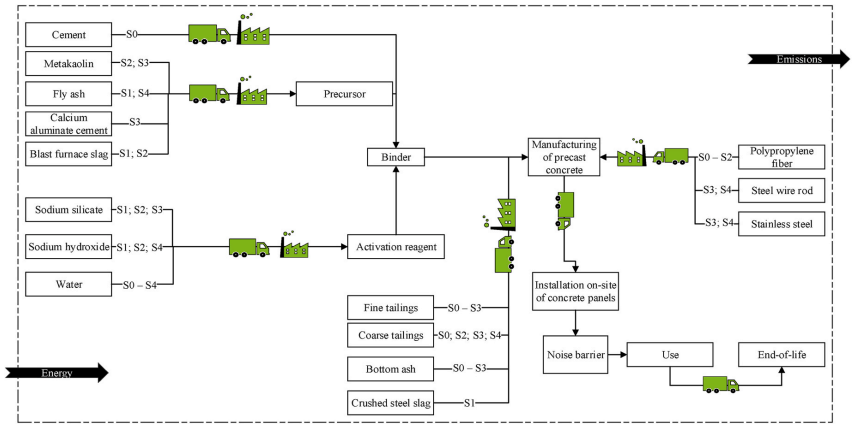

Fig. 2. System boundary depicting processes considered during the life cycle phase of the low-height noise barrier.

Table 1
Mix designs of the different scenarios (APILA Group, 2020).

Constituent	S0	S1	S2	S3	S4
Cement	27%				
Calcium aluminate cement				4%	
Activator		10%	15%	19%	0.3%
Waste precursor (CFA and GBFS)		25%	4%		37%
Metakaolin			9%	13%	
Fine aggregates	9%	13%	19%	13%	17%
Coarse aggregates	52%	45%	48%	43%	30%
Water	12%	6%	4%	6%	16%
Polypropylene fiber	0.14%	0.14%	0.14%		

CFA – coal fly ash; GBFS – granulated blast furnace slag.

needed for construction of S0 include cement, water, fine and coarse aggregates while materials required for construction of S1 – S4 are alkaline activator, precursors, water, fine and coarse aggregates as detailed in Table 1. The precursors used in S1 and S4 are mainly CFA and GBFS which have gone through beneficiation process while precursors for S2 combines GBFS and metakaolin, and precursor for S3 combines calcium aluminate cement and metakaolin. The fine aggregates are made up of fine tailings in all scenarios except S4 in which milled bio fly ash was used. Coarse tailings and bottom ash were used in S0, S2, and S3 respectively, as coarse aggregates while S1 contained bottom ash and crushed steel slag. Other materials include water and polypropylene fiber.

2.1.2. Preparation of pilot scale low-height noise barrier modules

In preparation of the pilot scale geopolymer composite LHNB, the activation reagent is prepared by weighing the solution reagents and then blending for a few minutes. The solution is left to dissolve completely and cooled. The geopolymer composite is prepared by weighing and mixing the dry ingredients. The activation reagent is poured into the dry mixture, stirred, and subsequently poured in molds or in a 3D printer with continuous mixing. The air bubbles are removed with a vibrator after casting. The products are cured at room temperature for 7 days shielded with a plastic film cover. The excess casting and other pieces are disposed with normal aggregate waste. This manufacturing applies to the geopolymer composite scenarios that are examined in this study (APILA Group, 2020).

According to preliminary product requirements, LHNB must be in two parts, a separate top of barrier and the foundation modules (Vahtera, 2011). For the precast LHNB, the modules are casted indoor and then transported to a construction site. The height of one module is 90 cm, a slab is placed 10 cm above ground surface making the total height of the LHNB to be 100 cm. The slab is not included in this study since it is same for all scenarios. The weight of one module as shown in Fig. 3 is 330 kg, and for a 20 m long LHNB 45 modules are used. The modules are attached to each other with stainless steel rebar welded to the caps screwed into the lifting anchors of the modules. The thickness of the LHNB is 150 mm which fits the Finnish standard concrete thickness (at least 100 mm) of a noise barrier (Liikennevirasto, 2017).

For the additive manufactured LHNB, the module is printed in factory and transported to the site for assembling. The weight and height of one module as shown in Fig. 4 is 57 kg and 45 cm, respectively. Two modules stacked on each other are needed to reach a 90 cm height and a slab is placed 10 cm above the ground making the total height of the barrier 100 cm. For a 20 m long LHNB, 90 modules are used. The module is hollow in shape and filled with 58.28 L of crushed aggregate per module. For 90 modules, 5245 L of crushed aggregate is utilized. The thickness of the concrete is 295 mm.

2.1.3. Carbonation (CO_2 uptake)

Carbonation "is a chemical reaction by which CO_2 penetrates concrete and reacts with hydration products, forming mainly calcium carbonate" (Andersson et al., 2019). When cement is produced, most of the CO_2 emitted is due to combustion of fuels required in production of cement and to some extent from calcination of limestone. The calcination reactions are reversible, thereby, CO_2 is absorbed into the concrete by a process referred to as carbonation. Carbonation is dependent on several factors such as the process lasting many years as it is a slow process. Other factors include CO_2 availability (as concrete must be exposed to CO_2 in air to carbonate), transport of CO_2 molecules into concrete (which can make carbonation rate faster when concrete is crushed), temperature, humidity, and porosity. Thus, considering carbonation in emission calculation of concrete is important (Stripple et al., 2018).

Carbonation reaction occurs in several steps but the main reaction is the reaction between the calcium and carbonate ions which takes place in water phase in the pore solution in the concrete, making water and moisture an important part of carbonation (Andersson et al., 2019). It is documented that half of the emissions that comes from raw materials required to produce concrete, can be reabsorbed during carbonation process of concrete during the use phase and partly in the end-of-life phase (Stripple et al., 2018). A report by Stripple et al. (2018) details carbonation reaction steps and has documented three different CO_2 uptake calculation methodologies based on complexity and accuracy. These different methods relate to an annual CO_2 uptake. In this study, the simplified methodology presented by Stripple et al. (2018) will be used to calculate the CO_2 uptake in the LHNB use and end-of-life phases.

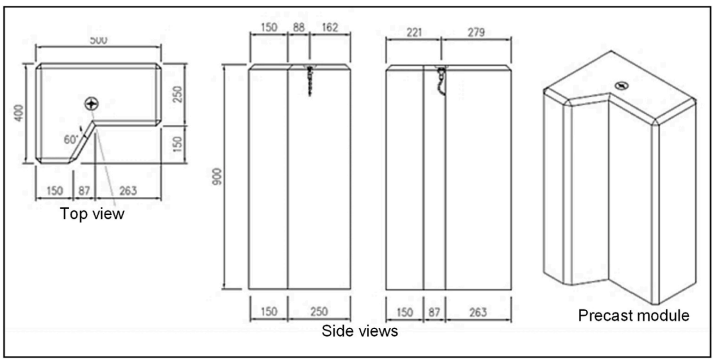

Fig. 3. Pilot precast LHNB module for the UIR project (Concept design by Design Reform ltd, 2020).

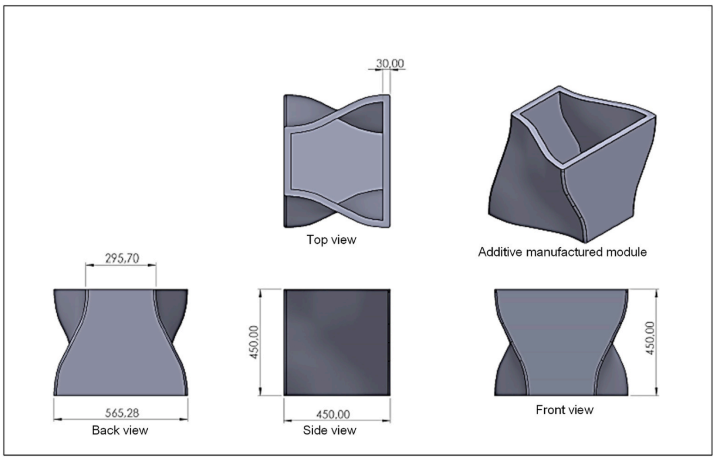

Fig. 4. Pilot additive manufactured LHNB element for the UIR project (Concept design by Design Reform ltd, 2020).

For the use stage, two alternative CO_2 uptake calculations are provided to handle uncertainty.

- Alternative A: annual CO_2 uptake for the use stage is estimated as "0.20 multiplied by the reported emission from calcination of consumed cement clinker"
- Alternative B: annual CO_2 uptake for the use stage is estimated as "0.15 multiplied by the reported emission from calcination of consumed cement clinker"

For the end-of-life phase (demolishing, crushing and storage).

- annual CO_2 uptake is estimated as "0.02 multiplied by the reported emission from calcination of consumed cement clinker".

Alternatively, if both the amount of annual concrete recycling and annual crushed concrete used as secondary raw material is known, the CO_2 uptake in the end-of-life and secondary use phase can be individually calculated as 10 kg CO_2/m^3 concrete (Stripple et al., 2018).

2.2. Life cycle inventory (LCI)

LCI is where data is collected and compiled on elementary flows for all processes in the product system. LCI data for sodium hydroxide, polypropylene fiber, transportation, cement, electricity, and water were sourced from GaBi database. LCI for sodium silicate and calcium aluminate cement were respectively sourced from Ecoinvent database and environmental product declaration by Cimsa Cimento (CIMSA, 2015). Pedigree matrix is applied to assess the quality of data utilized in this study. More information of the data quality can be found in the supplementary material (see Table S1). The data source for the different processes is shown in Table 2 below.

Data quality indexes are evaluated based on five independent characteristics namely, reliability, completeness, temporal correlation, geographical correlation, and further technological correlation, respectively as shown in the brackets (x,x,x,x,x). Each independent characteristic is scored between 1 and 5 quality levels (1-excellent; 5-poor) (Weidema et al., 2013).

To produce metakaolin, kaolin is calcined at 2.5 MJ/kg of thermal energy from natural gas (Heath et al., 2014; NLK, 2002). LCI data for kaolin is reported in GaBi database. LCI data for beneficiating fly ash, tailings and crushed steel slag were sourced from local companies producing these materials. Energy consumption for processing tailings and crushed steel slag is 0.011 MJ/kg and 0.063 MJ/kg respectively while energy consumption for processing bio fly ash and CFA is 0.045 MJ/kg and 0.11 MJ/kg, respectively. GBFS goes through the processes of granulation, drying, crushing and grinding (Marceau et al., 2007). Thus,

Table 2
Data source and quality.

Type of data	Source	Data quality indexes Pedigree matrix
Sodium hydroxide	GaBi database 2019 – EU-28: Sodium hydroxide (caustic soda mix, 100%)	(3,3,2,2,2)
Sodium silicate solution	Ecoinvent database – EU-28: Sodium silicate production, hydrothermal liquor, product in 37% solution state	(2,2,5,1,1)
Portland cement	Cement (CEM I) [Minerals]	(3,3,4,4,5)
Metakaolin	Kaolin calcination (Heath et al., 2014; NLK, 2002)	(3,3,2,3,3)
Water	GaBi database 2019 – EU-28: tap water	(3,3,4,4,3)
Electricity	GaBi database 2019 – FI: electricity grid mix	(3,3,4,3,4)
GBFS	GBFS beneficiation (Marceau and VanGeem, 2003)	(2,3,5,4,1)
Coal fly ash	Locally sourced	(1,2,1,1,1)
Tailings	Locally sourced	(1,2,1,1,1)
Calcium aluminate cement	Cimsa Cemento (CIMSA, 2015)	(2,2,1,4,2)
Crushed steel slag	Locally sourced	(1,2,1,1,1)
Crushed stone	GaBi database 2019 – DE: crushed stone 16/32 ts	(3,3,2,3,2)
Transportation	GaBi database 2019 – Truck-trailer, Euro 5, 34–40 t gross weight/27 t payload capacity	(3,3,2,2,2)
Diesel	GaBi database 2019 – Diesel mix at filling station	(3,3,2,3,3)
Landfill	GaBi database 2019 – Inert matter (unspecific construction waste on landfill)	(3,3,2,2,3)
Polypropylene fiber	GaBi database 2019 – EU-28: Polypropylene fibers	(3,3,2,4,2)

materials and energy required to process GBFS were modelled according to data from Marceau and VanGeem (2003). Data on electricity requirements for dissolving alkaline activator is 0.0084 kWh/kg (Passuello et al., 2017) and mixing of constituents is locally estimated to be 0.0045 MJ/kg. Electricity requirements for 3D printing is locally estimated to be 7 MJ/t (Jäppinen, 2017) while data for precast is estimated to be 2.16 MJ/t (Tahvanainen, 2020). It is assumed that limited to no-maintenance and repair activities are required. The distance covered for the different materials used in the LHNB scenarios can be found in Table S2 of the supplementary material.

2.3. Life cycle impact assessment (LCIA)

The LCIA phase is where information from LCI is translated to environmental impact scores and categories. In this step, an overview of significant environmental impact categories for LHNB is conducted. The relevant environmental impact categories in assigning LCI results to environmental issues according to different literature studies (Estévez et al., 2006; Kawai et al., 2005; Kikuchi and Kuroda, 2011; Zhang et al., 2006) are global warming potential (GWP) (kg CO2 eq.), fossil depletion (ADP_FF) (kg oil eq.), photochemical ozone creation potential (POCP) (kg NO_x eq.), and acidification potential (AP) (kg SO_2 eq.). These environmental impact categories are selected as they are associated with environmental issues related to concrete production such as fossil and resource depletion, emissions to air, water, and land (Chen et al., 2010; Stajanca and Estokova, 2012). Environmental performance modelling was conducted using GaBi 9.2.0.58 software and selected method was ReCiPe 2016 v1.1 (midpoint hierarchist timeframe). ReCiPe indicators provide information on the environmental issues associated with inputs and outputs of the product system at both midpoint and endpoint level. It also provides characterization factors for a variety of elementary flows for different environmental impacts (Výtisk et al., 2019). It is a widely adopted method due to its robustness (Hischier et al., 2010).

2.4. Sensitivity analysis

Sensitivity analysis is applied to evaluate the influence of modelling assumptions and choices in a product system (EC-JRC, 2010). Service life of geopolymer composite was assumed to be 40 years same as PCC. However, due to material differences in the mix designs of the LHNB scenarios, sensitivity analysis was conducted for the geopolymer composite (S1 – S4) in range 10 years–40 years to determine the influence of changes in service life on the environmental performance of the geopolymer composite LHNB scenarios.

3. Results

The LCIA results generated are based on the environmental assessment of the different LHNB scenarios (see Table 1). These results illustrate the environmental impacts of the LHNB in their different life cycle phases.

In the production phase, with respect to GWP, S1, S2, S3 and S4 had 44%, 7%, 32% and 96% lower global warming effects respectively, when compared to S0. With respect to ADP_FF, S1, S2 and S3 have 33%, 123% and 36% increased oil extraction respectively while S4 has 87% decrease, respectively, when compared to S0. With respect to POCP, S1, S2, S3 and S4 had 41%, 17%, 47% and 94% lower formation of photochemical oxidants, when compared to S0. Finally, with respect to AP, S1, S2, and S3 have respectively, 10%, 62%, and 27% potential increase in atmospheric deposition of acidifying compounds while S4 has 96% decrease when compared to S0. Still in the production phase, regarding GWP, cement is the most significant contributing material in S0 (90%). In S1, alkali activator and transportation were the most significant contributor at 80% and 16% respectively. In S2, alkali activator and metakaolin were the significant contributors at 70% and 19% respectively. Regarding S3, sodium silicate, metakaolin and CAC contributed 59%, 19% and 13% respectively. While in S4, transportation, aggregates, and alkali activator were the most significant contributor at 39%, 38%, and 11%. With respect to ADP_FF, cement (70%) and transportation (21%) mostly contributed to S0. Alkali activator and transportation contributed 73% and 16% respectively, to S1. In S2 and S3, alkali activator contributed 61% each and metakaolin contributed 24% and 29% to the scenarios, respectively. In S4, transportation and aggregates contributed 33% each. With respect to POCP, cement and transportation contributed 84% and 15% respectively to S0. Alkali activator and transportation are the most significant contributors to S1 at 70% and 27% respectively, S2 at 71% and 17% respectively, and S3 at 69% and 14% respectively. In S4, transportation and aggregates had 93% and 19% contribution, respectively. Finally, with respect to AP, cement (91%) is also the most significant contributing material in S0. Alkali activator is the most significant contributing material in S1 (90%), S2 (91%), and S3 (75%). In S4, transportation and aggregates contributed 45% and 26%, respectively. Other materials had minimal contribution lower than 10%. Visual representation of contribution of the input materials and energy to the respective impact categories in the production phase can be found in the supplementary material (see section B: LCIA results – contribution analysis in the production phase).

In the use phase, carbonation as discussed in section 2.1.3 is taken into account, and alternative B is used to calculate the annual CO_2 uptake for more conservative results. Calcination emission from cement is estimated to be approximately 49% (Stripple et al., 2018). For the geopolymer scenarios which have no cement content, CO_2 uptake is not calculated. This is because of the limited data availability for the CO_2 uptake of CFA and GBFS. Although, CO_2 uptake for GBFS has been estimated to be 35 kg CO_2/ton, it is recommended to include these additions when advanced CO_2 uptake methodology is applied. Since, simplified CO_2 uptake methodology is applied in this study, CO_2 uptake for scenarios with cement content (S0 and S3) are the only ones considered. Also, since minimal to no-maintenance and repair activities are expected during the usage of LHNB, the emissions in the use phase are limited to activities leading to carbonation and CO_2 uptake. Thus, annual CO_2 uptake for S0 and S3 is estimated to be 270 and 27 kg CO_2 eq./20m, respectively.

In the end-of-life phase, LHNB are demolished and transported to landfill. Emissions from demolition, crushing, and landfill are comparable for all the scenarios since the weights of the LHNB are equivalent. Annual CO_2 uptake is also considered in the end-of-life phase and estimated to be 36 and 4 kg CO_2 eq./20m for S0 and S3, respectively.

Fig. 5 presents the LCA results of the LHNB scenarios and on the secondary axis is the respective compressive strength (MPa at 28 days) of the scenarios. For the overall LCA results, S2 has the highest GWP emissions, with 0.35% increase above S0, while S1, S3 and S4 have 37%, 26% and 89% lower GWP emissions compared to S0. With respect to ADP_FF, S1, S2, and S3 have 28%, 107% and 31% increased oil consumption respectively, while S1 has 76% decrease in oil consumption compared to S0. With respect to POCP, S1, S2, S3, and S4 have 36%, 15%, 41%, and 83% lower potential of formation of photochemical oxidants when compared to S0. With respect to AP, S1, S2, and S3 have 9%, 54%, 24%, respectively, potential increase in atmospheric deposition of acidifying compounds while S4 has 85% decrease, when compared to S0.

When comparing the total LCA results with compressive strength, the LHNB mix designs produced different compressive strengths, with S0 having the highest strength (32 MPa) and S4 with the lowest strength (13 MPa). For a more consistent interpretation and assessment of results, environmental performance results with respect to compressive strength and service life was conducted and is discussed further in the next section.

3.1. Compressive strength related LCIA results

The environmental performance of the LHNB scenarios is analyzed

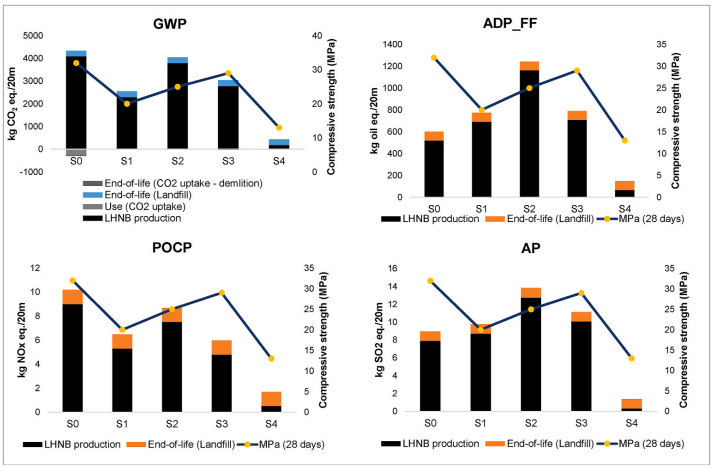

Fig. 5. Life cycle impact assessment results of the LHNB scenarios.

with respect to compressive strength using *Indicator*$_1$ (see Equation (1) in section 2.1). S2 has the highest emissions in the respective environmental impact categories, while S4 has the best environmental performance with this indicator as shown in Fig. 6.

3.2. Service life related LCIA results

For further consistent interpretation of results, the environmental performance of the LHNB scenarios is analyzed with respect to compressive strength and service life using *Indicator*$_2$ (see Equation (2) in section 2.1). As in the previous section, S2 is the worst scenario with this indicator while S4 has the best environmental performance as shown in Fig. 7. The limitation to this analysis is assumption of 40 years of service life for all the LHNB scenarios. As a result, a sensitivity analysis was conducted and is detailed in the next section.

3.2.1. Sensitivity analysis

The LHNB scenarios are made up of different mix designs with different materials which results in different compressive strength which can also influence the service life of the LHNB scenarios. Since PCC noise barrier has a desirable service life of averagely 40 years and an uncertainty on the service life of the geopolymer composites LHNB, a sensitivity analysis was conducted to determine how changes in the service life (10–40 years) of the geopolymer composite LHNB scenarios influence the LCA results. As shown in Fig. 8, the service life of S0 remains constant, thus, the environmental performance remains constant

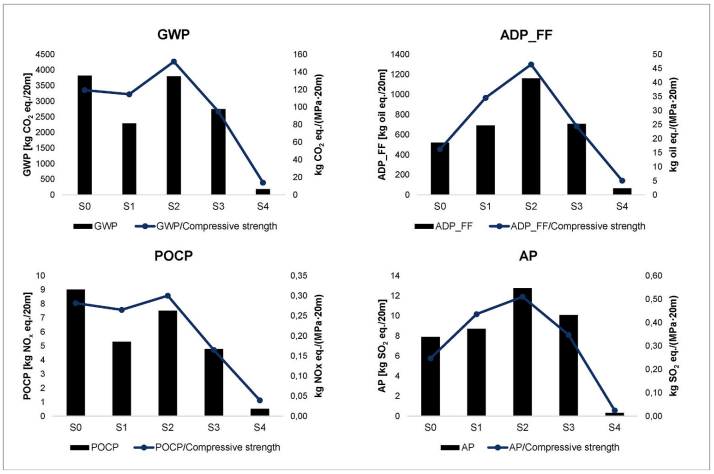

Fig. 6. Life cycle impact assessment results with respect to compressive strength of the LHNB scenarios.

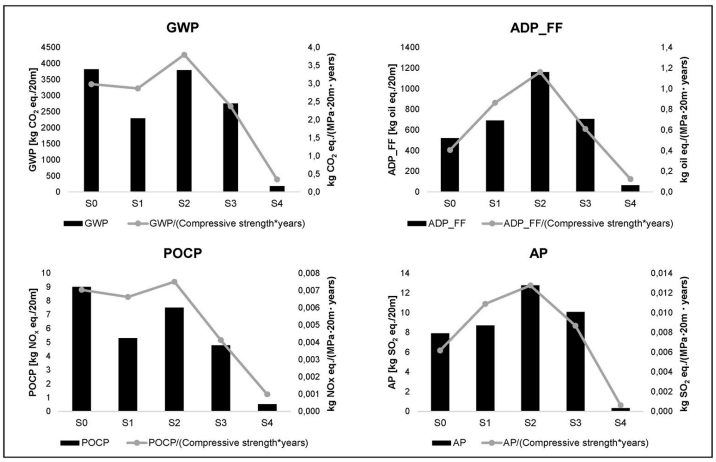

Fig. 7. Life cycle impact assessment results with respect to service life of the LHNB scenarios.

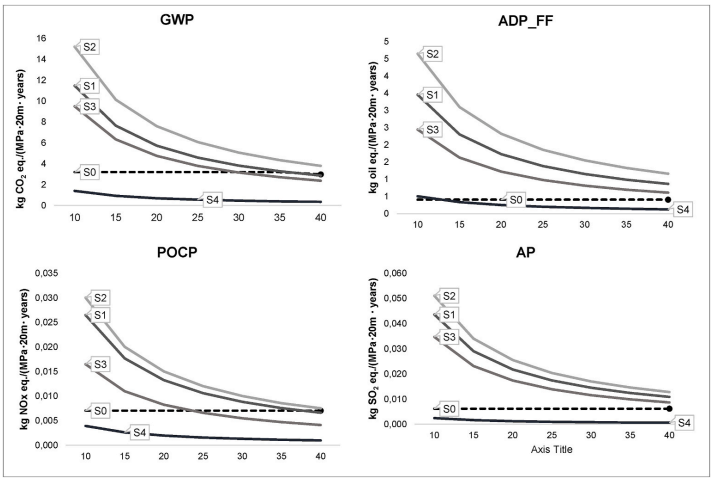

Fig. 8. Life cycle impact assessment results with respect to changing service life of the geopolymer composite LHNB scenarios.

whereas the environmental performance of the geopolymer composite scenarios is varied according to 10–40 years of service life duration.

With regards GWP, S4 has the best environmental performance with lower GWP emissions than S0 at the different years. The environmental impacts of S1, S2, and S3 is higher than S0. However, the environmental impacts of S1 and S3 becomes equal to S0 at 38 years and 32 years of service life respectively. With respect to ADP_FF and AP, only S4 has equivalent or better environmental performance than S0 whether it last 10 years or 40 years. With respect to POCP, S1, S2 and S3 have worse environmental performance when compared to S0. However, S1 and S3 become of equivalent environmental performance to S0 at 40 years and 25 years of service life while S4 remains environmentally favorable than S0 at the different years.

4. Discussion

It is essential to assess environmental impacts that will presumably occur during a product's life cycle and as such, it is possible to identify potential environmental problems and solutions. Resources and energy are much consumed in producing a LHNB. Thus, LCA of LHNB was achieved by analyzing different mix designs and proffering insight into details regarding their potential environmental impacts.

The assessment carried out shows that the production stage is the most significant life cycle phase. The major environmental problem associated with the reference scenario S0 (PCC LHNB) is due to cement production which has been known to be a major environmental pollutant (Andrew, 2018; Crossin and Carre, 2012). Most of the

environmental impacts from the production phase of the geopolymer composites LHNB S1–S4, originated from alkali-activator. Studies have shown that there is a possibility to produce alkali activator from silica-rich chemically modified waste products such as rice husk ash and waste glass without compromising on their mechanical properties (Tong et al., 2018; Vinai and Soutsos, 2019). Environmental assessment study by Abdulkareem et al. (2021), further demonstrated that environmental improvements are achieved from this substitute (Abdulkareem et al., 2021). Furthermore, transportation emissions were significant during production of S4. Transportation emissions is of importance due to environmental burden from long distance transportation of materials. Thus, most of the materials are transported only within regional scale (averagely 200 km).

When the environmental impact categories were initially assessed without considering compressive strength and service life (Fig. 5), S0 (PCC LHNB) had the worst environmental performance in GWP and POCP, while S2 had the worst environmental performance in ADP_FF and AP. When the environmental impacts were assessed with respect to compressive strength (Fig. 6), S2 had the worst environmental performance in all assessed impact categories followed by S1. Finally, when the environmental performance of the LHNB mix designs were assessed with respect to a fixed 40 years' service life (Fig. 7), S2 also had the worst environmental performance followed by S1. One of the limitations of this study is not calculating the specific service life of the different scenarios for a more consistent result, however, sensitivity analysis was conducted to determine effect of differences in service life on the overall results. When the service life of the geopolymer composites (S1–S4) were varied from 10 to 40 years due to uncertainty in the service life of geopolymer composites (Fig. 8), only S4 showed equivalent to better environmental performance than S0. Overall, S4 had the best environmental performance. These differences in results shows the significance of including compressive strength and service life for a more consistent interpretation of results.

Furthermore, Arenas et al. (2017) investigated noise properties of fly ash-based geopolymers and found the sound absorption of fly ash-based geopolymers is similar to commercial products. The study highlighted that sound absorption coefficient is dependent on ratio of aggregates to binder and not on the type of binder, activating solution ratio, and/or aggregates so far, the size distribution of the aggregates is alike. The study further highlights that sound absorption of a material depends on the thickness of a specimen, and a 120 mm thickness of material is appropriate as road traffic noise barriers which corresponds with the Finnish standard thickness for concrete noise barrier which is at least 100 mm (Liikennevirasto, 2017). Together, the standard thickness corroborates with the thickness of the precast LHNB (S0–S2) which is 150 mm and the thickness of the AM LHNB (S3 and S4) which is 295 mm (see section 2.1.2). Also, the specific mass of the LHNB scenarios is comparable with a safety marginal inclusive in the design.

S4 illustrates improvement potential in developing LHNB from 83% industrial waste materials and maximizing the efficient use of resources using AM construction method. The integration of AM in geopolymer makes it a superior and sustainable alternative to precast PCC (Yao et al., 2020) due to increased flexibility. This is also highlighted in this study comparing S2 and S3. Although, both mix designs are comparable, S2 had worse environmental performance than S3, as the later was constructed through additive manufacturing, with a unique hollow shape resulting in flexible LHNB development and lesser material consumption. Whereas S2 was produced in the traditional construction method resulting in more material consumption. Although, the environmental desirability of AM from carbon and energy viewpoint varies depending on how the printing is executed (Saade et al., 2020), other uniqueness include complexity-achievement and reduced hazardous exposure of workers etc. (Saade et al., 2020). Conversely, the shift to AM can lead to loss of jobs due to less manpower needed. There is still an open question on AM revolutionizing traditional construction, however, it can be said that AM will transform construction to highly sophisticated structures with improved environmental performance.

5. Conclusion

This study explores the environmental performance of five mix designs of low-height noise barriers (LHNB) from Portland cement concrete and geopolymer composite recipes, using LCA methodology. With compressive strength and service life (40 years) as indicators in assessing the environmental performance of the LHNB, S4 had the best environmental performance due to lower amounts of chemicals, virgin materials, and using additive manufacturing construction method whereas S2 had the worst environmental performance of the LHNB. When compared to S0, a potential decrease in emission between 40% and 73% is achieved in S4 in all assessed environmental impact categories. When compared to S1, a potential decrease in emission between 60% and 78% is achieved in S4. When compared to S2, a potential decrease in emission between 63% and 81% is achieved in S4. Finally, when compared to S3, a potential decrease between 37% and 72% is achieved in S4 in all the assessed environmental impact categories. Due to possibly different service lives of the geopolymer composites LHNB, sensitivity analysis carried out by varying the service lives of the LHNB geopolymer composites from 10 to 40 years and the result shows that only S4 has equivalent or better environmental performance compared to S0 at the different years.

The environmental hotspot of S0 is cement while alkali activator is the hotspot for S1, S2, and S3. Transportation emissions is the hotspot of S4. Based on the simplified methodology in calculating CO_2 uptake (Stripple et al., 2018), 270 and 27 kg CO_2 eq./20m can be absorbed during the use phase in S0 and S3, respectively, while in the end-of-life phase, 36 and 4 kg CO_2 eq./20m can be absorbed in S0 and S3, respectively.

S4 depicts solutions and concepts that result in environmental improvement potentials for a low-height noise barrier. This study highlights that although, geopolymer composites may be considered a low carbon alternative to Portland cement, this conclusion highly depends on the quantity of alkali activators in the mix design, its durability and service life. The results from this study supported decision-making and guided in local development of LHNB from geopolymer composites, by minimizing the use of alkali activators and natural precursors (metakaolin) in a mix design. These results show the possibility of developing a geopolymer composite LHNB from 83% industrial wastes and by-products and 0.3% alkali activator.

CRediT authorship contribution statement

Mariam Abdulkareem: Conceptualization, Formal analysis, Investigation, Data curation, Methodology, Software, Visualization, Roles. **Jouni Havukainen:** Conceptualization, Data curation, Funding acquisition, Investigation, Methodology, Project administration, Resources, Supervision, Validation, Visualization, Writing – review & editing. **Jutta Nuortila-Jokinen:** Conceptualization, Funding acquisition, Project administration, Resources, Visualization, Writing – review & editing. **Mika Horttanainen:** Conceptualization, Funding acquisition, Methodology, Project administration, Resources, Supervision, Validation, Visualization, Writing – review & editing.

Declaration of competing interest

The authors declare that they have no known competing financial interests or personal relationships that could have appeared to influence the work reported in this paper.

Acknowledgment

The authors would like to acknowledge the European Regional Development Fund, European Union through the Urban Innovative

Actions initiative for co-financing the Urban Infra Revolution project under the project number UIA02-155.

Appendix A. Supplementary data

Supplementary data to this article can be found online at https://doi.org/10.1016/j.jclepro.2021.129169.

References

Abbas, A.R., Liang, R.Y., Frankhouser, A., Cardina, J., Cubick, K.L., 2011. Green Noise Wall Construction and Evaluation.

Abdulkareem, M., Havukainen, J., Horttanainen, M., 2019. How environmentally sustainable are fibre reinforced alkali-activated concretes? J. Clean. Prod. 236 https://doi.org/10.1016/j.jclepro.2019.07.076.

Abdulkareem, M., Havukainen, J., Nuortila-Jokinen, J., Horttanainen, M., 2021. Environmental and economic perspective of waste-derived activators on alkali-activated mortars. J. Clean. Prod. 280, 124651 https://doi.org/10.1016/j.jclepro.2020.124651.

Amorim Júnior, N.S., Andrade Neto, J.S., Santana, H.A., Cilla, M.S., Ribeiro, D.V., 2021. Durability and service life analysis of metakaolin-based geopolymer concretes with respect to chloride penetration using chloride migration test and corrosion potential. Construct. Build. Mater. 287, 122970 https://doi.org/10.1016/J.CONBUILDMAT.2021.122970.

Andersson, R., Stripple, H., Gustafsson, T., Ljungkrantz, C., 2019. Carbonation as a method to improve climate performance for cement based material. Cement Concr. Res. 124, 105819 https://doi.org/10.1016/j.cemconres.2019.105819.

Andrew, R.M., 2018. Global CO 2 emissions from cement production. Earth Syst. Sci. Data 105194, 195–21710.

APILA Group, 2020. Apila Group [WWW Document]. URL. https://www.apilagroup.fi/en/. accessed 11.10.20.

Arenas, C., Luna-Galiano, Y., Leiva, C., Vilches, L.F., Arroyo, F., Villegas, R., Fernández-Pereira, C., 2017. Development of a fly ash-based geopolymeric concrete with construction and demolition wastes as aggregates in acoustic barriers. Construct. Build. Mater. 134, 433–442. https://doi.org/10.1016/j.conbuildmat.2016.12.119.

Asdrubali, F., 2006. Survey on the acoustical properties of new sustainable materials for noise control. In: Euronoise 2006. Tampere, Finland., pp. 1–10

Bendtsen, H., 2010. Noise Barrier Design: Danish and Some European Examples.

Brennan, J., Ding, G., Wonschik, C.-R., Vessalas, K., 2014. A closed-loop system of construction and demolition waste recycling. In: Isarc.

Cembureau, 2017. CEMBUREAU Activity Report 2017.

Chen, C., Habert, G., Bouzidi, Y., Jullien, A., 2010. Environmental impact of cement production: detail of the different processes and cement plant variability evaluation. J. Clean. Prod. 18, 478–485. https://doi.org/10.1016/j.jclepro.2009.12.014.

CIMSA, 2015. Environmental Product Declaration - Çimsa Çimento San. Ve Tic. A.Ş.

Crossin, E., Carre, A., 2012. Comparative Life Cycle Assessment of Concrete Blends.

Davidovits, J., 1994. Properties of Geopolymer Cements, Alkaline Cements and Concretes.

EC-JRC, 2010. International reference life cycle data system (ILCD) handbook - General guide for life cycle assessment - detailed guidance, International reference life cycle data system (ILCD) Handbook. In: General Guide for Life Cycle Assessment – Detailed Guidance. https://doi.org/10.2788/38479. Luxembourg.

EN ISO 14044, 2006. ISO 14044 – Environmental Management — Life Cycle Assessment — Requirements and Guidelines. https://doi.org/10.1007/s11367-011-0297-3. ISO 14044.

EN ISO 14040, 2006. SFS-EN ISO 14040 ENVIRONMENTAL MANAGEMENT. LIFE CYCLE ASSESSMENT . PRINCIPLES AND FRAME- WORK (ISO 14040 : 2006).

Environmental Protection Department Highways Department, 2003. Guidelines on Design of Noise Barriers.

Estévez, B., Aguado, A., Josa, A., 2006. Environmenta impact assessment of concrete recycling, coming from construction and demolition waste (C&DW). Deconstruction Mater. Reuse 250, 165–175.

Habert, G., D'Espinose De Lacaillerie, J.B., Roussel, N., 2011. An environmental evaluation of geopolymer based concrete production: Reviewing current research trends. J. Clean. Prod. 19, 1229–1238. https://doi.org/10.1016/j.jclepro.2011.03.012.

Heath, A., Paine, K., McManus, M., 2014. Minimising the global warming potential of clay based geopolymers. J. Clean. Prod. 78, 75–83. https://doi.org/10.1016/j.jclepro.2014.04.046.

Hischier, R., Weidema, B.P., Althaus, H., Bauer, C., Doka, G., Dones, R., Frischknecht, R., Hellweg, S., Humbert, S., Jungbluth, N., Köllner, T., Loerincik, Y., Margni, M., Nemecek, T., 2010. In: Implementation of Life Cycle Impact Assessment Methods. Ecoinvent report.

Huang, R., Riddle, M.E., Graziano, D., Das, S., Nimbalkar, S., Cresko, J., Masanet, E., 2017. Environmental and economic Implications of distributed additive manufacturing: the case of Injection mold tooling. J. Ind. Ecol. 21, S130–S143. https://doi.org/10.1111/jiec.12641.

Jäppinen, P., 2017. Electricity Consumption for 3D Printing.

Kawai, K., Sugiyama, T., Kobayashi, K., Sano, S., 2005. Inventory data and case studies for environmental performance evaluation of concrete structure construction. J. Adv. Concr. Technol. 3, 435–456. https://doi.org/10.3151/jact.3.435.

Kikuchi, T., Kuroda, Y., 2011. Carbon dioxide uptake in demolished and crushed concrete. J. Adv. Concr. Technol. 9, 115–124. https://doi.org/10.3151/jact.9.115.

Liikennevirasto, 2017. Radan Matalan Meluesteen Tuotevaatimukset. Liikennevirasto in Finnish.

Liu, Z., Jiang, Q., Cong, W., Li, T., Zhang, H.-C., 2018. Comparative study for environmental performances of traditional manufacturing and directed energy deposition processes. Int. J. Environ. Sci. Technol. 15, 2273–2282. https://doi.org/10.1007/s13762-017-1622-6.

Louise Rose Joynt, J., 2005. A Sustainable Approach to Environmental Noise Barrier Design. University of Sheffield.

Luukkonen, T., Abdollahnejad, Z., Yliniemi, J., Kinnunen, P., Illikainen, M., 2018. One-part alkali-activated materials: a review. Cement Concr. Res. 103, 21–34. https://doi.org/10.1016/j.cemconres.2017.10.001.

Marceau, M., VanGeem, M.G., 2003. Life Cycle Inventory of Slag Cement Manufacturing Process CTL Project No, 312012.

Marceau, M.L., Nisbet, M.A., Vangeem, M.G., 2007. Life Cycle Inventory of Portland Cement Concrete.

Marinković, S., Dragaš, J., Ignjatović, I., Tošić, N., 2017. Environmental assessment of green concretes for structural use. J. Clean. Prod. 154, 633–649. https://doi.org/10.1016/j.jclepro.2017.04.015.

Marinković, S., Carević, V., Dragaš, J., 2021. The role of service life in Life Cycle Assessment of concrete structures. J. Clean. Prod. 290, 125610 https://doi.org/10.1016/J.JCLEPRO.2020.125610.

Morgan, S.M., Kay, D.H., Bodapati, S.N., 2001. Study of noise barrier life-cycle costing. J. Transport. Eng. 127, 230–236. https://doi.org/10.1061/(ASCE)0733-947X(2001)127:3(230).

Müller, H.S., Moffatt, J.S., Haist, M., Vogel, M., 2019. A new generation of sustainable structural concretes – design approach and material properties. IOP Conf. Ser. Earth Environ. Sci. 290, 012002 https://doi.org/10.1088/1755-1315/290/1/012002.

Nematollahi, B., Xia, M., Sanjayan, J., 2017. Current Progress of 3D Concrete Printing Technologies.

NLK, 2002. Ecosmart Concrete Project: Metakaolin Pre-feasibility Study. British Columbia, Vancouver. Report EA2860.

Oltean-dumbrava, C., Richards, M., 2016. Assessing the Relative Sustainability of Long Parallel Noise Barriers and Related Noise Reducing Devices for a Motorway in Italy, pp. 4253–4260. Hamburg.

Panda, B., Tan, M.J., 2018. Experimental study on mix proportion and fresh properties of fly ash based geopolymer for 3D concrete printing. Ceram. Int. 44, 10258–10265. https://doi.org/10.1016/J.CERAMINT.2018.03.031.

Panda, B., Paul, S.C., Hui, L.J., Tay, Y.W.D., Tan, M.J., 2017. Additive manufacturing of geopolymer for sustainable built environment. J. Clean. Prod. 167, 281–288. https://doi.org/10.1016/J.JCLEPRO.2017.08.165.

Parker, G., 2006. Effective noise barrier design and specification. In: 1st Australas. Acoust. Soc. Conf. 2006, Acoust. 2006 Noise Prog, pp. 349–353.

Passuello, A., Rodríguez, E.D., Hirt, E., Longhi, M., Bernal, S.A., Provis, J.L., Kirchheim, A.P., 2017. Evaluation of the potential improvement in the environmental footprint of geopolymers using waste-derived activators. J. Clean. Prod. 166, 680–689. https://doi.org/10.1016/j.jclepro.2017.08.007.

Provis, J.L., 2018. Alkali-activated materials. Cement Concr. Res. 114, 40–48. https://doi.org/10.1016/j.cemconres.2017.02.009.

Raut, S.P., Ralegaonkar, R.V., Mandavgane, S.A., 2011. Development of sustainable construction material using industrial and agricultural solid waste: a review of waste-create bricks. Construct. Build. Mater. 25, 4037–4042. https://doi.org/10.1016/j.conbuildmat.2011.04.038.

Roads, Transport, Maritime Services, 2016. Noise Wall Design Guideline to Improve the Appearance of Noise Walls in NSW.

Saade, M.R.M., Yahia, A., Amor, B., 2020. How has LCA been applied to 3D printing? A systematic literature review and recommendations for future studies. J. Clean. Prod. 244, 118803 https://doi.org/10.1016/j.jclepro.2019.118803.

Stajanca, M., Estokova, A., 2012. Environmental impacts of cement production. Tech. Univ. Kosice, Civ. Eng. Fac. Inst. Archit. Eng. 296–302.

Stripple, H., Ljungkrantz, C., Gustafsson, T., Andersson, R., 2018. CO 2 Uptake in Cement-Containing Products Background and Calculation Models for IPCC Implementation Commissioned by Cementa AB and IVL Research Foundation.

Tahvanainen, T., 2020. Electricity Consumption of Casting.

Tong, K.T., Vinai, R., Soutsos, M.N., 2018. Use of Vietnamese rice husk ash for the production of sodium silicate as the activator for alkali-activated binders. J. Clean. Prod. 201, 272–286. https://doi.org/10.1016/J.JCLEPRO.2018.08.025.

Turk, J., Cotič, Z., Mladenovič, A., Šajna, A., Cotič, Z., Mladenovič, A., Šajna, A., 2015. Environmental evaluation of green concretes versus conventional concrete by means of LCA. Waste Manag. 45, 194–205. https://doi.org/10.1016/j.wasman.2015.06.035.

Vahtera, E., 2011. Raidemelun Vaimennuskyky Matalien Meluesteiden Tuotevaatimuksena (in Finnish).

Valdebenito, M.J., Dahmen, J., 2013. Life Cycle Assessment Screening: Environmental Impacts of a Novel Vegetative Sound Structure Authors.

Van Damme, H., 2018. Concrete material science: Past, present, and future innovations. Cement Concr. Res. 112, 5–24. https://doi.org/10.1016/J.CEMCONRES.2018.05.002.

Vanhooreweder, B., Marcocci, S., Alberto, D., 2017. Technical Report 2017-02. State of the Art in Managing Road Traffic Noise: Noise Barriers. Conference of European Directors of Roads.

Vieira, D.R., Calmon, J.L., Zulcão, R., Coelho, F.Z., 2018. Consideration of strength and service life in cradle-to-gate life cycle assessment of self-compacting concrete in a maritime area: a study in the Brazilian context. Environ. Dev. Sustain. 20, 1849–1871. https://doi.org/10.1007/s10668-017-9970-4.

Vinai, R., Soutsos, M., 2019. Production of sodium silicate powder from waste glass cullet for alkali activation of alternative binders. Cement Concr. Res. 116, 45–56. https://doi.org/10.1016/j.cemconres.2018.11.008.

Výtisk, J., Kočí, V., Honus, S., Vrtek, M., 2019. Current options in the life cycle assessment of additive manufacturing products. Open Eng. 9, 674–682. https://doi.org/10.1515/eng-2019-0073.

Weidema, B.P., Bauer, C., Hischier, R., Mutel, C., Nemecek, T., Reinhard, J., Vadenbo, C. O., Wernet, G., 2013. Overview and Methodology. Data Quality Guideline for the Ecoinvent Database Version 3.

Weil, M., Dombrowski, K., Buchwald, A., 2009. Life-cycle analysis of geopolymers. Geopolymers: Structures, Processing, Properties and Industrial Applications. Elsevier, pp. 194–210. https://doi.org/10.1533/9781845696382.2.194.

Yao, Y., Hu, M., Di Maio, F., Cucurachi, S., 2020. Life cycle assessment of 3D printing geo-polymer concrete: an ex-ante study. J. Ind. Ecol. 24, 116–127. https://doi.org/10.1111/jiec.12930.

Zhang, Z., Wu, X., Yang, X., Zhu, Y., 2006. BEPAS - A life cycle building environmental performance assessment model. Build. Environ. 41, 669–675. https://doi.org/10.1016/j.buildenv.2005.02.028.

ACTA UNIVERSITATIS LAPPEENRANTAENSIS

954. MUJKIC, ZLATAN. Sustainable development and optimization of supply chains. 2021. Diss.

955. LYYTIKÄINEN, JOHANNA. Interaction and barrier properties of nanocellulose and hydrophobically modified ethyl(hydroxyethyl)cellulose films and coatings. 2021. Diss.

956. NGUYEN, HOANG SI HUY. Model based design of reactor-separator processes for the production of oligosaccharides with a controlled degree of polymerization. 2021. Diss.

957. IMMONEN, HEIKKI. Application of object-process methodology in the study of entrepreneurship programs in higher education. 2021. Diss.

958. KÄRKKÄINEN, HANNU. Analysis of theory and methodology used in determination of electric motor drive system losses and efficiency. 2021. Diss.

959. KIM, HEESOO. Effects of unbalanced magnetic pull on rotordynamics of electric machines. 2021. Diss.

960. MALYSHEVA, JULIA. Faster than real-time simulation of fluid power-driven mechatronic machines. 2021. Diss.

961. SIEVINEN, HANNA. Role of the board of directors in the strategic renewal of later-generation family firms. 2021. Diss.

962. MENDOZA MARTINEZ, CLARA. Assessment of agro-forest and industrial residues potential as an alternative energy source. 2021. Diss.

963. OYEWO, AYOBAMI SOLOMON. Transition towards decarbonised power systems for sub-Saharan Africa by 2050. 2021. Diss.

964. LAHIKAINEN, KATJA. The emergence of a university-based entrepreneurship ecosystem. 2021. Diss.

965. ZHANG, TAO. Intelligent algorithms of a redundant robot system in a future fusion reactor. 2021. Diss.

966. YANCHUKOVICH, ALEXEI. Screening the critical locations of a fatigue-loaded welded structure using the energy-based approach. 2021. Diss.

967. PETROW, HENRI. Simulation and characterization of a front-end ASIC for gaseous muon detectors. 2021. Diss.

968. DONOGHUE, ILKKA. The role of Smart Connected Product-Service Systems in creating sustainable business ecosystems. 2021. Diss.

969. PIKKARAINEN, ARI. Development of learning methodology of additive manufacturing for mechanical engineering students in higher education. 2021. Diss.

970. HOFFER GARCÉS, ALVARO ERNESTO. Submersible permanent-magnet synchronous machine with a stainless core and unequal teeth widths. 2021. Diss.

971. PENTTILÄ, SAKARI. Utilizing an artificial neural network to feedback-control gas metal arc welding process parameters. 2021. Diss.

972. KESSE, MARTIN APPIAH. Artificial intelligence : a modern approach to increasing productivity and improving weld quality in TIG welding. 2021. Diss.

973. MUSONA, JACKSON. Sustainable entrepreneurial processes in bottom-of-the-pyramid settings. 2021. Diss.

974. NYAMEKYE, PATRICIA. Life cycle cost-driven design for additive manufacturing: the frontier to sustainable manufacturing in laser-based powder bed fusion. 2021. Diss.

975. SALWIN, MARIUSZ. Design of Product-Service Systems in printing industry. 2021. Diss.

976. YU, XINXIN. Contact modelling in multibody applications. 2021. Diss.

977. EL WALI, MOHAMMAD. Sustainability of phosphorus supply chain – circular economy approach. 2021. Diss.

978. PEÑALBA-AGUIRREZABALAGA, CARMELA. Marketing-specific intellectual capital: Conceptualisation, measurement and performance. 2021. Diss.

979. TOTH, ILONA. Thriving in modern knowledge work: Personal resources and challenging job demands as drivers for engagement at work. 2021. Diss.

980. UZHEGOVA, MARIA. Responsible business practices in internationalized SMEs. 2021. Diss.

981. JAISWAL, SURAJ. Coupling multibody dynamics and hydraulic actuators for indirect Kalman filtering and real-time simulation. 2021. Diss.

982. CLAUDELIN, ANNA. Climate change mitigation potential of Finnish households through consumption changes. 2021. Diss.

983. BOZORGMEHRI, BABAK. Finite element formulations for nonlinear beam problems based on the absolute nodal coordinate formulation. 2021. Diss.

984. BOGDANOV, DMITRII. Transition towards optimal renewable energy systems for sustainable development. 2021. Diss.

985. SALTAN, ANDREY. Revealing the state of software-as-a-service pricing. 2021. Diss.

986. FÖHR, JARNO. Raw material supply and its influence on profitability and life-cycle assessment of torrefied pellet production in Finland – Experiences from pilot-scale production. 2021. Diss.

987. MORTAZAVI, SINA. Mechanisms for fostering inclusive innovation at the base of the pyramid for community empowerment - Empirical evidence from the public and private sector. 2021. Diss.

988. CAMPOSANO, JOSÉ CARLOS. Integrating information systems across organizations in the construction industry. 2021. Diss.

989. LAUKALA, TEIJA. Controlling particle morphology in the in-situ formation of precipitated calcium carbonate-fiber composites. 2021. Diss.

990. SILLMAN, JANI. Decoupling protein production from agricultural land use. 2021. Diss.

991. KHADIM, QASIM. Multibody system dynamics driven product processes. 2021. Diss.

ISBN 978-952-335-738-9
ISBN 978-952-335-739-6 (PDF)
ISSN-L 1456-4491
ISSN 1456-4491
Lappeenranta 2021